



Development of a *Caenorhabditis elegans* model for
the assessment of toxicity and its application in
testing novel anthelmintics

Eyitayo Olufemi Oluwadare

A thesis submitted in partial fulfilment of the requirements of
Edinburgh Napier University, for the award of Doctor of Philosophy

October 2017

ABSTRACT

The nematode *Caenorhabditis elegans* is an alternative model used in biomedical research for the investigation of descriptive and mechanistic toxicity assessment of chemicals. There are considerable differences in published data, especially in terms of reproducibility and validation of toxicity endpoints, and the techniques used in the investigation of these endpoints. This thesis describes the evaluation of toxicological endpoints following the exposure of *C. elegans* to chemicals which include; zinc oxide nanoparticles (ZnONP), Diethylstilbestrol (DES) and derivatized target-specific anthelmintics.

The results suggest that ZnONP prepared in anionic and cationic dispersants (AZNP and CZNP respectively) were the most toxic against the nematode resulting in the 'bag of worms' (BOW) phenotype which can be exploited as a marker for reproductive toxicity. Also, worms treated with ZnONP prepared in 0.1% FBS (FZNP), molecular grade water (WZNP) or *E. coli* OP50 supernatant (SZNP) presented three-fold embryo elongation showing fully differentiated tissues encapsulated within the eggshell and still within the hermaphrodite gravid adult. The phenotype has been named accelerated embryonic development (AED) and could be used as a developmental toxicity endpoint. The results suggest that the AED endpoint is the most sensitive while lethality endpoint appears to be the least sensitive despite its extensive use in the literature. Also, microRNA microarray expression appears to be the most sensitive molecular endpoint while behavioural endpoints such as speed should be interpreted with caution, especially when performed manually. Importantly, good *C. elegans* culture practice (GCeCP) is required for reproducible chemical toxicity assessment and different endpoints may be required for different types of toxicity assessment.

Additionally, the thesis describes a second but related study which explores a potential for enhanced anthelmintic targeting. Novel fluorophore-based asparagine-containing oligopeptide substrate probes were used to target the helminth protease, legumain. These probes were selectively cleaved by legumain in *C. elegans*, *Haemonchus contortus* and *Teladorsagia circumcincta*. The protease-specific probes could potentially be exploited to achieve protease-mediated prodrug activation and drug delivery.

Declaration

I declare that this thesis is a result of my own independent work and all the work presented in it was undertaken and written by me. I also declare that no part of this work has been submitted for any other degree or professional qualification.

.....
Eyitayo Olufemi Oluwadare

.....
DATE

Dedication

To my brother

Olatubosun Oluwadare (1984 – 2015)

Tubo, your absence created an irreplaceable void in my heart.

I miss you so much, rest in peace.

Acknowledgement

I would like to thank all my colleagues, students and staff at Edinburgh Napier University who supported me through the process of this PhD. To Deborah McFarlane for her contribution to nanoparticle characterization, Hannah Bisby for some behavioural assessment of *C. elegans*, Elia Alcaniz Boada and Aiman Rehan for their contribution to lethality test of derivatized anthelmintics in *C. elegans*. I thank Patricia Gonzalez-Iglesias, Lisa McMillan and Jennifer Christie for making sure I was comfortable in the laboratory. To Sunil Mathur, who provided one of the probes (SM9) used in this research and for his support and friendship.

To Dr. Agnes Turnbull for the advice on chapter 5 of this thesis. To Dr. Iain Reid for the advice on image analysis, Ms. Sadie Kemp for assisting and training me on gene and protein expression techniques and Dr. Lesley Young for helping with the SEM characterization of nanoparticles.

Special thanks to Dr. Yao Ding; your presentation on the theranostic capability of legumain in cancer therapy inspired chapter 5 of this thesis. To Dr. Emma Marczylo of Public Health England for collaborating, sharing expert opinion and helping with the microRNA microarray analysis in this thesis. To Prof. David Gems of University College London for supplying 13 transgenic strains of *C. elegans*. To Dr. Kayode Imole of University of Twente, the Netherlands for his advice on nanoparticle characterization and his friendship of 17 years.

I am indebted to Robert Wright who was head of business and administration in the then FHLSS. Your contribution to my personal welfare was huge.

To my parents; Rufus and Christina for their prayers and care since my childhood and to Buki, Biyi and Gbenga my siblings.

To my supervisory team. Dr. David Mincher for the addition of kindness and cheerfulness to the research; thanks for showing me one bright side to life.

Dr Eva Malone; you constantly and painstakingly provided me with technical, academic and sisterly advice that has contributed immensely to my development as a research scientist.

To my director of studies; Dr. Lorna Proudfoot. From my first conversation with you, I found the family I left back in Africa. You have been my academic mentor, adviser, sister and mother. I could not have asked for any other person. I hope we would have the opportunity to work together again. Thank you.

Finally, to my wife, Opeyemi; thank you for all the sacrifice and love, I could not have done it without you and to Adura my son; I would be available to play with you for a bit longer now. I love you both!

Contents

List of Figures	xiii
List of Tables	xvi
List of Appendices	xvii
Chapter One	1
1 General introduction	1
1.1 Classification of <i>Caenorhabditis elegans</i>	4
1.1.1 Life Cycle	4
1.2 <i>C. elegans</i> and the human genome	8
1.3 History of <i>C. elegans</i> in biological research	9
1.4 Development of a <i>C. elegans</i> model for the assessment of chemical toxicity	10
1.4.1 Bag of worms phenotype	11
1.4.2 Transgenic GFP reporter expression	12
1.4.3 Behaviour in <i>C. elegans</i>	14
1.4.4 MicroRNAs as biomarkers of toxicity	15
1.5 The use of <i>C. elegans</i> as a representative model of parasitic helminths	17
1.5.1 Parasitic Helminths and their Economic Importance	17
1.5.2 <i>Haemonchus contortus</i>	17
1.5.3 <i>Teladorsagia circumcincta</i>	18

1.5.4	Overview of Anthelmintics	19
1.5.5	Anthelmintic resistance	20
1.6	Application of <i>C. elegans</i> in anthelmintic drug discovery	21
1.6.1	Legumain: A potential target for anthelmintic delivery	23
1.7	Aims of research	25
1.7.1	Objectives of aim 1	25
1.7.2	Objectives of aim 2	25
Chapter Two		26
2 Materials and Methods		26
2.1	Maintenance of <i>C. elegans</i> Strains	26
2.2	Stage specific synchronization	26
2.3	Toxicity assessment of zinc oxide nanoparticles	27
2.3.1	Preparation of zinc oxide nanoparticle treatments	27
2.3.2	Zinc oxide nanoparticle characterization	28
2.3.3	Dose response for ZnONP toxicity	29
2.3.4	Zinc oxide nanoparticles lethality test	29
2.3.5	Morphological analysis of ZnONP-treated worms	31
2.3.6	Reproductive analysis of ZnONP-treated worms	31
2.3.7	SOD expression of ZnONP-treated worms	32
2.3.8	RNA extraction from ZnONP-treated worms	32
2.3.9	<i>sod-3</i> gene expression and protein analysis of ZnONP-treated worms	34

2.3.10	Microarray analysis of MicroRNA expression.....	37
2.4	Toxicity assessment of Diethylstilbestrol.....	38
2.4.1	Diethylstilbestrol lethality test	38
2.4.2	Behavioural analysis of DES-treated worms	39
2.5	Toxicity assessment of derivatized tubulin-targeting anthelmintics.....	40
2.5.1	Anthelmintic derivative treatments.....	40
2.5.2	Derivatized anthelmintics lethality test.....	40
2.5.3	Behavioural analysis of derivatized anthelmintic-treated worms ...	40
2.6	Assessment of legumain-specific targeting in helminths.....	41
2.6.1	Fluorophore-based probes	41
2.6.2	Parasite Homogenates and Sheep Plasma.....	41
2.6.3	Preparation of somatic fractions.....	41
2.6.4	Removal of detergent from somatic fractions	42
2.6.5	BCA Protein Assay.....	43
2.6.6	Legumain activity.....	43
2.6.7	Legumain localization.....	44
2.7	Data analysis	45
Chapter Three.....		46
3	Toxicity assessment of zinc oxide nanoparticles	46
3.1	Introduction	46
3.1.	Results.....	49
3.2.1.	Zinc oxide nanoparticle characterization	49

3.2.2.	Effect of ZnONP on the survival of <i>C. elegans</i>	54
3.2.3.	Effect of ZnONP on worm morphology.....	57
3.2.4.	Effect of ZnONP on reproduction	59
3.2.5.	<i>sod-3::GFP</i> expression in ZnONP-treated <i>C. elegans</i>	63
3.2.6.	Molecular analysis of <i>sod-3</i> gene and protein expression.....	69
3.2.7.	Effect of ZnONP exposure on miRNA expression.....	73
3.3.	Discussion	75
3.3.1.	Zinc oxide nanoparticle characterization	75
3.3.2.	Effect of ZnONP on the survival of <i>C. elegans</i>	76
3.3.3.	Effect of ZnONP on worm morphology.....	78
3.3.4.	Effect of ZnONP on reproduction	79
3.3.5.	Effect of ZnONP on transgenic <i>sod-3::GFP</i> expression	81
3.3.6.	Effect of ZnONP on <i>sod-3</i> gene and protein expression	82
3.3.7.	Effect of ZnONP on microarray analysis of miRNA expression.....	83
Chapter Four	86
4	Toxicity assessment of Diethylstilbestrol.....	86
4.1	Introduction to diethylstilbestrol toxicity assessment.....	86
4.2	Results.....	87
4.2.1	<i>C. elegans</i> viability on exposure to DES	87
4.2.2	Effect of diethylstilbestrol on <i>C. elegans</i> survival	87
4.2.3	Effect of diethylstilbestrol on <i>C. elegans</i> reproduction.....	89
4.2.4	Effect of diethylstilbestrol on <i>C. elegans</i> behaviour.....	90

4.3 Discussion	94
Chapter Five	97
5 Toxicity assessment and prove of concept of target-specific anthelmintics.....	97
5.1 Part one	97
5.1.1 Introduction to tubulin-specific derivatized anthelmintic toxicity assessment	97
5.1.2 Results	101
5.1.3 Discussion.....	106
5.2 Part two.....	109
5.2.1 Introduction to legumain-specific anthelmintic targeting: A proof of concept	109
5.2.2 Results	110
5.2.3 Discussion.....	126
Chapter Six	135
6 General discussion.....	135
6.1 Lethality as a toxicological endpoint in <i>C. elegans</i>	138
6.2 Morphology as a toxicological endpoint in <i>C. elegans</i>	139
6.3 Behavioural endpoints for toxicological assessment.....	140
6.4 Reproductive and developmental toxicity endpoints should be classified in terms of embryogenesis and egg-laying.....	143
6.5 Transgenic GFP-reporter expression analysis.....	145

6.6	MiRNA expression as a biomarker for toxicity	151
6.7	Designing realistic exposure scenarios.....	152
6.8	The <i>C. elegans</i> model in the application of anthelmintic drug delivery	153
6.9	Conclusion	153
References.....		155
Appendices.....		179
	Appendix A: Synchronization.....	179
	Appendix B: Anthelmintic derivatives	181
	Appendix C: Fluorophore-based probes.....	185
	Appendix D: Reagents and treatment preparation	187
I.	LB agar preparation	187
II.	NGM preparation	187
III.	Concentrated <i>E. coli</i> OP50 (Pellets)	187
IV.	M9 Buffer	188
V.	S Basal solution	188
VI.	Potassium Citrate (pH6)	189
VII.	Trace metal solution	189
VIII.	S medium	189
IX.	20% Sodium hypochlorite (NaOCl).....	189
X.	Zinc Oxide nanoparticle treatment preparation	189
XI.	Preparation of Phosphate-Citrate Buffer.....	195

XII.	Preparation of MES buffer	195
XIII.	Preparation of Cysteine Protease Inhibitors	196
XIV.	Preparation of LS9 and TL11 probes.....	196
XV.	Preparation of <i>C. elegans</i> treatments with different pH	196
XVI.	Preparation of nematode parasite treatments at different pH	197
XVII.	Legumain assay plate plan.....	198

List of Figures

Figure 1.1: Transparent internal structure of the adult hermaphrodite <i>Caenorhabditis elegans</i>	4
Figure 1.2: Life cycle of <i>C. elegans</i>	6
Figure 1.3: General life cycle of gastrointestinal parasitic worms.....	19
Figure 1.4: Delivery mechanism of anti-cancer drug.....	24
Figure 2.1: Schematic representation of treatment plan for ZnONP assay	30
Figure 3.1: Scanning electron micrograph of ZnONP in different dispersants.....	50
Figure 3.2: Z-average diameter of ZnONP in dispersants.....	52
Figure 3.3: Particle size distribution of ZnONP in dispersants.	53
Figure 3.4: Effect of ZnONP on wild-type <i>C. elegans</i> survival.....	55
Figure 3.5: Effect of 12.5mM ZnONP exposure on survival of wild type <i>C. elegans</i>	56
Figure 3.6: Effect of ZnONP on worm morphology.	58
Figure 3.7: Egg-laying phenotype observed following exposure of wild-type gravid adult <i>C. elegans</i> to ZnONP.	59
Figure 3.8: Representative images of ZnONP effect on worm embryogenesis.	61
Figure 3.9: Representative images depicting egg laying in accelerated embryonic development (AED) phenotype.	62
Figure 3.10: Effect of 12.5mM ZnO NP exposure on survival of transgenic <i>sod-3::GFP C. elegans</i> strain.....	63
Figure 3.11: Comparison of <i>sod-3::GFP</i> expression in four developmental stages of worms.....	65
Figure 3.12: Egg-laying phenotype observed following exposure of <i>sod-3::GFP</i> adult <i>C. elegans</i> to ZnONP.	66

Figure 3.13: Effect of ZnONP on <i>sod-3::GFP</i> expression during embryogenesis.....	67
Figure 3.14: Stress response in first filial generation of ZnONP-treated worms.	68
Figure 3.15: Effect of ZnONP on <i>sod-3</i> gene expression.....	71
Figure 3.16: Effect of ZnONP on SOD-3 protein expression.....	72
Figure 3.17: Principal component analysis (PCA) of significantly altered miRNAs	73
Figure 3.18: Heatmap of those significantly altered miRNAs	74
Figure 4.1: Effect of diethylstilbestrol on wild-type <i>C. elegans</i> survival.	88
Figure 4.2: Effect of diethylstilbestrol on <i>C. elegans</i> brood size.....	89
Figure 4.3: Effect of diethylstilbestrol on <i>C. elegans</i> average speed.....	91
Figure 4.4: Effect of diethylstilbestrol on <i>C. elegans</i> average body bend per minute (BBPM).....	93
Figure 5.1: Effect of an anthraquinone derivative and its TPP conjugate on <i>C. elegans</i> survival	102
Figure 5.2: Effect of MB2 and MB2-TPP on <i>C. elegans</i> survival.....	103
Figure 5.3: Effect of colchicine and colchicine-based drugs on <i>C. elegans</i> survival.....	104
Figure 5.4: Effect of colchicine and colchicine-based drugs on <i>C. elegans</i> body bend.....	105
Figure 5.5: Effect of colchicine and colchicine-based drugs on <i>C. elegans</i> speed.....	106
Figure 5.6: Activation of TL11 by wild type <i>C. elegans</i> homogeneate.....	112
Figure 5.7: Activation of TL11 by <i>T. circumcincta</i> homogenate.	113
Figure 5.8: Activation of TL11 by <i>H. contortus</i> homogenate.	114

Figure 5.9: pH effect on the activation of LS9 by <i>T. circumcincta</i> homogenate.	115
Figure 5.10: pH effect on the activation of LS9 by <i>H. contortus</i> homogenate.	116
Figure 5.11: pH effect on the activation of LS9 by sheep plasma.	117
Figure 5.12: Comparison between LS9 activation in <i>H. contortus</i> homogenate and sheep plasma.....	118
Figure 5.13: Activation of LS9 by sheep liver tissue homogenate.....	119
Figure 5.14: Rhodamine-based probe (SM9) uptake in <i>C. elegans</i>	121
Figure 5.15: Detergent effect on the activation of LS9 by recombinant legumain.	122
Figure 5.16: Activation of LS9 by resin-recovered (RR) recombinant legumain.	123
Figure 5.17: LS9 activation by somatic fractions of <i>C. elegans</i>	125
Figure 5.18: Structural representation of probes used for legumain localization.	132

List of Tables

Table 3.1: Influence of lysis agents on the quantity and quality of nucleic acid extraction in <i>C. elegans</i>	70
Table 4.1: Comparison between two methods used for the assessment of DES effect on <i>C. elegans</i> brood size.....	90
Table 4.2: Comparison between two methods used for the assessment of DES effect on <i>C. elegans</i> speed	92
Table 6.1: Toxicological assessment of chemicals performed in the current research.....	137
Table 6.2: Rationale for the use of transgenic strains for toxicity assessment of chemicals.....	148

List of Appendices

Appendix A: Synchronization	179
Appendix B: Anthelmintic derivatives	181
Appendix C: Fluorophore-based probes probes.....	185
Appendix D: Reagents and treatment preparation	187

Chapter One

1 General introduction

Toxicology can be defined as the study of the adverse effect of chemical or physical agents of known structure on biological systems. Research in toxicology entails the examination of cellular, biochemical and molecular mechanisms, and the functional effects of chemicals and their risk assessment. In order to accomplish this, there is a need to understand the relationship between the exposure of chemical substances and the responses they induce. One of the benefits of toxicological assessment is to produce risk assessments of the possible effects and significance of chemicals on humans and their environment. Since there are a variety of chemicals which include drugs, there are also corresponding diverse types of effects. In the current research, chemicals have been evaluated using:

1. Descriptive toxicology which is toxicity testing that offers information about safety assessment, and
2. Mechanistic toxicology that identifies and explains the biochemical, cellular and molecular mechanisms chemicals use to induce toxic effects.

Appropriating the right toxicity model that would provide the information needed to evaluate potential risks of chemicals is not limited to humans but also other animals, plants and the environment, and this could be challenging. However, the current work focuses on using a singular model to develop a standardized tool that would not only be applicable to different chemicals based on the classification above but would be predictive when considering different exposed groups.

The specialized areas of toxicology considered in this research include environmental toxicology, reproductive toxicology and pharmaceutical toxicology. For the purpose of the current research, a brief definition of these areas is stated below.

Environmental toxicology: This investigates the adverse impact of chemical pollutants in the environment on biological organisms which usually excludes humans. Environmental toxicology should not be misrepresented with

Ecotoxicology which is a specialized area within the former. Ecotoxicology is specifically concerned with the impacts of toxic substances on population dynamics in an ecosystem.

Reproductive toxicology: This investigates the adverse effects which can result from exposure of chemicals to the reproductive system of chemical or physical agents. Indeed, reproductive toxicology does not exist without developmental toxicology. Developmental toxicology refers to the adverse effects of chemicals on the developing organism that occurs any time through the life span of the organism which could result from exposure to chemicals before conception, prenatal development, or postnatally.

Pharmaceutical toxicology: The study of the adverse effect of medicinal drugs on humans, plants and animals with the purpose of ensuring safety of these classes of chemicals following controlled administration. This aspect of toxicology is an interface between pharmacology and toxicology. It should be noted that the aspect of pharmaceutical toxicity also covers the development of drug targets since mechanistic evaluation is considered.

All three aspects mentioned above are inter-related. For instance, Zinc oxide nanoparticles; one of the reference toxicants in the current research could be assessed either as an environmental or a reproductive toxicant. Also, diethylstilbestrol is a pharmaceutical agent but it is also the reference chemical for reproductive toxicity in this study. Furthermore, anthelmintic derivatives such as the ones considered in the current research can be analysed in terms of their pharmaceutical implications as well as their effect in the environment.

The increasing impact of toxicology on society is accompanied by the duty to be ever sensitive to the ethical, social, and legal implications of research in toxicology. Regulatory studies using animals have been traditionally adopted for assessing the safety of chemicals to protect humans and the environment. However, there should be regular reviews as our understanding of science and technical processes continually improve. In 1959, Russell and Burch published their work on "The Principles of Humane Experimental Technique" which gave birth to the concept of replacement, refinement and reduction of animals in

research (3Rs). It took almost half a century for this concept to be established with the European Registration, Evaluation, Authorisation and Restriction of Chemicals (REACH) legislation leading the cause. This was necessary to ensure that the appropriate animals are used for toxicity testing whilst consistently improving their predictive value and reducing their overall usage. With an increasing number of studies using *in vitro* and *in silico* models as predictive tools of chemical safety, it is expected that a good number of chemicals would be excluded for further evaluation, thus, reducing the need for animal testing. One general purpose of this research is to provide a suitable alternative model for toxicity testing.

The understanding of most hereditary, physiological, developmental and molecular processes is a result of studies on model organisms. Experimental amenability to specific research interest and the phylogenetic position of organisms determine their choice as model organisms. In general, multicellular model organisms share basic biological processes with their corresponding target organisms. Hence, the identification of genes, biological processes or molecular pathways of interest in a model may create opportunities for comparative studies in its target organism or organisms. The major difference between the model and target organisms is that model organisms respond better to experimental manipulations. It is with qualities like this that increasing wealth of knowledge that relate to certain model organisms have been gained.

The nematode *Caenorhabditis elegans* was first used as a model organism in 1963 (Brenner, 2009). When compared to other multicellular organisms like *Drosophila melanogaster*, it is simpler to manipulate because it has less than a thousand cells that divide in conventional manner; indicating that every cell lineage can be traced back to the egg. Although models such as *Danio rerio* (Zebra fish) are arguably better suited for vertebrate target organisms as they are genetically accessible for appendage and heart regeneration, *C. elegans* exhibits all the hallmarks of a multicellular organism with complex organ systems (*C. elegans* Consortium, 1998). These include a reproductive system, a metabolically active digestive tract, a nervous system and an endocrine system; allowing it to exhibit social, sexual and learning behaviours (de Bono and aricq 2005). In order to justify some characteristics of *C. elegans* as a model, it is necessary to describe its classification and life cycle.

1.1 Classification of *Caenorhabditis elegans*

C. elegans is a multicellular organism that belongs to the family Rhabditidae in the order Rhabditida of the class Secernentea and from the phylum Nematoda. The classification of *C. elegans* places it in a position where it is free-living, possesses oesophagosal functions as well as an excretory system and is also bilaterally symmetrical. The nematode possesses an elongated cylindrical body and has no appendages or segmentation. The adult worm is approximately 1 to 1.3mm in length. *C. elegans* exists usually as a hermaphrodite which is self-fertilizing and occasionally as male that can mate with the hermaphrodites to produce their young. The young larva to its adult stage is transparent allowing morphological features of the worm to be observed with a basic stereo microscope or compound microscope (Figure 1.1).

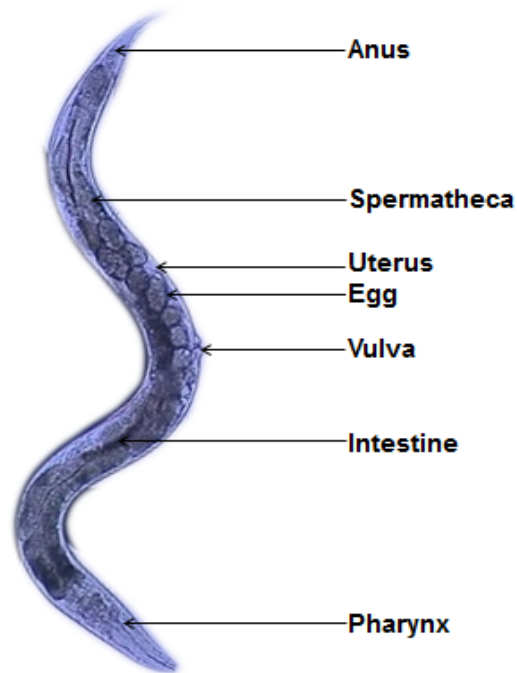


Figure 1.1: Transparent internal structure of the adult hermaphrodite *Caenorhabditis elegans*

1.1.1 Life Cycle

The common habitats of the worm include compost or rotten fruits and occasionally in the soil where it feeds on microorganisms for a source of nutrient. They thrive in moisture-rich environments and in temperate regions around the world. *C. elegans* like most round worms help in improving soil structure due to their burrowing activity hence, it is pivotal in the development of soil nutrient for

ecological balance. The life cycle of *C. elegans* (Figure 1.2) takes between two and three days depending on the temperature (16 to 25°C). The stages in the life cycle below are based on temperatures between 20 and 22°C.

1.1.1.1 Embryogenesis

The development of the embryo starts inside the hermaphrodite and eggs are laid through the vulva opening. This is subsequent to the fertilization of the oocyte by the spermatheca of the hermaphrodite or the spermatozoa from the male nematode. The complete process of embryogenesis after the eggs are laid takes between one and three hours and is divided into two stages.

1.1.1.1.1 Proliferation

This process involves the division of a single cell to over 500 undifferentiated cells. At 22°C, it takes up to 5 hours and 30 minutes after fertilization for this process to occur. The first two and a half hours of the process takes place within the hermaphrodite's uterus where the zygote and the embryonic founder cells are formed. This is followed by the laying of the embryo outside the worm as soon as approximately 30-cell stage is reached at gastrulation (Bucher and Seydoux, 1994). The final stage of proliferation is the organization of cells within the embryo into three germ layers known as the ectoderm, mesoderm and endoderm; these three develop into the neurons, hypodermis and muscles, respectively.

1.1.1.1.2 Organogenesis

This process involves the terminal differentiation of cells with no further cell division. At 22°C, it takes approximately 6 to 8 hours for the completion of organogenesis. The worm forms inside the egg and begins to roll around its longitudinal axis prior to cell cleavage. It is at this point that the pharynx begins to function and the egg is hatched (Sulston *et al.*, 1983). Proliferation and organogenesis make up the whole process of embryogenesis and it is at the end of embryogenesis that the physiology and the sex of the adult worms are determined.

1.1.1.2 L1 Stage

At this stage, five of the eight motor neurons in the adult hermaphrodite's ventral cord are developed to support nervous function. Also, somatic gonad precursors begin to produce cells while the germ line precursors begin to divide continuously from the L1 through to the end of adult development. The ventral cells that eventually develop into the vulva in L3 and L4 stages are created at the end of the L1 stage. However, two dorsal coelomycytes develop from the mesoblast in the hermaphrodite which is not present in the male (Sulston and Horvitz, 1977).

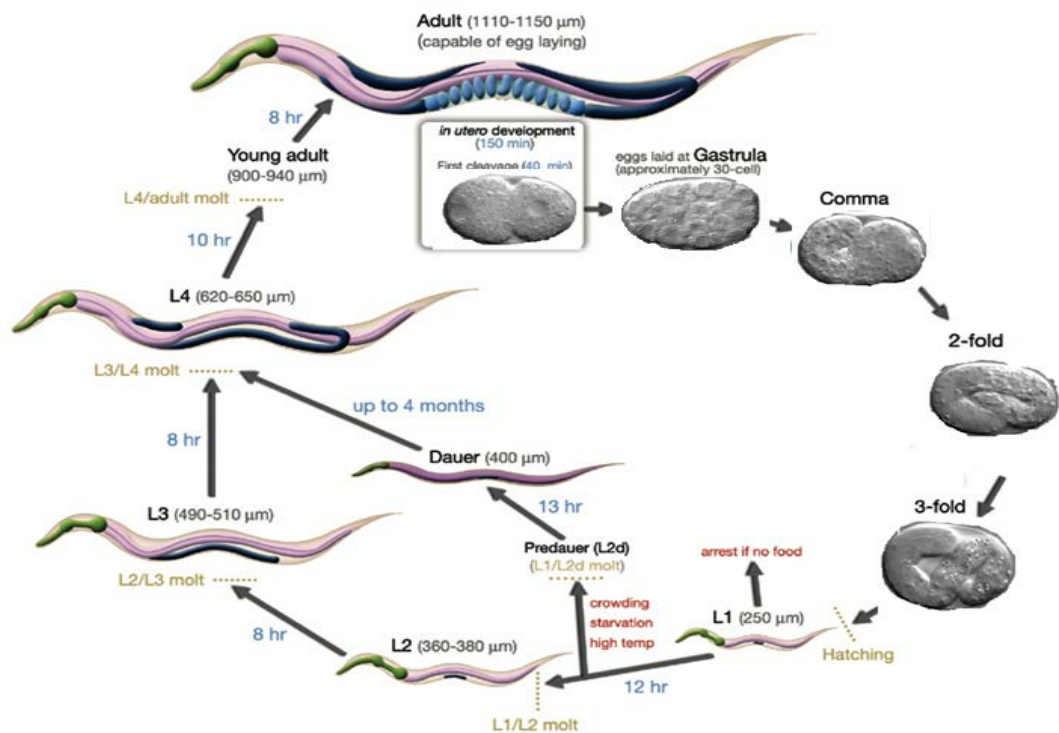


Figure 1.2: Life cycle of *C. elegans*.

(Image adapted from Wormatlas)

1.1.1.3 L2 Stage

In the nervous system, two ventral ganglion neurons are formed to improve nerve coordination while the germ cell division in the reproductive system continues. The germ cells are interwoven with somatic cells until the molt phase between L2 and L3 where the cells are arranged appropriately to establish the organization of the gonad. The extension of the gonad starts at the distal tip cells at both the posterior and anterior end of the hermaphrodite while the gonad in the male worm elongates only at the anterior (Kimble and White, 1981).

1.1.1.4 Dauer Stage

Unfavourable environmental conditions such as lack of food, high population density or high temperature may prevent the L1 larva from developing into the L2 stage (Golden and Riddle, 1984). At the dauer stage, the larva does not age because its duration has no effect on post-dauer life span, hence the longevity of the worm can be said to be increased (Kimura *et al.*, 1997, Mihaylova *et al.*, 1999). There is no feeding in the dauer phase and movement is highly reduced. However, as soon as the environment becomes conducive, the worm exits the dauer and begins to feed and after approximately 10 hours, molts directly into L4 stage skipping the L3 stage.

1.1.1.5 L3 Stage

There is extensive development in the reproductive system at the L3 stage. In the hermaphrodite, 143 cells that form the gonadal sheath, the uterus and the spermathecae are produced by the somatic gonad precursors (Kimble and Hirsh, 1979). The anterior and posterior gonadal sheath extends continuously at the tips until the distal tip cells stop and slowly start arranging themselves in the dorsal direction. Also, 16 sex muscles are generated from the sex myoblasts. In the male L3 larva, the germ line that produces only meiosis and spermatozoa starts. The somatic gonad blast cells undergo cell division to the somatic gonads that differentiate into the seminal vesicle and the vas deferens. The proximal gonad extends and 6 male sex myoblasts are produced and the tail begins to swell as a result of posterior blast cell division (Sulston, 1988).

1.1.1.6 L4 Stage

The formation and development of gonads is completed in the L4 phase. During the L4/adult molt, the production of spermatozoa ceases while other germ line cells continue to undergo meiotic division and differentiation generating only oocytes. Tissue development increases as the vulval and uterine cell generation ends and the egg-laying neurons and sex muscles interact with the uterus and vulva to form the egg-laying apparatus (Greenwald, 1997). In the male worm, all sex muscles become completely developed with the inclusion of a coelomocyte

generated from the mesoblast. The vas deferens and the seminal vesicle differentiation are also completed in the male L4 worm (Antebi *et al.*, 1997).

1.1.1.7 Adult worm

It takes *C. elegans* between 60 and 65 hours at temperature ranges of 22-25°C to develop from embryogenesis to adulthood. In the first 94 hours of adulthood, the hermaphrodite produces oocytes and reproduction, resulting from self-fertilization, would produce up to 300 offspring. The adult male on the other hand fertilizes the oocytes to produce between 1200 and 1400 progeny (Hodgkin, 1988). Although the adult hermaphrodite generates a total of 1090 somatic cells during its development, 131 of these experience apoptosis at specific stages in development (Driscoll, 1995) a remainder of 959 cells. Unlike the adult hermaphrodite, the adult male worm possesses 1031 somatic cells. The total number of neurons in the adult hermaphrodite is 302 while the male has an additional 81 (White *et al.*, 1986).

1.2 *C. elegans* and the human genome

The entire worm from its single cell embryo to the 959 somatic cells present in the adult has been fully studied. *C. elegans* genes have more than 40% gene homologs that share similar functions with human genes (Kaletta and Hengartner, 2006) including those associated with diseases (Shaye and Greenwald, 2011). Despite having more than 40% gene homology with the human genome, it encodes over 22,000 proteins (*C. elegans* Consortium, 1998); a number slightly fewer than that in humans. In 2002, *C. elegans* became the first multicellular eukaryote to have its over 100 million bases completely sequenced. The sequencing project, which was funded by the National Human Genome Research Institute (NHGRI) and the National Institutes of Health (NIH), has an estimated error rate of less than 1 in 100,000. It is no understatement that *C. elegans* has transformed methodologies used in genetic studies to understand how regulation of genes affects cellular processes. The worm's modest genetics,

transparent structure and simplicity of cultivation make it a model system for studies in developmental biology, neurobiology, toxicology and the molecular basis of some human diseases.

1.3 History of *C.elegans* in biological research

In 2002, Sydney Brenner, John Sulston and Robert Horvitz were awarded the Nobel Prize in Physiology or Medicine for their work on the genetics of organ development and programmed cell death in the nematode. Andrew Fire and Craig C. Mello also received the Nobel Prize in 2006 for their discovery of RNA interference during translation in *C. elegans*. Again, in 2008, a Nobel Prize in Chemistry was awarded to Martin Chalfie for his work on green fluorescent protein, a tool used extensively in *C. elegans* research.

Apart from being a model choice for Nobel Prize winners, *C. elegans* has played key roles in biomedical discoveries. For instance, in 1993, presenilin, a transmembrane protein associated with Alzheimer's disease, was discovered in the nematode (Sundaram and Greenwald, 1993) and in 1995, genetic alterations in the human presenilin-1 gene were linked to early-onset of Alzheimer's disease (Levitan and Greenwald, 1995; Sherrington *et al.*, 1995). With the discovery of presenilins in *C. elegans*, the understanding of Alzheimer's disease has advanced due to the identification of the protein as a constituent of an important target site in the disease known as the γ -secretase complex (De Strooper *et al.*, 1999); a prospective target in the treatment of the disease.

Also, *C. elegans* has helped improve the understanding of diabetes type 2. The loss of function of the forkhead transcription factor FOXO was found to save the diabetic phenotype of insulin-resistant mice (Nakae *et al.*, 2002). This was made possible based on findings five years earlier that identified the negative regulators of insulin signalling pathway including daf-16 gene which encodes the *C. elegans* orthologue of FOXO (Ogg *et al.*, 1997). Again, *C. elegans* can be used to investigate mechanisms involved in pharmacological processes. An example was shown in the increase of serotonergic signalling in the nematode following

exposure to the antidepressant fluoxetine. This was possible due to the inhibition of the *C. elegans* orthologue of the serotonin re-uptake transporter SERT (Ranganathan *et al.*, 2001) a monoamine transporter associated with depression. This finding has suggested that there are other modes of action of fluoxetine and has stimulated investigations to understand the molecular basis of depression. Having explored some previous work with *C. elegans*, the following sections in this chapter describe the focus and rationale for the current research.

1.4 Development of a *C. elegans* model for the assessment of chemical toxicity

As mentioned earlier, *C. elegans* is transparent (Figure 1.1) allowing the observation of morphological and developmental changes within the individual worm. It is an attractive option as it is capable of reproducing within three to five days with an approximate lifespan of three weeks (Fielenbach and Antebi, 2008) which would facilitate high throughput screening; these advantages make *C. elegans* a good model for toxicity. Moreover, from an ecological perspective, its sensitivity to a wide variety of toxicants including organic phosphates, heavy metals and pesticides suggests its appropriateness for toxicological screening (Leung *et al.*, 2008).

The prevalent use and release of chemical substances in the environment has influenced the need for the development of rapid and affordable testing techniques to protect humans and other living species. Similarly, pharmaceutical industries depend on the assessment of toxicity and safety of new chemical substances as a prerequisite in the development of new drugs. Accomplishing this task with conventional animal models such as rodents or higher animals have some disadvantages such as the requirement of ethical approval, high cost and long assessment time. The *C. elegans* model system can allay these concerns.

For the *C. elegans* model, as with most animal models, the most commonly used endpoint for the assessment of chemicals is lethality testing; however, there are variances in the literature that depend on lethality as an endpoint probably due to

technical differences in exposure approach or the preparation of chemicals for exposure which may change their physicochemical characteristics. It is as a result of these setbacks that better screening techniques involving a wide range of toxicologically applicable endpoints such as lifespan, reproduction, behaviour and morphology were introduced. In the current research, the suitability of *C. elegans* for the assessment of chemical toxicity with emphasis on environmental as well as developmental and reproductive toxicity was investigated. For the purpose of the current research, zinc oxide nanoparticles (ZnONP), diethylstilbestrol (DES) and anthelmintic derivatives that target specific organelles or enzymes have been selected as reference toxicants for the assessment of toxicity. An overview of some sub-lethal endpoints used in the current research for toxicity assessment using the *C. elegans* model system is discussed below.

1.4.1 Bag of worms phenotype

As the adult worm ages, decline in the reproductive function is imminent and this begins after or around five days into adulthood with cessation being around ten to fourteen days into adulthood (Mendenhall *et al.*, 2011). Self-fertile hermaphrodites produce their highest progeny size on day 2 of becoming an adult and stop production with 5-6 days of adulthood as a result of self-sperm depletion while male-fertilized hermaphrodites produce their highest progeny size within 2-4 days of adulthood and cease production at about the 12th day due to age-related degeneration of the reproductive system (Hughes *et al.*, 2007). Ideally, fertilized eggs are laid within approximately 12.5 hours in young and healthy adults. Where the time between fertilization and egg-laying is exceeded as a result of loss of reproductive function, the eggs may hatch within the adult worm and the young larva will feed on the adult, killing it. This manifestation is referred to as matricidal hatching which is the intra-uterine hatching and development of larvae leading to the destruction of the mother worm by the larvae (Luc *et al.*, 1979). In *C. elegans*, matricidal hatching; colloquially called 'bag of worms' (BOW) phenotype or 'bagging', was described by Pickett & Kornfeld (2013) as a form of cannibalism that enhances larval viability and promotes dauer formation. Prior to this time, Johnson (1984) had shown that high population densities could lead to the BOW phenotype. Chen & Caswell-Chen (2003) further showed that

lack of food or any form of stress could lead to BOW phenotype. They also showed that the condition can be reversed provided food is returned to the environment and stress is reduced in time. Their findings led to the suggestion that the condition is a form of parental influence (altruism) to protect the progeny. Chen and Caswell-Chen further showed that under stress, the progeny obtain nutrients directly from the adult parent body before becoming dauers. They concluded that even the production of only one stress-resistant, long-lived dauer instead of progeny that cannot achieve the dauer is a fitness advantage (Chen and Caswell- Chen, 2003). The BOW phenotype can be used as a marker for unfavourable conditions such as exposure to chemicals.

While BOW is a measure of reproductive fitness, it is not an unusual phenotype in *C. elegans*, and by definition, it focuses on the viability of the adult worm rather than its embryo. Seidel & Kimble (2011) investigated embryo viability in terms of number of viable embryo produced by adult worms following starvation and observed that the number of embryos are reduced in starved worms; suggesting that unfavourable conditions may deplete embryo number. The combination of reproductive fitness and embryo viability can be utilized for the assessment of chemical toxicity and this could be possible by investigating the process that leads to bagging. Angelo & Gilst (2009) showed that embryos in the morphogenic stage of embryogenesis within starved gravid adult worms had terminally differentiated cells, tissues and organs which had started developing prior to egg-laying but classified this as a process leading to bagging. In the current research, we examined the process of embryogenesis in chemical-exposed gravid adult worms to investigate the effect of chemical on their viability.

1.4.2 Transgenic GFP reporter expression

Although *C. elegans* has many advantages as a toxicity model, it is less sensitive to most environmental stressors when compared with models such as *Daphnia*. This is likely a reflection of the robust set of cellular defence pathways the worm utilizes occasionally as part of its opportunistic lifestyle in the terrestrial habitat. Nonetheless, some studies have shown that transgenic strains of *C. elegans* that are sensitive markers of stress resulting from exposure to reproductive or pharmaceutical chemicals can also be utilized as indicators of environmental

stressors (Hägerbäumer *et al.*, 2015). The use of gene expression from transgenic worms is easily reproducible with minimal variability unlike endpoints such as worm motility which measures lethality (Roh *et al.*, 2006).

One of the ways of limiting variances such as the one experienced with lethality testing in toxicity assessments is by taking advantage of transgenic green fluorescent protein (GFP) reporter strains to evaluate sublethal effect in terms of biochemical responses induced following exposure to chemicals. For example, one characteristic of the effect of toxicants is that they can induce oxidative stress in biological systems exposed to them. Oxidative stress is a condition involving the disturbance between the balance of free radicals or reactive molecules from oxygen (prooxidants) and the ability of a biological system to detoxify their damaging effects (antioxidants) in which case the free radical production exceeds that of the antioxidant. There are suggestions that free radicals and reactive molecules from oxygen collectively referred to as reactive oxygen species (ROS) play a role in activation and processes of cell signalling including gene expression (Hancock *et al.*, 2001). This can be advantageous in the development of toxicity assays using *C. elegans* because markers of oxidative stress like superoxide dismutase genes can be investigated with transgenic and knockout strains. Superoxide dismutase (SOD) is an antioxidant or a detoxifying enzyme that converts or takes part in the process of conversion of ROS products to hydrogen peroxide and subsequently water. SOD production is an indication of self-defence of biological systems; hence, an increase in the production or expression of SOD is a function of the severe effect of toxicant exposure to the biological system. Also, since most of the ROS present in cells is believed to be produced in the mitochondria, mitochondrial viability can be investigated by measuring SOD in the cell. There are five SOD genes in *C. elegans*:

- *sod-1* encodes a Cu and Zn-containing intracellular enzyme that is principally localized in the cytosol (Jensen and Culotta, 2005) and is also found in the mitochondrial intermembrane space. It acquires its copper through a glutathione pathway.
- *sod-2* gene is responsible for the production of the main Fe / Mn SOD found in the cytosol based (Giglio *et al.*, 1994)

- *sod-3* also encodes iron and manganese-containing SOD but is a minor cytosolic isoform of SOD. However, over 60% of SOD produced by *sod-3* is believed to be mitochondrial-based. This could be relevant for the assessment of mitochondrial function (Hunter *et al.*, 1997).
- *sod-4* encodes an extracellular Cu/Zn SOD and is believed to play a role in insulin /IGF-1 signalling pathway which coordinates growth, differentiation and metabolism in response to change in the environment or nutrient supply (Yoko Honda *et al.*, 2008). It is also involved in the redox regulation during vulval development (Shibata *et al.*, 2003); an advantage that could be useful to assess the influence of chemicals on reproduction.
- *sod-5* gene encodes an intracellular Cu/Zn SOD but very little SOD is found in the cytosol (Hoogewijs *et al.*, 2008) although it effectively compensates for *sod-1* where the latter is not functional (Yanase *et al.*, 2009).

Also, a master regulator gene *daf-16* which controls multiple stress-response pathways can be used as marker alongside the *sod* genes. The only *C. elegans* forkhead box O (FOXO) homologue is encoded by *daf-16* which is a transcription factor for the insulin/IGF-1-mediated signaling pathway that regulates stress responses (Yen *et al.*, 2011). *Daf-16* determines the transcription of genes that code for enzymes which take part in immunity as part of a general stress response.

The application of concurrent testing of multiple gene output would give insight into stress response patterns that are expressed in transgenic and knockout *C. elegans* strains with green fluorescent protein (GFP) reporters. The current research has utilized the conventional lethality endpoint and have included the investigation of *sod-3::GFP C. elegans*.

1.4.3 Behaviour in *C. elegans* as a toxicity assessment tool

One characteristic of animals is their ability to change their behaviour in response to changes in their external environment and also changes in their internal physiological state. These behavioural alterations are achieved through the activities of the nervous systems. *C. elegans* displays robust behavioural

response to changes in its environment. Such changes alter the worm's movement in terms of the effect on locomotion velocity (speed) and turning frequency (body bends per time). The movement of *C. elegans* is affected by the presence of xenobiotics in its local environment and the worm's neurosensory awareness about these environmental changes is driven by behavioural shifts that are central to survival. In order to understand the *C. elegans* behaviour, the knowledge of how the activity of its muscles translates into movement within the mechanical framework and physical environment is important. The forward movement of the worm is achieved by undulatory waves in a dorsal-ventral plane from head to tail and are affected by responses to conditions in the worm environment that determine the locomotory behaviour of the worm (Pierce-Shimomura *et al.*, 2008). The alternate contraction and relaxation of two dorsal and two ventral muscle groups running along the length of the body of the worm creates its bending characteristic (Von Stetina *et al.*, 2005).

1.4.4 MicroRNAs as biomarkers of toxicity

A microRNA (miRNA) is a non-coding RNA of about 18 to 22 nucleotides that selectively bind one or more messenger RNA (mRNA) molecules to effect the post-transcriptional regulation of gene expression (Bartel 2009). MiRNA was first identified in *C. elegans* by Lee *et al.* (1993) who identified a small temporal RNA named *lin-4* which was shown to be a regulator of the *lin-14* mRNA which is important in the timing of the development of L1 larva to the L2 stage in the worm. It was concluded that *lin-4* resulted in reduced protein expression by *lin-14*. Seven years later Reinhart *et al.* (2000) identified another small RNA; *let-7* which is involved in the timing and development of *C. elegans* L4 stage to adult worm. In the same year, Pasquinelli *et al.* (2000) also found that *let-7* was conserved in *Drosophila* and in humans. By 2001, more miRNAs had been identified in *C. elegans* (Bartel *et al.*, 2001; Lee and Ambros, 2001) and other animals (Lagos-quintana *et al.*, 2001). While the number of miRNAs encoded by the human genome is about 1000, the number of mRNAs are estimated at approximately 30,000 (Pritchard *et al.*, 2012) which suggests that single or multiple mRNAs can be targeted by miRNA genes.

The biogenesis of miRNA starts with the transcription of mRNA from miRNA-encoding genes by the influence of RNA polymerase II and III. The primary mRNA transcripts are referred to as pri-miRNA and are about 100 to 1000 nucleotides in length. In the nucleus, the pri-miRNA is cleaved by a ribonuclease III enzyme known as Drosha and its co-factor; DGCR8, to form a precursor miRNA called pre-miRNA. Exportin 5 in the nucleus transports the pre-miRNA to the cytoplasm where it interacts with another ribonuclease III enzyme known as Dicer. Dicer cleaves the pre-miRNA to a short miRNA duplex of approximately 20 base pairs. The duplex is then bound by an argonaute protein known as AGO2. AGO2 is part of the RNA induced silencing complex (RISC) which responsible for the activity and transport of miRNA to its target site. AGO2 interacts with dicer to unwind the strands of the duplex and allow one of the strands to be selectively retained within the RISC (Rüegger and Großhans, 2012). The retained strand is called the guide strand because it guides the RISC to its mRNA target where it either inhibits translation or degrades the mRNA of the target gene.

Previous studies have shown that miRNA is implicated in human pathology such as diabetes (Trajkovski *et al.*, 2011) and cancer (Iorio and Croce, 2012). The stability of miRNA and its protection from endogenous RNase in plasma (Mitchell *et al.*, 2008) have encouraged its use as a biomarker of liver drug-induced toxicity (Wang *et al.*, 2009). These findings coupled with its association with specific cellular pathways (Arzate-Mejía *et al.*, 2011) including those implicated in diseases would help improve our understanding of the role miRNA plays in mechanisms involved in toxicity. In the current research, we investigate the use of miRNA as indicators of toxicity in *C. elegans*.

1.5 The use of *C. elegans* as a representative model of parasitic helminths

1.5.1 Parasitic Helminths and their Economic Importance

Parasitic helminths are known to be major infectious agents of humans and livestock, especially in developing nations. Current data suggests that over 1.4 billion people worldwide suffer from helminthiasis; majorly from poor communities of developing Africa, Asia and the Americas (Caffrey, 2012). In the agricultural sector, many nations of the world have arranged projects for nematode control; however, anthelmintic resistance has been on the increase. Many parasites of domestic livestock resist broad spectrum anthelmintic drugs (Kaplan and Vidyashankar, 2012) and there is also a growing concern that the mass administration of these drugs may not sustain human parasite control programs in the near future (Prichard *et al.*, 2012). Thus, it is imperative that new methods of managing these parasites be discovered. Unfortunately, the challenge is not being met as new anthelmintic medicines are not developed based on the consideration that agricultural livestock industries are minor markets for these drugs. Yet, recent reports have suggested that multiple-anthelmintic resistance is growing fast among major agricultural livestock producers (Geurden *et al.*, 2014). *C. elegans* as a model in this thesis focuses on two of the major economically important gastrointestinal parasites of sheep, *Haemonchus contortus* and *Teladorsagia circumcincta*. These two helminth parasites were utilized for some of the experiments in chapter five of this thesis.

1.5.2 *Haemonchus contortus*

Haemonchus contortus is a stongylid nematode that infects millions of sheep and goats worldwide (Scott & Sutherland, 2010). Barber's pole worm, as it is also called, feeds on blood from the capillaries in the stomach mucosa of its host leading to haemorrhagic gastritis, oedema, anaemia and other related complications. Ultimately, the infected host dies where infection is severe and in the absence of treatment or presence of resistant strains (Nikolaou and Gasser, 2006).

The minimum life cycle of *H. contortus* is between four to six weeks. The adult male resides in the abomasum of its ruminant host where it mates with the female

to produce eggs which are excreted in the faeces into pasture. In the faeces, embryogenesis takes place and the eggs hatch producing the L1 larva which is the first larval stage of development. The L1 larva develops and molts to the L2 stage and then the L3 stage. Larval stages 1 to 3 all take place in the faeces. At the L3 stage, the larva migrates on to the pasture where it is ingested by grazing ruminants.

In the rumen of the ruminant, the retained L2 cuticle known as the exsheath is shed and allows the L3 larva to move to the abomasum where it develops into the L4 larval stage. Following successful migration and development of the L4 larva in the abomasum, the nematode develops into the adult worm between 14 and 21 days (Prichard, 2001).

An adult female is capable of producing about 10,000 eggs a day (Waller *et al.*, 2004) and one host may harbour thousands of such females. Although *H. contortus* infections occur rapidly in tropical regions, the L4 larva can undergo arrested development in order to evade adverse conditions such as prolonged drought or cold winters (Hoberg *et al.*, 2004). This ability coupled with the movement of livestock from place to place has encouraged global distribution and survival of the parasite despite having its etiology from sub-Saharan Africa (Blouin *et al.*, 1995).

1.5.3 *Teladorsagia circumcincta*

About a decade ago, *T. circumcincta* was recorded as the dominant parasitic nematode affecting sheep in the United Kingdom (Nieuwhof and Bishop, 2005). The life cycle of *T. circumcincta* is similar to that of *H. contortus* in that it is also a gastrointestinal strongylid nematode. Like *Haemonchus*, the eggs develop in faeces and hatch within 24 hours to release the L1 larva which is the first stage of larval development. The L1 develops through L2 to the third larval stage known as the L3 larva which is the infective stage. The period of larva development from L1 to L3 takes about a week and the process takes place in the faeces. The L3 moves on to the pasture and is ingested by a ruminant host. In the rumenorecticulum of the host, the L3 exsheath is shed and the larva moves through the abomasum to the gastric glands where it moults to the fourth larval

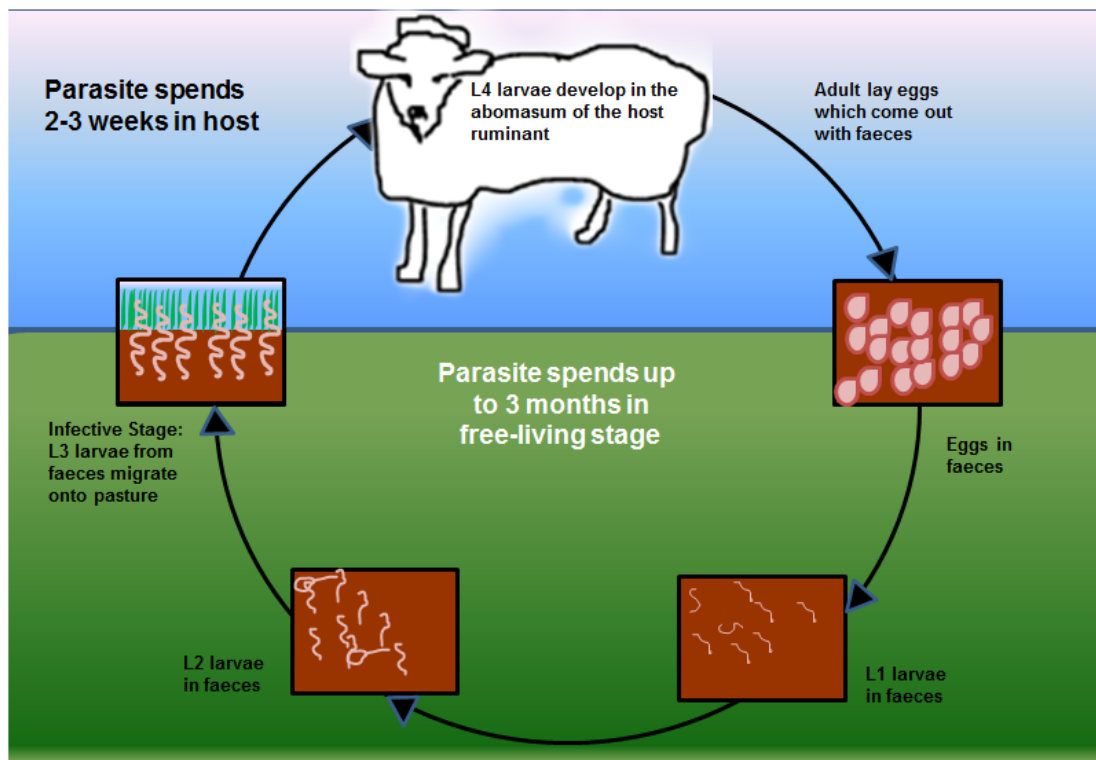


Figure 1.3: General life cycle of gastrointestinal parasitic worms.

(Adapted from SCOPS, 2012)

stage of development (L4). It is in the gastric gland that the L4 develops into either the male or female adult parasite which mates with the opposite sex to produce more parasites. The adult *T. circumcincta*; like *Haemonchus* can live for up to 12 weeks before dying; a time frame that is capable of decimating the host. *T. circumcincta* infection can lead to poor productivity in livestock resulting from deaths and failure to reproduce (O'Connor *et al.*, 2006).

1.5.4 Overview of Anthelmintics

Many drugs and chemicals are available to combat helminth parasites but with regards to host-parasite interaction, a drug requires high selectivity for a parasite in order to meet the criteria for the definition of an anthelmintic. The margin between the minimal therapeutic dose and the minimal toxic dose of most anthelmintics is wide and these drugs often have a broad spectrum of activity. Having said this, in principle, the utility of an anthelmintic can be restricted by its pharmacokinetic properties, its mechanism of action and the characteristic of the

infected host. Moreover, the increased use of available anthelmintics is accompanied by increasing frequency of parasite resistance to them (Sutherland and Leathwick, 2011). Since most anthelmintics are classified either based on their chemical structure, their site of action or their biochemical mechanisms, resistance of a parasite to any member of a class may also mean resistance to other members of that class. Therefore, it is important to synthesize better targeted anthelmintics that can circumvent such resistance. Any mention of parasites here on refers to helminth parasites.

1.5.5 Anthelmintic resistance

Although there is a growing public, media and political attention on antimicrobial resistance, it does not seem that anthelmintic resistance is seen as equally important. For more than two decades, no new antimicrobials have been produced but two novel anthelmintics; monepantel (Sager *et al.*, 2009) and the oral derquantel-abamectin formulation (Little *et al.*, 2011) have been made in the last five years. It is probable that new antimicrobials are carefully guarded because of their public health implications. Unfortunately, it could be damaging if such approach is used for anthelmintics because the available number of anthelmintics are fewer compared to antimicrobials and the attempt to wait until available drugs become ineffective as a result of resistance may increase the selection pressure on the new anthelmintics for resistance when they become available for use. Moreover, the use of new anthelmintics in the absence of resistance would achieve an effective kill rate on both organisms that are or not resistant to existing anthelmintics; as a result the overall level of resistance in worm parasite population would be reduced. Regrettably, there is a thin line between the use and management of anthelmintics, like antimicrobials. The affordability and availability of the drugs have led to their rapid routine use and this has caused the development and increase of anthelmintic resistance.

Prior to the introduction of amino-acetonitrile derivative monepantel (AAD) in 2009, the three major classes of broad spectrum anthelmintic drugs were macrocyclic lactones, benzimidazoles and levamisoles. Most worm parasites were usually controlled with a combination of the anthelmintic administration and

management strategies. However, the emergence of resistance to these drugs has compromised effective control as multiple drug resistance is on the increase in Europe and North America (Falzon *et al.*, 2013; Martínez-Valladares *et al.*, 2013; Sargison *et al.*, 2007). Furthermore, multiple drug resistance has been reported in temperate and tropical regions of the world. Even more challenging is the report of the case of resistance to monepantel in New Zealand last year (Scott *et al.*, 2013). It is becoming clearer that the current chemical control strategies may not be sufficient any more. Hence, there is a need to adopt new approaches of targeted selective treatments with the novel exploitation of legumain in this case.

1.6 Application of *C. elegans* in anthelmintic drug discovery

The classification of nematodes into two classes; Adenophorea and Secernentea by the Catalogue of Life (Roskov *et al.*, 2014) seems to be an easy sorting as it is based on morphology. However, morphological characteristics are not enough to reflect the relationship between free-living and parasitic nematodes as the sharing of characters by a set of species which are not present in their common ancestry (homoplasy) are widespread. Hence characters cannot be used, without ambiguity, to determine how related free-living nematodes are to their parasitic counterparts. A more suitable approach for comparison would be molecular phylogenetics which involves the use a gene or genes from different taxa to construct a dataset of homologous traits. Specifically, *C. elegans* small subunit rRNA (18S rRNA) analysis suggests that the worm is closely related to parasitic nematodes in the order Strongylida (Fitch and Kelly-Thomas, 1997) which includes *Teladorsagia* and *Haemonchus*.

As an experimental model system, the genome of *C. elegans* has been completely sequenced with the inclusion of expressed sequence tags (ESTs) which are DNA found in the coding region of a gene used to identify full gene lengths and which is also important in gene mapping. These *C. elegans* ESTs have been used as reference points for the generation of most human nematode parasite ESTs (Mitreva *et al.*, 2005). The success of the *C. elegans* genome

project inspired scientists like Blaxter *et al.* (1999) to start the Filarial Genome Project where parasite genome research is ongoing. Blaxter *et al.* (2002) worked on *Brugia malayi*; the causative agent of elephantiasis, which is similar to *C. elegans* in many respects. The size of their base size is similar (100Mb), although *B. malayi* has higher adenine-thymine ratio (Rothstein *et al.*, 1988). Also, the main features in the organisation of genes in both organisms are alike. With reference to ESTs, the closest homologue to most *B. malayi* EST genes is a *C. elegans* gene and a good number of parasite and free-living worms gene pairs do not have any other homologues. More so, because of the evolutionary gap between *B. malayi* and *C. elegans*, any common motif would possibly be of functional importance and it would be appropriate to examine the operation of such already known sequence in *C. elegans* in the *Brugia* species.

As a result of successful molecular study on *C. elegans*, similarities based on nematode morphology can be revisited. For instance, collagen is a common feature in members of the class Secernentea and although *C. elegans* collagen is more complex than that of parasitic worms, its complexity makes it an important model for the study of developmental regulation in the parasitic worms (Kingston, 1991).

The process of dauer formation in *C. elegans* can also help in understanding how parasitic worm infection can be controlled. This is possible because for some parasites, the infective form is the dauer stage (Riddle and Albert, 1997). Pheromone produced by peroxisomal fatty acid β -oxidation in the *C. elegans* environment is the first signal in the process of dauer formation (Bucher and Seydoux, 1994) and it is proportionate to population density or other stress producing conditions. Although pheromones are also present in parasitic worms (Braendle 2012), they have extensively conserved pathways. However, the understanding of *C. elegans* dauer gene cascade can help understand how the cascades work in parasitic worms. Hence, pheromone-mediated activities in parasitic worm life cycle may become drug design targets as chemosensory drugs could disrupt the dauer formation pathway.

1.6.1 Legumain: A potential target for anthelmintic delivery

In 1993, legumain was identified in leguminous seed and classified as a cysteine protease (Kembhavi *et al.*, 1993). It requires asparagine in the P1 position adjacent to the C-terminus to cleave protein substrates (Jinq-may Chen *et al.*, 1997). In mammals, legumain was first identified in the lysosome/endosome systems (Chen *et al.*, 1998) and it can also be found on cell surfaces (Liu *et al.*, 2003) and in the nucleus (Andrade *et al.*, 2011; Haugen *et al.*, 2013). In the lysosome, legumain plays an important role in MHC class II-mediated antigen presentation (Maehr *et al.*, 2005; Manoury *et al.*, 2003) with studies showing that its activities are highly correlated with activation of macrophages and that it is an ideal marker for primary tumour inflammation as well as early stage metastatic lesions (Edgington *et al.*, 2013). It has been shown to be an important enzyme in the regulation of cathepsins B, H and L activities in the immune system (Shirahama-Noda *et al.*, 2003). The activation of legumain is triggered by acidic pH and has been shown to be autocatalytic (Berven *et al.*, 2013).

There are suggestions that the localisation of legumain expression can be used to predict the outcome of a patient's survival from cancer (Ohno *et al.*, 2010). Also, studies have shown that legumain can be used as a component of therapeutics in the treatment and management of certain cancers. Some cancer therapy studies are focused on taking advantage of the expression of legumain in diseased individuals (Guo *et al.*, 2013, Haugen *et al.*, 2013, Ohno *et al.*, 2010, Wang *et al.*, 2012). Helminths have been shown to possess legumain (Adisakwattana *et al.*, 2007; Ju *et al.*, 2009; Oliver *et al.*, 2006; Skelly and Shoemaker, 2001; Wawrzyniak *et al.*, 2012).

Within the School of Applied Sciences in Edinburgh Napier University, Dr. David Mincher's group have spent over a decade in the area of cancer research, prodrugs and molecular probes targeting legumain associated with cancer cells. His team showed that prodrugs can enhance drug delivery and efficacy by exploiting the expression of legumain in cancer cells to identify with high accuracy and precision; the release of the active drug at the cancer site whilst sparing normal cells (Ding 2014). Hence, the current research intends to explore legumain in *C. elegans* and trichostrongylid nematodes with a view to improving the targeting of anthelmintic drugs. In theory, drugs attached to asparagine-

containing tripeptide substrates (prodrugs) which can be cleaved by legumain would release the active drugs into the locality of the enzyme. Dr. David Mincher's group has developed fluorescent-based probes containing tripeptide conjugates to prove this concept. We intend to show that the interaction of the probe with legumain would result in the cleavage of the tripeptide and the release of the fluorophore which would fluoresce (Figure 1.4).

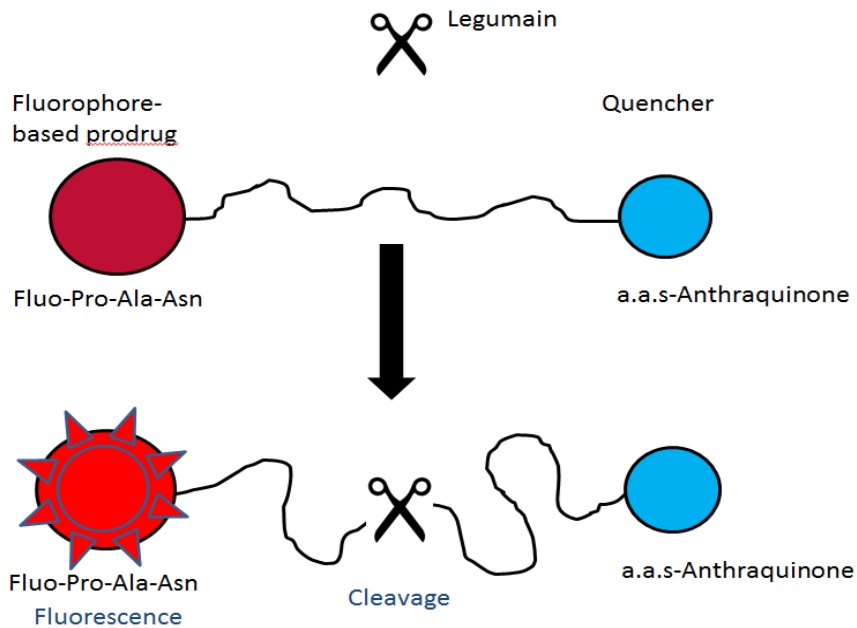


Figure 1.4: Delivery mechanism of anti-cancer drug.

The fluorophore-based prodrug is linked to the quencher and cleaved by legumain expressed in the tumour region.

1.7 Aim of research

1. To development and standardize techniques for chemical evaluation using the *C. elegans* model system.
2. To use *C. elegans* as a representative model in the application of anthelmintic treatment for parasitic helminth infections.

1.7.1 Objectives of aim 1

1. To develop a high-throughput and reliable technique for toxicity assessment of zinc oxide nanoparticles, diethylstilbestrol and tubulin-targeting derivatized anthelmintics.
2. To utilize transgenic GFP reporter strains for descriptive and mechanistic toxicology evaluation.
3. To differentiate bag of worms and embryo development phenotypes as two different endpoints of reproductive toxicity.
4. To standardize behavioural assay as an endpoint for toxicity
5. To investigate the suitability of microRNA expression as a marker for toxicity

1.7.2 Objectives of aim 2

1. To proof the concept that the legumain cysteine protease can be exploited as a potential for enhanced anthelmintic targeting using *C. elegans* as a representative model of parasitic helminths.
2. To investigate the anthelmintic and enhanced anthelmintic properties of colchicine derivative and their TPP conjugate respectively.

The research work addresses the challenges of documented toxicity assessment of emerging chemical substances such as nanoparticles and this would help achieve the objectives of the European Union's Registration Authorization and Restriction of Chemicals (REACH) project of attaining the replacement, reduction and refinement of animals used for toxicity testing. Also, the success of the research on the use of *C. elegans* as a model for parasitic helminths would also open new doors to the development of anti-parasite drugs including protozoan parasites.

Chapter Two

2 Materials and Methods

2.1 Maintenance of *C. elegans* Strain

Wild-type (N2 strain) *C. elegans* from the *Caenorhabditis* Genetics Centre, University of Minnesota, USA was originally collected from J. Hodgkin of Oxford University in 1993. The superoxide dismutase III Green Fluorescent Protein (*sod-3::GFP*) – CF1553 strain was originally collected from Kenyon, C. of the University of California, San Francisco, USA in 2004. The worms were maintained at 20°C on nematode growth medium (NGM) seeded with *Escherichia coli* OP50 in 60mm diameter Petri dishes (VWR, UK) or in 100mm diameter Petri dishes (Thermo Fischer Scientific, UK). *E. coli* OP50 was purchased from the Leibniz Institute DMSZ- German collection of microorganisms and cell cultures. The nematode strain was maintained by chunking (Stiernagle 2006) where a portion of agar from a previous plate was cut out using a sterilized scalpel into an NGM plate already seeded with *E. coli* OP50 (see page 179 for synchronization protocol). Regular transfer of nematodes to fresh plates prevents overcrowding and subsequent stress or formation of the resistant dauer forms.

Freezing was also used to store *C. elegans* by transferring starved L1 or L2 larvae into vials of soft agar freezing solution and storing in a -80°C freezer (Stiernagle, 2006).

2.2 Stage specific synchronization

Mixed culture or age-synchronized populations were prepared for the experiments. The age-synchronized worms were for the analysis of stage-specific assessment of endpoints investigated and included L1, L3, L4/ young adults (L4YA) and gravid adult (GRA) worms. An adaptation of the synchronization protocol as described by Sulston & Hodgkin (1988) was used for the current research (See appendix). All the exposures were performed in S

medium (see appendix); which is a liquid medium for worm maintenance, with or without treatments for 4 or 24 hours at 20 °C in the presence of *E. coli* OP50 as food source.

2.3 Toxicity assessment of zinc oxide nanoparticles

2.3.1 Preparation of zinc oxide nanoparticle treatments

Zinc oxide nanoparticle (ZnONP) in proprietary dispersants (colloidal dispersion with anionic or cationic dispersants) were produced by Alfa Aesar (ZnO NanoShield™ ZN-3014A or ZN-3008C respectively). The manufacturer's preparation contained 50% ZnONP in water. ZnONP (ZnO NanoShield™) and bulk zinc oxide (-325 mesh powder = 44µm) in powdered form were also obtained from Alfa Aesar. The average particle size of the ZnONP was 70nm (data provided by the manufacturer). Reagent-grade ZnCl₂ for Zn ion (Zn²⁺) was purchased from Sigma Aldrich.

We prepared two dispersants; 0.1% foetal bovine serum (FBS) and *E. coli* OP50 supernatant as our in-house dispersants for ZnONP dispersion. The working stocks of powdered ZnONP and bulk ZnO were prepared by adding an equal volume of S basal to a mixture of one part of 1M ZnONP or bulk ZnO (prepared in molecular grade water) and four Parts 10% FBS, *E. coli* OP50 supernatant or molecular grade water. The resulting 100mM ZnONP was used as the working stock for ZnONP. For the preparation of the working stocks of ZnONP in proprietary dispersants, molecular grade water was used for the preparation of 1M ZnONP from the readily available suspension ZnONP containing 6.14175M ZnO (see appendix for details). This was followed by adding one part of the 1M ZnONP to nine parts of S basal to give a working stock of 100mM ZnONP.

Summarily, the five stocks of ZnONP in dispersant were prepared and these include; ZnONP dispersed in FBS (FZNP), ZnONP dispersed in *E. coli* OP50 supernatant (SZNP), ZnONP dispersed in molecular grade water, ZnONP dispersed in propriety anionic dispersant (AZNP) AND ZnONP dispersed in

propriety cationic dispersant. The stock suspensions of all ZnONP and bulk ZnO were sonicated (Grant Ultrasonic Bath XB6; Grant Instruments, Cambridge, UK) for 30 minutes to enhance dispersion and homogeneity of suspensions. The zinc ion (Zn^{2+}) stock solution (100mM) was prepared by dissolving ZnCl_2 in molecular grade water. All treatment applications were in staggered time points (Kaszuba, 2015).

2.3.2 Zinc oxide nanoparticle characterization

2.3.2.1 Scanning Electron Microscopy (SEM)

The SEM was used for capturing images of the ZnONP to identify their shape, arrangement and the measurement of size. The working stocks described above (Section 1.3.1) were diluted in filtered molecular grade water ($0.2\mu\text{m}$) to a concentration of 1.25mM and centrifuged (1500rpm) onto round glass coverslips using a Shandon Cytospin 3 (Thermo Scientific). The 1.25mM sample concentrations are required for easy viewing on the SEM as higher concentration (3.125 to 25mM) will make microscopic viewing difficult due to saturation of particles. The ZnONP on the coverslips were allowed to air-dry and mounted onto stubs using silver paint to hold the coverslips firmly. The stubs were placed in a sputter coater (Emitech K550X, Quorum Technologies, Kent) and sputter-coated with gold at a coating current of 15mA for 2 minutes. This is important to help form an even coat on the surface of the prepared ZnONP suspension in order to inhibit charging and reduce thermal damage to the sample. It also helps improve the secondary electron emission of the ZnONP suspension for easy viewing on the SEM. Images were captured using a Hitachi S4800 Ultra High Resolution Field Emission Scanning Electron Microscope at an accelerating voltage of 10000 volts and a calibration scan speed of 25.

2.3.2.2 Dynamic Light Scattering (DLS)

DLS was used to establish the effect of dispersants on ZnONP size and the distribution of the size following dispersion. The technique measures the diameter of a hypothetical spherical and rigid particle, which diffuses at the same speed as the ZnONP. This measurement represents an equivalent of the irregular shaped

NP and is known as the hydrodynamic diameter. A Malvern Zetasizer Nano ZS was used to measure the hydrodynamic diameter presented as Z average at 25 °C. ZnONP in dispersants from working concentrations described above (Section 1.3.1) were used to prepare 12.5mM ZnONP samples, which were sonicated for 30 minutes and analysed by taking three measurements per sample at 3 minute intervals.

2.3.3 Dose response for ZnONP toxicity

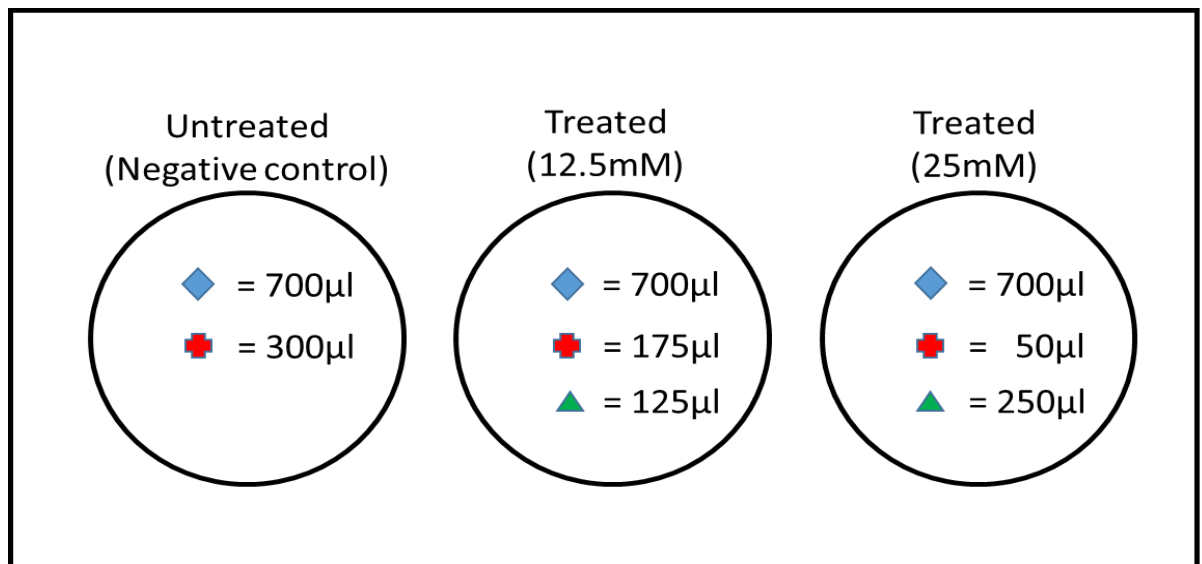
Due to variations of ZnONP concentrations in available literature, pilot experiments were conducted in order to choose the appropriate range for ZnONP concentrations. The concentrations considered included those relevant to ecotoxicology (Ma *et al.*, 2013) as well as cosmetics and industrial exposure scenarios as documented in the Scientific Committee on Consumer Safety opinion (SCCS, 2012) of the European Commission. Based on results from the pilot experiments on wild type *C. elegans* strain, the concentrations chosen for the study ranged from 3.125mM to 25mM. Although, these concentrations were seemingly high ($LC_{50} \geq 25mM$) they were within the remits of possible exposure scenarios such as accidental spillage in the environment. More so, the research focus is to evaluate methodologies to ensure the model organism is well suited for toxicity assays, so high concentrations would be useful in understanding toxic effects.

A detailed description of the preparation of the treatment concentrations is in the appendix. Liquid media was chosen over solid media for the toxicity experiments because ZnONP and bulk particles do not disperse evenly on solid media, restricting worm exposure to the toxicants.

2.3.4 Zinc oxide nanoparticles lethality test

For the lethality test, synchronized L4 worms were exposed to treatments for 4 or 24 hours in 24-well tissue culture plates. Each test consisted of 12.5mM or 25mM ZnONP in dispersant (FZNP, SZNP, WZNP, AZNP or CZNP), a negative control which is the untreated group and a Zn^{2+} ion control (12.5mM or 25mM $ZnCl_2$ [ZN]). A 700 μ l volume of synchronized L4 worms in liquid culture (S medium) and in the presence of food (*E. coli* OP50) was added into each of the

wells in the 24-well plate. For the untreated worms, 300 μ l of S medium was added to the well to make up a final volume of 1ml. For the treated samples, 175 μ l or 50 μ l of S medium was added to each of the wells to make up a volume of 875 μ l or 750 μ l respectively. A 125 μ l or 250 μ l of 100mM ZnCl₂, ZnONP in dispersant or bulk ZnO in molecular grade water (BZ) was added to the treatment wells to make a concentration of 12.5mM or 25mM respectively, in a final volume of 1ml in the wells. All treatment and controls were run in three replicate wells and repeated three or four times with changes to the positions of treatment in the 24-well plate for each repeat experiment. Figure 2.1 below shows a schematic representation of the treatment plan. The 24-well plate was incubated for 4 or 24 hours at 20°C and all treatments were in staggered time. Following exposure, counts were read from samples in each well that were diluted with M9 buffer and aliquoted into clear empty Petri dishes to allow for visible counting under a stereomicroscope (Leica Microsystems, Germany) with a 6.3:1 zoom and 6.3X-40X magnification. Worms that did not respond to gentle probing under the microscope were scored as dead. Percentage survival was calculated as number of living worms per count divided by total number of worms per count (dead and alive) and multiplied by 100.



- ◆ = *C. elegans* in S medium containing *E. coli* OP50
- ⊕ = S medium
- ▲ = 100mM ZnCl₂, 100mM ZnONP in dispersant or 100mM bulk ZnO

Figure 2.1: Schematic representation of treatment plan for ZnONP assay

2.3.5 Morphological analysis of ZnONP-treated worms

In order to investigate the effect of ZnONP on worm size, synchronized L4 worms were exposed to treatments for 24 hours in 24-well tissue culture plates at 20°C. Each test consisted of 12.5mM ZnONP in dispersant, a negative control and a Zn²⁺ ion control which were prepared as described in section 1.3.1. Following exposure, worms were anaesthetized with 25mM levamisole to prevent movement and digital images of the worms were taken using a compound microscope equipped with a camera (Olympus DP25) and analysed with ImageJ (Fiji) software (Schindelin *et al.*, 2012). The body length of the worms was measured from the tip of the worms' mouth through the centre of the body to the tip of the tail. The width measurement was calculated from a perpendicular cross through the middle of the vulva. The morphology assay was repeated twice for each treatment and the mean measurement (n=15) per treatment was calculated.

2.3.6 Reproductive analysis of ZnONP-treated worms

The current research utilized an embryogenic assay instead of the conventional brood size assay as the reproductive toxicity endpoint. This was because our pilot experiments indicated that there was a broad variation in fecundity results. Based on a previous experiment (not shown) the bag of worms (BOW) phenotype, which is the internal hatching of eggs in the worms, was observed to occur under unfavourable conditions such as overpopulation and exposure to high concentration of ZnCl₂ (25mM). We decided to utilize this as a marker for toxicity. Synchronized L1 larvae from first feed following hatching in liquid medium were incubated for 72 hours (20°C). After 72-hour incubation, the adult worms were treated with the test solutions in the presence of food (*E. coli* OP50) and in S medium for 24 hours. The treatment plan was as described above and the test solutions consisted of either 12.5mM FZNP, SZNP, WZNP, AZNP or CZNP. The controls also included untreated negative control and the Zn²⁺ control (12.5mM ZN). Following exposure, gravid worms were anaesthetized with 25mM levamisole, which importantly also induced the release of eggs allowing clear visibility of embryonic development. Worms were then analysed for the BOW phenotype using a compound microscope equipped with a camera (Olympus DP25) to take videos in form of sequence frame shots. Gravid worms containing completely hatched worms within them were scored as BOW phenotypes while

those with 3-fold embryo development within the eggs were termed accelerated embryonic development (AED) phenotypes.

2.3.7 SOD expression of ZnONP-treated worms

Superoxide dismutase (SOD) is a natural antioxidant produced in biological systems in order to detoxify free radicals or reactive molecules from oxygen by converting them to peroxides and water molecules. There are five types of SOD in *C. elegans* and one of this is the mitochondrial-based iron-manganese SOD known as SOD-3. To study the effect of ZnONP on SOD-3 transgenic *C. elegans* strain CF1553 (*sod3::GFP*) was used. Synchronized CF1553 eggs were transferred into S medium in the presence of *E. coli* OP50 as food source and L1, L3, L4 and adult hermaphrodite worms that developed from the eggs were treated with the test samples described in section 1.3.1 for 4 or 24 hours at 20°C.

Living *sod-3::GFP* worms from treatments were briefly centrifuged (30 seconds) and mounted on microscope slides with 3% agarose pads, anaesthetised with 25mM levamisole and capped with cover slips. Fluorescence images were collected from a Laser Scanning Confocal Microscope (Carl Zeiss microscopy, USA) suited with an enhanced GFP channel set (excitation, 385 nm; emission, 495 nm) using a x10 objective and / or an epifluorescence microscope (Carl Zeiss microscopy, USA) using x5, x10 or x20 objectives. Both microscopes were equipped with ZEN-lite freeware (Zeiss). Subsequent to observation of uniform intensity patterns among worms in the same field of view (x5 magnification), the expression of the *sod-3::GFP* reporter was examined on a worm by worm basis for each treatment.

2.3.8 RNA extraction from ZnONP-treated worms

While the methods described in sections 1.3.4 to 1.3.7 above were used for investigating physiological and phenotypic responses following chemical exposure, molecular responses at genomic level were also important in reinforcing the establishment of the effect of the chemicals on *C. elegans*. High-quality RNA from treated *C. elegans* RNA is required to generate sensitive and relevant results from molecular analysis. A modification of the RNeasy mini kit (Qiagen) technique was used for the RNA extraction as described below.

Having cultured *C. elegans* on NGM plates containing *E. coli* OP50, nine 5-day old plates were washed into 900ml S. medium in a 5L flask. This was incubated (20°C) for 120hrs in an incubator shaker (Innova 44 series, New Brunswick Scientific) at 160rpm. A 296.25ml volume of the mixed population culture was aliquoted into three 2L flasks with 3.75ml of 1M ZnONP in cationic dispersant (CZNP) added to one of flasks making a final 300ml worm culture treated with 12.5mM CZNP. A 3.75ml volume of S medium was added to each of the remaining two 2L flasks to make up a final volume of 300ml culture. One of the two flasks was incubated for 2 hours at 37°C for the heat shock control while the other was incubated at 20°C along with the CZNP-treated worms for 24 hours as the untreated control and treated sample respectively. Following incubation and exposure the contents in the flasks were transferred into 50ml falcon tubes and centrifuged at 4000rpm (1520g) for 3 minutes using a benchtop centrifuge (Universal 320, Hettich Zentrifugen) and left for 2 minutes at room temperature to allow most bacteria to settle at the bottom of the tube while the worms remained mixed with the supernatant. The centrifugation and aspiration was repeated twice with the final centrifugation at 12000rpm (11750g) for 6 minutes in a Mikro 200 centrifuge (Hettich Zentrifugen) allowing the worms settle at the bottom of the tube. The supernatant was carefully aspirated leaving no more than 2ml residue which was transferred into an already weighed 2ml Eppendorf tube to help in calculating the wet weight of worms in the tube. The tube was centrifuged at 12000rpm (11750g) for 1 minute and the supernatant was aspirated leaving in the tube about 0.2-0.3ml pellet. The worms were washed twice by filling the Eppendorf tube with M9 buffer, vortexing for 5 seconds and centrifuging at 13500rpm (17136g) for 1 minute in a perfect spin 24R refrigerator centrifuge (Peglab) before aspirating the supernatant leaving a final wet weight of no more than 300mg. Lysis buffer [Buffer RLT (600µl) or qiazol (1.1ml)] was added to the Eppendorf tube and vortexed for 15-20 seconds to ensure proper mix. The tube was placed in a tissue-lyser and homogenized for 6 minutes at 50 oscillations per second (50Hz). Following homogenization, the lysate was centrifuged for 3 min at 13500rpm (17136g); the supernatant was removed and transferred to a new Eppendorf tube. An equal volume of 70% ethanol was added to the cleared lysate and mixed immediately by pipetting. 700µl of the sample was transferred into an RNeasy spin column placed in a 2 ml collection tube and centrifuged for 20

seconds at 13500rpm (17136g). The flow-through was discarded and the collection tube was reused by adding 700µl Buffer RW1 to the RNeasy spin column and centrifuging for 20 seconds at 13500rpm (17136g) to wash the spin column membrane. The flow-through was discarded and buffer RPE was added to the RNeasy spin column, centrifuged for 20 seconds at 13500rpm (17136g) to wash the spin column membrane before 500µl Buffer RPE was added to the RNeasy spin column again and centrifuged for 2 minutes at 13500rpm to wash the spin column membrane. The RNeasy spin column was placed in a new 2 ml collection tube, centrifuged at full speed for 1 minute and placed in a new 1.5 ml collection tube adding 30µl RNase-free water directly to the spin column membrane. The column was centrifuged for 1 min at 13500rpm (17136g) to elute the RNA and the sample was stored at -80°C for nucleic acid measurement.

2.3.9 *sod-3* gene expression and protein analysis of ZnONP-treated worms

2.3.9.1 Real time PCR

The integrity and concentration of RNA (extraction described above) was evaluated using a Nanodrop 2000 spectrometer (Thermo Scientific) and an Agilent 2100 bioanalyzer (Agilent technologies). Total RNA was reverse transcribed using the Precision nanoScript™ 2 Reverse Transcription kit (Primerdesign).

2.3.9.1.1 cDNA synthesis

Using the protocol provided by the manufacturer, each of the RNA samples was diluted in RNase free water to make 5µl of 1µg RNA in a 0.2ml PCR tube. RT primer (1µl) and RNase free water (4µl) were added sequentially to the PCR tube to make a final volume of 10µl. A lid was applied to the sample which was heated to 65°C for 5 minutes followed by immediate cooling on ice. To complete the reverse transcription (+RT) reaction, 5µl nanoScript 2 4X buffer, 1µl dNTP mix, 3µl RNase free water and 1µl nanoScript enzyme were mixed together to give a final volume of 10µl. Also, a 10µl negative control (-RT) was prepared by mixing 5µl nanoScript 2 4X buffer, 1µl dNTP mix, 4µl RNase free water without nanoScript. The 10µl of +RT or -RT was added to the 10µl sample on ice and the tube was mixed briefly by vortexing for 10 seconds followed by pulse spinning.

Using a thermal cycler (Peqlab), the samples were incubated at 25°C for 5 minutes, followed by a change in temperature to 42°C for 20 minutes and subsequent heat inactivation at 75 °C for 10 minutes. The resulting cDNA was then stored at -20 °C for qPCR experiments.

2.3.9.1.2 Selection of *C. elegans* reference genes

In order to quantify gene expression, a relative analytic method in which the amount of the gene transcript is calculated in relation to a pre-defined gene is required. This requirement is necessary to correct the differences between gene expressions in different samples. The pre-defined gene is known as the reference gene (RG) and its expression is usually unaffected by factors that influence the expression of genes of interest. In order to select the reference genes for the *sod-3* gene expression experiment, six *C. elegans* RG (Actin, EIF3C, MDH1, CANX, TUBULIN and UBC3) were chosen based on previous use in literature (Zhang *et al.*, 2012). From the six RG, three were selected based on their stability. As described in the protocol, RG primer mix with SYBR green (Primerdesign) were suspended in RNase free water (220µl), briefly centrifuged, vortexed, left for 5 minutes and centrifuged again. In each well of a 96-well plates (ABI optical plates), a primer master mix was prepared by adding 1µl of the RG primer mix to 10µl PrecisionPLUS™ master mix (Primerdesign) and making up 15µl with 4µl RNase free water. cDNA from section 1.3.9.1.1 above was diluted (10µl cDNA in 90µl RNase free water) and 5µl of the diluted cDNA was added into wells of the 96-well plate. For each RG considered, 26 wells were needed which included duplicates of four untreated control samples, four heat shock-treated samples, four CZNP-treated samples and a RNase free water control. The plate plan is as described in table A1 in the appendix. The plate was placed in StepOne Plus™ Real-Time PCR System (Applied Biosystems) and the enzymes in the wells were activated for 10 minutes at 95°C and, then denaturation and, amplification using 40 cycles of 10 seconds at 95 °C and 60 seconds at 60°C, respectively. The amplification was quantified using a melting curve analysis post run.

2.3.9.1.3 *sod-3* qPCR analysis

Based on the result of the three most stable RG tested in section 1.3.9.1.2 above (see Figure A1 of the appendix for average expression stability graph), actin, CANX and MDH1 were chosen as reference genes for the *sod-3* gene expression normalization. The designed primers used for *sod-3* qPCR (Chun *et al.*, 2015)

were 5'-TATTAAGCGCGACTTCGGTCCCT-3' for the forward primer and 5'-CGTGCTCCCAAACGTCAATTCCAA-3' for the reverse (Eurofins genomics). The primers were reconstituted to 100pmol/μl and 6μl of the forward and 6μl of the reverse primers were diluted in 88μl of RNase free water give a concentration of 300nM in 20μl reaction (This concentration is the same for the reference genes). Similar to the description in section 1.3.9.1.2 above, in each well of a 96-well plate (ABI optical plates), a primer master mix was prepared by adding 1μl of the RG primer mix or *sod-3* primer mix to 10μl PrecisionPLUS™ master mix (Primerdesign) and making up to 15μl with 4μl RNase free water. cDNA from section 1.3.9.1.1 above was diluted in 10-fold (10μl cDNA in 90μl RNase free water) and 5μl of untreated, CZNP-treated or heat shock-treated cDNA was added into wells of the 96-well plate. For each gene considered, 12 wells were needed which included a negative control (-RT) and triplicates (+RT) of untreated control samples, heat shock-treated samples and CZNP-treated samples; for each of the four genes (*sod-3* and the three RG) considered. The experiment was carried out on four sets of samples (n=4). The plate plan is as described in table A2 in the appendix. The plate was placed in StepOne Plus™ Real-Time PCR System (Applied Biosystems) and the enzymes in the wells were activated for 10 minutes at 95°C and, then denaturation and, amplification using 40 cycles of 10 seconds at 95°C and 60 seconds at 60°C, respectively. This was followed by quantification using a melting curve analysis post run.

For the normalization of data (ΔCt) the mean Ct in each condition for *sod-3* gene was subtracted from that of actin, CANX and MDH1. Subsequently, the derived ΔCt for *sod-3* under CZNP or heat shock exposure conditions was subtracted from that in untreated controls to get the $\Delta\Delta Ct$ and the fold changes were calculated as $2^{-\Delta\Delta Ct}$. An increase in gene expression by at least 1.5-fold was considered upregulation while a decrease by at least 0.5-fold was considered significantly down-regulated.

2.3.9.1.4 Immunoblot analysis of SOD-3 protein expression

Mixed populations of worms from 100μl liquid culture that had been treated with either CZNP at 20°C for 24 hours or heat shock at 37°C for 2 hours, or an untreated population were homogenized in 2ml Eppendorf tubes with a bead using 400μl lysis buffer (1ml of 20% SDS, 800ul of 1M, 500ul β-mercaptoethanol,

1.5ml glycerol and 6.2ml deionized water) in a tissue lyser (Qiagen) at 50Hz for 2 minutes. The tubes were heated at 97°C for 2 minutes and samples were allowed to cool on ice. Following centrifugation of the samples for 2 minutes at 15000rpm, the total protein concentration in the supernatant was quantified using Bradford reagent (Biorad) and equal amounts (20µg in 20µl) were loaded on the gel. Before loading the samples, the gel cassette was filled with running buffer (30g Tris Base, 144g Glycine, 10g SDS diluted in a 1L final volume of deionized water) and 5µl ladder was added to one well while 20µl of untreated, heat shock-treated or CZNP-treated samples was added into each of the subsequent wells. The sample buffer was pipetted unto an empty well and the gel was run at 120V for 60 minutes. The gel was transferred to a nitrocellulose membrane using a transfer buffer (30g Tris Base and 144g Glycine in a 1L final volume of deionized water) at 270V for 60 minutes. The nitrocellulose membrane was blocked using a 2% milk blocking solution; 2g milk powder in 100ml of 0.1% PBS tween (5 PBS tablets (Sigma-Aldrich) dissolved in 9.99L deionized water added to 10ml of 10% Tween) for 60 minutes on a shaker at room temperature. After pouring off the blocking solution, the membrane was incubated with 1:1000 primary MnSOD antibody (S8060-10B-USBiological) raised in rabbit against rat as previously used by (Doonan *et al.*, 2008) and 1:1000 human actin antibody raised in goat (C-11: sc-1615-Santa Cruz) in 10ml fresh blocking solution overnight on a shaker at 4°C. The membrane was then washed three times in PBS tween for 20 minutes for each wash. This was followed by incubation with 1:20000 anti-rabbit produced in goat (Green- Licor 926-32211) and anti-goat produced in donkey (Red-Licor 926-68024) secondary antibodies for SOD and Actin respectively at room temperature for 2 hours using a foil to cover the dish to prevent photo bleaching due to light. The membrane was washed twice with PBS tween and once with PBS before scanning with the Licor Odyssey machine and quantifying immunofluorescence with Licor image studio lyte imaging system (Li-cor Bioscience).

2.3.10 Microarray analysis of MicroRNA expression

MicroRNAs (MiRNAs) are non-coding small RNAs processed from primary RNA transcripts. MiRNAs are important in the regulation of genes. In the current research, miRNAs were used as biomarkers to investigate the effect of ZnONP

exposure on *C. elegans* by using miRNA microarray to help elucidate expression patterns that could be ascribed to chemical toxicity. RNA samples from section 1.3.8 above were sent to Dr. Emma Marczylo of Public Health England, Oxford, United Kingdom for microarray analysis of miRNA expression. This was part of a collaboration with Public Health England. The experiments were performed by Dr. Emma Marczylo and the heatmap visualization of miRNA expressions of hybridization intensities with a cut off fold change of two and four were recorded.

2.4 Toxicity assessment of Diethylstilbestrol

2.4.1 Diethylstilbestrol lethality test

In order to investigate the lethal effect of Diethylstilbestrol (DES) on *C. elegans*, 1M DES (D4628-Sigma Aldrich, Germany), was prepared by diluting 268.35mg of DES in 1ml DMSO. A working stock of 100mM DES was prepared from the 1M solution using a 10-fold dilution. 10-fold serial dilutions were made from the working stock (100mM) and a 10mM treatment concentration was prepared by adding 100µl of 100mM DES to 900µl S. medium containing synchronized L4 worms. Other resulting dilutions from the 100mM stock were used to prepare the lower treatment concentrations in that order. Each concentration of DES was vortexed immediately before use. Controls included 0.1%, 1%, DMSO prepared with M9 as diluent. The different concentrations of DES were similar to real life exposure doses. Following exposure, counts were read from samples in each well under a stereomicroscope (Leica Microsystems, Germany) with a 6.3:1 zoom and 6.3X-40X magnification. As described by Chalfie & Sulston (1981) and Sulston *et al.* (1975), worms that did not respond to gentle probing under the microscope were scored as dead. Percentage survival was calculated as number of living worms per count divided by total number of worms per count (dead and alive), and multiplied by 100.

2.4.2 Behavioural analysis of DES-treated worms

The behavioural assessment of worms exposed to DES was investigated using a computer tracking. In this experiment, synchronized L4 worms were exposed to DES concentrations ranging from 1nM to 10mM in a final volume of 1ml treatment in a 24-well plate setting. The controls included untreated synchronized L4 worms in S medium and L4 worms in 0.1%, 1% and 10% DMSO. The worms were monitored using a computer tracking system composed of a Leica M125 dissecting microscope (Germany) equipped with a 5 Megapixel Olympus DP5 camera (United Kingdom) interfaced with a Windows computer. Following exposure, 500µl of each treatment containing worms was transferred onto empty petri dishes. Behavioural tracking was monitored on liquid medium and not solid medium because worms that burrow into the agar prevent clear frame capture. Also, desiccation resulting from dry solid agar surface might influence movement of the worms if tracking was monitored on agar. Digital captures tracking worm movement were acquired for 15 seconds at approximately five frames per second using Cellsens Life Science imaging software. The speed (length covered in pixels per second) and thrashing frequency (body bend per second) of the worms were recorded using ImageJ (Fiji) software and the wrMTrck plugin as described by Nussbaum-Krammer *et al.* (2015). The thrashing frequency was converted to body bends per minute to normalize the data. The wrMTrck permits the concurrent tracking of the worms by recording their rate of movement. A description of the steps for the manipulation of wrMTrck parameters can be found in the supplementary document provided by Dr. Jesper Pederson (See Pederson in the references).

2.5 Toxicity assessment of derivatized tubulin-targeting anthelmintics

2.5.1 Anthelmintic derivative treatments

The anthelmintic derivatives; GEO1, GEO2, MB2, MB2-TPP, NU:UB 238 and SH1 used in this study were supplied by Dr David Mincher of Edinburgh Napier University, Edinburgh, United Kingdom. Aiman Rehan of Edinburgh Napier University graciously supplied AM1 and AM2. GEO1, AM1 and MB2 are colchicine derivatives while GEO2, AM2 and MB2-TPP are their respective triphenylphosphonium (TPP) conjugates. NU:UB 238 is an anthraquinone derivative and SH1 is its TPP conjugate. The structures and molecular details of the anthelmintic derivatives can be found in the appendix (Section B).

2.5.2 Derivatized anthelmintics lethality test

Concentrations of colchicine (Sigma Aldrich), TPP (Sigma Aldrich), GEO1, GEO2, AM1, AM2, MB2, MB2-TPP, NU:UB 238 and SH1, ranging from 0 to 400µM were considered for the toxicity assessment. Untreated L4 worms in S medium was used as negative control. Other controls included the DMSO (0.1%, 1% and 10% DMSO) which was the solvent used in the preparation of treatment suspensions. All samples containing the worms and their food (*E. coli* OP50) were exposed to the treatments in a total of 1ml in a 24-well plate setting. Exposure times were either 4 or 24 hours at 20°C incubation temperature with all treatments run in staggered time. Experiments were repeated at least once. Following exposure, counts were read from samples in each well and percentage survival was calculated as described in section 1.4.1 above.

2.5.3 Behavioural analysis of derivatized anthelmintic-treated worms

Whilst the major aim of studying the toxicity of derivatized anthelmintics in *C. elegans* is to investigate their helminthocidal properties, the effect of the derivatives on worm behaviour was necessary to give a broader descriptive toxicity assessment. In order to investigate the effect of derivatized anthelmintics on *C. elegans* behaviour, synchronized L4 worms were exposed to treatments as

described in section 1.5.2 above. The worms were monitored using the same computer tracking system described in section 1.4.2 above. Behavioural video tracking was accomplished by capturing images for 20 seconds at approximately 6 frames per second using Cellsens Life Science imaging software. The wrMTrck plugin on ImageJ (Fiji) was used to compute the speed and thrashing frequency of the worms as described in section 1.4.2 above.

2.6 Assessment of legumain-specific targeting in helminths

2.6.1 Fluorophore-based probes

For the investigation of the potential for legumain-specific anthelmintic targeting, Ding Y., Turnbull A. and Mathur S. from the Department of Chemistry and Drug Design, Edinburgh Napier University synthesized and graciously provided the probes TL11, LS9 and SM9 respectively. TL11 is a fluorescein-labelled probe while LS9 and SM9 are rhodamine-based. The structure and details of the probes can be found in section C of the appendix.

2.6.2 Parasite Homogenates and Sheep Plasma

Homogenates of the sheep parasites, *Haemonchus contortus* and *Teladorsagia circumcincta* (both containing 1mg/ml protein) were provided by Dr Alasdair Nisbet of Moredun Research Institute, Edinburgh, United Kingdom while sheep plasma was provided by Dr Mick Rae of Edinburgh Napier University Edinburgh, United Kingdom.

2.6.3 Preparation of somatic fractions

A protocol for the preparation of somatic fractions in *C. elegans* was developed to identify whether legumain was water soluble (S1), membrane-associated (S2) or membrane-bound (S3). The protocol was originally designed by McAllister *et al.* (2011) for the preparation of trematode somatic fractions and was modified in

our laboratory for *C. elegans*. For the preparation of the somatic fractions, equal volumes of *C. elegans* pellet (wet weight) and homogenizing buffer (HB; PBS, 2mM EDTA 1mM phenylmethylsulphonyl fluoride (PMSF) pH7.4) were mixed and the worms were homogenized using a tissue-lyser for 4 minutes at 50 oscillates per second followed by centrifugation at 20,000g for 20 minutes at 0°C. The supernatant was removed but retained as S1 fraction. The pellet was resuspended in HB with 0.1% Tween-20 and homogenized with the tissue-lyser for 30 seconds at 50 oscillates per second. This was followed by centrifugation at 16,500g for 20 minutes at 2°C before aspirating the supernatant (S2) for retention. The Tween-20 extraction was repeated before aspirating the supernatant which was discarded this time. The pellet from the repeated extraction was resuspended in 0.5ml 2% w/v reduced Triton X-100 in PBS pH7.4 and homogenized with the tissue-lyser for 30 seconds at 50 oscillates per second. The homogenate was stirred for 30 minutes using a shaker at 4°C (160rpm). This was followed by centrifugation at 50,500g for 30 minutes at 2°C before aspiration and retention of the supernatant (S3).

2.6.4 Removal of detergent from somatic fractions

Whilst Tween 20 and Triton X-100 were used to solubilize, stabilize and disaggregate the protein content to produce S2 and S3 somatic fractions respectively (see section 1.6.3 above), the detergents in the somatic fractions seem to interfere with legumain activity as observed in a pilot legumain activity assay. Therefore, it was important to remove non-bound detergents from the somatic fractions. The Pierce detergent removal resin column (87778-Thermo Scientific) was used for the detergent removal. As described in the manufacturer's protocol, after the loosening the resin column cap and removing its bottom closure, the resin column was placed into a 15ml collection tube and centrifuged at 1000g for 2 minutes to remove the storage solution in the column. In order to wash the resin column free of the storage solution, 2ml phosphate citrate buffer (pH5) was added to the column which was subsequently centrifuged at 1000g for 2 minutes. The buffer and storage solution in the collection tube was discarded and the 2ml phosphate citrate buffer wash, centrifugation and discarding of the content in the collection tube was repeated twice. The resin column was placed in a new 15ml collection tube and 400µl the somatic fraction

(S2 or S3) was carefully pipetted onto the compact resin bed in the column. The column was incubated for 2 minutes at 25°C. This was followed by centrifugation at 1000g for 2 minutes to collect the detergent-free somatic fraction for legumain assay.

2.6.5 BCA Protein Assay

To estimate the total protein concentration in homogenates, Bovine Serum Albumin (BSA) standards were prepared from 2mgml⁻¹ stock solution. BCA working reagent was prepared by combining 20µl copper (II) sulphate pentahydrate 4% solution with 1ml bicinchoninic acid. 10µl of homogenate or Bovine Serum Albumin (BSA) standard was added into a 96 well micro plate followed by 80µl of the BCA working reagent and the mixture was mixed carefully for 30 seconds before incubating at 37°C for 30 minutes. The plate was allowed to cool for 5 minutes and the absorption was measured at 600nm using an LT5000 ELISA plate reader. After taking the average of replicate values, a standard curve was generated by plotting mean standard values against their respective concentrations. The standard curve was used to interpolate the concentration of each nematode parasite homogenate sample based on its mean absorbance value.

2.6.6 Legumain activity

The legumain assay involved the determination of legumain in worms (*C. elegans*, *H. contortus* or *T. circumcincta*), sheep plasma and sheep liver tissue based on the selective cleavage of the fluorophore-based substrate attached to a quencher to release fluorescence. The probes use the Fluorescence Resonance Energy Transfer (FRET) application to measure fluorescence. For the experiment, homogenates of *C. elegans*, *H. contortus*, *T. circumcincta*, sheep liver tissue or sheep plasma samples were treated with 10µM of either TL11 or LS9 in a final volume of 100µl in a 96-well plate. Each treatment well of the 96-well plate contained the sample diluted in either MES buffer (pH5) or phosphate citrate buffer (pH4, 5, 6, or 7). The buffers were necessary to allow for activation of legumain as this is pH-dependent (see section D of appendix for buffer

preparation). A 3.5 μ l, 3.6 μ l or 3.7 μ l volume of protease inhibitors; N-phenylmaleimide (1mM), E-64 (100 μ M) or Iodoacetamide (1mM) respectively, were added to 95.4 μ l, 95.3 μ l or 95.2 μ l respectively, of sample in buffer. This was followed by the addition of 1.1 μ l of the provided working stock solution of TL11 (902.5 μ M) or LS9 (895.75 μ M) to make a final volume of 100 μ l treatment containing 10 μ M probe in each well. E-64 is a general cysteine protease inhibitor which has no inhibitory effect on legumain (Barrett *et al.*, 1982 and Chen *et al.*, 1997), while N-phenylmaleimide and Iodoacetamide inhibit legumain activity. The negative control included 98.9 μ l each of MES (pH5) or phosphate citrate buffer with 1.1 μ l of the LS9 or TL11 probe (10 μ M concentration of the probe) while the positive control included 98.9 μ l recombinant legumain in buffer (2.5ng/ μ l) with 1.1 μ l probe. Details of the preparation of treatment samples can be found in section D of the appendix. The 96 well plates were analysed in the fluorimeter (Fluorostar Omega – BMG Labtech) for 2 hours at excitation spectrum of 544nm and emission of 590nm for treatments containing LS9 or excitation spectrum of 485nm and emission of 520nm for treatments containing TL11.

2.6.7 Legumain localization

SM9 probe was employed to investigate whether the probe is permeable to the worms. This was important to establish the possible interaction of the rhodamine-based probe, and identify the legumain localized region(s) in the worm following the cleavage of tripeptide group from the probe. For the experiment, an adult population of worms was exposed to 1 μ M SM9 in a final volume of 100 μ l and incubated (20°C) in a shaker incubator for 18 or 24 hours. Controls included worms that were untreated with the SM9 probe and the SM9 probe alone. Worms from the treatments were washed with M9 buffer and centrifuged briefly (30 seconds). The worms were mounted on microscope slides with 3% agarose, anaesthetised with 25mM levamisole and capped with cover slips. Fluorescence images were captured using a Laser Scanning Confocal Microscope (Carl Zeiss microscopy, USA) suited with an enhanced multiple channel set using a x10 objective and / or an epifluorescence microscope (Carl Zeiss microscopy, USA) using x5, x10 or x20 objectives. Both microscopes were equipped with ZEN-lite

freeware (Zeiss). Imaging analysis was performed using the ImageJ (Fiji) software.

2.7 Data analysis

Significant differences among treatment groups or concentrations and their controls were compared for one or two exposure times. For lethality test experiments involving one time exposure, One-way ANOVA was calculated. Where two exposure times were compared within different groups of treatments, Two-way ANOVA was calculated for the experiments. Also, One-way ANOVA was used for statistical evaluation of experiments involving cumulative data. Where data from individual worms was used for toxicity assay data analysis, graphs were developed from contingency tables with 95% confidence intervals. Statistical significance from pairwise comparison was established as $p < 0.05$ for biological replicates. All statistical analysis was performed with Sigmaplot 12 (Systat Software, Inc., San Jose California USA).

Chapter Three

3 Toxicity assessment of zinc oxide nanoparticles

3.1 Introduction

The term nanotechnology describes the manipulation of materials by one atom or one molecule to dimensions as small as 100nm. Hence, the word nanomaterial describes materials between 1 and 100nm size ranges (Boholm and Arvidsson, 2016). The physical and chemical properties of nanomaterials encourage their application in engineering (Ahn *et al.*, 2014), textile industries (Ilanchezhian *et al.*, 2015), food industries (Danza *et al.*, 2015), cosmetics industry (Fakhravar *et al.*, 2015) and medicine (Fan *et al.*, 2015). The global economy currently benefits from the lucrative application of nanotechnology and nanomaterials, and is predicted to be worth about £140.84 billion by 2025 (Global Nanotechnology Market Analysis & Trends, 2016).

One of the common nanomaterials used in various industries is zinc oxide nanoparticles (ZnONP). ZnONP are used in food additives, paints, cosmetics and personal hygiene products. More specifically, they are constituents of body moisturizers and sunscreens because of their translucence and ability to prevent exposure to ultraviolet A and B (UVA and UVB) radiation (Nohynek *et al.*, 2007). Again, ZnONP protection against UV light makes it a necessary ingredient in painting and coating materials used in building and construction (Steele *et al.*, 2009). ZnONP in the form of a dietary Zn supplement can improve the growth performance and red blood cell counts in fish. Their antibacterial properties also make them useful in mouthwashes, toothpastes and ointment production for the prevention of microbial growth (Jones *et al.*, 2008).

The small size, large surface area and increased surface reactivity due to high percentage of atoms on the particle surface and quantum effects, are characteristics that make ZnONP different from their bulk equivalents. Concerns have been raised regarding the implications of these characteristics on human health and the environment because of increasing manufacture, use and exposure to ZnONP (Nowack and Bucheli, 2007). Although ZnO is generally recognized as safe by agencies like the FDA in the United States, in its

nanoparticulate form, it can develop new toxic characteristics. Consequently, its toxicity evaluation is important.

There have been a number of *in vitro* studies on ZnONP toxicity assessment. In the lung epithelial cell culture assay, ZnONP induced intracellular Ca^{2+} (George *et al.*, 2010), mitochondrial damage caused by the generation of reactive oxygen species (ROS), and increase in the pro-inflammatory cytokine IL-8 (Saptarshi *et al.*, 2015). ZnONP have also been found to induce antioxidant activities as well as altering cell viability in adipocytes and mouse myoblast cell lines (Pandurangan *et al.*, 2014). Similarly, the investigation of the effect of ZnONP on mouse macrophages revealed that non-cytotoxic concentrations of the NP in consumer products elicited cellular pro-inflammatory responses and resulted in significant cell death following 24-hour exposure to the NP (Giovanni *et al.*, 2015). Prach *et al.* (2013) investigated the cytotoxic effect of ZnONP on the human monocyte cell line; THP1. Their results showed that ZnO cytotoxicity was dependent on size and charge of the NP. Zijno *et al.* (2015) investigated the induction of oxidative stress (OS) by ZnONP on human colon carcinoma cells. Their study revealed that ZnONP caused micronucleic and DNA damage. They further compared the genotoxic abilities of ZnONP to titanium oxide (TiO_2) NP and realized that while TiO_2 could repair oxidative DNA through the involvement of 8-oxoguanine glycosylase, Zn NP could not. Hence ZnONP are suggested to also affect repair pathways as Zijno *et al.* (2015) and (De Angelis *et al.*, 2012) suggest that their fast dissolution when compared to TiO_2 is a major factor which contributes to their toxicity.

Although a substantial amount of study on ZnONP has been done *in vitro*, *in vivo* assays are needed to understand their long-term effects in biological systems and to investigate their fate; if they indefinitely remain in the systems; dissolve and/ or get cleared from the system. Moreover, *in vivo* screening authenticates the initial *in vitro* assay in order to allow the latter to be used as a primary toxicity assessment method. Some researchers have studied ZnONP in organisms like bacteria (Read *et al.*, 2016), algae (Bhuvaneshwari *et al.*, 2015), crustaceans (Xiao *et al.*, 2015), Zebra fish (Wehmas *et al.*, 2015) and mice (Gosens *et al.*, 2015). Wehmas *et al.* (2015) showed that the toxicity of ZnONP in zebra fish was stage specific. This is likely, as physiological zinc levels play a crucial role in

growth and development, including the immune system through the regulation of various enzymes (Truong-Tran *et al.*, 2001). While some mammalian *in vivo* models may be preferred for toxicity assessments, they are relatively expensive in comparison to some invertebrate models and their assessments may also be time-consuming. For example, the assessment of one chemical for reproductive toxicity would involve the use of many animals and such processes require time. Hartung & Roviada (2009) estimated that 54 million vertebrate animals and testing costs of £6.8 billion would be required to implement the European Registration, Evaluation, Authorisation and Restriction of Chemicals (REACH). The REACH was initiated to minimize the use of animals in chemical testing through the implementation of the 3Rs (reduction, refinement or replacement of animal use). Such challenges as mentioned above have encouraged the development of more accessible and acceptable models for *in vivo* screening. One of such models is the nematode *Caenorhabditis elegans*. A detailed overview of *C. elegans* was included in chapter one of the current research.

The aim of the current research was to develop a *C. elegans* model system for ZnONP toxicity assessment and to gain more understanding of the physicochemical characteristics of ZnONP that influence toxicity. In order to accomplish the goals, wild-type and transgenic *C. elegans* strains were exposed to ZnONP nanoparticle prepared in five different types of dispersants; molecular grade water, 0.1% FBS, *E. coli* OP50 supernatant, anionic and cationic colloidal dispersants that allowed us to investigate the effect of dispersion on worm response. The potential toxic effects of ZnONP were investigated using lethality, morphology, reproduction, green fluorescent protein (GFP) reporter expression, gene and protein expression, and miRNA expression analysis to elucidate a new perspective to ZnONP toxicity assessment.

3.1. Results

In order to investigate viability of the worms following exposure to zinc oxide nanoparticles (ZnONP), physicochemical properties of the ZnONP and endpoints that are measures of toxicity were investigated. We characterized ZnONP in different dispersants using direct light scattering (DLS) and scanning electron microscopy (SEM) to determine effect of the dispersants on the ZnONP size, distribution, shape and arrangement.

3.2.1. Zinc oxide nanoparticle characterization

3.1.1.1 Scanning Electron Microscopy analysis of ZnONP

The SEM was used for capturing images of the ZnONP to identify their shape, arrangement and the measurement of size. ZnONP dispersed in molecular grade water (WZNP), 0.1% FBS (FZNP), *E. coli* OP50 supernatant (SZNP), anionic dispersant (AZNP) or cationic dispersant (CZNP) all had irregular shapes and the particles were majorly clustered (Figure 3.1, panels A-E), however; WZNP, FZNP and SZNP seemed to have more clusters while AZNP and CZNP appeared to have more uniform side by side alignment of the particles (Figure 3.1, panels F-J). Furthermore, although the details from the commercially produced ZnONP datasheet state that the ZnONP used is approximately 70nm, the size range of the ZnONP in all the dispersants were between 27nm and 451nm.

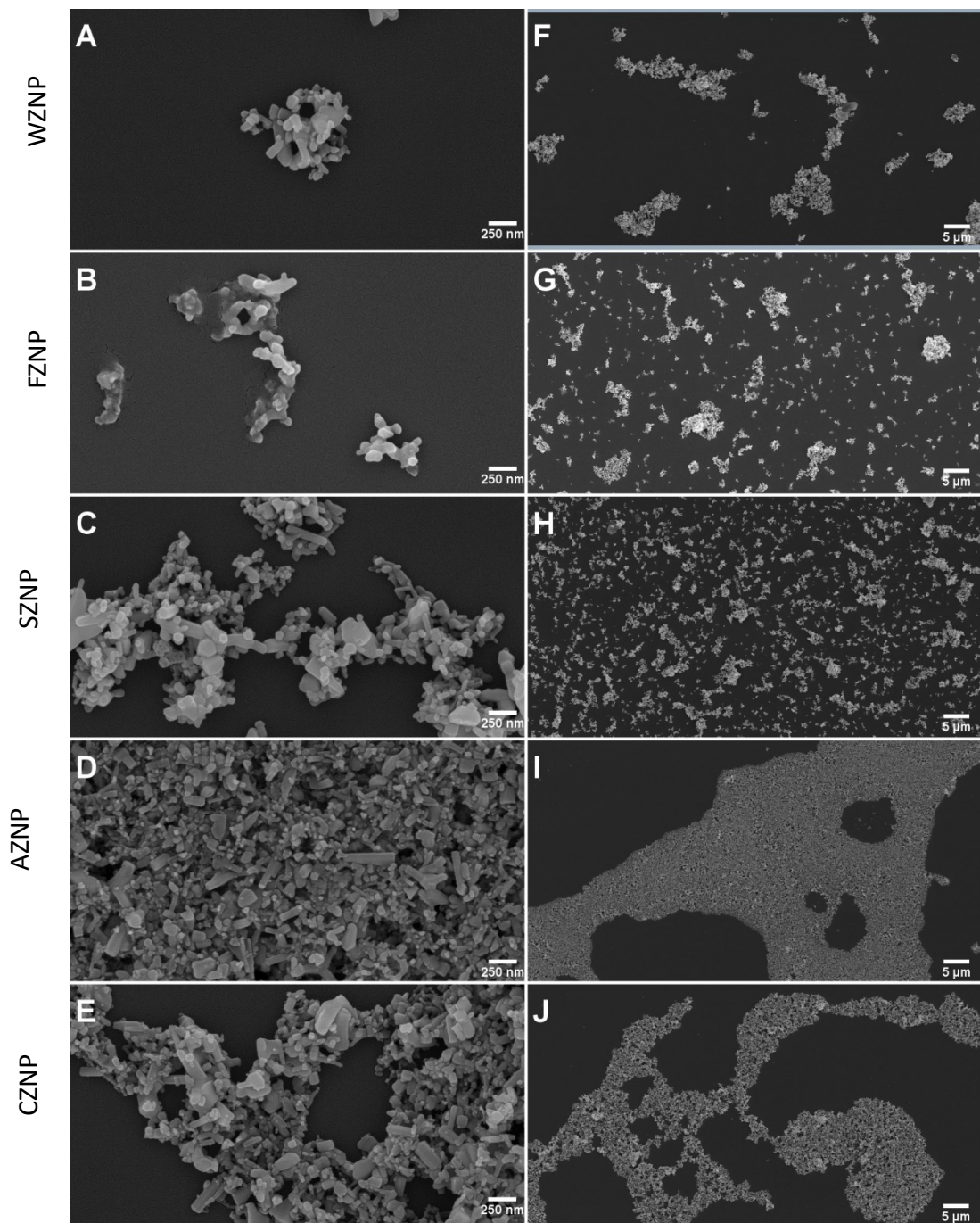


Figure 3.1: Scanning electron micrograph of ZnONP in different dispersants.

All samples for characterization were prepared at a concentration of 1.25mM in molecular grade water represented by WZNP (A & F), 0.1% FBS represented by FZNP (B & G), *E. coli* OP50 supernatant represented by SZNP (C & H), anionic dispersant represented by AZNP(D & I) or cationic dispersant represented by CZNP (E & J). The samples were mounted on aluminium pin mounts and coated with gold for electrical conductivity in a plasma chamber for 2 minutes to prevent particle distortion.

3.1.1.2 Dynamic light scattering analysis of ZnONP

DLS was used to establish the effect of dispersants on ZnONP size and the distribution of the size following dispersion. The technique measures the diameter of a hypothetical spherical and rigid particle which diffuses at the same speed as the ZnONP. This measurement represents an equivalent of the irregular shaped NP and it is known as the hydrodynamic diameter. Assessment of the ZnONP in dispersants with the DLS produced the Z-average diameter which is the intensity weighted mean size or cumulant mean of the collective total ZnONP hydrodynamic diameter in each dispersant. In Figure 3.2, ZnONP prepared in molecular grade water WZNP had the highest Z-average diameter ($1256 \pm 134.1\text{nm}$) while ZnONP prepared in cationic dispersant CZNP had the lowest ($197.6 \pm 1.504\text{nm}$). Figure 3.2 also detail point blots of the triplicate readings from the bar graph. The order of size of the triplicate Z-average values was required to establish aggregation or sedimentation in the ZnONP preparations. The difference among the Z-average measurements is expected to be within 2% of one another. The first Z-average reading was taken (red) 3 minutes before the second reading (green) and the third reading (blue) was taken 3 minutes after the second reading for each of the dispersed ZnONP samples. There was a decreasing Z-average diameter ($\geq 6\%$) in WZNP suggesting ZnONP sedimentation while SZNP, FZNP and AZNP had increasing Z-average values, however; these were within acceptable threshold. The differences in Z-average values obtained from the repeats of CZNP were within less than 1% of one another suggesting that CZNP was the most stable of all ZnONP investigated.

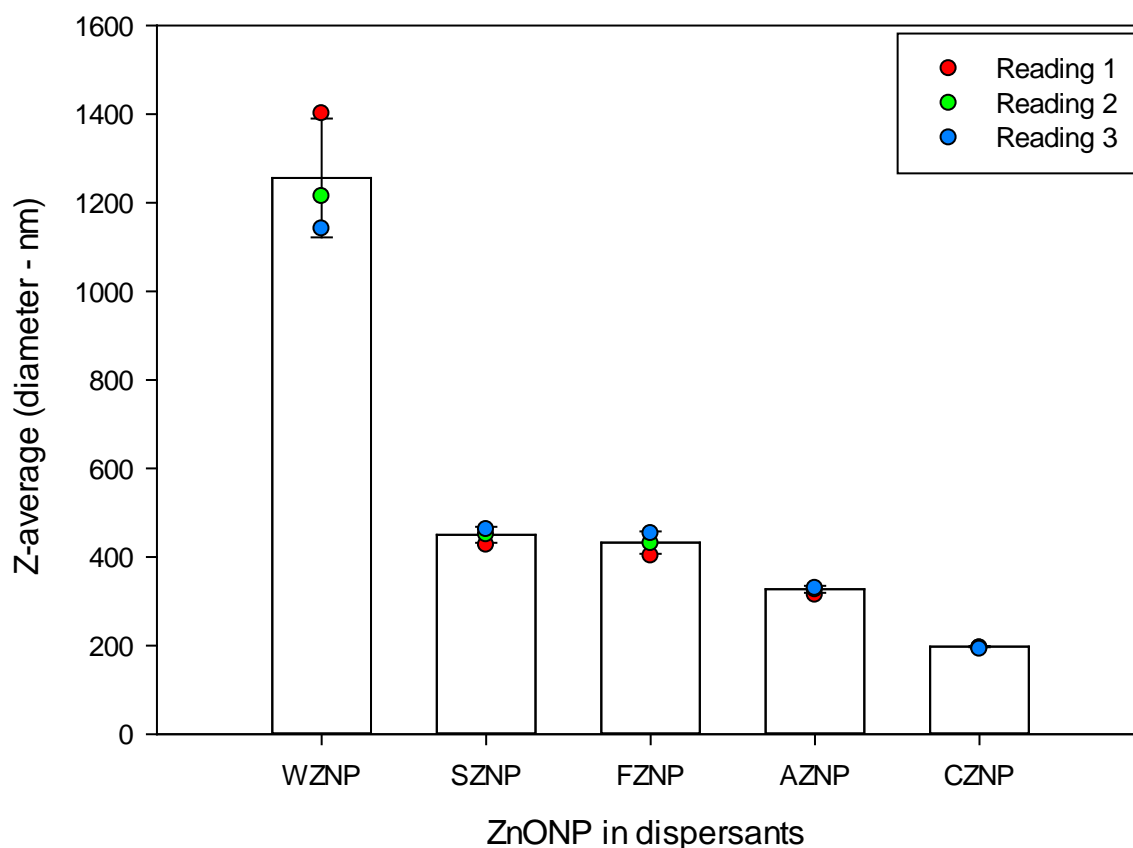


Figure 3.2: Z-average diameter of ZnONP in dispersants.

12.5mM ZnONP was prepared in molecular grade water (WZNP), *E. coli* OP50 supernatant (SZNP), 0.1% FBS (FZNP), anionic dispersant (AZNP) or cationic dispersant (CZNP). DLS was used to analyse the samples with three readings taken for each sample at 3 minute intervals. First reading is represented by the red dot, second reading is represented by the green dot and the third reading is represented by the blue dot. Temperature was maintained at 25°C while light scattering angle was 173°.

To reinforce the finding above, the ZnONP size distribution was also evaluated (Figure 3.3) and the result revealed that WZNP was excessively polydispersed with its size ranging between 450 to 6500nm. The occurrence of particles of around 712nm in diameter was the highest (38%) of the WZNP distribution. On the other hand, the highest peak of CZNP was around 220nm (14.7%) and the range of distribution was between 78nm and 620nm. Also, CZNP was the only sample that had all three readings imposed on one another with a monomodal peak for each reading (Figures 2 and 3) suggesting that it is the most stable of all ZnONP samples.

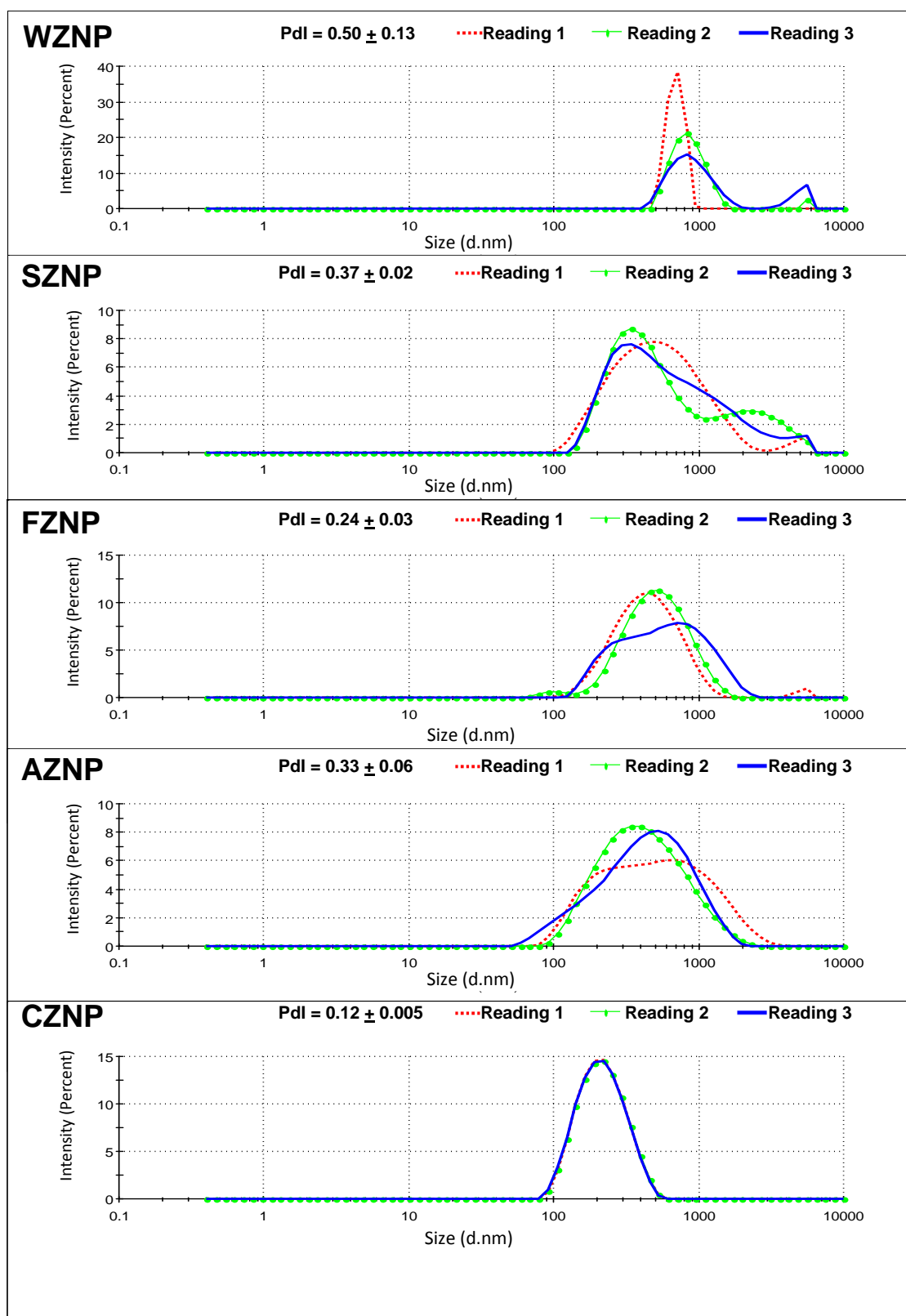


Figure 3.3: Particle size distribution of ZnONP in dispersants.

12.5mM ZnONP was prepared in molecular grade water (WZNP), *E. coli* OP50 supernatant (SZNP), 0.1% FBS (FZNP), anionic dispersant (AZNP) or cationic dispersant (CZNP). DLS was used to analyse the samples with three reading taken for each sample at 3 minute intervals. First reading is represented by the red dot, second reading is represented by the green dot and the third treading is represented by the blue dot. Temperature was maintained at 25°C while light scattering angle was 173°. Polydispersity index (Pdl) which is a measure of the width of the distribution was within acceptable threshold (0.05-0.7). Count rate per second was within acceptable threshold (117.8-460.1 kilo count per second)

3.2.2. Effect of ZnONP on the survival of *C. elegans*

L4 adults from synchronized cultures of wild-type worms were exposed to varying concentrations of ZnONP in two different dispersants (anionic and cationic) to investigate the lethal effect of the NP on the worms. The concentrations chosen for the pilot study ranged from 3.125mM to 25mM. Although, these concentrations were high, they were within the remits of possible exposure scenarios. More so, high concentrations were included to give informed understanding of suitable concentrations to be considered for subsequent experiments. A negative control (S medium) and a Zn²⁺ control (ZnCl₂) were included as part of the experiment. Following a 4-hour exposure time to ZnONP treatments, the results revealed that more than 95% of all treatment groups and control groups survived (data not shown). After 24-hour exposure, about 95% of worms exposed to all treatment groups below 12.5mM survived with no significant difference between the untreated group and other treatment groups. At 25mM, more than 60% of worms exposed to ZnCl₂ (ZN) for 24 hours died, while about 16% and 10% death was recorded among worms exposed to ZnONP dispersed in anionic dispersant (AZNP) and cationic dispersants (CZNP) respectively (Figure 3.4A). The viability observed at 12.5mM was similar for 25mM AZNP and CZNP-exposed worms but about 95% of the ZN-treated worms survived (Figure 3.4B). The results described above reveal that the lethal effect of ZnONP is dose-dependent.

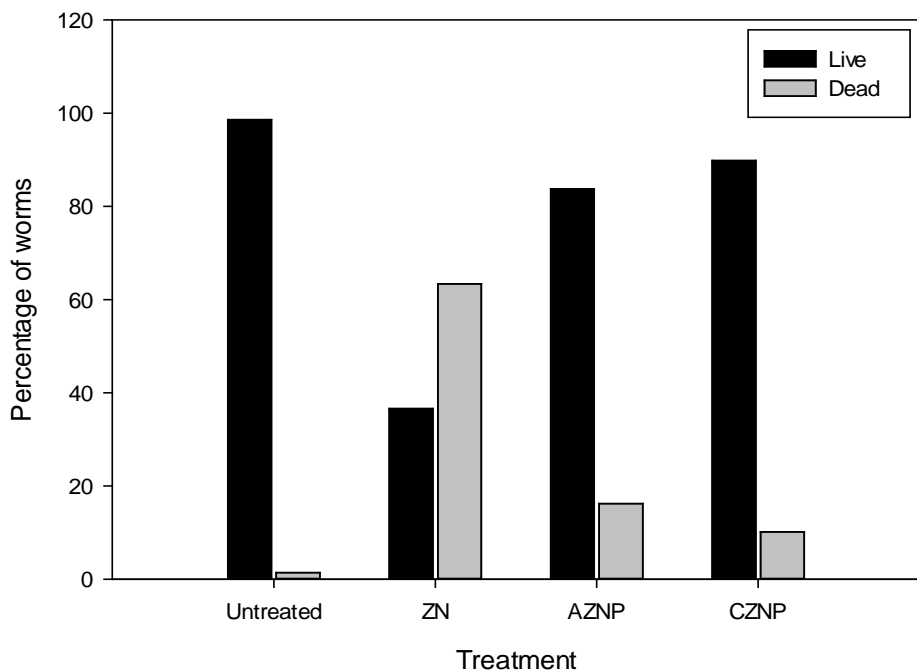
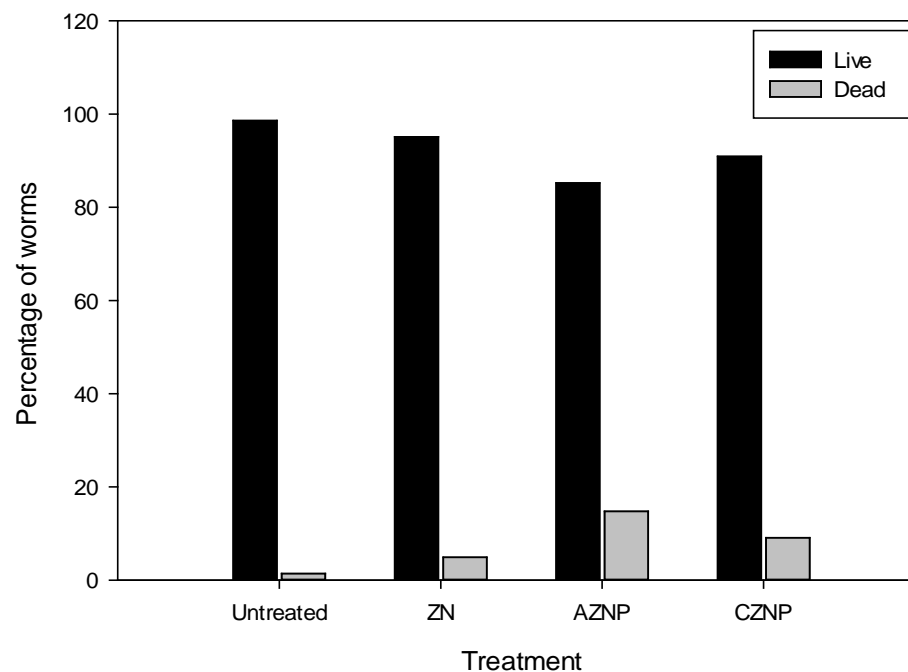
A**B**

Figure 3.4: Effect of ZnONP on wild-type *C. elegans* survival.

Percentage of live and dead synchronized L4 worms following exposure to (A) 25mM or (B) 12.5mM ZnCl₂ (ZN), ZnONP in anionic dispersant (AZNP) or cationic dispersant (CZNP) for 24 hours where the untreated group and ZN-treated group were the negative and positive controls respectively. Counts were read under a stereomicroscope (Leica Microsystems, Germany) with a 6.3:1 zoom and 6.3X-40X magnification. Worms that did not respond to gentle probing under the microscope were scored as dead. Percentage survival was calculated as number of living worms divided by the total number of worms (dead and alive) multiplied by 100. Chi-square analyses of the contingency table from the experiments were used for statistical analysis. For graph A, chi-square= 236.198 with 3 degrees of freedom (P = <0.001) where a total of 703 worms were analysed over three separate experiments with each treatment containing between 148 and 215 worms and power of chi-square test = 1. For graph B, chi-square= 30.237 with 3 degrees of freedom (P = <0.001) where a total of 850 worms were analysed over three separate experiments with each treatment containing between 205 and 220 worms and power of chi-square test = 0.999.

Following on from the pilot study, ZnONP in three other dispersants were investigated added to the previously considered treatment groups (SM, ZN, AZNP and CZNP). The three additional treatments included ZnONP prepared in molecular grade water (WZNP), 0.1% fetal bovine serum (FZNP) and *E. coli* OP50 supernatant (SZNP) to attempt investigating the effect of dispersants alone. The worms were exposed to 12.5mM concentrations of the ZnONP for 24 hours. The results in Figure 3.5 showed that there was no significant difference observed among all the treatment groups and the controls with less than 5% death recorded in all cases.

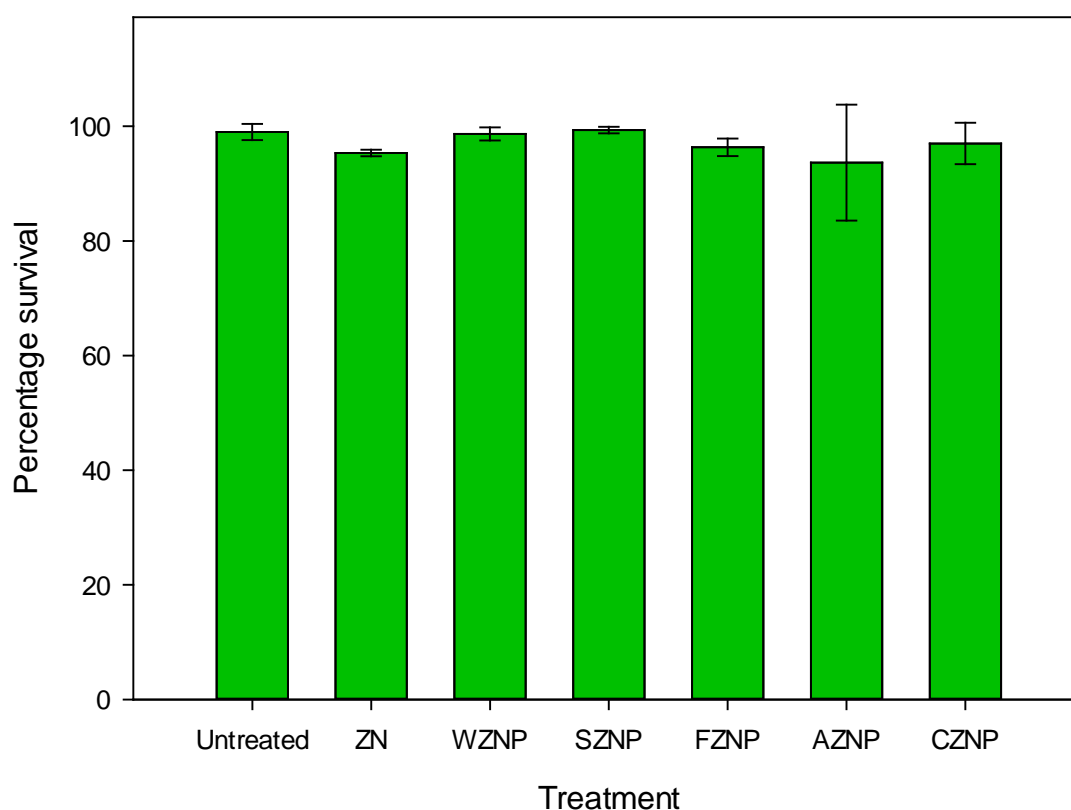


Figure 3.5: Effect of 12.5mM ZnONP exposure on survival of wild type *C. elegans*.

Percentage survival of synchronized L4 worms exposed to 12.5mM ZnCl₂ (ZN), ZnONP prepared in molecular grade water (WZNP), *E. coli* OP50 supernatant (SZNP), 0.1% fetal bovine serum (FZNP), anionic dispersants (AZNP) or cationic dispersant (CZNP) at 20°C for 24 hours where untreated group and ZN-treated group were the negative and positive controls respectively. The controls for dispersants used in the preparation of AZNP and CZNP were unavailable due to manufacturer's proprietary confidentiality. Survival counts were read under a stereomicroscope with a 6.3:1 zoom and 6.3X-40X magnification. Worms that did not respond to gentle probing under the microscope were scored as dead. Percentage survival was calculated as number of living worms divided by the total number of worms (dead and alive) multiplied by 100. ANOVA on ranks was used for statistical analysis with error bars representing \pm SD where $n \geq 155$ over three separate experiments.

3.2.3. Effect of ZnONP on worm morphology

The effect of ZnONP treatments prepared in different dispersants with a final concentration of 12.5mM, on individual worm morphology was investigated by measuring the body length and body width of worm post treatment (Figure 3.6). Following a 24-hour exposure to the ZnONP in different dispersants, the results revealed that the length of worms exposed to SM was significantly longer than ZN-treated worms ($p < 0.02$). AZNP-treated worms were significantly shorter than untreated worms ($p < 0.001$) suggesting that AZNP affect the length of the worms. SM and SZNP treatments had similar length averages suggesting that the length of untreated worms and SZNP-treated worms are not affected by the treatments. Also, there was a significant difference between the width of untreated worms and ZN-treated worms with the former having a broader width ($p < 0.001$). Furthermore, the width of the AZNP-treated worms and CZNP-treated worms were significantly narrower than the untreated control group ($p < 0.001$ and $p = 0.004$ respectively). Interestingly, the SZNP-treated group were significantly broader than FZNP ($p < 0.019$), WZNP ($p < 0.048$), AZNP ($p < 0.001$), CZNP ($p < 0.001$) and ZN ($p < 0.001$) -treated groups. The results indicate that worm morphology is not affected by SZNP treatment; hence, the type of dispersants may have an effect on worm morphology. Again, the possible effect on worm morphology observed in AZNP and CZNP-treated worms could implicate the dispersants used in the preparation of the treatments.

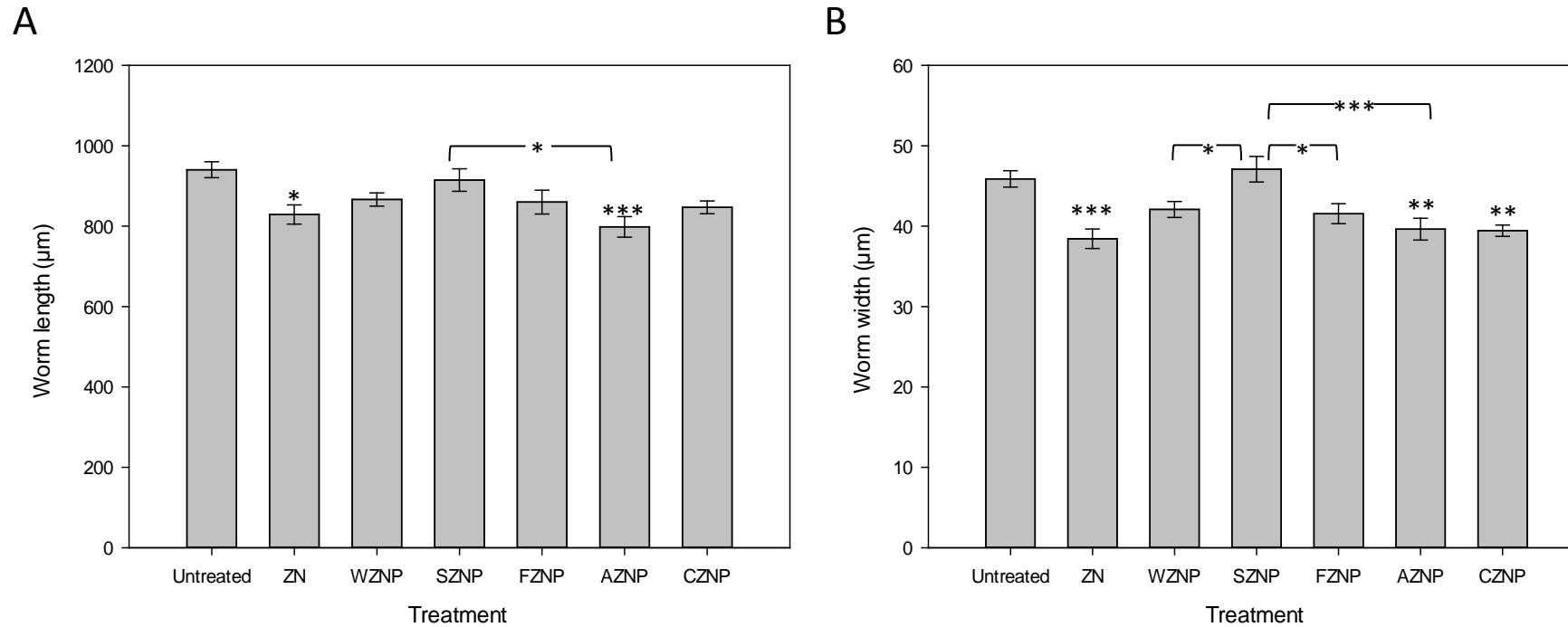


Figure 3.6: Effect of ZnONP on worm morphology.

(A) Worm length and **(B)** worm width of synchronized L4 worms exposed to 12.5mM ZnCl₂ (ZN), ZnONP prepared in molecular grade water (WZNP), *E. coli* OP50 supernatant (SZNP), 0.1% fetal bovine serum (FZNP), anionic dispersants (AZNP) or cationic dispersant (CZNP) at 20°C for 24 hours were measured using imageJ analysis of camera-captured images. The untreated group and ZN-treated group were the negative and positive controls respectively while controls for dispersants used in the preparation of AZNP and CZNP were unavailable due to manufacturer's proprietary confidentiality. The length measurement was taken from the tip of the worms' mouth through the centre of the body to the tip of the tail. The width measurement was calculated from a perpendicular cross through the middle of the vulva. One-way analysis of variance (ANOVA) was used for statistical analysis with error bars representing \pm SEM where n=15 for each treatment group analysed over 3 separate experiments. All pairwise multiple comparisons were investigated and the degree of significance was represented by * where $p \leq 0.05$, ** where $p \leq 0.01$ and *** where $p \leq 0.001$. Asterix directly above bars represent degree of significance of comparisons between the negative control (untreated) and other treatments, while asterix connecting two bars represent the significance between the two connected bars.

3.2.4. Effect of ZnONP on reproduction

3.1.1.3 Bag-of-worms (BOW) Phenotype

Endotokia matricida, also known as bagging or bag-of worm (BOW) phenotype is the internal hatching of eggs in the worms. Although the condition is believed to be a worm fitness advantage (Chen and Caswell-Chen, 2003), the phenotype is in response to a change in environmental conditions hence, its utility as a marker of toxicity was attempted. Worms exposed to 12.5mM ZnONP in different dispersants were investigated for BOW phenotype (Figure 3.7). Untreated and SZNP-treated worms had similar responses with 1% untreated worms exhibiting the BOW phenotype and no worm exposed to SZNP presenting the phenotype. At least, 20% of worms exposed to FZNP, AZNP and CZNP had BOW phenotype. This suggests that SZNP-treated worms are not affected to the same extent as other types of dispersants for ZnONP.

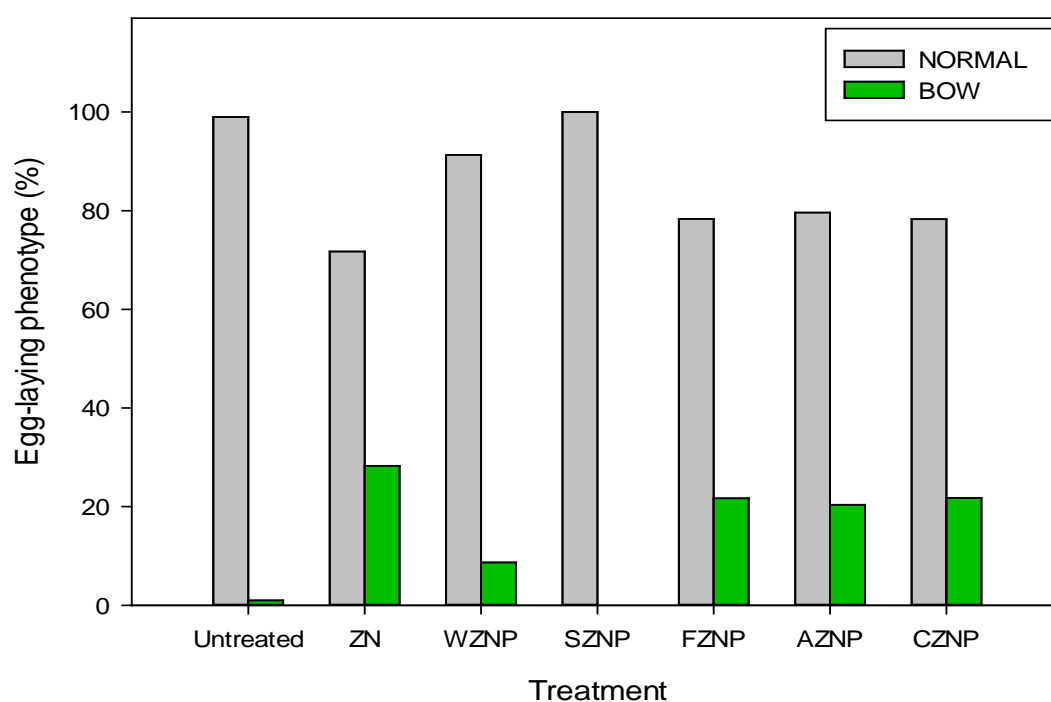


Figure 3.7: Egg-laying phenotype following exposure of wild-type adult *C. elegans* to ZnONP.

Adult worms (60 hours after first feed) from synchronized populations were exposed to 12.5mM ZnCl₂ (ZN), ZnONP prepared in molecular grade water (WZNP), *E. coli* OP50 supernatant (SZNP), 0.1% fetal bovine serum (FZNP), anionic dispersants (AZNP) or cationic dispersant (CZNP) at 20°C for 24 hours where untreated group and ZN-treated group were the negative and positive controls respectively. The controls for dispersants used in the preparation of AZNP and CZNP were unavailable due to manufacturer's proprietary confidentiality. Chi-square analyses of the contingency table from the experiments were used for statistical analysis. Chi-square= 47.532 with 6 degrees of freedom (P = <0.001) where n=474 over three separate experiments and power of chi-square test = 0.997.

3.1.1.4 Effect of ZnONP on embryogenesis

Under favourable conditions, worms lay their eggs with the embryo intact within the eggshell as expected immediately after the generation of embryonic founder cells. This is the second phase of proliferation process during embryogenesis. The effect of ZnONP on the proliferation process was investigated by exposing the adult hermaphrodite worms to 12.5mM ZnONP treatments prepared in different dispersants. Representative screenshots from videos highlighting the effect of ZnONP in different dispersants on worm reproduction revealed that the untreated worm lays its eggs in short bursts (<1 second) with the embryo intact within the eggshell (Figure 3.8, panel A) as expected immediately after the generation of embryonic founder cells. On the other hand, worms treated with FZNP presented three-fold embryo elongation showing fully differentiated tissues encapsulated within the eggshell and still in the hermaphrodite gravid adult (Figure 3.8, panel B). This phenotype was consistent in worms treated with WZNP (not shown) and SZNP (Figure 3.9). We have named the phenotype accelerated embryonic development (AED). Figure 3.8, panel C highlights a representative image of worms exposed to CZNP. The images reveal larvae within the hermaphrodite adult worm; the bag of worm (BOW) phenotype. The BOW phenotype was also present in worms treated with AZNP (data not shown but observed in n=4). In SZNP-treated worm (Figure 3.9), the short bursts of egg release during the process of proliferation occurs at the three-fold elongation stage of egg development and the worm bursts out of the eggshell as seen in the top panels. This was not always the case in the same worm as some three-fold elongation stage worms were still intact when released from the adult worm (lower panel); however, the bursting of the eggshell was observed in several AED phenotypes. This result implies that the type of ZnONP dispersion or dispersant may affect the process of embryogenesis in the worm.

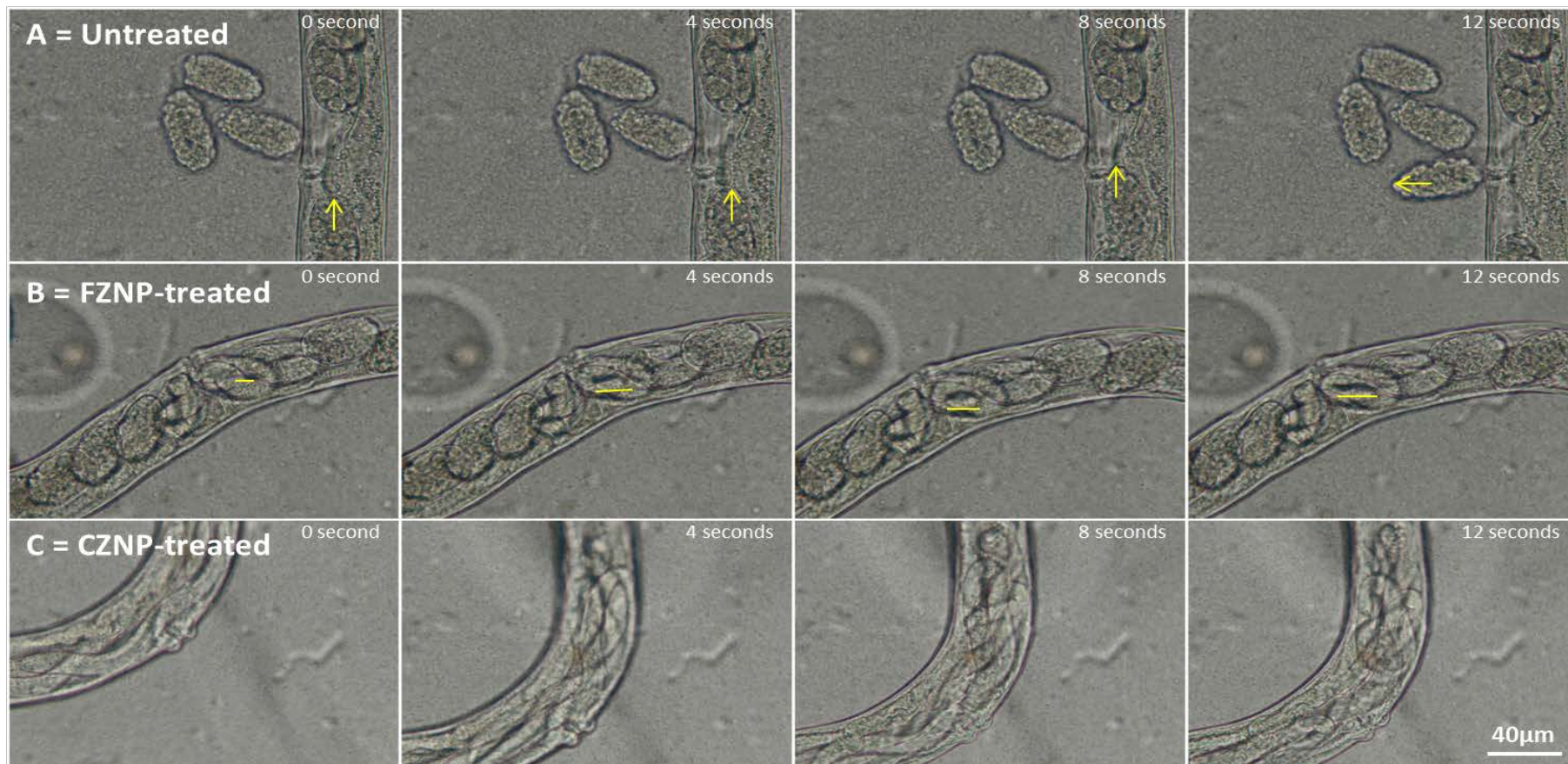


Figure 3.8: Representative images of ZnONP effect on worm embryogenesis.

Panel A: Untreated worm (control) laying eggs. Yellow arrows show the process movement of an egg during egg-laying. **Panel B:** A worm that has been treated with ZnONP dispersed in 0.1% FBS (FZNP). The yellow lines show the change in curling size due to movement of larvae within the egg enclosure (accelerated embryonic development). **Panel C:** A worm that has been treated with ZnONP dispersed in cationic dispersant (CZNP) showing the body filled with hatched worms (Bag of worms phenotype). Worms used in each experiment were from the same synchronized population. The worms were exposed to 12.5mM treatments for 24 hours before image capture using a compound microscope connected to an Olympus camera and cellsens image analysis application. Conditions are consistent in repeated experiments (n=4).

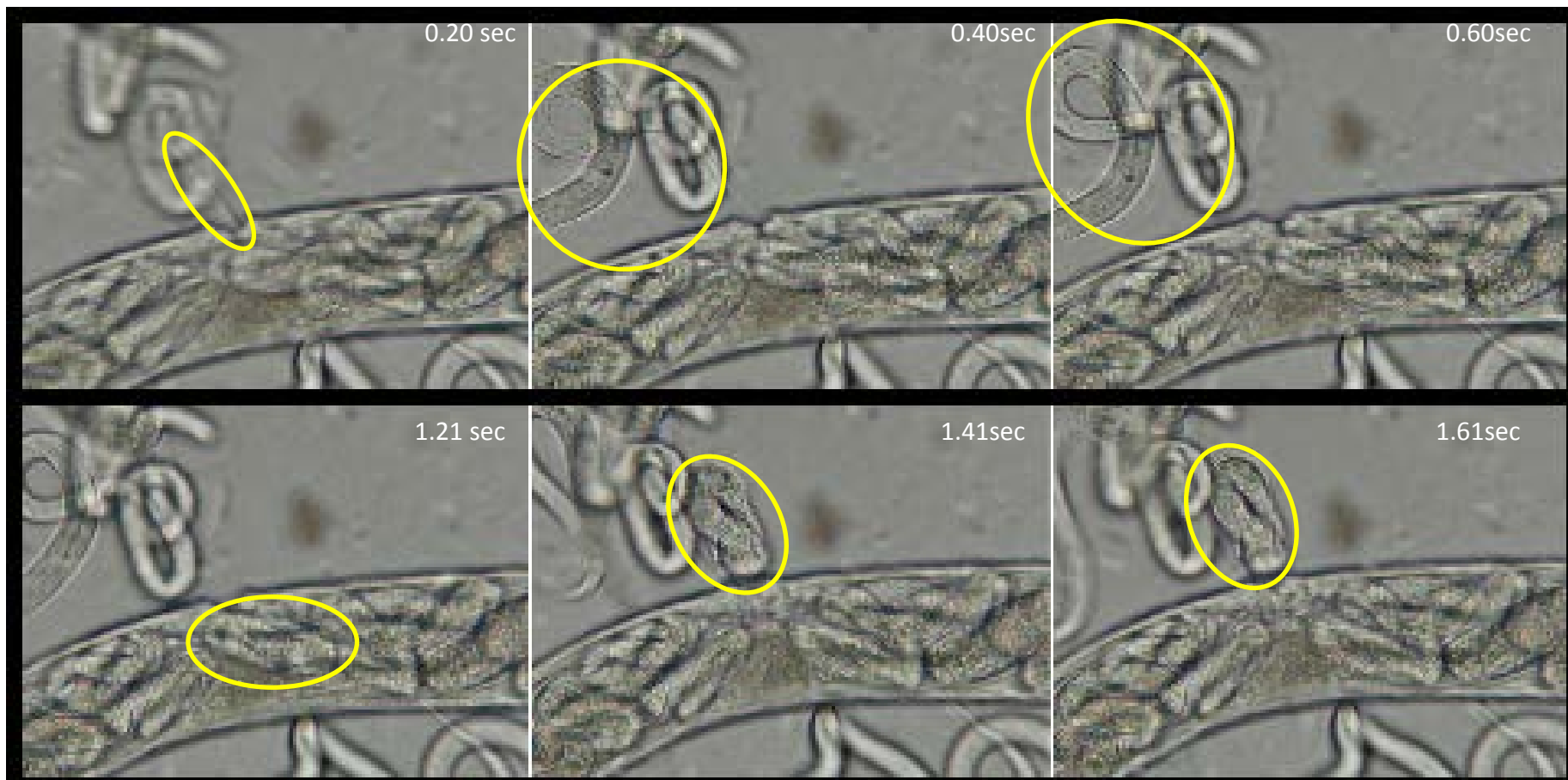


Figure 3.9: Representative images depicting egg laying in accelerated embryonic development (AED) phenotype.

Image is taken from worms exposed to 12.5mM ZnO NP dispersed in *E. coli* OP50 supernatant (SZNP). Yellow ovals in upper panels reveal simultaneous hatching as egg is laid. Lower panels reveal hatching of AED egg. Note that AED is not scored as bag of worm phenotype unless complete hatching occurs within the gravid adult worm. The worms were exposed to 12.5mM treatments for 24 hours before image capture using a compound microscope connected to an Olympus camera and cellsens image analysis application. Conditions are consistent in repeated experiments (n=4).

3.2.5. *sod-3::GFP* expression in ZnONP-treated *C. elegans*

A characteristic effect of toxicants is that they can induce oxidative stress in biological systems; therefore, analysing changes in stress-responsive genes can be useful for the assessment of toxic responses. This can be assessed in *C.elegans* by using the transgenic *sod-3::GFP* *C. elegans* strain. Superoxide dismutase 3 (*sod-3*) is a natural antioxidant that takes part in the conversion of reactive oxygen species products to hydrogen peroxide and subsequently water and is upregulated in response to oxidative stress. Transgenic *sod-3::GFP* *C. elegans* strain was employed to measure stress in worms exposed to ZnONP; however, in order to effectively utilize the *sod-3::GFP* strain, it was important to repeat lethality assays performed on wild type worms on the transgenic strain.

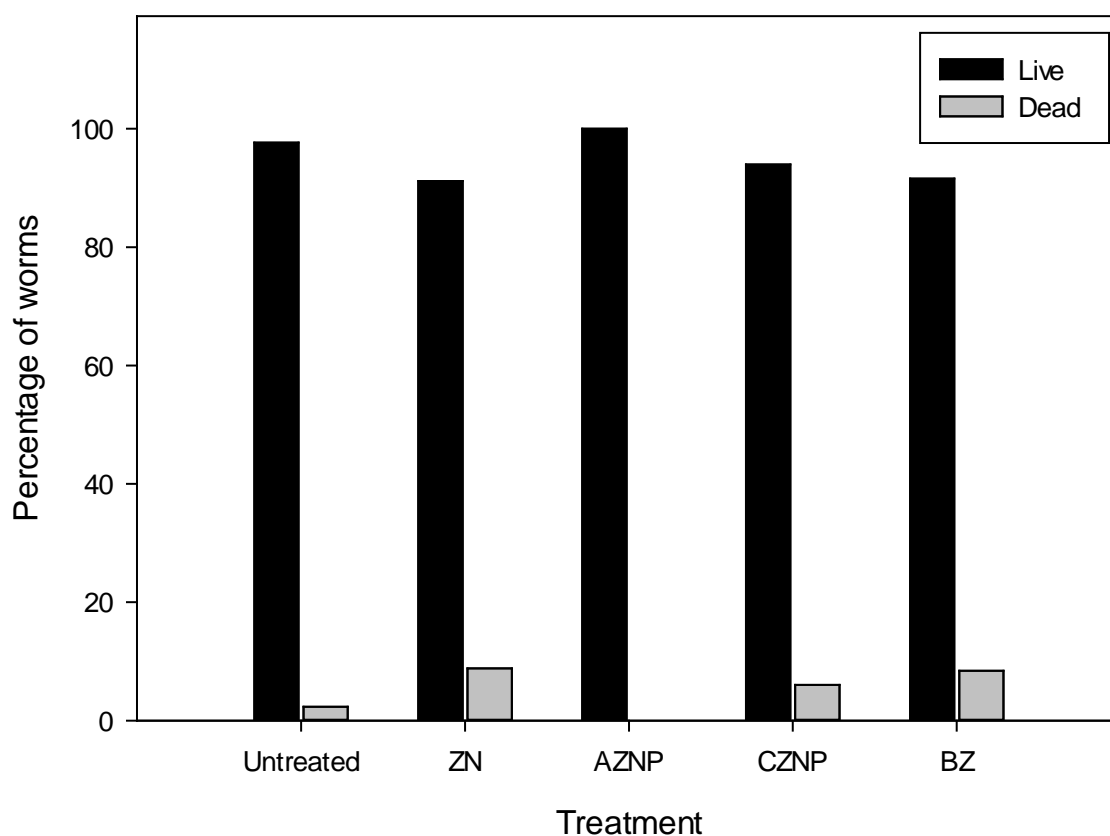


Figure 3.10: Effect of 12.5mM ZnO NP exposure on survival of transgenic *sod-3::GFP* *C. elegans* strain.

Percentage of live and dead synchronized L4 worms following exposure to 12.5mM ZnCl₂ (ZN) or 12.5mM ZnONP prepared in anionic dispersants (AZNP), cationic dispersant (CZNP) or 12.5mM bulk ZnO in molecular grade water (BZ) at 20°C for 24 hours where untreated group and ZN-treated group were the negative and positive controls respectively. The controls for dispersants used in the preparation of AZNP and CZNP were unavailable due to manufacturer's proprietary confidentiality. Chi-square analyses of the contingency table from the experiments were used for statistical analysis. Chi-square= 14.008 with 4 degrees of freedom (P = <0.007) where a total of 539 worms were analysed with each treatment containing between 68 and 128 worms over three separate experiments and the power of chi-square test = 0.873.

Results (Figure 3.10) revealed that *sod-3::GFP* strain exposed to 12.5mM ZnONP in dispersants showed a different result from that observed in their wild-type counterparts previously investigated (see Figure 3.4B). There was no death recorded for worms exposed to anionic dispersants (AZNP),

Subsequent to the lethality assay, transgenic *sod-3::GFP C. elegans* strain was employed to investigate oxidative stress in worms exposed to 3.125mM ZnONP prepared in anionic dispersants (AZNP), cationic dispersant (CZNP), and bulk ZnO (BZ). The lower concentration was chosen to investigate the effect of the prepared ZnONP samples at the sublethal level. In the L1 larval stage, worms exposed to CZNP appeared to have the highest fluorescence intensity (Figure 3.11). L3 larvae exposed to ZnONP had higher fluorescence intensity than BZ-treated L3 larvae. L4/young adults and gravid adult stages all had relatively high fluorescence intensities post exposure to ZnONP. Fluorescence intensities were characteristically found in the pharynx region of the head and at the tail post ZnONP treatment. CZNP induced the highest fluorescence intensities across each developmental stage.

We investigated the egg-laying phenotypes in transgenic *sod-3::GFP* worms exposed to 3.125mM ZnONP in different dispersants (Figure 3.12) and examined whether ZnONP influenced oxidative stress response in the worms during the proliferation stage of embryogenesis. While less than 3% of untreated worms had BOW phenotype, about 60% of the ZN-treated worms were BOW while over 80% of CZNP-treated worms became BOW (Figure 3.12). Also, about 30% of AZNP-treated worms resulted in BOW. These results were different from the observations in wild-type worms which were exposed to a higher concentration (Figure 3.7). The results suggest that ZnONP have a higher toxic effect on transgenic *sod-3::GFP* worms than their wild-type counterparts.

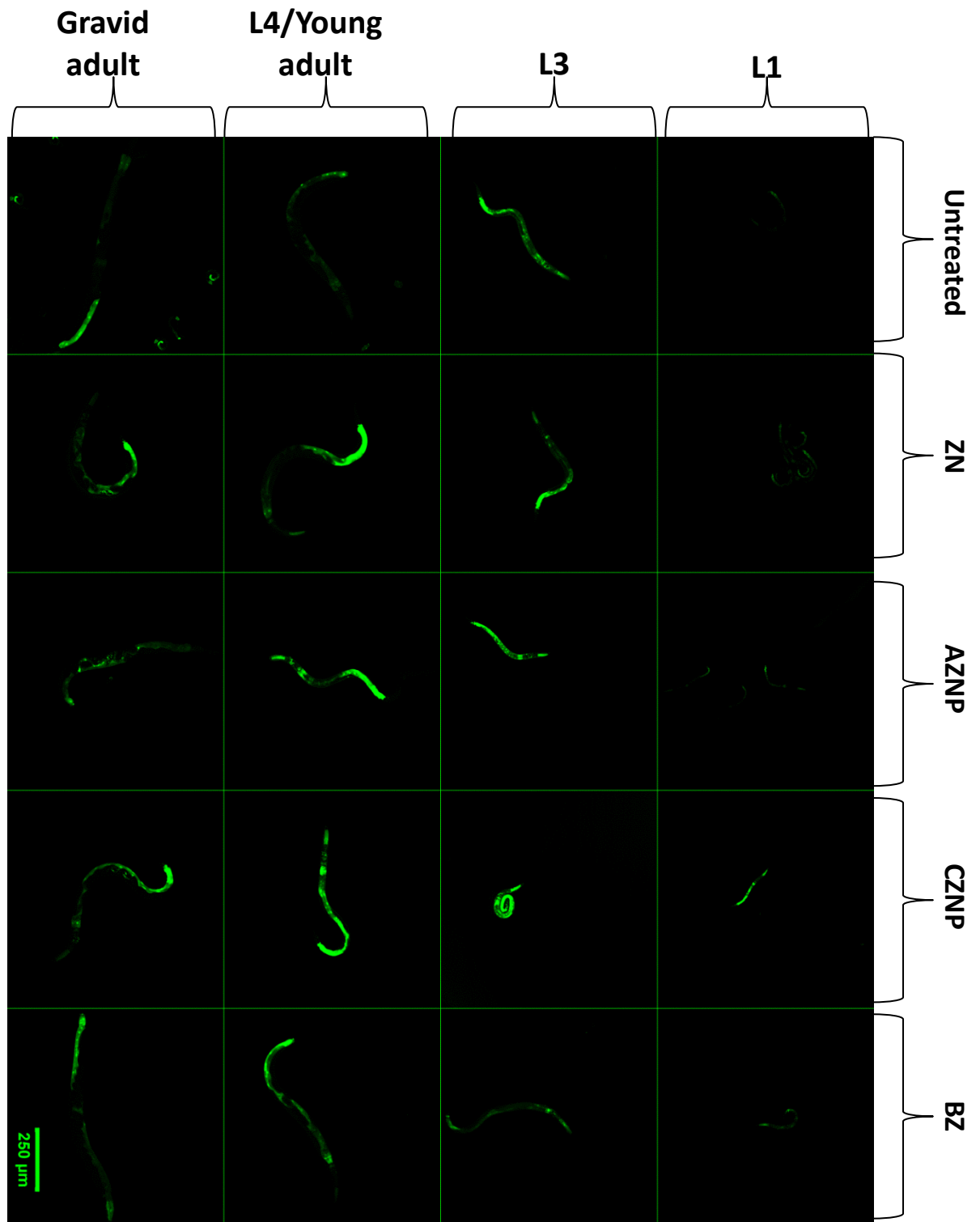


Figure 3.11: Comparison of *sod-3::GFP* expression in four developmental stages of worms.

Transgenic *sod-3::GFP* worms from synchronized populations were exposed 3.125mM $ZnCl_2$ (ZN), ZnONP dispersed in anionic dispersants (AZNP), or in cationic dispersant (CZNP) or bulk ZnO dispersed in molecular grade water (BZ) for 24 hours where the untreated group and ZN-treated group were the negative and positive controls respectively. The controls for dispersants used in the preparation of AZNP and CZNP were unavailable due to manufacturer's proprietary confidentiality. All images are representative images of each treatment group and were taken with a LSM 880 using Zeiss plan apochromat 10 x/0.45 Ph1 M27 microscope objectives. Detection wavelength was between 493-598nm. The enhanced green fluorescent protein (EGFP) channel with an excitation and emission wavelength of 488 and 546nm respectively was used. The parameters were the same for all images.

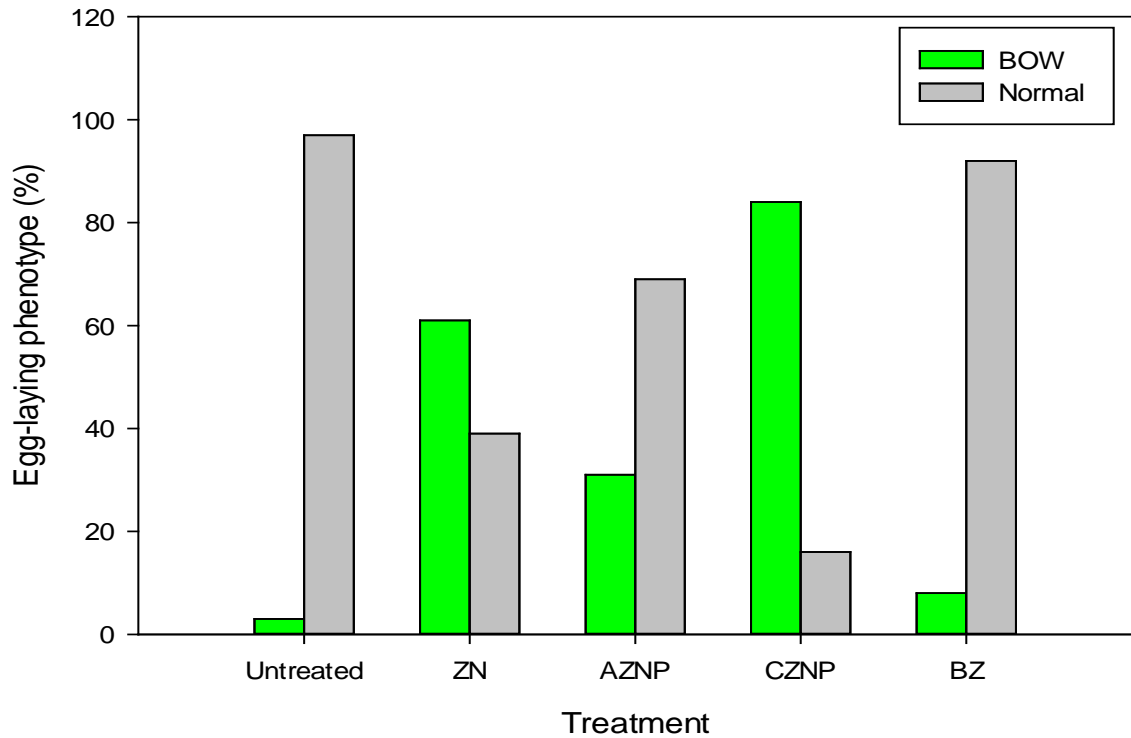


Figure 3.12: Egg-laying phenotype observed following exposure of *sod-3::GFP* adult *C. elegans* to ZnONP.

Adult worms from synchronized populations were exposed to 3.125mM ZnCl₂ (ZN), ZnONP prepared in anionic dispersants (AZNP) or cationic dispersant (CZNP), or bulk ZnO prepared in molecular grade water (BZ) at 20°C for 24 hours. The untreated group and ZN-treated group were the negative and positive controls respectively while controls for dispersants used in the preparation of AZNP and CZNP were unavailable due to manufacturer's proprietary confidentiality. Chi-square analyses of the contingency table from the experiments were used for statistical analysis. Chi-square= 52.957 with 4 degrees of freedom ($p = <0.001$) where a total of 147 worms were analysed with each treatment containing between 19 and 45 worms and the power of chi-square test = 1.0.

In Figure 3.13A, an untreated gravid worm had its egg intact eggs within the worm; however, a relatively higher fluorescence intensity was observed in larvae within the BOW of a ZN-treated gravid worm that also contained AEDs (Figure 3.13B). Representative images of worms exposed to 12.5mM ZnONP in dispersant revealed that hatched larva within a worm exposed to 12.5mM CZNP (Figure 3.13D) seemed to have the highest relative fluorescence intensity in comparison to other groups of treated worms. Furthermore, a comparison between worms exposed to AZNP for four and 24 hours (Figure 3.13C and F) revealed that eggs released from four hour treated worms had relatively low fluorescence intensity. Each representative image in Figure 3.13 was consistent with the phenotypes in the treatment groups

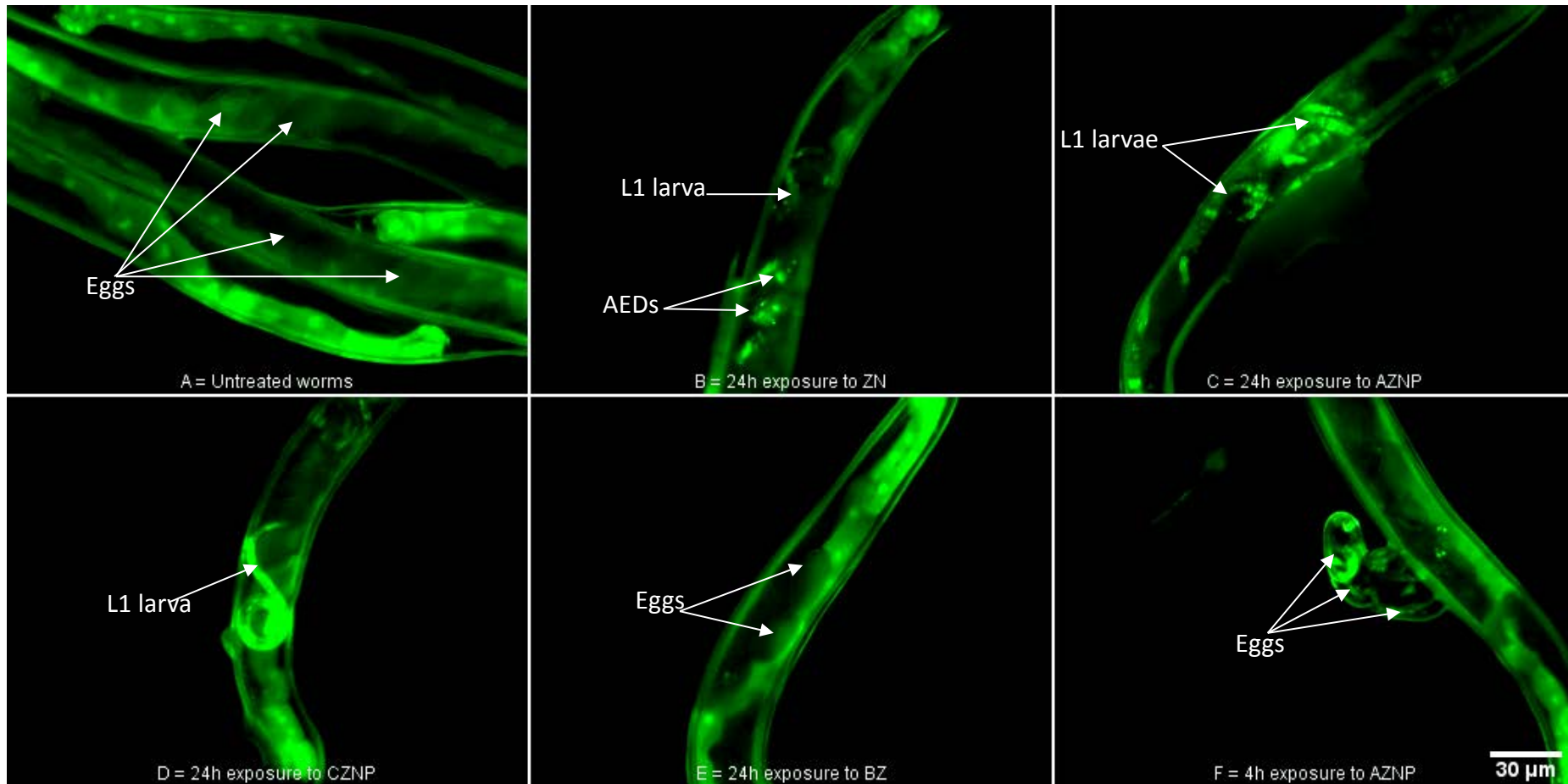


Figure 3.13: Effect of ZnONP on *sod-3::GFP* expression during embryogenesis.

Fluorescence images of (A) untreated worms, and worms exposed to (B) 12.5mM $ZnCl_2$ [ZN], (C) 12.5mM ZnONP prepared in anionic dispersant [AZNP], (D) 12.5mM ZnONP prepared in cationic dispersant [CZNP] and (E) 12.5mM bulk ZnO prepared in molecular grade water [BZ] following 24 hours at 20°C. (F) Fluorescence image of a worm following a 4h exposure to AZNP. Worms used in each experiment were from the same synchronized population. Conditions are consistent in repeated experiments (n=3).

L1 larvae that were successfully hatched from gravid adults exposed to 12.5mM ZnONP prepared in dispersants were observed (Figure 3.14). The pattern of fluorescence expression in the larva from ZN-treated adult (Figure 3.14B) revealed that GFP expression was clear from below the pharynx region down to the tail of the larva and this was consistent with the pattern observed in larva within a ZN-treated gravid adult (see Figure 3.13B). Similarly, consistency was observed in successfully hatched L1 larva from CZNP-treated adults (Figure 3.14C) and L1 larva within CZNP-treated gravid adult (Figure 3.13D) with the expression pattern appearing in the whole larva body.

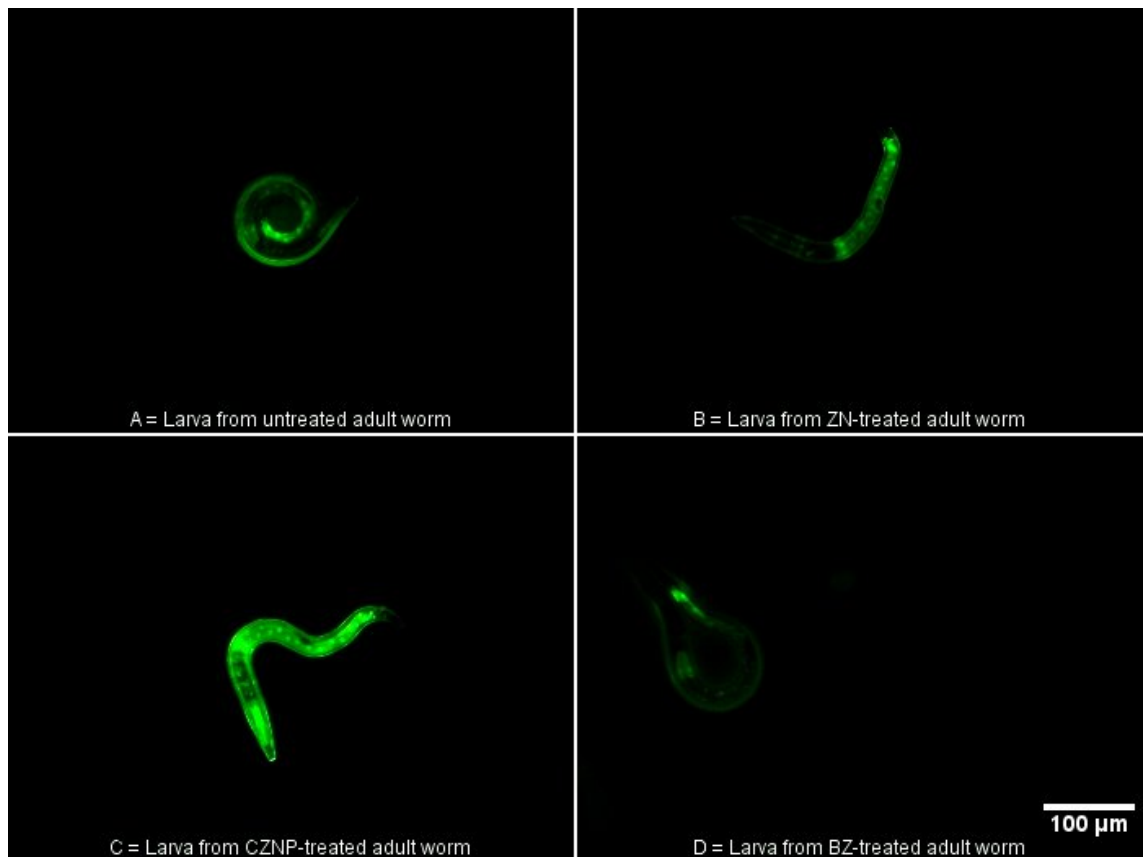


Figure 3.14: Stress response in first filial generation of ZnONP-treated *sod-3::GFP* worms.

Less than 18 hour old hatched larvae from (A) untreated adult *sod-3::GFP* transgenic worm and worms treated with 12.5mM (B) $ZnCl_2$ [ZN], (C) ZnONP prepared in cationic dispersant [CZNP] and (D) bulk ZnO prepared in molecular grade water [BZ] over a 24h period were captured using a compound microscope connected to a camera. Conditions are consistent in repeated experiments (n=3). Adult worms were from the same synchronized population.

3.2.6. Molecular analysis of *sod-3* gene and protein expression.

Experiments such as real-time PCR and microarray analysis require pure nucleic acids with high concentration yield for molecular analysis. Table 3.1 reveals that higher amount of starting *C. elegans* sample yields higher concentration of nucleic acid. Lysis involving the use of RLT buffer yielded 0.61µg/µl nucleic acid while the use of trizol yielded 2.42µg/l. The values of the yield revealed that the trizol-treated sample was higher than the RLT buffer-treated sample suggesting that trizol is more effective for RNA extraction than the RLT buffer in kits. Table 3.1 also revealed that both RLT buffer-treated or trizol-treated samples yielded nucleic acids that were free from protein contamination with absorbance ratios (260/280) in the samples (in bold) above 2.0 suggesting that both RLT buffer-treated or trizol-treated samples were free from protein contamination. The 260/230 ratio which is a secondary measure of nucleic acid purity also revealed the same value (2.4) for the two lysis agents.

Table 3.1: Influence of lysis agents on the quantity and quality of nucleic acid extraction in *C. elegans*.

S/N	Sample	Wet Weight	Lysing agent	Nucleic acid conc. ($\mu\text{g}/\mu\text{l}$)	A260	A280	260/280	260/230
1	Rnase-free water	Not applicable	Not applicable	0.4	0.01	0.037	0.24	-0.04
2	<i>C. elegans</i>	181mg	RLT buffer	0.61	15.2	7.141	2.12	2.4
3	<i>C. elegans</i>	194mg	Trizol	2.42	60.4	28.27	2.14	2.4

*Up to 20ul of M9 buffer was present in total mass of each sample as the movement of the worms prevented total liquid removal.

RNA was extracted by homogenizing a mixed population of *C. elegans* (approximately 1500 L4/ml of mixed culture) using beads in a tissue-lyser for 2 minutes at 50Hz. Protocol for extraction as described in commercially available kit (Qiagen) was followed with a replacement of the RLT buffer (blue above) with trizol (red). All measurements were taken on the Nanodrop spectrophotometer. Absorbance ratios (260/280) in samples (**bold**) were above 2.0 indicating the samples were free from protein contamination. The 260/230 ratio is a secondary measure the nucleic acid purity and values are higher than the corresponding 260/280 values.

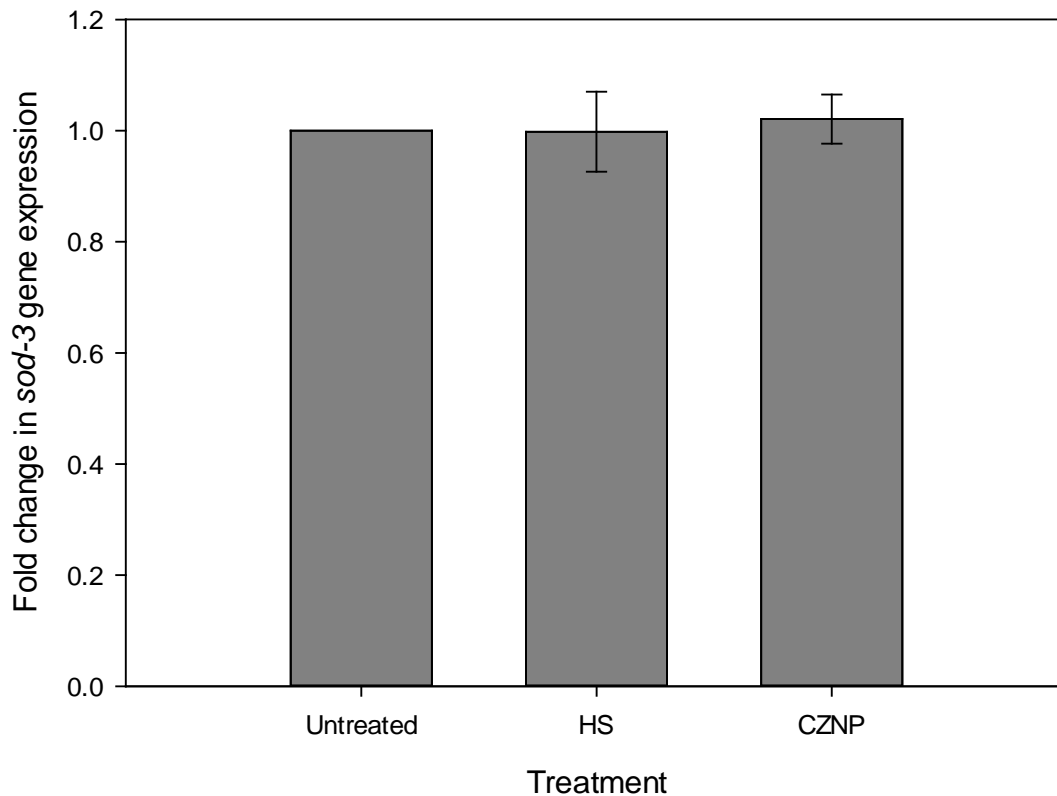


Figure 3.15: Effect of ZnONP on *sod-3* gene expression.

Mixed culture of wild-type *C. elegans* was exposed to heat shock (HS) for 2 hours at 37°C or 12.5mM ZnONP in cationic dispersant (CZNP) for 24 hours at 20°C where the untreated group is the control. The gene expression values were normalized with mean expression of ACTIN, CANX and MDH1 from three separate experiments (n=3) were performed.

Sod-3 encodes a mitochondrial Mn superoxide dismutase (SOD) and as mentioned earlier, SOD is an antioxidant that neutralizes oxidative stress (OS), hence it's production is a measure of toxicity resulting from OS in the worms. To examine whether ZnONP-treated worms experience an increase in OS, real-time PCR (qPCR) was performed in three treatment groups (Figure 3.15). The 12.5mM ZnONP in cationic dispersant (CZNP) was chosen over other ZnO NP treatment types because of the high occurrence of BOW phenotype observed previous toxicity assays (Figures 3.11, 3.13D and 3.14D). The result revealed that there was no significant fold change between the *sod-3* expression in CZNP-treated and untreated worms (Control). Also, although SOD-3 protein was detectable in the worms (Figure 3.16A), there was no significant difference between the protein expression in CZNP-treated sample and the control (Figure 3.16B).

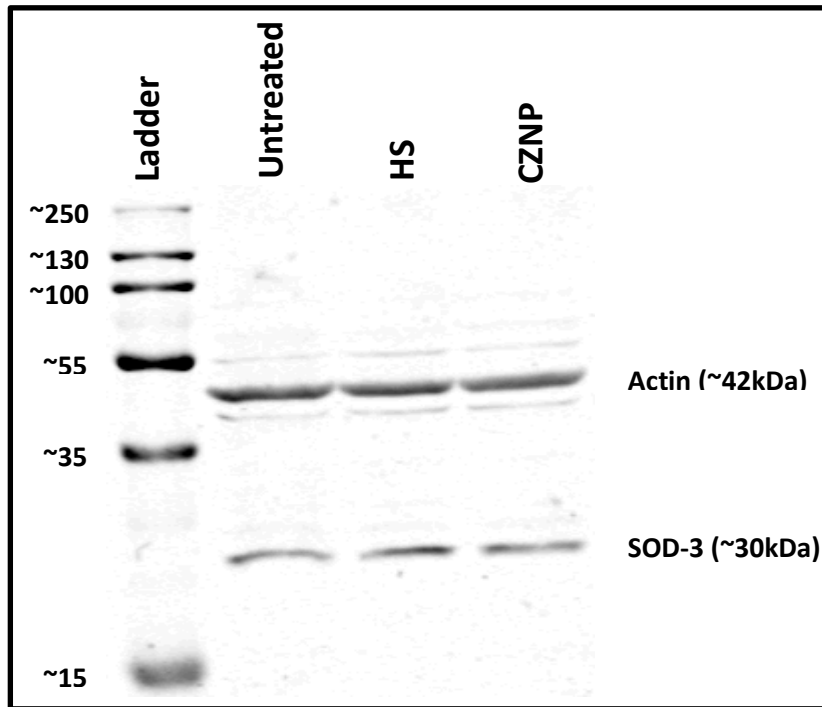
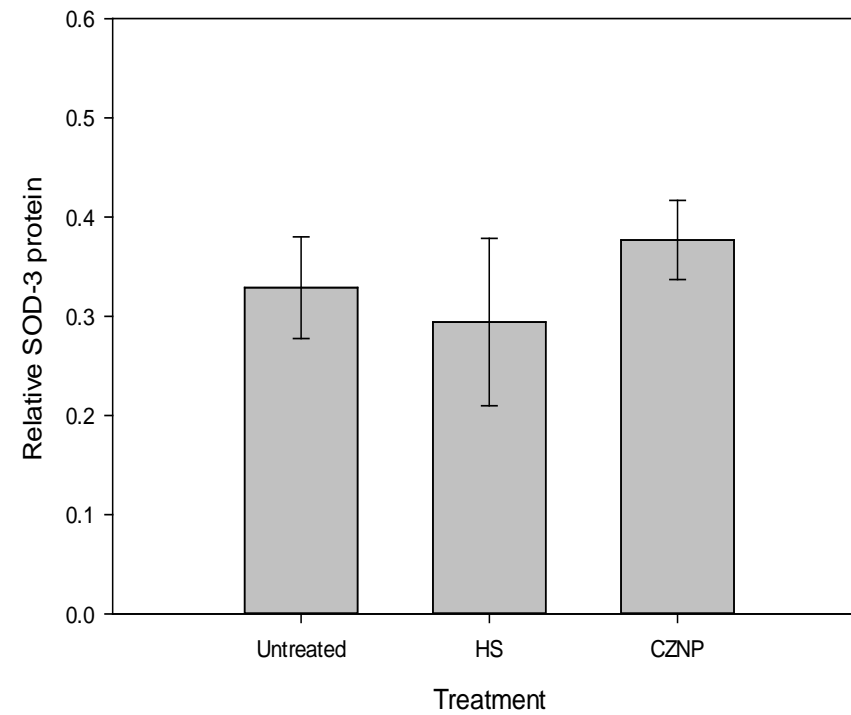
A**B**

Figure 3.16: Effect of ZnONP on SOD-3 protein expression.

(A) Western blots of SOD-3 and actin protein and (B) Relative SOD-3 protein levels. Samples were from mixed population of *C. elegans* (>1500 worms/ml) and include untreated worms (control), heat shock-treated (HS) worms (37°C for 2 hours) or worms exposed to cationic dispersed ZnONP (CZNP) for 24 hours at 20°C. Four separate experiments were performed (n=4). Relative protein levels were derived using densitometry.

3.2.7. Effect of ZnONP exposure on miRNA expression

Genome wide miRNA expression was profiled by microarray analysis. Principal component analysis (PCA) confirmed that there was significant differential microRNA expression between the control (untreated) and ZnONP (CZNP) treatment groups (Figure 3.17). PCA identifies fewer number of uncorrelated variables referred to as principal components (PC), from a large data set like the microarray in order to reveal the maximum amount of variance from the fewest number of PC. CZNP induced the differential expression of approximately 90 miRNAs at the $p < 0.01$, $q < 0.05$ significance level (q represents a multiple comparison correction with a false discovery rate of 5%). Those miRNAs with a fold change greater than 2 in three separate experiments are shown in Figure 3.18. Despite some variability in miRNA expression levels between experiments, there is a trend, predominantly down regulation of miRNAs in the three tests. Specifically, the *C. elegans* miR-42-3p, miR-49-3p, miR-67-3p, miR-239a-5p and miR-253-3p were significantly down-regulated across the three tests. In contrast, *C. elegans* miR-76-3p and miR-42-5p were upregulated. One of the controls; zebra fish miR-124-3p probe was upregulated across the three experiments indicating cross reactivity with *C. elegans* miRNA.

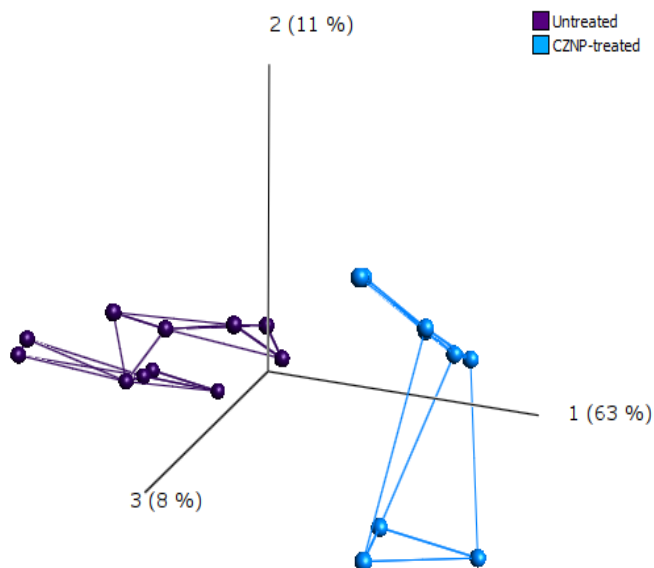


Figure 3.17: Principal component analysis (PCA) of significantly altered miRNAs ($p < 0.01$, $q < 0.05$) with a fold change > 2 following treatment with CZNP ($n=3$). Lines connect nearest 4 neighbours. RNA samples were from mixed population of *C. elegans* (>1500 worms/ml) treated with CZNP (12.5 mM) or without CZNP (untreated-control) for 24 h at 20°C.

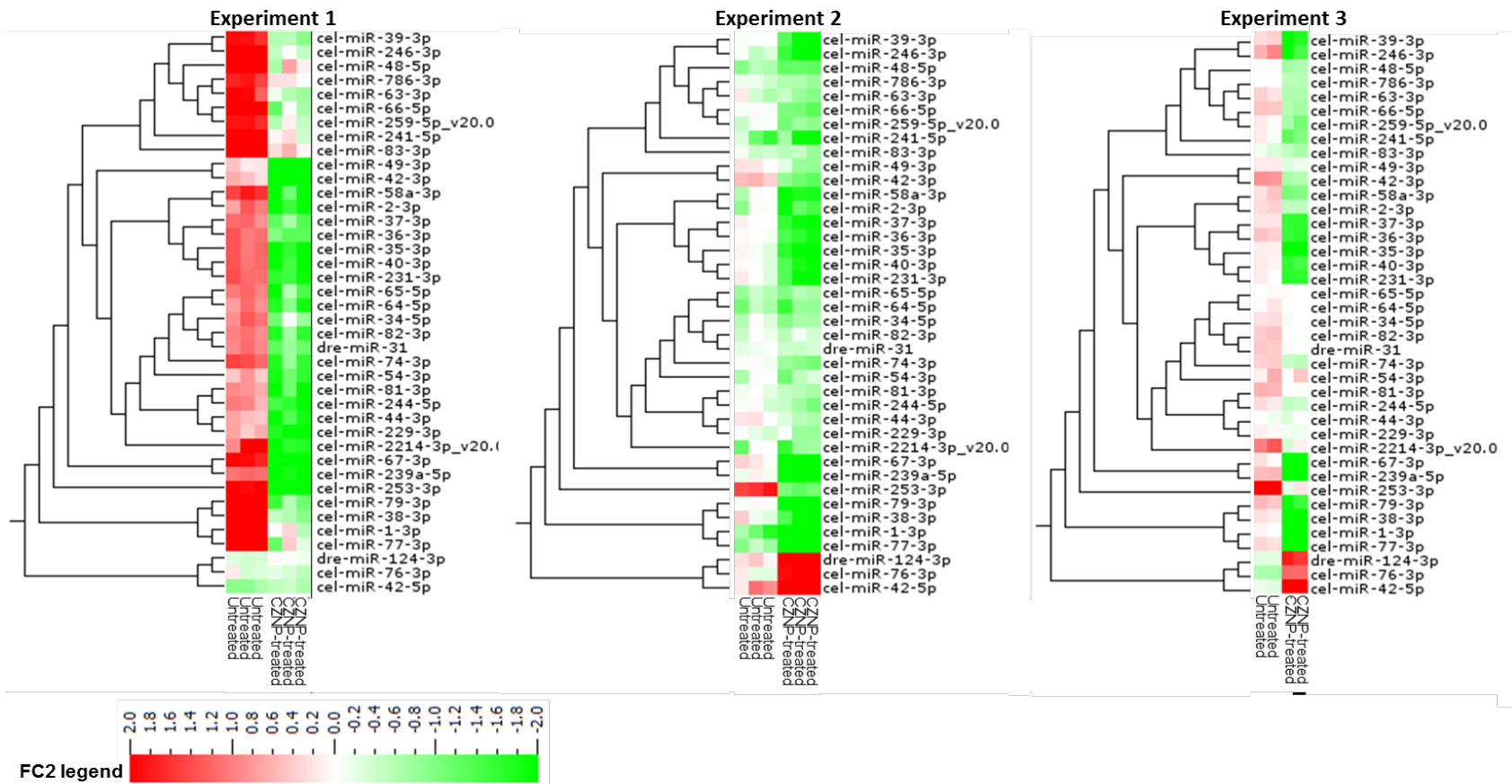


Figure 3.18: Heatmap of those significantly altered miRNAs

($p < 0.01$, $q < 0.05$) with a fold change > 2 following treatment with CZNP. Expression levels represent \log_2 [CZNP/Control] (Log₂ R), with downregulations shown in green and upregulations in red. RNA samples were from mixed population of *C. elegans* (>1500 worms/ml) treated with CZNP (12.5mM) or without CZNP (untreated-control) for 24 h at 20°C. Experiments 1 and 2 were performed in triplicate, whilst Experiment 3 was in duplicate.

3.3. Discussion

3.3.1. Zinc oxide nanoparticle characterization

Our results revealed that the size of the commercially available ZnONP (detailed as 70nm) for all the preparations ranged between 27 and 451nm when measured by SEM and DLS analysis revealed that the hydrodynamic Z-average was between 197 and 1256nm. Although these values were dependent on the dispersant used for the preparation of the ZnONP suspensions, data gathered from the instruments recorded different values for the same ZnONP in dispersant. Supposedly, the difference between the size reported by the suppliers and the measurements taken during the investigation could have been due to the fact that DLS measures motion of hypothetical spherical particles which is translated into a mean of hydrodynamic diameter of the particle movements as against the actual particle size. The mean hydrodynamic diameter in DLS is typically larger than the measurement taken from the SEM or the supplier's specification because for DLS to work effectively, samples are always in liquid phase (Hradil *et al.*, 2007) and the interaction of nanoparticles with liquid alters its physical properties. On the other hand, despite the preparation of SEM samples in dispersants, the samples were not in suspension as they were dehydrated and fixed, so the lack of a liquid phase in the SEM sample preparation could have been responsible for alteration in the ZnONP size (McClements and McClements 2015). Another consideration for the difference in ZnONP sizes is that since DLS reports its measurement using intensity weighted averages of a collection of particles, the polydispersity of the sample may skew the hydrodynamic average diameter to favour larger particles. Although the observation of SEM images of ZnONP in different dispersants appear to have different cluster arrangement patterns (Figure 3.1, panel A), classification as agglomerates and or aggregates would be difficult. The reason is implied in the definitions and relationship between the two terms which are sometimes used incorrectly or interchangeably. Agglomeration is the assembly of individual particles joined together at different angles to one another to form a unit while aggregation is the formation of a common crystal structure by individual particle through the side by side alignment of the particles. In other words, the surface area of an agglomerate does not differ from the total surface area of particles in that agglomerate while the surface area in an aggregate is lower than the total surface area of individual particles in the

aggregate (Walter, 2013). Hence, the inability to capture and measure all the sides of the individual irregular-shaped particles on the SEM makes it difficult to distinguish agglomeration from aggregation. Nevertheless, whilst Sokolov *et al.* (2015) suggests the use of new techniques such as electrochemical nanoimpact; which gives individual particle analysis, to distinguish between agglomeration and aggregation, DLS with a combination of other techniques such as SEM remains a popular way of characterizing nanoparticles. The order of the repeat measurements of Z-average values and the number of peaks in a size distribution are indicators of aggregation where a decreasing Z-average diameter and bimodal or multimodal distributions suggest the presence of aggregation and an increasing Z-average diameter indicates sedimentation (Kaszuba, 2015). Although the aggregation can only be compared relatively among samples, the results (Figures 2 and 3) suggest that WZNP had the highest number of aggregates while CZNP had the least aggregate and was almost monodispersed; that is most of the CZNP had a uniform size. This implies that cationic dispersants are likely to provide better stability and dispersion of ZnONP while water is less likely to disperse ZnONP as the ZnONP would sediment.

3.3.2. Effect of ZnONP on the survival of *C. elegans*

The survival assay results reveal that the lethal effect of ZnONP is dose-dependent. Although it is recommended that concentrations examined in toxicity assays must be relevant to realistic exposure scenarios and high concentrations should be cautiously interpreted (Oberdörster, 2010), our highest ZnONP concentration was 25mM (~2g/L) because LC₅₀ was not yet achieved at this point. For the present study, the relatively short exposure times (4 and 24 hours) compensates for the high concentration used when compared to some studies where lower concentrations were used at the expense of longer exposure times of up to 72 hours (Roh *et al.*, 2009; Jiang *et al.*, 2016; Bhuvaneshwari *et al.*, 2015 and Khare *et al.*, 2014). In fact, one study exposed L4 worms to treatments until the rest of their lifespan for reproductive toxicity assessment (Contreras *et al.*, 2014). The question that remains unanswered is that of developing an acceptable standard of acute or chronic exposure time versus concentration with realistic exposure scenarios in mind.

Contrary to some previously published works on ZnONP toxicity in *C. elegans* (Wu *et al.*, 2013), ZnONP appears to be non-toxic to the worm unless at higher (millimolar) concentrations where AZNP and CZNP were effective at inducing lethal toxicity in *C. elegans*. Although the assessment of ZnONP surface charge was not investigated, Prach *et al.* (2013) had previously shown that the zeta potential which measures the charge on the ZnONP used in our experiments reflected the information provided by the manufacturer. High surface charge of nanoparticles or particles influences the breaking down of clusters and nanoparticle dispersion. Nanoparticles with zeta potential between -30 and +30 mV show a tendency to form clusters. This information coupled with our results implies that apart from the stability and low aggregation of AZNP and CZNP, their charge may influence their toxicological effect in the *C. elegans* model. Whilst it can be assumed that lethal toxicity of ZnONP is based on soluble Zn ions as seen in the Zn²⁺ control results (Figure 3.4A), it is not unexpected that the toxicity could be partly dependent on the dispersant used and consequently the dispersion of the ZnONP in preparation. This is revealed in the ZnONP characterization results (Figures 2 and 3) coupled with the effect of soluble Zn ions from lower ZnCl₂ concentration on the worms (Figure 3.4B). With the consideration that information was not available on the composition of the proprietary dispersant in the commercially supplied AZNP and CZNP, our results emphasize the findings of Anand & Varghese (2015) who suggested that the quality of nanoparticles dispersion is dependent on the ionic composition of the dispersant. Although, in their work, they prepared non-ionic, anionic and cationic surfactants to disperse ZnONP and showed that the anionic surfactant produced the best stability, Dennis *et al.* (1997) observed that a proprietary non-ionic surfactant was more toxic to *C. elegans* than its anionic and cationic counterparts. Nonetheless, the strength of the ionic charge is likely responsible for the variations in the results of Dennis *et al.* (1997).

One challenge with lethality is that subsequent to treatment, analysis is usually performed manually by counting live worms (reviewed by Jiang *et al.* (2016)). This qualitative technique is subjective depending on a scientist's skill of assessment and accuracy hence, increase in experimental error is likely. The comparison for sensitivity and consistency between lethality and other endpoints considered in

our experiments revealed that lethality is not as sensitive as sublethal endpoints at indicating toxicity. This agrees with the work of Dhawan *et al.* (1999) who compared toxicological endpoints in *C. elegans* treated with alcohol. In their work, they found sublethal endpoints such as behaviour and reproduction to be more sensitive than lethality assessment and also, there was correlation between these sublethal responses. Our survival results suggest that ZnONP is lethal to *C. elegans* at high (millimolar) concentrations, and is dependent on length of exposure and the type of dispersant in which the ZnONP is prepared.

3.3.3. Effect of ZnONP on worm morphology

Our research suggests that the dispersant used in the preparation of ZnONP influenced the effect of the ZnONP on worm morphology despite the effect of soluble Zn ions, which resulted in both diminished growth as seen in the ZnCl₂ controls. The AZNP had the highest effect on body length, resulting in diminished length, and AZNP and CZNP had the highest effect on width, resulting in leaner larval structure (Figure 3.6). Interestingly, SZNP-treated worms were unaffected by the ZnONP. This may have been due to the sequestering of the ZnONP. Biofilm-forming secreted bacterial extracellular polymeric substances (EPS) could be present in the *E.coli* OP50 supernatant used as dispersants in SZNP and might have coated the nanoparticles. With the assumption that the worms eat the bacteria, it is possible that the secreted EPS modulates the bioavailability of ZnONP, probably by sequestering it, hence preventing any adverse effect (Polak *et al.*, 2014). On the other hand, a possible explanation for the morphological anomaly observed in the FZNP-treated worms could have been that the lipid content from the 0.1% FBS, whilst improving dispersion, does not necessarily sequester the ZnONP due to its low lipid content. Furthermore, ZnONP uptake could have contributed to poor morphological development in affected worms. There is the possibility of direct ingestion of the nanoparticles which could have formed clusters in the pharynx or within the worm gut making the worm constipated or finding it difficult to feed efficiently. There could be an argument that the same effect should be experienced when bulk ZnO is consumed but it is likely that bulk ZnO can easily be avoided by the worms as it is large enough to be detected easily by the worm's sensory system while the

ZnONP are likely to have been attached directly to the worms food source (*E. coli* OP50) giving the worm no choice but to ingest them.

3.3.4. Effect of ZnONP on reproduction

Whilst reproduction is assumed to be a more sensitive endpoint than lethality, it shares a similar challenge with lethality in terms of quantification of brood size. For example, variability in reproducibility of brood size assay in one experiment was as high as 11.5% (Höss *et al.*, 2009). The present research has addressed this concern by classifying the reproductive endpoint in terms of embryogenesis. Embryogenesis in *C. elegans* involves the formation and development of the embryo to the point of hatching. Embryonic assay proposes a semi qualitative but more effective way of assessing reproductive toxicity than brood size because it is less time-consuming (at least 18 hours) and variability in reproducibility is likely to be lower.

In the present study, embryonic assessment involves the identification of Bag of Worms (BOW) phenotypes. BOW phenotypes or *endotokia matricida* (Johnson, 1984) are a result of matricidal hatching. Matricidal hatching may occur when worms are starved (Seidel and Kimble 2011), transferred from solid to liquid medium (Shook and Johnson 1999), exposed to toxic substances (Walker and Tsui 1968) or have a high population density. Essentially, in BOW phenotypes, egg-laying ceases and embryos within the gravid hermaphrodites continue to develop and hatch inside their parent. Chen & Caswell-Chen (2004) suggested that the bagging of worms could be reversible provided the cause of the induction is removed before the adult worm experiences any lethal injury resulting from larval movement, hence; it is an adaptive response that allows progeny, from adults experiencing unfavourable conditions, to reach the resistant dauer stage following provision of sufficient nutrient and protection from their parent.

We investigated the BOW phenotype as a marker of ZnONP toxicity and the results suggest that there is a correlation between the morphological and reproductive toxicity endpoints. SZNP-treated worms did not exhibit the BOW phenotype and this is probably due to the EPS-ZnONP interaction discussed

above (section 3.3). The relative toxicity patterns among the treatment groups were consistent with the patterns described in the morphological assessment.

Interestingly, we discovered a condition prior to internal hatching which we refer to as accelerated embryonic development (AED) phenotype. The AED phenotype presents three-fold embryo elongation showing fully differentiated tissues encapsulated within the eggshell and still in the hermaphrodite gravid adult (Figure 3.8, panel B). To the best of our knowledge, it has not been classified in the literature. The assessment of AED phenotype augmented the sensitivity of the embryonic reproductive assay in that it includes a mechanistic toxicology approach to reproductive toxicity assessment. For example, BOW phenotype was not observed in SZNP-treated worms, whereas we observed AED phenotype in the worms. This suggests that there is a delayed toxic response in SZNP-treated worms. In order to fully understand the reason for the delayed response, further analysis would be required. Although we did not investigate the presence of ZnONP in the embryo to determine if the nanoparticle crosses the egg barrier, Meyer *et al.* (2010) showed that AgNP was detected in unlaidd *C. elegans* eggs. In zebrafish, ZnONP accumulated in the embryo and eleuthero-embryo, and also inhibited hatching (Brun *et al.*, 2014).

One limitation that may affect the embryogenic assay technique is that the rate of feeding of the gravid worms with bacteria might affect their egg-laying and hatching (Fasseas *et al.*, 2013) but in comparative studies such as the current research this is inconsequential since the feeding condition of all samples are the same and the worms used in each experiment are from synchronized populations.

In conclusion, the evaluation of survival, morphology and reproduction as toxicity endpoints suggests that at the same concentration, there is a significant difference in the effect of ZnONP on *C. elegans* among these endpoints. As suspected, survival appears to be the least sensitive of all the endpoints because significant effects were only observed in ZnONP dispersed in two dispersants (AZNP or CZNP). On the other hand, reproduction (embryonic assessment) seems to be the most sensitive endpoint because significant effects were observed in ZnONP prepared in the five dispersants (WZNP, FZNP, SZNP, AZNP

or CZNP) considered. However, this reproductive toxicity effect is based on consideration that AED is included as a measure of ZnONP toxic effect.

3.3.5. Effect of ZnONP on transgenic *sod-3::GFP* expression

So far, the current research has shown that ZnONP may only be a lethal toxicant of *C. elegans* at high millimolar concentrations. This could only be a limitation where lethality is used as the major measure of toxicity. In our study, we introduced transgenic GFP reporter strains to measure gene expression as a more sensitive approach for toxicity evaluation of ZnONP. We utilized *sod-3::GFP* strain for our experiments knowing that in terms of fold change in gene expression, *sod-3*, a mitochondrial MnSOD is the most upregulated of all the 5 *sod* genes. *sod-3* only accounts for 1% of the total *sod* mRNA while the other mitochondrial MnSOD (*sod-2*) accounts for 18% of total *sod* mRNA (Doonan *et al.*, 2008). The results showed that transgenic strains vary slightly in their responses to lethal toxicity when compared to wild-type *C. elegans*; however, the pattern of toxicity is similar. It is likely that the creation of transgenic strains with GFP reporters could have influenced the change. When using the transgenic strains for toxicity assay (specifically gene expression assay), it is worthwhile to run a parallel test with the wild type strain at least to compare the difference between lethal toxicity.

The expression of *sod-3::GFP* was highest in CZNP -treated worms (Figure 3.11). This strengthens the findings from morphological and reproductive assays that suggested that the Zn²⁺ contents and the dispersants could have contributed to the toxic effect of ZnONP. More interesting is that the concentration used for the *sod-3::GFP* expression analysis was four times lower than that used for the lethal, morphological and reproductive assays. This suggests that *sod-3::GFP* expression is highly sensitive. Another point of note is that *sod-3* expression could be stage-specific but this would be dependent on the type of chemical exposure as observed in L1 larva exposed to CZNP (Figure 3.11).

The assessment of transgenic *sod-3::GFP* gravid hermaphrodite worms and their embryo, BOWs and AEDs suggests that ZnONP induced oxidative stress on the hatched embryo and 3-fold embryo of BOWs and AEDs respectively (Figure

3.13). This is not unlikely as the embryo and hatched larva would require a lot of energy to adapt to their temporary environment. In a way, the altruistic response of the adult worm may encourage adaptive skills to survive in unfavourable conditions prior to release into a safe environment.

Although the loss of *sod-3* gene function can be complemented by *sod-2*, the choice of *sod-3::GFP* over *sod-2* was because the loss of *sod-2* would prevent the detection of MnSOD in the worms (Honda and Honda 1999). This may alter the effect of ZnONP exposure by preventing the ability of the worm to function against severe oxidative stress thus discouraging sublethal assessment as worms may die due to imbalance of free oxygen radicals. One downside to the GFP reporter approach is that while it is feasible to cover ZnONP responses and oxidative stress pathways, the *sod-3* gene considered here represents only a meagre part of an extensive array of genes that are implicated in ZnONP toxicity and oxidative stress. Consequently, this approach is only reliable for the quick measurement of stress-response gene expression where the GFP variant is stable as subtle responses involving internal regulatory mechanisms could be missed. Overall, this current research shows that the use of transgenic *C. elegans* GFP stress-reporter strains can offer an indication of the patterns of gene response to ZnONP toxicity.

3.3.6. Effect of ZnONP on *sod-3* gene and protein expression

Increased reactive oxygen species (ROS) production may disrupt the functionality of the mitochondrion which results in oxidative stress responses in affected organisms (Dickinson and Chang, 2012). The presence of antioxidant defence mechanisms such as superoxide dismutase (SOD) in biological systems help to counter oxidative stress. SOD was chosen as the antioxidant analyzed because it is the only enzyme that directly uses free radicals as substrate; thus its activity is generic in organisms (Silvestre *et al.*, 2006). In the current research, exposure to CZNP did not cause change in the expression and activity of SOD-3. This finding corroborates the result of Huang *et al.* (2010) who investigated the effect of nanoparticulate ZnO on human bronchial epithelial cells and observed that the expression of antioxidant genes including SOD was not changed following exposure. In contrast, Syama *et al.* (2013) observed that SOD was

significantly elevated following exposure of mouse liver cells to ZnONP. An explanation for lack of change in *sod-3* gene expression is the exposure of *C. elegans* to dauer pheromone. This pheromone induces a high resistance to stress in active worms, so while a mechanistic basis for toxicity can be demonstrated in responses as observed in transgenic *sod3::GFP* strain, these responses cannot be observed beyond a threshold that can be seen at mRNA transcription or protein translation level (Hunt, 2016).

Furthermore, while the assessment of *sod-3* gene regulation under oxidative stress could be subjective due to its dependence on relative comparison with *sod-3* gene expression levels in control samples, the inclusion of a *sod-3* mutant (null strain) and / or a *sod-2; sod-3* mutant (hypomorphic strain) as controls in the qPCR and protein analysis could have provided a more authentic validation of the analysis. This is because these mutants are hypersensitive to oxidative stress (Doonan *et al.*, 2008). SOD-2 is the major MnSOD protein and it can complement SOD-3, hence the suggestion for the inclusion of *sod-2* mutant.

3.3.7. Effect of ZnONP on microarray analysis of miRNA expression

Descriptive assessment of ZnONP toxicity described in the current research did not seem to bolster the observations at the molecular level. However, the addition of microRNA (miRNA) expression analysis to ZnONP toxicity assessment as a mechanistic toxicity assay in *C. elegans* revealed that the miRNA expression of treated worms reinforced the behavioural, morphological, reproductive and transgenic GFP expression results.

Because a single miRNA (especially conserved ones) has an affinity for multiple biological targets (Bartel 2009), the predicted targets of 38 *C. elegans* miRNAs with fold change greater than two were themed around oxidative stress and embryogenesis. The choice for oxidative stress was to elucidate further on SOD expression while embryogenesis was chosen based on the egg-laying phenotypes observed following CZNP treatment. The changes in miRNA expression observed in CZNP-treated worms were predominantly downregulation. Using the computational method; RNA22, developed by Miranda *et al.* (2006), over 19000 miRNA target sites were predicted for mir-253-3p which

was downregulated following exposure to CZNP. These include four of the five *C. elegans* SOD genes; *sod-2* and *sod-3* genes which encode mitochondrial MnSOD, and *sod-1* and *sod-5* that encode cytosolic Cu/ZnSOD. MiR-253-3p was also predicted to target *let-502* which encodes a Rho-binding serine/threonine kinase that takes part in the regulation of nonmuscular contraction in humans. In *C. elegans* *let-502* takes part in the regulation of embryonic morphogenesis (Piekny *et al.*, 2003) which starts with transformation of embryo cell migration to pharyngeal pumping development.

In contrast to miR-253-3p, miR-42-5p expression is upregulated following CZNP but it also predictively targets *sod-1*, *sod-2*, *sod-3* and *sod-5* as well as *let-502*. While the contrasting response between miR-253-3p and miR-42-5p should be carefully considered based on the uncertainty of the predictive ability of any computational methods, the opposite expressions could be a matter of perspective. For example, the purpose of SOD in biological systems is to combat oxidative stress (OS) by neutralizing free oxygen radicals; so the induction of OS could be an indication of toxicity. With this in mind, there is a possibility that miR-42-5p is expressed to control the expression of the SOD genes which would degrade or silence the transcription of their mRNA. Conversely, miR-253-3p is downregulated to allow the SOD genes to code for the protein. Either way, it is a question of regulation. Chen *et al.* (2011) also showed that there is a possibility of one miRNA to destabilize another. They showed that a *let-7* miRNA can be targeted by miR-107 thereby decreasing its expression to promote tumor progression in humans and mice. Another explanation for the contrast in miR-253-3p and miR-42-5p expression could be that the stability of the miRNAs is dependent on the target sites. Previous studies on *C. elegans* miRNA revealed that a reduction in the available target sites for miRNA decreased the accumulation of the miRNAs (Chatterjee *et al.*, 2011). Again, some exonucleases of *C. elegans* can influence the expression of miRNA as their depletion can result in the accumulation of miRNAs (S Chatterjee and Grosshans 2009).

MiR-42-3p which belongs to the same family with miR-42-5p and miR-49-3p were downregulated and both were predicted to target only *sod-4* gene out of the five *C. elegans* SOD genes. Mir-239a-3p which is highly expressed at all larval

developmental stage and weakly expressed in the embryo was downregulated. The RNA22 prediction for miR-239a-3p included only two sod genes; *sod-2* and *sod-3*. Like miR-42-5p, miR-76-3p was upregulated and it was predicted to target only *sod-5* of the five *C. elegans* SOD genes. For MiR-42-3p, miR-49-3p, Mir-239a-3p and miR-76-3p, RNA22 predicted *let-502* as a potential target. The inclusion of *Danio rerio* miR-124-3 probe revealed that mir-124-3p is conserved across species as it was picked up by the *C. elegans* RNA in the microarray. MiR-124 is implicated in oxidative stress and increase in lipofuscin which is a marker for aging and the the protein responsible for autofluorescence in *C. elegans*. It also plays a vital role in the control of whole worm ATP level (Dallaire *et al.*, 2012).

The results of the microarray suggest that CZNP has an effect on *C. elegans* which can be observed at the post-transcriptional level. This is a plausible basis for the conflicting results between qPCR and immunoblot, and microarray analysis of miRNA expression. Some other advantages of the miRNA over qPCR and immunoblot is that mixed populations of worms can easily reveal effects in miRNA analysis as there are more mechanisms to analyse due to the broad range of miRNA in the array. Due to the limit of the number of gene expression analysed with qPCR, any gene of interest which is not expressed in all developmental stages of the worm may prove difficult to analyse; hence known stage-specific gene expression using synchronized population are best suited for qPCR analysis. Although, the development of miRNA as biomarkers is still in its early stages and target sites are still not known for many miRNAs, the technique is highly sensitive in deciphering the effects of ZnONP.

Chapter Four

4 Toxicity assessment of Diethylstilbestrol

4.1 Introduction to diethylstilbestrol toxicity assessment

Diethylstilbestrol (DES) is a synthetic nonsteroidal chemical with properties that interfere with the physiological effects of oestrogen in humans and animals; hence it is an endocrine disruptor. Between 1938 and 1971, DES was administered to pregnant women to prevent abortion and other pregnancy-related complications. However, its use was abolished later in 1971 when there were strong suggestions that *in utero* exposure to DES was closely associated with vaginal clear cell adenocarcinoma (Herbst *et al.*, 1971). Further studies within the next four decades identified other health hazards including obesity (Newbold *et al.*, 2009) and psychosexual development changes in those exposed to DES (Mahalingaiah *et al.*, 2014; Harris & Waring 2012; Hoover *et al.*, 2011) while their offspring had reproductive anomalies such as underdeveloped sexual organs, vaginal adenosis (Laronda *et al.*, 2012) and testicular steroidogenesis (Maeda *et al.*, 2013). In the United States alone, no less than 2 million women were given DES during the period of its use (Noller *et al.*, 1988); thus the continuous studies to understand its adverse effect on the body. Studies using animal cell line models (Kuzbari *et al.*, 2013) and rats (Horiguchi *et al.*, 2014) have been consistent with DES in terms of the effect of DES on enzymes essential for hydroxylation of steroid hormones and understanding how DES suppresses erythropoietin; thereby inducing anaemia, respectively. The extensive volume of literature verifying the adverse effects of exposure to DES collected over the last forty years using DES-exposed experimental animal models, combined with observations from DES-exposed humans, have led to the use of DES as a chemical of interest for the assessment of reproductive toxicity in humans and animals and it is also representative of environmental endocrine disruptors that may pollute the environment causing diseases in humans and animals.

Steinmetz *et al.* (1997), Tran *et al.* (1997) and White *et al.* (1994) have used the identification of oestrogen-like activity as the basis for endocrine-disrupting compounds (EDC) detection in biological systems; however, the inability of the EDCs to bind oestrogen receptors may not encourage the detection of oestrogen-

like activities. Hence there is a need to develop an assay to identify and assess the toxicity of EDCs.

In the current research, the effect of DES on *C. elegans* viability was investigated. The possible application of *C. elegans* as a model organism for EDC assays is discussed in the thesis.

4.2 Results

4.2.1 *C. elegans* viability on exposure to DES

In order to investigate viability of the worms following exposure to Diethylstilbestrol (DES), three measures of toxicity were investigated. These endpoints include survival of worms based on lethality of DES, reproduction and behavioural responses to DES.

4.2.2 Effect of diethylstilbestrol on *C. elegans* survival

In order to investigate the lethal effect of diethylstilbestrol (DES) on *C. elegans*, synchronized L4 worms were treated with concentrations of DES ranging from 0.001 μ M to 10 μ M. A negative control (S medium) which is the untreated group and a DMSO control (solvent used for treatment preparation) were included as part of the experiment. Following 24-hour exposure DES treatments, the results (Figure 4.1) revealed that more than 80% of all treatment groups and control groups survive with 10 μ M DES treatment recording the highest number of live worms (approximately 93%). There was no significant statistical difference among the DES treatment groups and the controls. The results suggest that the DES treatments had minimal lethal effect on the worms.

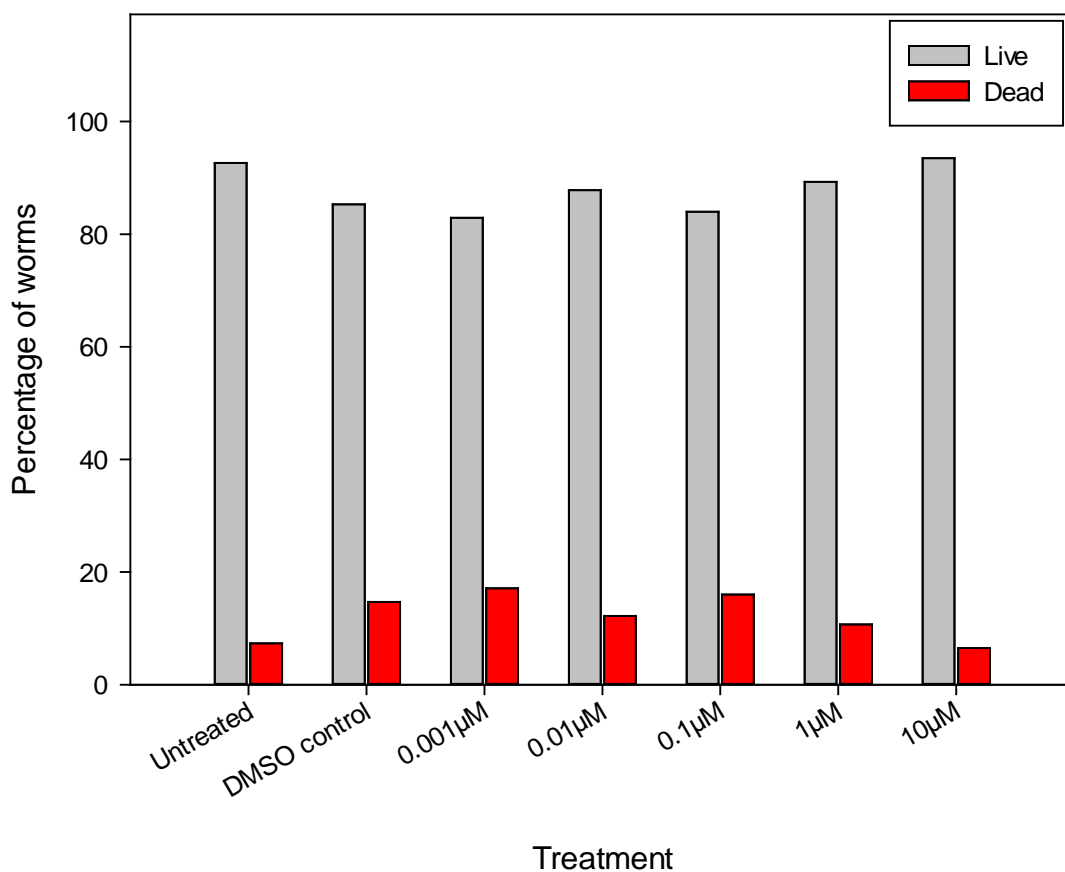


Figure 4.1: Effect of diethylstilbestrol on wild-type *C. elegans* survival.

L4 worms from synchronized populations were exposed to 0.001µM, 0.01µM, 0.1µM, 1µM or 10µM diethylstilbestrol for 24 hours at 20°C in liquid medium where the negative controls included untreated worms and DMSO (0.1%) used in the preparation of treatments. Viable and dead worms were recorded after exposure to the treatment. Chi-square analyses of the contingency table from the experiments were used for statistical analysis. Chi-square= 9.399 with 6 degrees of freedom (P = 0.152) where a total of 698 worms were analysed over two separate experiments and each treatment contained between 62 and 136 worms. Power of performed test = 0.604.

4.2.3 Effect of diethylstilbestrol on *C. elegans* reproduction

The reproductive endpoint considered in the investigation of DES effect on the worms was fecundity. Due to challenges of monitoring offspring of adult worms from the same synchronized population, two DES concentrations (10 μ M and 100 μ M), a negative control (S medium - no treatment) and a DMSO control. Brood size from the DES and DMSO treatments were presented as percentages of the brood size from untreated worms. In figure 4.2, the percentage control brood size of worms treated with DES was higher than the DMSO control with 10 μ M DES almost twice as high as the DMSO control. All the brood size from the three treatment groups were lower than the brood size of the untreated worms. Similarly, one of our undergraduate students; Hannah Bisby, repeated the experiment using a different approach consisting of mixed culture and her result (Table 4.1) showed that the brood size of worms treated with 100 μ M DES was higher than the DMSO control.

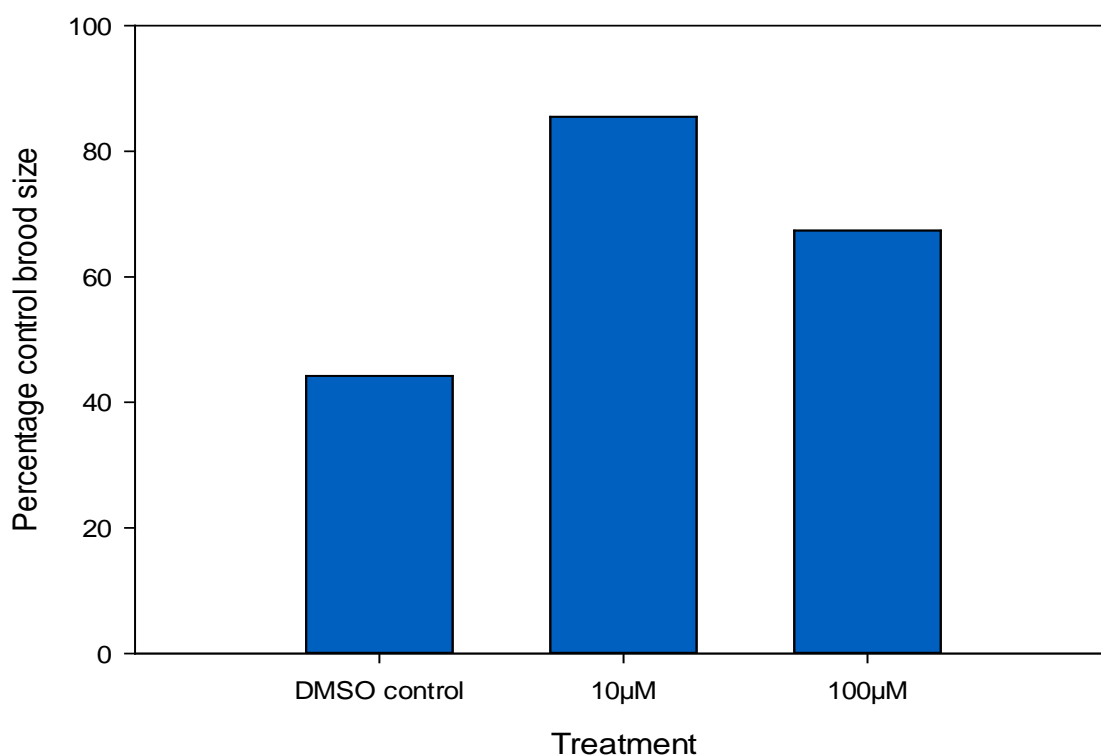


Figure 4.2: Effect of diethylstilbestrol on *C. elegans* brood size.

Two adult worms were treated with 10 μ M or 100 μ M diethylstilbestrol for 24 hours at 20°C in liquid medium where worms treated with 0.1% DMSO were the negative controls and data was calculated as a percentage of brood size from untreated worms. The brood count was over 96 hours following exposure to treatment.

Table 4.1: Comparison between two methods used for the assessment of DES effect on *C. elegans* brood size

Experimental design		
Developmental stage analyzed	Synchronized L4	Mixed
DES exposure time in media	24 hours in liquid medium	4 hours in solid medium
Medium in which brood was produced	Solid	Solid
Worms examined per treatment group	2	8
Counting period for brood size	96 hours	48 hours
Brood size of untreated control group	138	1,2,10,12,15,19,24,53 $\bar{x} = 17$ Med = 13.5 SD = 16.51
Brood size of 0.1% DMSO -treatment group	61	1,1,3,4,4,9,11,29 $\bar{x} = 7.75$ Med = 4 SD = 9.30
Brood size of 100 μ M DES prepared in 0.1 DMSO -treatment group	93	1,5,6,6,7,13,35,41 $\bar{x} = 14.25$ Med = 6.5 SD= 15.11

The table compares brood size of worms from a synchronized population of adults with a mixed population. For the brood size of worms from a synchronized population, two adult worms were placed on a NGM plate seeded with *E. coli* OP50 and moved to a fresh plate after 24 hours while the F1 worms were counted on each changed plate daily following removal of the adult worms before summing the F1 counts over a four-day period (96 hours). For the brood size of worms from a mixed population, one adult worm was placed in each of eight replicate NGM plates seeded with *E. coli* OP50 as food source and the number of F1 worms in each plate was counted after 48-hour period. All plates containing worms were incubated at 20°C. \bar{x} , Med and SD represent the mean, median and standard deviation of brood size respectively, for the mixed population.

4.2.4 Effect of diethylstilbestrol on *C. elegans* behaviour

Due to the limited effect of DES on worm survival, the effect DES on worm average speed and body bend per minute (BBPM) was investigated. This was necessary to explore sublethal effects of DES on the worms. The average speed and number of body bends were generated using a computer tracking system. Worms were treated with 0.01 μ M, 0.1 μ M, 1 μ M, 10 μ M or 100 μ M DES or a DMSO

control for 24 hours at 20°C. Visual observation showed that the worms experienced twitching which lasted approximately 4 minutes on exposure to DES treatments and the controls. This was followed by monitoring the behaviour of the worms using a computer tracking system (ImageJ). In Figure 4.3, the bar graph compares the mean of the average speed of the worms in each treatment group. Whilst the results in figure 4.3 revealed no statistically significant difference among treatment groups, there seems to be an undulating average speed with increasing concentration of DES with a high average speed of about 7.5px/s at 0.01µM in comparison to the DMSO control and the 0.1µM DES. However, worms treated with 0.1µM, 1µM and 10µM recorded increasing speed in that order but worms treated with 100µM DES otherwise showed a lower than average speed. Again, behavioural data from a second experiment performed by Hannah Bisby using the manual assessment method for speed measurement (Table 4.2) revealed that there was no difference between the DMSO control and the 100µM DES-treated worms; however, the untreated worms seemed faster than both the DMSO control and the 100µM DES-treated worms (data not shown).

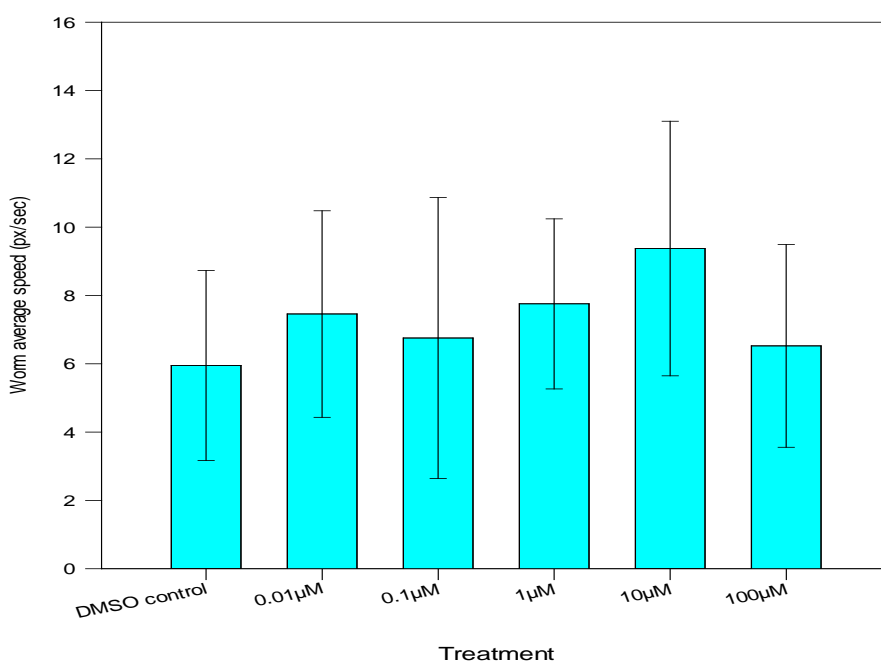


Figure 4.3: Effect of diethylstilbestrol on *C. elegans* average speed.

L4 worms from synchronized populations worms were exposed to 0.01µM, 0.1µM, 1µM, 10µM or 100µM diethylstilbestrol (DES) for 24 hours at 20°C where the negative control included worms treated with 0.1% DMSO which was used in the preparation of DES treatments. The video frames were captured in 24 well plates over a 15 second period. Data was generated from 60 worms with each treatment group containing between 7 and 12 worms and speed was measured in pixels per second (px/s). Statistical analysis was by One-way ANOVA ($p=0.348$).

Table 4.2: Comparison between two methods used for the assessment of DES effect on *C. elegans* speed

Experimental design		
Developmental stage analyzed	Synchronized L4	Mixed
DES exposure time in media	24 hours in liquid medium	4 hours in solid medium
Medium in which speed was measured	Liquid medium	Solid medium
Worms examined per treatment group	15	8
Speed measurement technique	Automated (Quantitative)	Manual (Qualitative)
Speed of 100µM DES prepared in 0.1% DMSO – group (SD)	5.95 (2.78)	++
Speed of 100µM DES prepared in 0.1% DMSO - treatment group (SD)	6.52 (2.97)	++

The table compares speed of worms from a synchronized population of L4 worms with a mixed population. For the synchronized population, the ImageJ WrmTrack plugin was used to determine the speed of the worms in pixel per second (px/sec) while visual observation was used to investigate the speed of worms in the mixed population. The motion of the worms in the synchronized and mixed population was recorded in S medium solution and NGM agar respectively in the presence of *E. coli* OP50 as food source and an incubation temperature of 20°C. SD represents the standard deviation of brood size for the synchronized population.

The box plot shows (Figure 4.4) the BBPM among each treatment group. There was no statistically significant difference in the BBPM of worms across the treatment groups but there was a steady increase in DES-treated worms with a steady increase observed at treatment concentrations of 0.1 an increasing number of 1µM and 10µM DES and above.

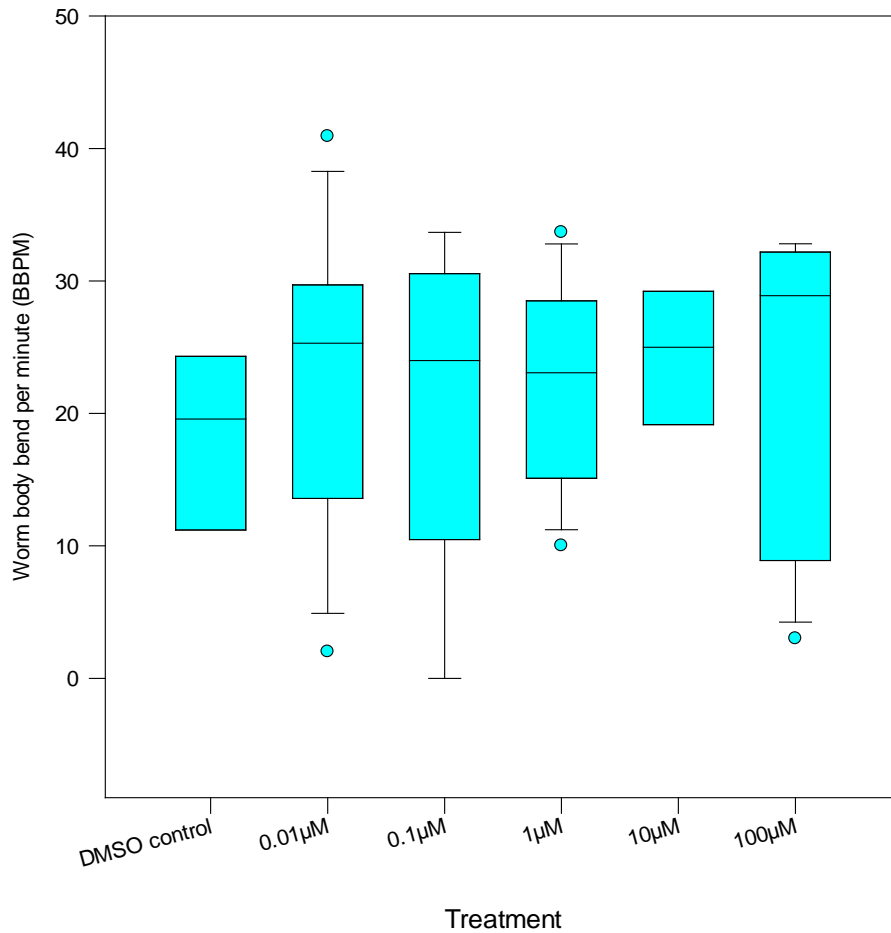


Figure 4.4: Effect of diethylstilbestrol on *C. elegans* average body bend per minute (BBPM)

L4 worms from synchronized populations worms were exposed 0.01µM, 0.1µM, 1µM, 10µM or 100µM diethylstilbestrol (DES) for 24 hours at 20°C where the negative control included worms treated with 0.1% DMSO which was used in the preparation of DES treatments . The video frames were captured in 24 well plates over a 15 second period. Individual body bends per minute was calculated from computer tracking-generated body bend per second using the worm tracker plugin on ImageJ. Data was generated from 60 worms with each treatment group containing between 7 and 12 worms. Due to the unequal variance among sample groups, ANOVA on ranks (H-test) was used for statistical analysis where $H = 3.883$ with 5 degrees of freedom ($P = 0.718$).

4.3 Discussion

In the current research, DES treatments ranging 0.001 μ M and 10 μ M did not reveal significant difference in terms of lethality on worms when compared with controls (Figure 4.1). This suggests that the concentrations used in the experiments were not high enough to induce a lethal effect. The results correlate with the work of Maranghi *et al.* (2008) who reported that low doses of DES showed no sign of general toxicity in mice. Consequently, the concentrations of treatments were further increased to ranges between 100 μ M and 10mM but the results for survival of treated worms remained relatively unchanged. In fact, there seemed to be improved viability specifically the apparent increase in size of worms from some treatments when compared to controls (data not shown). The result would appear logical to support the use of DES to enhance the growth of agricultural animals as was the case about sixty years ago (Dinusson *et al.*, 1950).

The concentration range maintained for the lethal toxicity analysis above was similarly used to analyse fecundity. Again, the results showed that there was an increase in brood size with DES treatment; although these differences were in comparison to the solvent control (0.1% DMSO) used in the preparation of the DES concentrations (Figure 4.2). Interestingly, similar results were obtained with a different experimental set-up using mixed populations of worms detailed in table 4.1. While only two DES concentrations were considered, the results seem to agree with the initial basis for the use of DES in the treatment of reproductive-related conditions as it was generally used for preventing spontaneous abortion which was believed to be a result of reduction in oestrogen level (Smith 1948). At the point of investigating the effect of DES on fecundity, the requisite skill required for using computer-based tracking of offspring had not been acquired. This would have allowed the monitoring of multiple adult worms for their brood size. This limitation resulted in the use of manual counting of brood that can create errors. Whilst some scientists depend on the manual approach for brood count (Li *et al.*, 2014; Gonzalez-Moragas *et al.*, 2015), the technique could be daunting (Polak *et al.*, 2014) and the reproducibility of the technique could be subjective depending on the technical skill of the scientist.

The results in figures 3 and 4 suggest that there is variability in the behaviour of the worms in terms of speed and body bends respectively. One major challenge

with the data analysed for behaviour is that it was generated from the computer worm tracking programme which is limited in accurately tracking every worm in an experiment. The algorithm for the tracking programme includes laying-off outliers from threshold of behaviour specification. For example, when two tracked worms overlay each other, the sequence of tracking in the two worms may be excluded from the data and this resulted in unequal worm number in each treatment group. One factor that can improve the output of the computer tracking system is the quality of plate preparation for camera capture. For instance, particle-free worm plates with moderate number of worms (20-30) might generate better data. Despite the challenges automated analysis of worm behaviour may pose, it is still more efficient than manual assessment. In table 4.2, a comparison between the automated and manual behavioural tracking system revealed that the latter could be qualitative and subjective, depending on the researcher's observatory skills. More so, good *C. elegans* culture practice (GCeCP) would reduce the magnitude of errors in behavioural as well as other toxicity endpoint assessment. For example, in table 4.2, while the current research measured speed on liquid medium, solid medium would have served the purpose better as particles that vibrate in liquid medium due to worm movement may be misrepresented by the automation system as worms. Also, synchronized population would reduce the probability of error than mixed population.

Another observation in behaviour was the initial twitching of larvae on exposure to treatments. This could have been as a result of the 0.1% DMSO. DMSO concentration as low as 0.25% could trigger twitch in the worms (Raizen *et al.*, 2012).

The DES treatment exposure time (24 hours) used in the experiments is consistent with real life scenarios. For example, Karnaky (1949) administered daily doses of DES to women with high risk of abortion. However, it should be noted that DES usage, right from the 1940s (Shimkin and Grady, 1941) to the current decade (Zhang *et al.*, 2014) have shown that consistent exposure to the synthetic oestrogen can lead to reproductive disorders.

It is not out of place to suggest that for *C. elegans*, DES appears to support reproduction and growth. This is not surprising as a report suggested that DES is at least five times more potent than the naturally occurring oestradiol; the most

potent oestrogen in mammals (Noller and Fish 1974). Also, since cholesterol is important in the fluidity of lipid bilayers and membrane permeability in *C. elegans* as with other multicellular organism, it is likely that the worm expresses enzymes that can utilize cholesterol (Kurzchalia and Ward, 2003) as well as other sterol-like compounds converting them to usable compounds in order to meet its sterol requirement. This possibility is likely because *C. elegans* cannot synthesize sterols de novo (Chitwood *et al.*, 1983). It may be that DES is being modified by the nematode for its utilization. Further investigation such as the use of nuclear hormone receptor or oestrogen receptor mutant strains of *C. elegans* (Magner *et al.*, 2013 and Lindblom *et al.*, 2001) can be used to further understand the effect of the synthetic oestrogen on *C. elegans*.

Chapter Five

5 Toxicity assessment and prove of concept of target-specific anthelmintics

5.1 Part one

5.1.1 Introduction to tubulin-specific derivatized anthelmintic toxicity assessment

Anthelmintics are drugs or chemical compounds that selectively target helminth parasites in a host to inflict an effect that can halt reproduction and / or survival of the parasite while having minimal effect on the host. The selectivity of an anthelmintic can be influenced by its pharmacokinetic properties; which may cause the host to be exposed to lower concentrations of the drug than the parasite would. Anthelmintic selectivity can also be dependent on the inhibition of metabolic processes that are important for the parasite but not the host. In order for parasites to survive within their hosts, they require a steady diet, the ability to maintain homeostasis regardless of host immune response and the ability to reproduce successfully. Any interference to one or more of these processes may lead to the treatment and control of parasite infections. In other words, the compromise of the cellular integrity, neuromuscular coordination and / or host immunity evasion mechanisms are the answers to effectively treating parasitic infections. However, the increased use of available anthelmintics is accompanied by increasing frequency of parasite resistance to them (Sutherland and Leathwick, 2011). Since most anthelmintics are classified either based on their chemical structure, their site of action or their biochemical mechanisms, resistance of a parasite to any member of a class may also mean resistance to other members of that class. Therefore, it is important to synthesize better targeted anthelmintics that can circumvent such resistance. Any mention of parasites hereon refers to helminth parasites.

Some anthelmintics are able to disrupt the process of the effective communication of the nervous system with muscles in parasites leading to their paralysis and eventual flushing out from the host system. The anthelmintics that

induce this response do so by binding to two types of protein molecules; receptors and ion channels. One example is the nicotinic agonist that bind to the nicotinic acetylcholine receptor (nAChR) whose natural substrate is acetylcholine (ACh); a neurotransmitter that is commonly found in the central nervous system. When ACh binds to the nAChR it relays signal to the nerves to stabilize movement and balance. The nicotinic agonists also act on nAChR of some parasites by stimulating the ganglion activity in the parasite somatic muscle cells leading to paralysis following neuromuscular blockade (Martin and Robertson, 2010). A classical member of this group is levamisole. Another group of anthelmintics that disrupts neuromuscular efficiency are the glutamate-gated chloride channels potentiators. These include the macrocyclic lactone of which avermectin is a classical representative. They bind to the glutamate-gated chloride channel receptors (GluClR) in nerve cells of parasites to open the channel which allows an inflow of chloride ions. Due to the presence of different chloride channel subunits, parasites may show different responses to macrocyclic lactones as different parts of the parasites may be paralyzed. The most effective macrocyclic lactone usually paralyzes the pharynx of nematodes but the macrocyclic lactones do not affect cestodes and trematodes, probably because they do not possess GluClR. Although macrocyclic lactones are potent against parasites, some members like avermectin and other structurally related compounds can bind or modulate pentameric ligand-gated ion channel receptors of mammalian hosts (Lynagh *et al.*, 2011 and Adelsberger *et al.*, 2000); however with relatively low potency. One of the latest anthelmintics that affect neuromuscular efficiency are the amino-acetonitrile derivative (AAD). Monepantel is currently the only available member of this group that has been produced commercially. There are suggestions that it is an agonist that binds specifically to a nematode clade of AChR subunits precisely, a homomeric channel known as *mptl-1* which belongs to the DEG-3 family of nAChR (Kaminsky *et al.*, 2008). Depolarization of muscle cells in parasites occurs following a constant influx of ions and this leads to irreversible paralysis and eventual parasite death. The specificity of monepantel is high because the nAChR it binds to is only found in nematodes.

Anthelmintics that disrupt cellular integrity such as benzimidazole and its derivatives are often used as the first line of action in the treatment of parasitic infections. This group of anthelmintics inhibit tubulin polymerization. They are

also likely responsible for the inhibition of cellular transport and energy metabolism. The result of their inhibitory characteristics is the depolymerization of microtubules that encourages the depletion of energy and constipation in parasites; thus, leading to death (Vinaud *et al.*, 2008). There are suggestions that the selectivity of benzimidazoles for parasite infection treatment is encouraged by the ability of the host cells to augment genetic adaptation that prevents the disruption of microtubules in the host following exposure to benzimidazoles (Aleyasin *et al.*, 2014).

5.1.1.1 Tubulin-specific anthelmintic targeting

Colchicine is an anti-inflammatory derived from extracts of the flower *Colchicum autumnale* used generally for the treatment of gout. It is suggested that colchicine stops the assembly of microtubules leading to the disruption of inflammasome activation, leukotrienes and cytokine generation, phagocytosis and microtubule-based inflammatory cell chemotaxis (Dalbeth *et al.*, 2014). The information on colchicine reveals that it has a high affinity to bind tubulin and copolymerizes into microtubules rather than depolymerizing them. When colchicine binds to β -tubulin, a curved tubulin dimer is formed because of the steric action between α -tubulin and colchicine. This leads to the inhibition of microtubule assembly (Ravelli *et al.*, 2004). While colchicine may not affect the mitochondrion directly, its action on microtubules disrupts the biogenesis of the mitochondrion (Heggeness *et al.*, 1978). This is because the depolymerisation of microtubules is suggested to be responsible for the inhibition of mitochondrial content during the interphase of cell cycle (Karbowski *et al.*, 2001). Apart from the generation of cellular energy, the mitochondrion produces reactive oxygen species (ROS) in form of by-products of the electron transport chain. The production ROS is a reflection of cellular oxidative stress level and it can influence the destruction of biomolecules in biosystems where antioxidants are not sufficient to neutralize the ROS. Thus, cellular oxidative stress which is implicated in cell death and aging can originate from mitochondrial dysfunction (Balaban *et al.*, 2005). In addition, the mitochondrion plays a pivotal role in cellular calcium balance as the accumulation of mitochondrial calcium takes part in the regulation of aerobic metabolism (Contreras *et al.*, 2010). Furthermore, there are suggestions that

mitochondrial metabolic anomalies resulting from compromised or mutated mitochondrial DNA are factors that contribute to aging via apoptosis (Payne and Chinnery, 2015). Therefore, due to its role in cell life and death, the current research explores the mitochondrion as a viable target for colchicine in the treatment of parasitic helminth infections. Although colchicine is not an anthelmintic, it shares a similarity with benzimidazoles in that they both interact with the colchicine binding site in cells (Lacey, 1988; Lu *et al.*, 2012) thus, there is the prospect to develop colchine-based anthelmintics for the treatment of parasitic infections.

A major challenge that colchicine would face as an anthelmintic is its low therapeutic index. In order to address this concern, an approach that can be exploited is to take advantage of the negative potential (150 -180mV) of the mitochondrion's inner membrane (Zielonka *et al.*, 2017). Finichiu *et al.* (2013) demonstrated that lipid bilayers of the mitochondrion allow the easy passage of lipophilic cations due to the dispersion of their charge over a large surface area. This and the potential gradient of the lipophilic cations support their accumulation into the mitochondrial matrix. Triphenylphosphonium (TPP), which is one of the most common lipophilic cations, was demonstrated to accumulate preferentially in the inner core of the mitochondrion (Armstrong, 2007). In comparison to other lipophilic cations such as thiopyrylium AA-1 and rhodamine 123 that inhibit mitochondrial ATP synthesis (Sun *et al.*, 1994; Modica-Napolitano *et al.*, 1984), TPP is less toxic to the mitochondrion (Modica-Napolitano and Aprille, 2001) and have been successfully used to facilitate the delivery of drugs to the mitochondria (Patel *et al.*, 2010; Diers *et al.*, 2010). Luque-Ortega *et al.* (2010) revealed that TPP derivatives can induce low toxicity on mammalian cells while inflicting lethal effect on the protozoan parasite belonging to the genus *Leshmania*. This is achieved by targeting complex II of the respiratory chain thus, leading to decrease in both cytoplasmic ATP and electrochemical mitochondrial potential. They also inhibit oxygen consumption rate by using succinate as substrate.

Our collaborators at the chemistry department of Edinburgh Napier University have designed and produced prodrugs consisting of colchicine derivatives with TPP conjugates that can be activated within biological systems. The aim of the current research is to investigate the anthelmintic property of the prodrugs; precisely the colchicine derivatives and the enhanced activity of the colchicine-

TPP conjugates. Also, we examine the suitability of *C. elegans* as a representative model of parasitic helminths.

5.1.2 Results

5.1.2.1 Effect of tubulin-targeting drugs on *C. elegans* survival

Triphenylphosphonium (TPP) is a lipophilic cation which when conjugated with drugs delivers them to the mitochondrion. In order to show the effect that TPP has on the efficacy of drugs, L4 adults from synchronized cultures of wild-type worms were exposed to varying concentrations of an anthraquinone derivative; NU:UB 238 (see section B of the appendix for structure) or a NU:UB 238 and triphenylphosphonium conjugate (NU:UB 238-TPP) for 24 hours. The results (Figure 5.1) revealed that at 100 μ M, NU:UB 238 treatment resulted in less than 25% worm survival while NU:UB 238-TPP resulted in about 40% worm survival. On the other hand, 0.01 μ M, 0.1 μ M, 1 μ M and 10 μ M NU:UB 238 and NU:UB 238-TPP were not significantly different from one another with more than 95% of the worms surviving after exposure. The results imply that at 100 μ M, worms exposed to NU:UB 238-TPP survived almost twice as much as worms exposed to NU:UB 238.

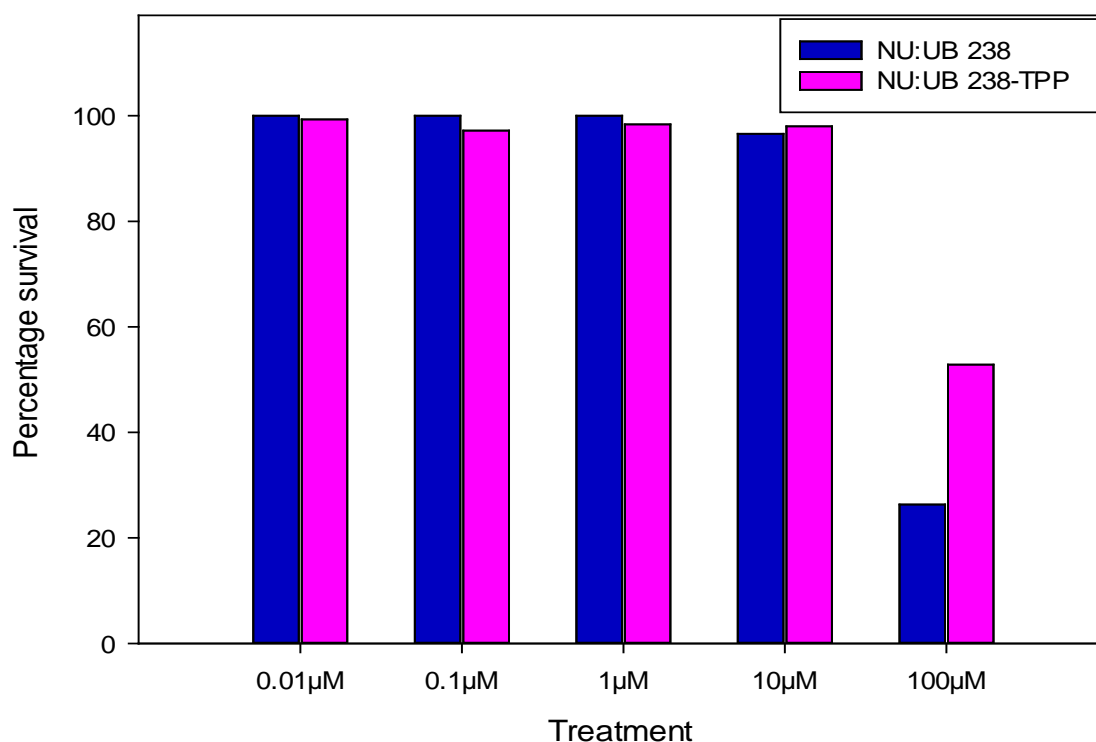


Figure 5.1: Effect of an anthraquinone derivative and its TPP conjugate on *C. elegans* survival

L4 worms from synchronized populations were exposed to 0.01 μM, 0.1 μM, 1 μM, 10 μM or 100 μM NU:UB 238 or NU:UB 238-TPP for 24 hours at 20°C where the control include untreated worms with percentage survival >98% (not shown). The number of live worms in each treatment group was divided by the total number of worms in the group and multiplied by 100 to get the percentage survival. The data was drawn from three separate experiments where $178 \geq n \geq 123$ for each treatment group.

While the aim of the results in figure 5.1 was to describe the effect of TPP on drug enhancement, the anthraquinone derivative used was originally designed for the inhibition of DNA topoisomerase I and II enzymes (Pettersson 2004) in cancer chemotherapy. However, because one interest in the current research is anthelmintic therapy, a colchicine derivative; MB2 and a MB2-TPP conjugate were designed to test their anthelmintic and enhanced anthelmintic properties respectively. In figure 5.2 the 100 μM MB2 treatment resulted in about 50% worm survival while 100 μM MB2-TPP resulted in about 95% worm survival. On the other hand, 0.01 μM, 0.1 μM, 1 μM and 10 μM MB2 and MB2-TPP were not significantly different from one another with more than 95% of the worms surviving after exposure. The results suggest that at 100 μM, MB2 is more effective than MB2-TPP.

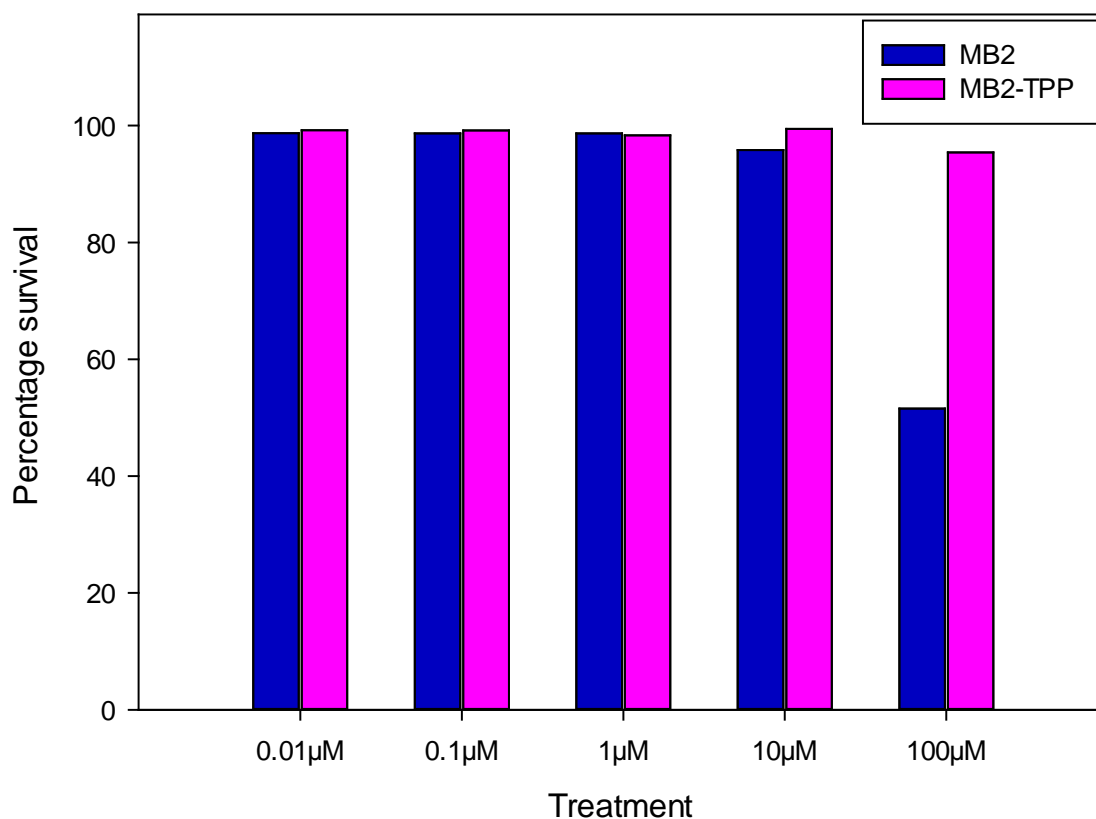


Figure 5.2: Effect of MB2 and MB2-TPP on *C. elegans* survival.

L4 worms from synchronized populations were exposed to 0.01 μM, 0.1 μM, 1 μM, 10 μM or 100 μM MB2 or MB2-TPP for 24 hours at 20°C where the control include untreated worms with percentage survival >97% (not shown). The number of live worms in each treatment group was divided by the total number of worms in the group and multiplied by 100 to get the percentage survival. The data was drawn from three separate experiments where $205 \geq n \geq 122$ for each treatment group).

Apart from the MB2 series of compounds, another series of colchicine derivatives, GEO1 and GEO2 (GEO1-TPP conjugate) were tested for their anthelmintic properties. More than 90% of worms exposed to 1 μM, 25 μM, 50 μM, 75 μM and 100 μM GEO1 or GEO2 survived with no significant difference among the groups of treatments (Figure 5.3). Unlike the observations in figures 5.1 and 5.2, there was no significant difference between the survival of worms treated with 100 μM GEO1 and GEO2.

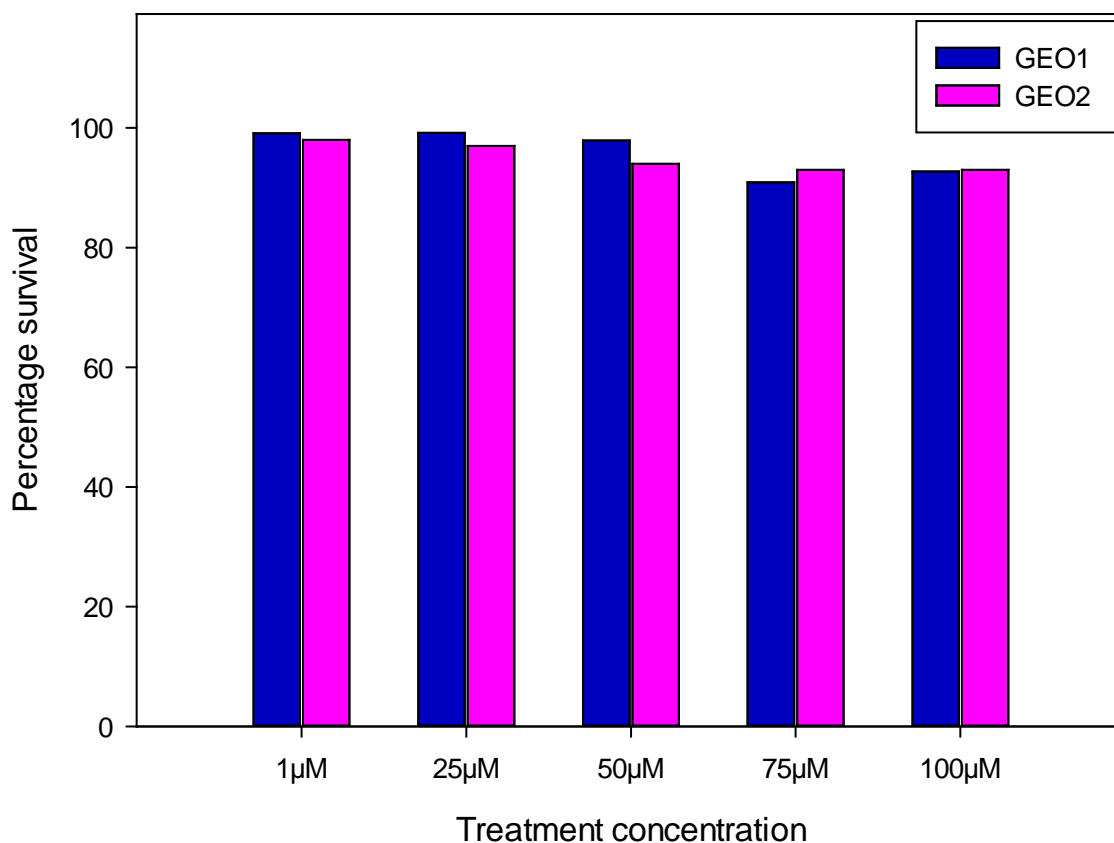


Figure 5.3: Effect of colchicine and colchicine-based drugs on *C. elegans* survival.

L4 worms from synchronized populations were exposed to 1 μM, 25 μM, 50 μM, 75 μM or 100 μM GEO1 or GEO2 (where GEO2 is GEO1-TPP conjugate) for 24 hours at 20°C where the control include untreated worms with percentage survival >99% (not shown). The number of live worms in each treatment group was divided by the total number of worms in the group and multiplied by 100 to get the percentage survival. The data was drawn from three separate experiments where $248 \geq n \geq 121$ for each treatment group.

5.1.2.2 Effect of tubulin-targeting drugs on *C. elegans* behaviour

The behaviour of *C. elegans* is modulated in response to a number of stimuli including drugs. As a representative model of helminth parasites, the effect of derivatized anthelmintics was investigated in *C. elegans*. Having previously investigated the lethality of some colchicine derivatives (Figures 5.2 and 5.3), the effect of GEO compounds on worm body bend was investigated (Figure 5.4). While there is a random pattern in the concentration response of the worms to each treatment in figure 5.4, the trend for colchicine (COL), GEO1 and GEO2 were similar. Generally, for the three aforementioned treatment groups, there was a percentage increase in the number of worm body bends at 400 μM in comparison to the untreated group (12%, 16% and 33% for COL, GEO1 and GEO2 respectively).

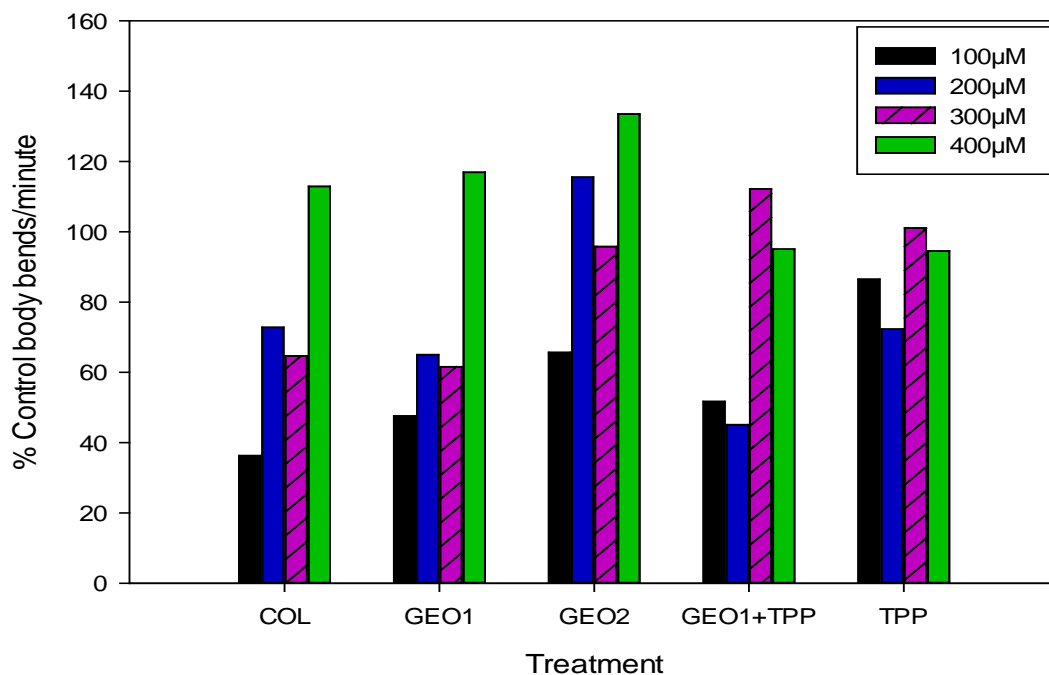


Figure 5.4: Effect of colchicine and colchicine-based drugs on *C. elegans* body bend.

First day adult worms were exposed to colchicine (COL), a colchicine derivative (GEO1), GEO1 conjugated with a triphosphonium moiety (GEO2), a mixture of GEO1 and triphosphonium (GEO1+TPP), or triphosphonium (TPP) for 24 hours. The worms were from a synchronized population (20°C) and were captured in 60mm Petri plates over a 20 second period. Individual worms were tracked and body bends per seconds were recorded using the worm tracker plugin on ImageJ. The mean of data from each treatment concentration was normalized by calculating body bend per minute (BBPM) and subsequently the percentage BBPM as a percentage of BBPM from untreated worms. The untreated worms were incubated in S medium. Data was generated from 403 worms with each treatment containing between 1 and 53 worms. Due to the unequal variance among sample groups, ANOVA on ranks (H-test) was used for statistical analysis where $H = 119.059$ with 19 degrees of freedom ($P = <0.001$).

Also, within the three treatment groups, GEO2 seemed to have the highest percentage of body bends at all four concentrations (100µM, 200µM, 300µM and 400µM). The additional effect of GEO1 and triphenylphosphonium (GEO1+TPP) was also investigated in the experiment and its concentration response pattern was similar to that of triphenylphosphonium (TPP) alone.

Furthermore, the effect of GEO compounds on worm speed was investigated (Figure 5.5). There was a random pattern in the concentration response of the worms to each treatment in the trend for experiment with an inconsistent pattern across the treatment groups. One notable observation was that there was a percentage increase in speed of worms exposed to COL, GEO1 and GEO2 in comparison to the untreated group.

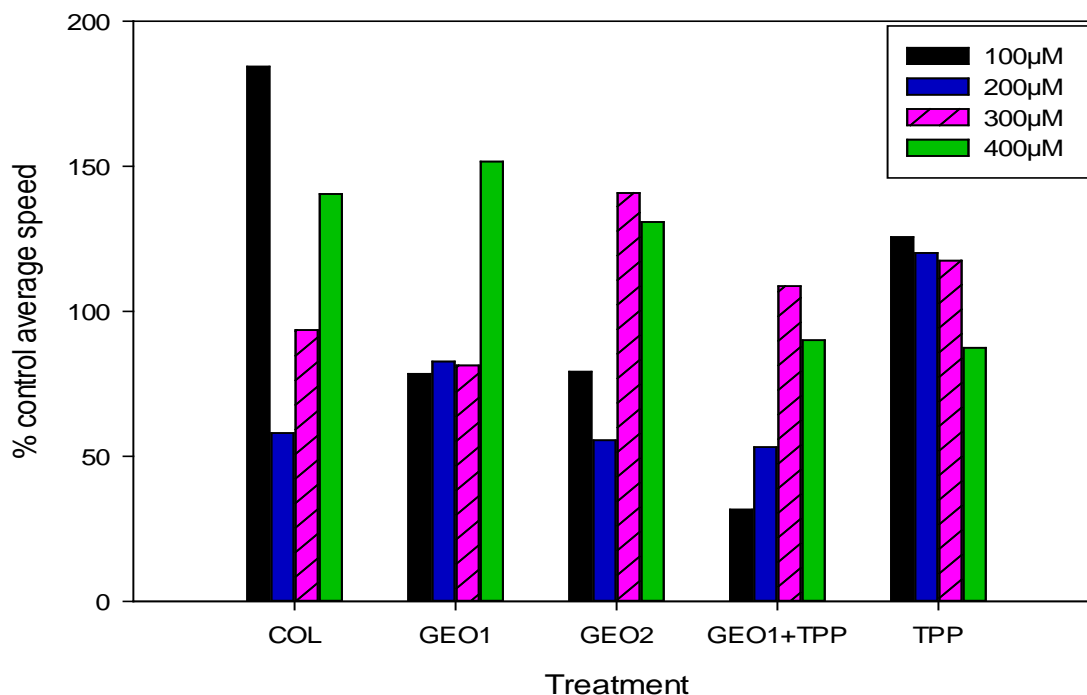


Figure 5.5: Effect of colchicine and colchicine-based drugs on *C. elegans* speed.

First day adult worms were exposed to colchicine (COL), a colchicine derivative (GEO1), GEO1 conjugated with a triphosphonium moiety (GEO2), a mixture of GEO1 and triphosphonium (GEO1+TPP), or triphosphonium (TPP) for 24 hours. The worms were from a synchronized population (20°C) and were captured in 60mm Petri plates over a 20 second period. Individual worms were tracked and speed was recorded in pixel per second using the worm tracker plugin on ImageJ. The mean of data from each treatment concentration was normalized by calculating the speed as a percentage of untreated worms' average speed. The untreated worms were incubated in S medium. Data was generated from 465 worms with each treatment containing between 1 and 60 worms. Due to the unequal variance among sample groups, ANOVA on ranks (H-test) was used for statistical analysis where $H = 97.254$ with 19 degrees of freedom ($P = <0.001$).

5.1.3 Discussion

Anthelmintic derivatives made up of colchicine-based drugs and their triphenylphosphonium (TPP) conjugates were tested on *C. elegans* to investigate their anthelmintic properties. The conjugates are made up of the derivatized drugs which are linked to a TPP moiety with an ester bond. The in-house synthesized derivatized anthelmintic compounds were screened against *C. elegans* owing to its anatomical and physiological resemblance with the parasite helminth. For the colchicine-based drug; MB2 (Figure 5.2), it is likely that the compounds exhibit anthelmintic activity in a dose-dependent manner given that about 50% of the worms died at 100µM. On the other hand, while it was expected that MB2-TPP conjugate would be more effective than MB2, this was not the case as more than 90% of the worm survived. One possible cause of this observation is the solubility of MB2-TPP. Although, MB2-TPP dissolves in DMSO, its

administration to the *C. elegans* test samples resulted in reprecipitation in solution (observed during treatment preparation and microscopic investigation). This could have resulted in a reduction of the actual concentration of MB2-TPP in the treatment. A similar observation was noticed in the NU:UB compounds and this was also reflected in the results (Figure 5.1) which showed that NU:UB 238 was more effective than NU:UB 238-TPP conjugate. One difference between the lethal effect of NU:UB 238-TPP and GEO2 is that NU:UB 238-TPP seemed more potent than GEO2. This was expected as the NU:UB series of compounds are anthroquinone-based and were originally designed as cancer therapeutics so they are suspected to be naturally toxic to cells. The NU:UB compounds were only included in the current study to show the potential of TPP in enhancing drug delivery.

The results of the GEO1 and its TPP conjugate (GEO2) suggest no lethal effect on the worms at 100 μ M following a 24h exposure (Figure 5.3). A further increase in concentration and incubation for 24h (i.e. 48-hour exposure) suggests that there was a clear difference between the GEO1 and GEO2-treated samples with more than 20% lethality observed in worms treated with 200 μ M to 800 μ M GEO2 (observation with Dr. Rosa De Llanos). This suggests that the effect of the derivatized anthelmintics TPP conjugate (GEO2) is time and concentration-dependent, and the TPP is likely responsible for the enhanced effect of GEO2 due to the affinity of TPP for mitochondria. This is likely due to the ability of TPP to cross phospholipid bilayers without requiring a transporter allowing easy uptake of GEO1 (product of the conjugate following suspected cleavage of ester bond by worm esterase) into the mitochondria (Finichiu *et al.*, 2013) thereby causing the disruption of the organelle and eventual death of the worm. One unanswered question with respect to high concentrations of the anthelmintic derivatives is the effect they may pose to the host and possibly the environment when discharged through waste products.

A possible reason for the low anthelmintic effect of GEO series of compounds exhibited at 100 μ M may be due to the lack of characterization of the compound for predictive anthelmintic properties. Characterization of anthelmintic should be the first step in the design of anthelmintic drugs. Technological advancement in the development of techniques that can be used to acquire the atomic structure of protein-ligand interaction has created an avenue for the development of

molecules that target specific sites (Gore and Desai, 2014). This approach is a computer structure-based design of drugs. A common example of this is molecular docking which refers to the process of refining drug molecular structure by manipulating the separation between the drug and its target site whilst maintaining their relative fixed orientation and internal geometry at computational level (Kitchen *et al.*, 2004) and (Meng *et al.*, 2011). This helps to predict the best interaction between the drug and its target site. In the inhibition of enzymatic processes, ligand-binding is important, thus forming a foundation for strategy of drug design (Sliwoski *et al.*, 2013). Molecular docking has been successfully used to design prospective antimicrobial agents against infections such as *Mycobacterium tuberculosis* (Obiol-Pardo *et al.*, 2011) or *Plasmodium falciparum* (Guggisberg *et al.*, 2014). This evidence suggests that molecular docking analysis of the anthelmintic derivatives described in this study might provide the feasibility of their efficiency in the treatment of helminth infections.

For behavioural analysis, two endpoints; body bends per minute and the average speed of worms were investigated. The treatment of *C. elegans* with GEO compounds revealed that while there was variability in terms of concentration response to the GEO compounds, there was increased number of body bends per minute (BBPM) in GEO2 in comparison to GEO1; suggesting that the TPP enhanced the effect of GEO1 (Figure 5.4). GEO1+TPP were included in the experiment to show the unconjugated additional effect of GEO1 and TPP. The BBPM observed in in GEO1+TPP was relatively lower than that observed in GEO2. It was clear from the findings that the effect of GEO2 was not as a result of the additional effect of TPP to GEO1 but rather, the supposed release and accumulation of active GEO1 in the cell. Moreover, a close look at colchicine and GEO1 revealed similar behavioural activity in terms of BBPM. On the other hand, the average speed of treated worms (Figure 5.5) did not clearly reflect the observations of worm BBPM. One notion is that exposure to the drugs induced an effect which could be high or low speed. Specifically, the effect of drugs on worm tubulin would likely affect the functionality of the sensory cilia associated with movement (Hurd *et al.*, 2010).

Summarily, the behavioural analysis results reveal that BBPM is more sensitive and have a low variability when compared to speed as endpoints of toxicity.

5.2 Part two

5.2.1 Introduction to legumain-specific anthelmintic targeting: A proof of concept

From the ecological viewpoint, the effect of chemical substances on *C. elegans* can be used as a measure of toxicity on the biota of an ecosystem. Parasitic helminths may share a common ecosystem with *C. elegans* hence; chemical substances that have toxic effects on *C. elegans* may have similar effects on parasites from the same ecosystem. *C. elegans* can be used as a model for the study of anthelmintic properties. Parasitic helminths are difficult to keep alive over a long period of time outside their host and access to the infective stage parasites would require killing the host so; they are not best suited to be used directly in the study of anthelmintic properties. *C. elegans* has been used as an experimental model in the study of commercial anthelmintic effects and meets some requirements needed for testing as it can be easily genetically manipulated besides being cost-effective and readily available.

Because *C. elegans* is a representative member of the phylum Nematoda which has some parasitic members, it is important to understand its relationship with the parasites in the phylum. Taxonomic classification of nematodes has been quite difficult as evolutionary relationships are challenged by constant reviews and ongoing discoveries; however, one classification is based on molecular phylogenetics which involves the use of a gene or genes from different taxa to construct a dataset of homologous traits. Specifically, *C. elegans* small subunit rRNA (18S rRNA) analysis suggests that the worm is closely related to parasitic nematodes in the order *Strongylida* (Fitch and Kelly-Thomas, 1997) which includes *Teladorsagia* and *Haemonchus*. As a result of successful molecular study on *C. elegans*, genetic similarities between the nematode and parasitic nematodes make it a potential model for the study of anthelmintics.

Having described the challenges of anthelmintic resistance (chapter one, section 1.5.5), there is a need to develop more effective or better-targeted drugs that would combat resistance. Cysteine proteases are common in *C. elegans* and are also conserved in some parasitic worms from the same class (Jasmer *et al.*, 2001). Specifically, it has been demonstrated that the cysteine protease; legumain is present in parasitic worms (Oliver *et al.*, 2006). It cleaves asparagine in the P1 position adjacent to the C-terminus of protein substrates (Chen *et al.*,

1997). In order for active drug molecules to be released into a biosystem, legumain in the biosystem cleaves a prodrug consisting of an amino acid substrate and the active drug to release the active drugs into its locality. The current research hypothesizes that this would improve the target of such drug. There are some other rational approaches to developing more efficient anthelmintics such as targeting endosymbionts that are essential for parasite development (Slatko *et al.*, 2010), protein-protein interaction (Taylor *et al.*, 2011) or receptor binding (Sager *et al.*, 2009). However, the choice of these anthelmintic candidates is sometimes flawed by the function, existence or conservation of their target in parasitic helminth species. These challenges can be overcome using the current legumain-target approach.

The aim of the research is to show proof of concept that the legumain cysteine protease can be investigated as a potential for enhanced anthelmintic targeting using *C. elegans* as a representative model of parasitic helminths. We explore the use of the *C. elegans* and a probe containing a fluorophore which is used as a biomarker, attached to a tripeptide group that would serve as a quencher. Initially, the legumain-targeting probes were designed for the purpose of targeting cancer cells which express increased legumain compared to normal healthy cells (Jinq-may Chen *et al.*, 1997). The probe is activated once legumain cleaves the tripeptide to release the fluorophore which would fluoresce. This would be measured by a fluorimeter. It is intended that this concept be replicated in the target parasitic helminth. The success of this would reduce the use of higher concentrations of anthelmintic drugs but improve the efficacy of the drugs.

5.2.2 Results

5.2.2.1 Legumain activation of TL11 probe by helminth homogenates

In order to demonstrate legumain enzyme activity in helminths, homogenate of the free-living worm; *Caenorhabditis elegans* and the parasitic worms, *Teladorsagia circumcincta* and *Haemonchus contortus* were exposed to a fluorescein-based probe TL11 that fluoresces following cleavage by legumain (see introduction). Two cysteine protease inhibitors, Iodoacetamide and N-phenylmaleimide that are specific inhibitors of legumain, and a general cysteine protease inhibitor (E-64) with no inhibitory effect on legumain (Barrett *et al.*, 1992

and Chen *et al.*, 1997) were introduced into the experiment. Fluorescence resulting from fluorescein after cleavage of the probe which acts as substrate is directly proportional to legumain activity in the homogenates.

After 120 minutes of exposure to TL11 (Figure 5.6), fluorescence intensity was observed in all the treatment groups with a linear relationship maintained over the time course suggesting activation of TL11 probe by the *C. elegans* homogenate in all the treatments; however, the fluorescence intensity of the treatment group that had no inhibitor (CeT) was significantly higher ($p < 0.001$) than other treatment groups that contained inhibitors. At 120 minutes, fluorescence of the treatment group containing E-64 (CeET) was significantly higher ($p < 0.001$) than that containing N-phenylmaleimide (CeNT) which recorded the lowest fluorescence intensity; however, CeET was not statistically different from the treatment group containing Iodoacetamide (CeIT). CeIT and CeNT were similar in terms of their low fluorescence intensities. The reduction in the relative fluorescence intensity of CeIT and CeNP as compared to CeT suggests that the activation of the TL11 probe was inhibited. The speed of the increase in relative fluorescence intensity which is a measure of the rate of probe cleavage reaction was highest for CeT and lowest for CeNT.

In order to determine enzyme activity following interaction of the fluorescein-labelled probe with parasitic worms, *T. circumcincta* homogenate was treated with TL11 in the presence or absence of a legumain-specific inhibitor (Iodoacetamide) or a non-legumain inhibitor (E-64). The results in figure 5.7 revealed that fluorescence occurred following exposure of *T. circumcincta* homogenate to the probe suggesting activation of the probe by the homogenate, thus enzyme activity. Like the *C. elegans* homogenate, a linear relationship was maintained over a two-hour time course in the treatment group without the protease inhibitors (TcT) and the E-64-treated group (TcET). TcT recorded the highest fluorescence intensity at 120 minutes (approximately 5700 relative fluorescence unit (RFU)), while the rate of reaction of TcET was slower reaching around 3860RFU at 120 minutes. The Iodoacetamide-treated group (TcIT) tended towards optimal fluorescence intensity at about 1160RFU suggesting the stoppage of reaction, hence an inhibition of enzyme activity.

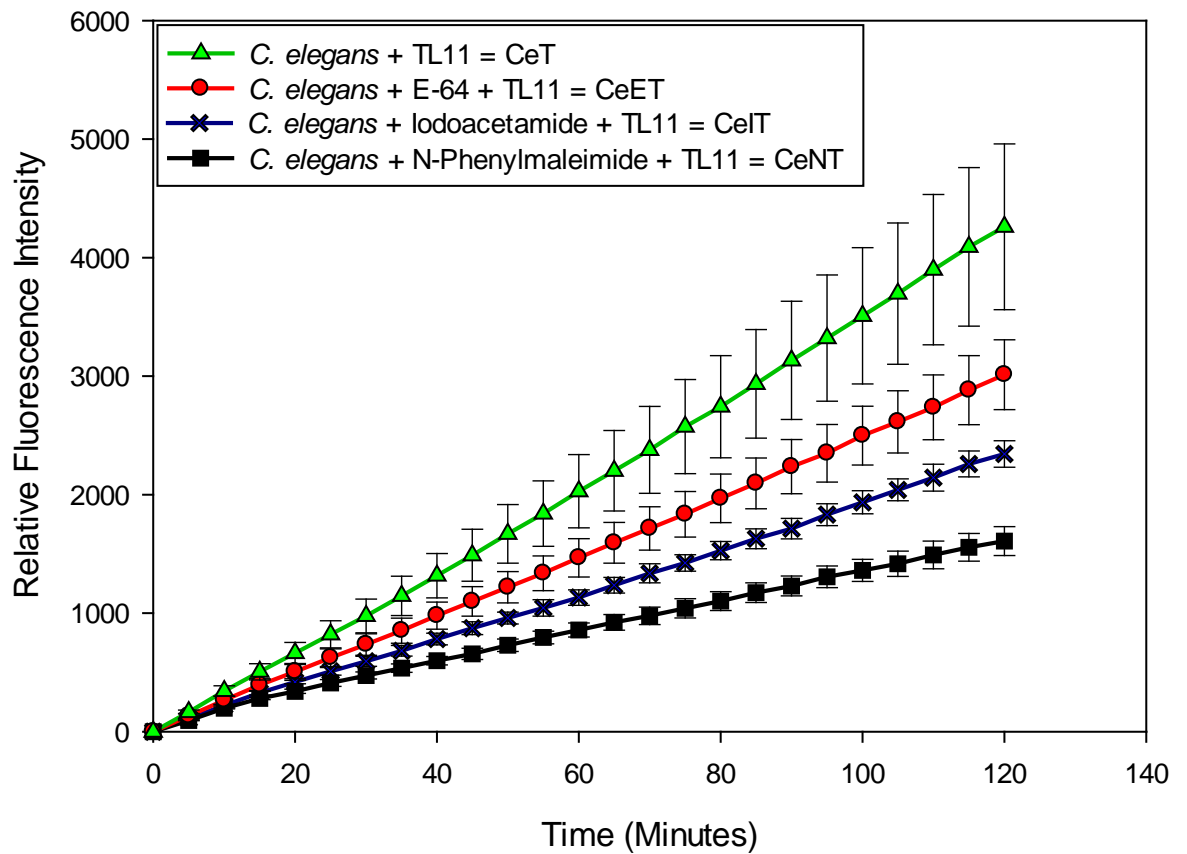


Figure 5.6: Activation of TL11 by wild type *C. elegans* homogenate.

Mixed population of homogenized *C. elegans* (approximately 3000 L4 worms in mixed culture) was treated with TL11 (10 μ M) probe with or without either iodoacetamide (1mM), N-phenylmaleimide (1mM) or E-64 (100 μ M). The final treatment volume of 100 μ l per well in a 96 well plate was made up using 2-(N-morpholino) ethanesulfonic acid (MES) buffer at pH5. Controls (not shown) included fluorescein, TL11 in MES buffer, *C. elegans* homogenate in MES buffer and MES buffer alone. Treatments were incubated at 22 $^{\circ}$ C in triplicate and fluorescence intensity with excitation and emission wavelength of 485nm and 520nm respectively, was monitored over a 2-hour period. Each treatment data recorded by the Omega fluorimetric software (Biostar) was normalized to a starting relative intensity unit of zero. Statistical analysis was performed using two-way ANOVA with error bars representing \pm SD.

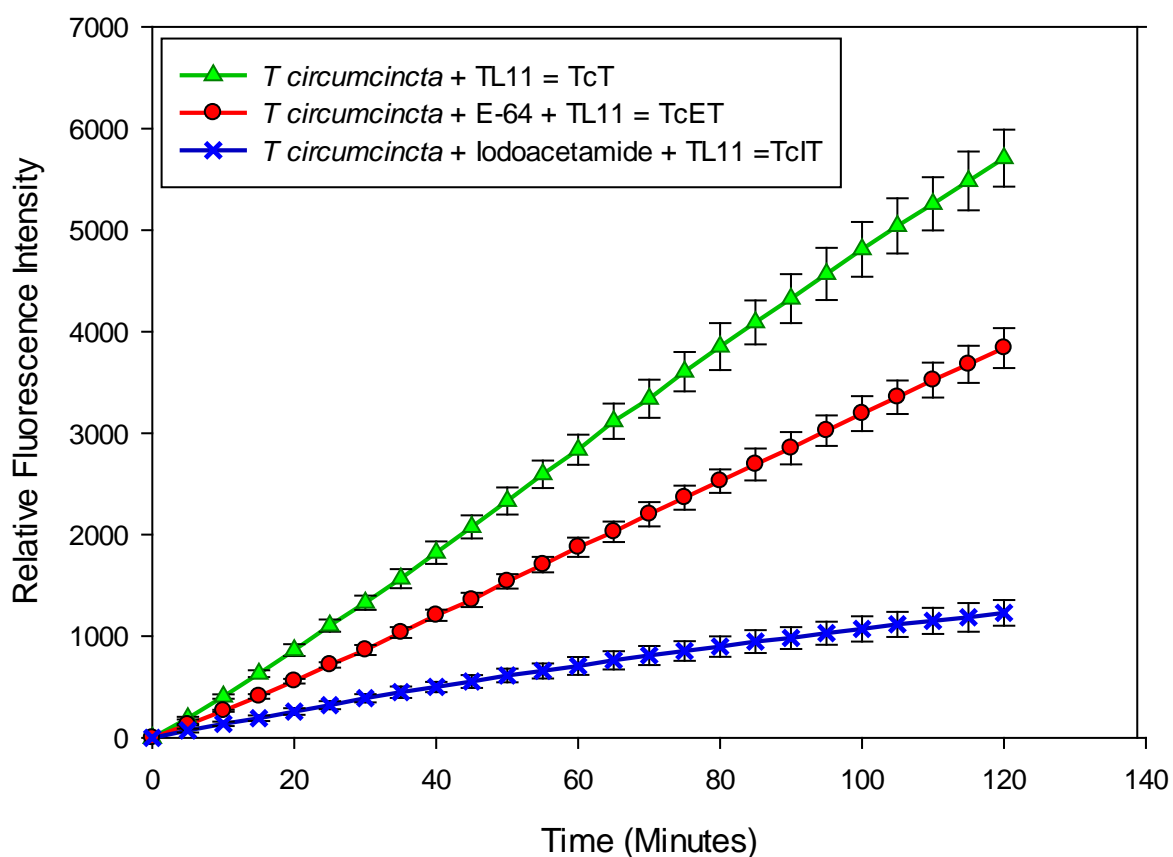


Figure 5.7: Activation of TL11 by *T. circumcincta* homogenate.

T. circumcincta homogenate was treated with TL11 (10µM) probe with or without either iodoacetamide (1mM) or E-64 (100µM). The final treatment volume of 100µl per well in a 96 well plate was made up using MES buffer (pH5). Controls (not shown) included fluorescein, TL11 in MES buffer, *T. circumcincta* homogenate in MES buffer and MES buffer alone. Treatments were incubated at 22°C in triplicate and fluorescence intensity with excitation and emission wavelength of 485nm and 520nm respectively, was monitored over a 2-hour period. Each treatment data recorded by the Omega fluorimetric software (Biostar) was normalized to a starting relative intensity unit of zero. Statistical analysis was performed using two-way ANOVA with error bars representing ±SD.

H. contortus homogenate was treated with TL11 in the presence or absence of iodoacetamide or E-64 and the results (Figure 5.8) reveal that *H. contortus* homogenate without inhibitor treatment (HcT) was high and was not statistically different from homogenate treated with iodoacetamide (HcIT) with the rate of reaction of both treatment groups tending towards an optimal relative fluorescence intensity of approximately 14000RFU and suggesting the activation of the probe molecules by enzyme in the samples was almost complete. At 120 minutes, E-64-treated *H. contortus* homogenate (HcIT) recorded a relative fluorescence intensity of approximately 1600RFU that was significantly lower (p

< 0.001) than HcT and HcIT with the line of reaction tending towards a curve thus, indicating inhibition of reaction.

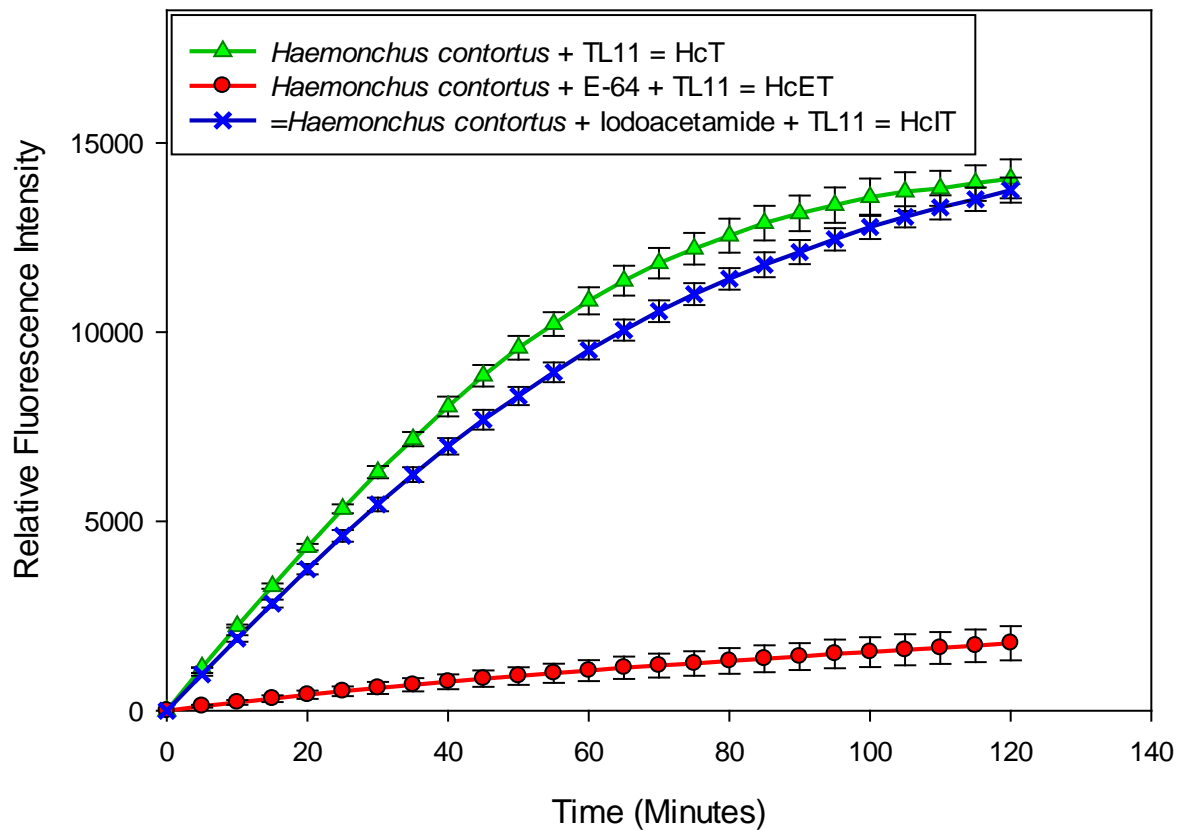


Figure 5.8: Activation of TL11 by *H. contortus* homogenate.

H. contortus homogenate was treated with TL11 (10 μ M) probe and with or without either iodoacetamide (1mM) or E-64 (100 μ M). The final treatment volume of 100 μ l per well in a 96 well plate was made up using MES buffer (pH5). Controls (not shown) included fluorescein, TL11 in MES buffer, *H. contortus* homogenate in MES buffer and MES buffer alone. Treatments were incubated at 22 $^{\circ}$ C in triplicate and fluorescence intensity with excitation and emission wavelength of 485nm and 520nm respectively, was monitored over a 2-hour period. Each treatment data recorded by the Omega fluorimetric software (Biostar) was normalized to a starting relative intensity unit of zero. Statistical analysis was performed using two-way ANOVA with error bars representing \pm SD.

5.2.2.2 Effect of pH on activation of LS9 probe by parasitic helminth homogenates

According to Chen *et al.* (1998), the optimal pH at which mammalian legumain cleaves protein substrates best is pH5. In order to determine the sensitivity of parasite homogenate legumain activity to pH, four different pH levels were tested. This was necessary to accommodate the different pH in infection or parasitic worm localized sites of mammal hosts. Homogenate of *T. circumcincta* was prepared in phosphate citrate buffer of pH4, 5, 6 or 7 and incubated with LS9; a

rhodamine-based probe for two hour. The progress curve graph (Figure 5.9) revealed that at pH5, the reaction between *T. circumcincta* homogenate and LS9 (TcL) maintained a distinct linear progression with approximately 2800RFU and the highest fluorescence intensity thus, the fastest rate of reaction at 120 minutes. For TcL at pH4, 6 and 7, the curves were approaching a non-linear part with pH4 and 6 exhibiting was no statistical difference between the fluorescence intensities and reaching approximately 2000RFU.

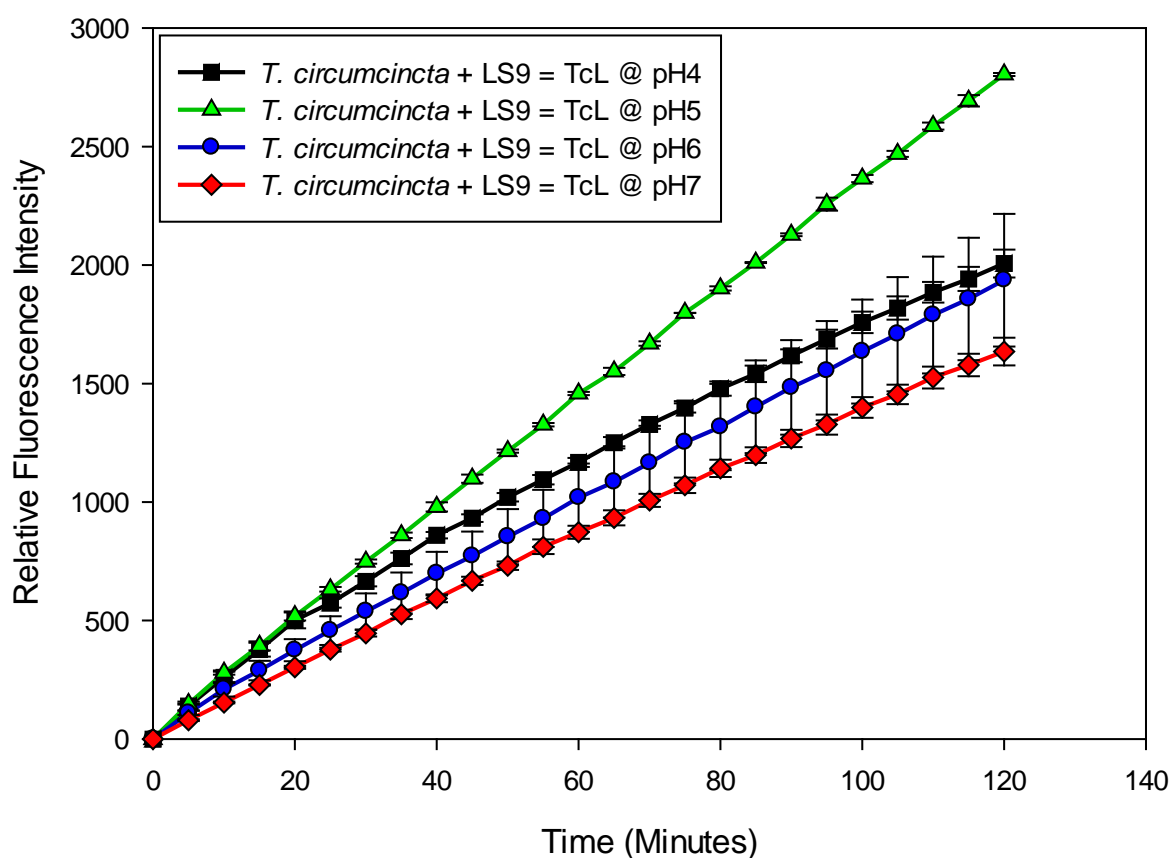


Figure 5.9: pH effect on the activation of LS9 by *T. circumcincta* homogenate.

T. circumcincta homogenate was treated with LS9 probe (10 μ M) using Phosphate citrate (PCB) buffer of pH4, 5, 6 or 7 to make up a final volume of 100 μ l per well in a 96 well plate. Controls (not shown) included rhodamine in PCB buffer (pH 4, 5 6 and 7), LS9 in PCB, *T. circumcincta* homogenate in PCB and PCB buffer alone. Treatments were incubated at 22 $^{\circ}$ C in triplicate and fluorescence intensity with excitation and emission wavelength of 544nm and 590nm respectively, was monitored over a 2-hour period. Each treatment data recorded by the Omega fluorimetric software (Biostar) was normalized to a starting relative intensity unit of zero. Statistical analysis was performed using two-way ANOVA with error bars representing \pm SD.

For *H. contortus* exposure to LS9 (HcL) at varying pH over a two-hour period (Figure 5.10), the highest intensity was recorded for HcL at pH5 which peaked an optimal fluorescence intensity of approximately 16000 RFU while at pH6 HcL

recorded the fastest rate of reaction but an optimal intensity around 12200RFU was recorded suggesting inhibition at pH6. HcL incubated at pH4 was the only treatment group that exhibited a linear progression after 120 minutes reaching approximately 13600RFU.

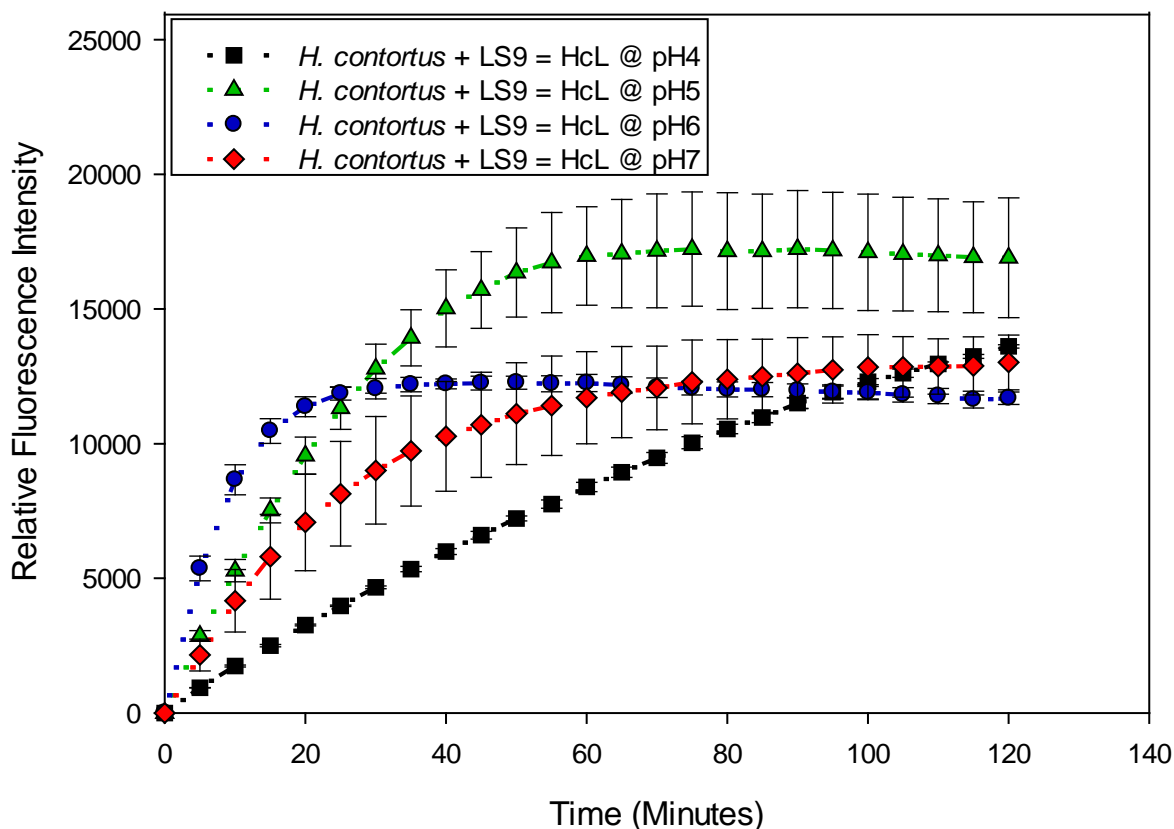


Figure 5.10: pH effect on the activation of LS9 by *H. contortus* homogenate.

H. contortus homogenate was treated with LS9 probe (10 μ M) using PCB buffer of pH4, 5, 6 or 7 to make up a final volume of 100 μ l per well in a 96 well plate. Controls (not shown) included rhodamine in PCB buffer (pH 4, 5 6 and 7), LS9 in PCB, *H. contortus* homogenate in PCB and PCB buffer alone. Treatments were incubated at 22 $^{\circ}$ C in triplicate and fluorescence intensity with excitation and emission wavelength of 544nm and 590nm respectively, was monitored over a 2-hour period. Each treatment data recorded by the Omega fluorimetric software (Biostar) was normalized to a starting relative intensity unit of zero. Statistical analysis was performed using two-way ANOVA with error bars representing \pm SD.

5.2.2.3 Legumain activation of LS9 probe in sheep plasma

For the investigation of the presence of legumain in sheep plasma, dilution was made in phosphate citrate buffer (pH4, 5, 6 or 7), and incubated with LS9 probe for two hours (Figure 5.11). The result revealed no activity among the treatment groups as there was no significant fluorescence intensity (less than 40RFu) at all pH observed. This suggests that the probe was not activated by sheep plasma.

A repeat analysis on the sheep plasma experiment at pH5 was set up with *H. contortus* homogenate (HcL). The result showed ample difference in LS9 activation with HcL almost peaking its optimal fluorescence intensity at approximately 15300RFU thus tending towards the completion of the reaction at about 120 minutes after incubation while no quantifiable change was seen in sheep plasma (Figure 5.12).

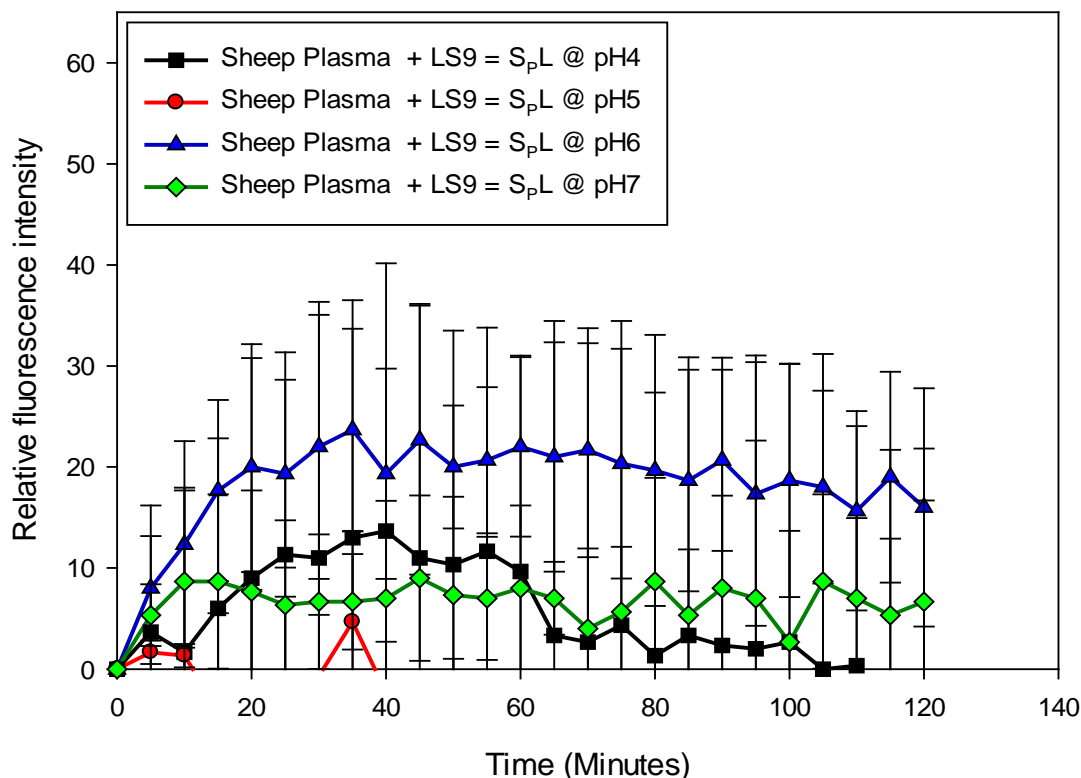


Figure 5.11: pH effect on the activation of LS9 by sheep plasma.

Sheep plasma was treated with LS9 probe (10 μ M) using PCB buffer of pH4, 5, 6 or 7 to make up a final volume of 100 μ l per well in a 96 well plate. . Controls (not shown) included rhodamine in PCB buffer (pH 4, 5, 6 and 7), LS9 in PCB, sheep plasma in PCB and PCB buffer alone. Treatments were incubated (22 $^{\circ}$ C) in triplicates and fluorescence intensity with excitation and emission wavelength of 544nm and 590nm respectively, was monitored over a 2-hour period. Each treatment data recorded by the Omega fluorimetric software (Biostar) was normalized to a starting relative intensity unit of zero. Statistical analysis was performed using two-way ANOVA with error bars representing \pm SD.

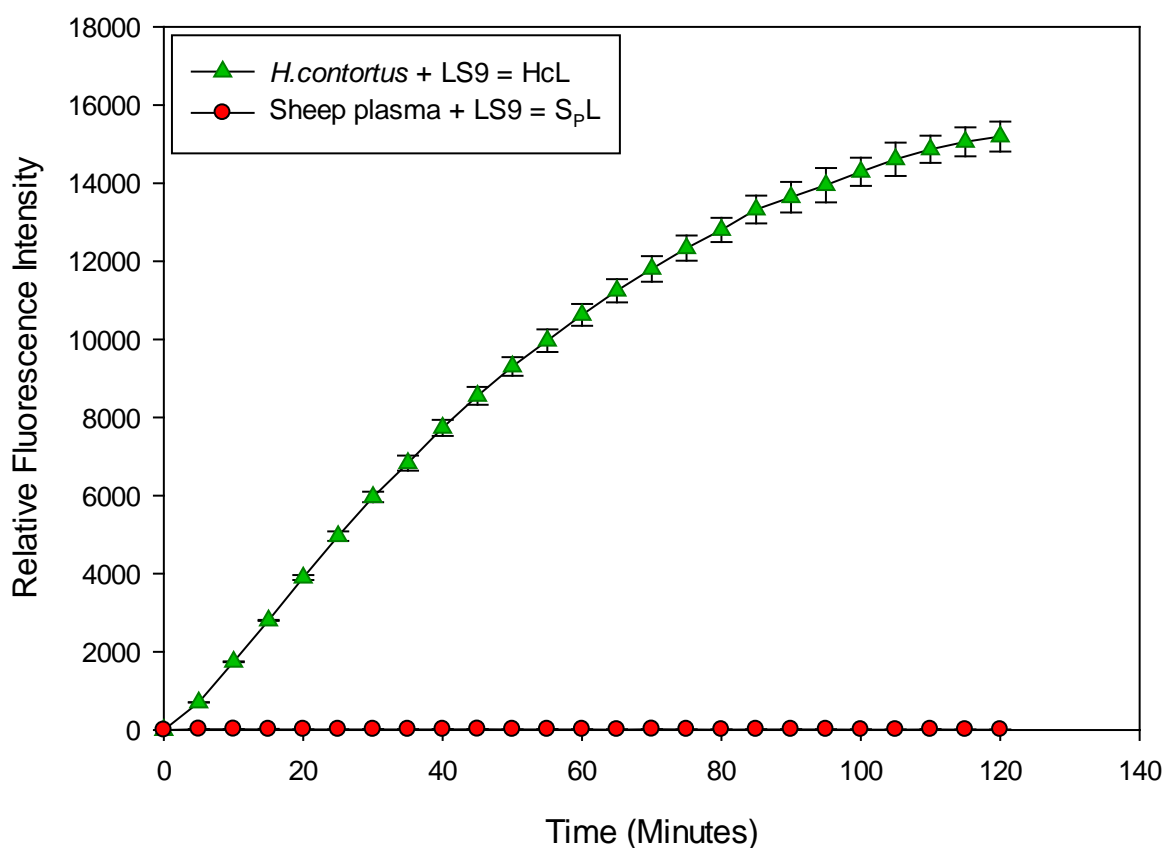


Figure 5.12: Comparison between LS9 activation in *H. contortus* homogenate and sheep plasma.

H. contortus homogenate or sheep plasma was treated with LS9 (10 μ M) probe. The final treatment volume of 100 μ l per well in a 96 well plate was made up using PCB buffer (pH5). Controls (not shown) included rhodamine in PCB buffer, LS9 in PCB, *H. contortus* homogenate in PCB and PCB buffer alone. Treatments were incubated at 22 $^{\circ}$ C in triplicate and fluorescence intensity with excitation and emission wavelength of 485nm and 520nm respectively, was monitored over a 2-hour period. Each treatment data recorded by the Omega fluorimetric software (Biostar) was normalized to a starting relative intensity unit of zero. Statistical analysis was performed using two-way ANOVA with error bars representing \pm SD.

5.2.2.4 Legumain activation of LS9 probe in sheep liver tissue homogenate

Having examined sheep plasma for LS9 activation, legumain activation in sheep liver tissue was investigated. The result (Figure 5.13) showed that at pH5, sheep liver tissue homogenate treated with LS9 in the absence of protease inhibitors (L τ L) revealed the highest fluorescence intensity but progressed towards a non-linear curve, however, a similar pattern was observed by liver tissue treated with E-64 (L τ EL) but the reaction rate was slower and the progression into a non-linear curve was faster. The treatment containing iodoacetamide (L τ IL) was beginning to reach its optimal intensity at 120 minutes following exposure. N-phenylmaleamide-treated sample (L τ NL) did not exhibit any fluorescence

suggesting complete non-activation of LS9 thus, no enzyme activity was observed.

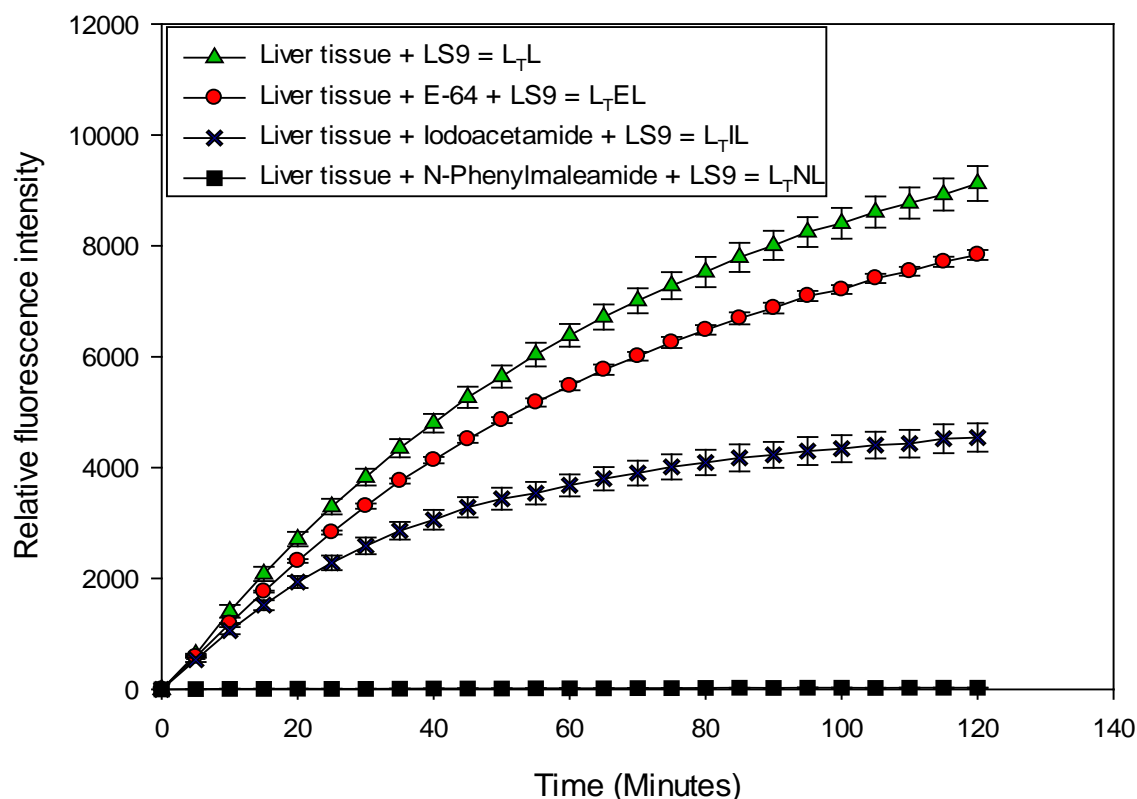


Figure 5.13: Activation of LS9 by sheep liver tissue homogenate.

Sheep liver tissue homogenate was treated with LS9 (10 μ M) probe and with or without E-64 (100 μ M), Iodoacetamide (1mM) or N-phenylmaleamide (1mM). Controls (not shown) included rhodamine in PCB buffer, LS9 in PCB, liver tissue homogenate in PCB and PCB buffer alone. The final treatment volume of 100 μ l per well in a 96 well plate was made up using PCB buffer (pH5). Treatments were incubated at 22 $^{\circ}$ C in triplicate and fluorescence intensity with excitation and emission wavelength of 485nm and 520nm respectively, was monitored over a 2-hour period. Each treatment data recorded by the Omega fluorimetric software (Biostar) was normalized to a starting relative intensity unit of zero. Statistical analysis was performed using two-way ANOVA with error bars representing \pm SD.

5.2.2.5 Localization of legumain enzyme in *C. elegans*

Localisation of legumain is useful in investigating the specificity and successful delivery of the fluorophore-based prodrug to its target site (where legumain is expressed in the worm). *C. elegans* worm culture was exposed to TL11, LS9 and SM9 probes to investigate whether the probes were toxic to the worms and to observe if the probes could gain entry into the worms *in vivo*. Following a 22-hour exposure of young L4 and adult worms to 0.001 μ M to 1 μ M concentrations of the probes, there was no significant toxicity to the worms since the control sample and test samples had similar low mortality results (data not shown). For the

observation of fluorescence following treatment of the worms with the probes, after a 24 hour exposure period, images of SM9-treated (1 μ M) worms revealed distinct patterns of intensities on the worms (Figure 5.14). The fluorescence was localized in specific regions of the worm; specifically areas around the pharynx, the vulva and close to the tail (Figure 5.14). On the other hand, TLL and LS9 probes were not retained (images not shown).

As part of the investigation to localize the legumain enzyme in *C. elegans*, we attempted to identify if the enzyme was water soluble (S1), membrane-associated (S2) or membrane-bound (S3) in fractions of the worm. Due to the unknown interaction of detergents used in extraction of the somatic fractions, the activity of recombinant legumain in the detergents; 0.1% Tween 20 and 2% Triton X which would mimic reactions for S2 and S3 fraction respectively, was investigated to ascertain if the detergents prevented legumain activity. The results (Figure 5.15) indicated that while recombinant legumain prepared at pH5 (R_{LL}) maintained non-linear curve progressing toward a plateau at 120 minutes (approximately 7000RFU), recombinant legumain in 0.1% Tween 20 at pH5 treated with LS9 (R_{LT20L}) produced low fluorescence intensity and thus; low enzyme activity while the recombinant legumain in 2% Triton X-100 solution at pH5 (R_{LT100L}) revealed no activity. The result suggested that detergents hindered or reduced enzyme activity.



Figure 5.14: Rhodamine-based probe (SM9) uptake in *C. elegans*.

Fluorescent imaging of cultured *C. elegans* exposed to (A) no treatment and (B) 1 μ M SM9 probe. Worms were treated for 24h in liquid medium. Uptake excitation and emission wavelengths were 544nm and 590nm respectively. All labelled points in panel B display distinct fluorescence intensities representative of observations from approximately 30 worms per well of treatment in biological triplicates (n=3). HSN refers to hermaphrodite specific neurons and RVG refers to retrovesicular ganglion. The labelled regions are subject to confirmation.

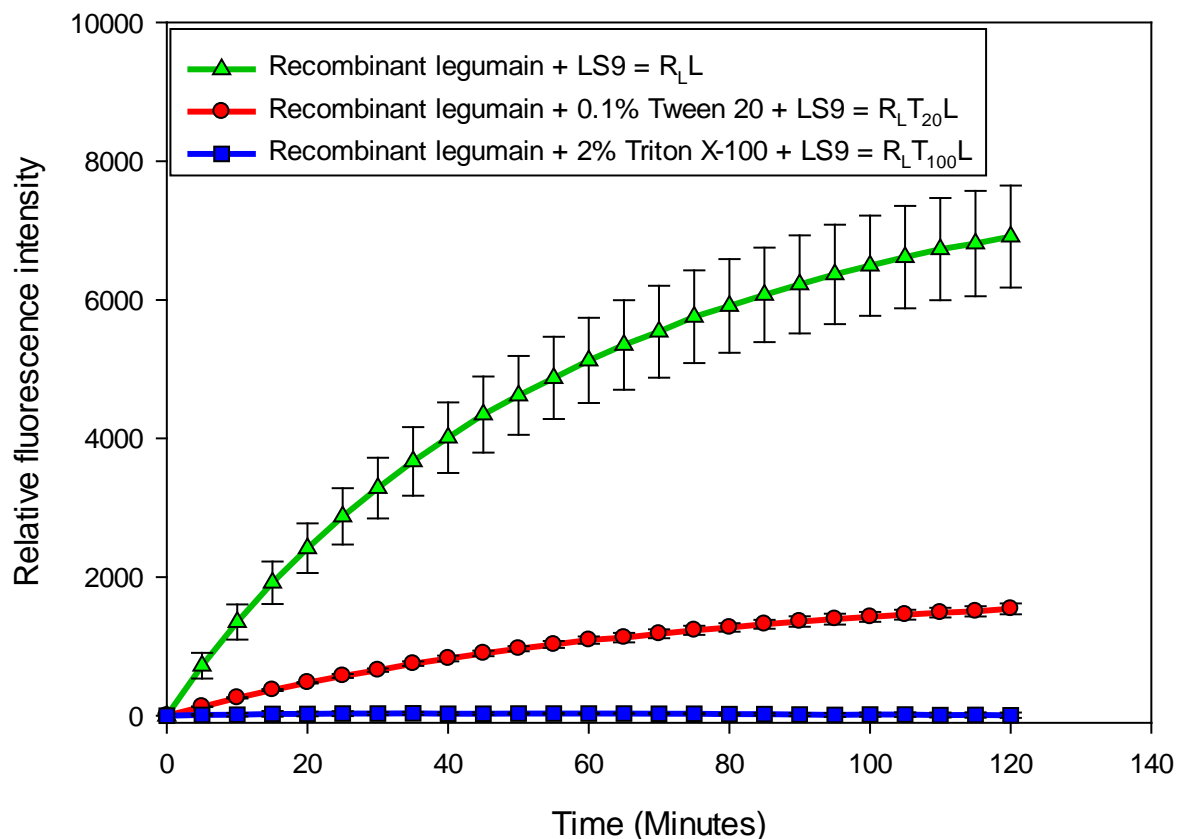


Figure 5.15: Detergent effect on the activation of LS9 by recombinant legumain.

Recombinant legumain (250ng/100 μ l) was prepared in PCB (pH5), 0.1% Tween 20 in phosphate-buffered saline (PBS) solution adjusted to pH5 or 2% Triton X-100 in PBS (pH5). Each sample was treated with LS9 probe (10 μ M) using PCB buffer (pH5) to make up a final volume of 100 μ l per well in a 96 well plate. Treatments were incubated (22 $^{\circ}$ C) in triplicates and fluorescence intensity with excitation and emission wavelength of 544nm and 590nm respectively, was monitored over a 2-hour period. Each treatment data recorded by the Omega fluorimetric software (Biostar) was normalized to a starting relative intensity unit of zero. Statistical analysis was performed using two-way ANOVA with error bars representing \pm SD.

In order to recover the recombinant legumain from the detergents a detergent gel extraction was utilized using a resin-recovery technology (see methods). The resin-recovered recombinant legumain from recombinant legumain in 0.1% Tween 20 was exposed to LS9 (RR- $R_L T_{20} L$) for 120 minutes and the result (Figure 5.16) revealed that there was no significant difference between recombinant legumain ($R_L L$) and RR- $R_L T_{20} L$ as both fluorescence intensities at 120 minutes were approximately 1800RFU compared to $R_L T_{20} L$ which had reached its optimal fluorescence intensity (approximately 330RFU) at about 105 minutes suggesting inhibition of enzyme activity.

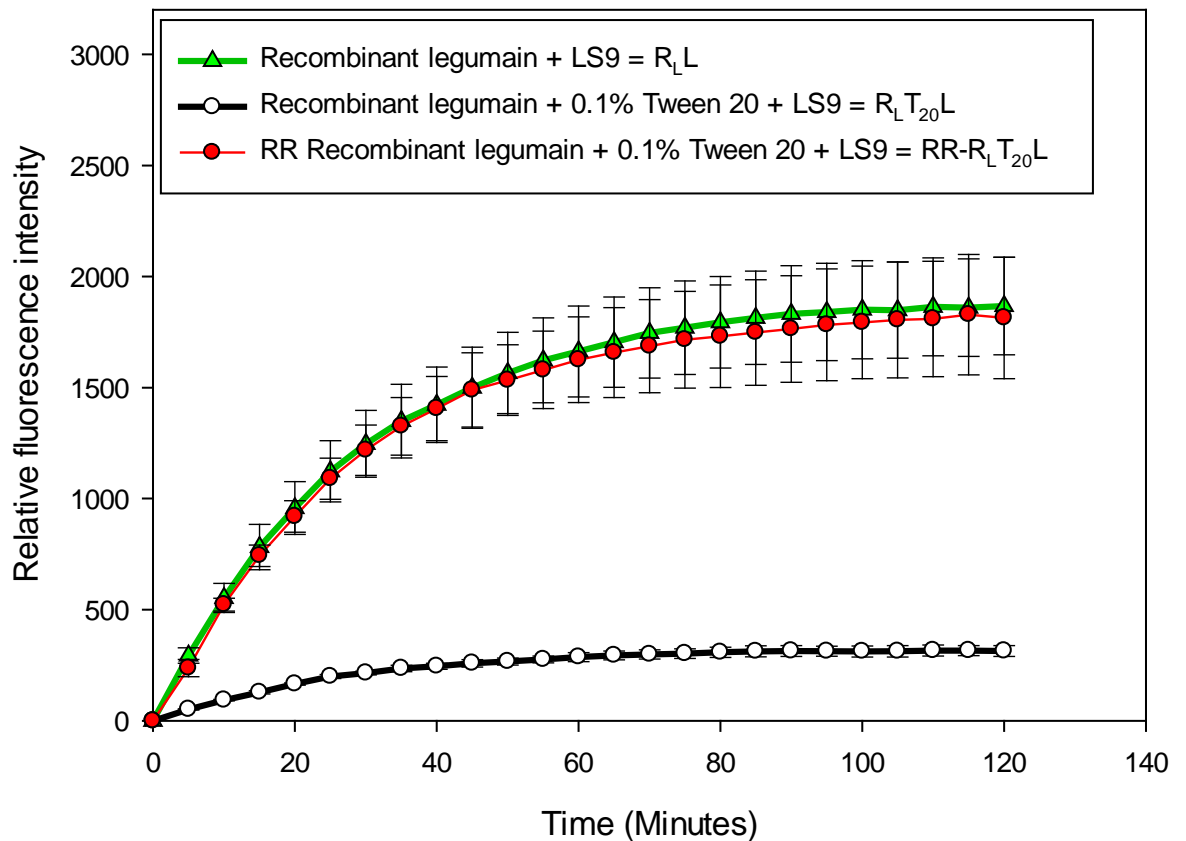


Figure 5.16: Activation of LS9 by resin-recovered (RR) recombinant legumain.

Recombinant legumain (167ng/100 μ l) was prepared in PCB (pH5), 0.1% Tween 20 in PBS solution (pH5) or resin-recovered (RR) recombinant legumain (167ng/100 μ l) in 0.1% Tween 20 in PBS solution (pH5). Each sample was treated with LS9 probe (10 μ M) using PCB buffer (pH5) to make up a final volume of 100 μ l per well in a 96 well plate. Treatments were incubated (22 $^{\circ}$ C) in triplicates and fluorescence intensity with excitation and emission wavelength of 544nm and 590nm respectively, was monitored over a 2-hour period. Each treatment data recorded by the Omega fluorimetric software (Biostar) was normalized to a starting relative intensity unit of zero. Statistical analysis was performed using two-way ANOVA with error bars representing \pm SD.

Having successfully shown above that samples could be recovered from detergents, *C. elegans* somatic fractions S2 and S3 were prepared with either homogenizing buffer (HB) or phosphate buffered saline (PBS) solution containing 0.1% Tween 20 (for S2 extraction) or 2% Triton X-100 (for S3 extraction). The somatic fractions and their resin-recovered samples were exposed to LS9 probe for 2 hours. The results in Figure 5.17 reveal that samples prepared in HB had generally low fluorescence intensities (Figure 5.17a) when compared to their PBS-prepared equivalents (Figure 5.17b) with the HB-containing samples exhibiting distorted curve progression. Fluorescence though initiated at the blank (zero point), did not visibly progress over time until approximately 15, 20 and 45

minutes for CeL, CeS3L and RR-CeS3L (Figure 5.17a). Figure 5.17b showed that the CeL in PBS was significantly higher ($p < 0.001$) and the reaction rate was faster than all other treatment groups in PBS while the other treatments were not significantly different from one another. Furthermore, although RR-CeS2L and RR-CeS3L prepared in PBS exhibited fluorescence, their detergent-containing equivalents did not reveal any fluorescence intensity (Figure 5.17b).

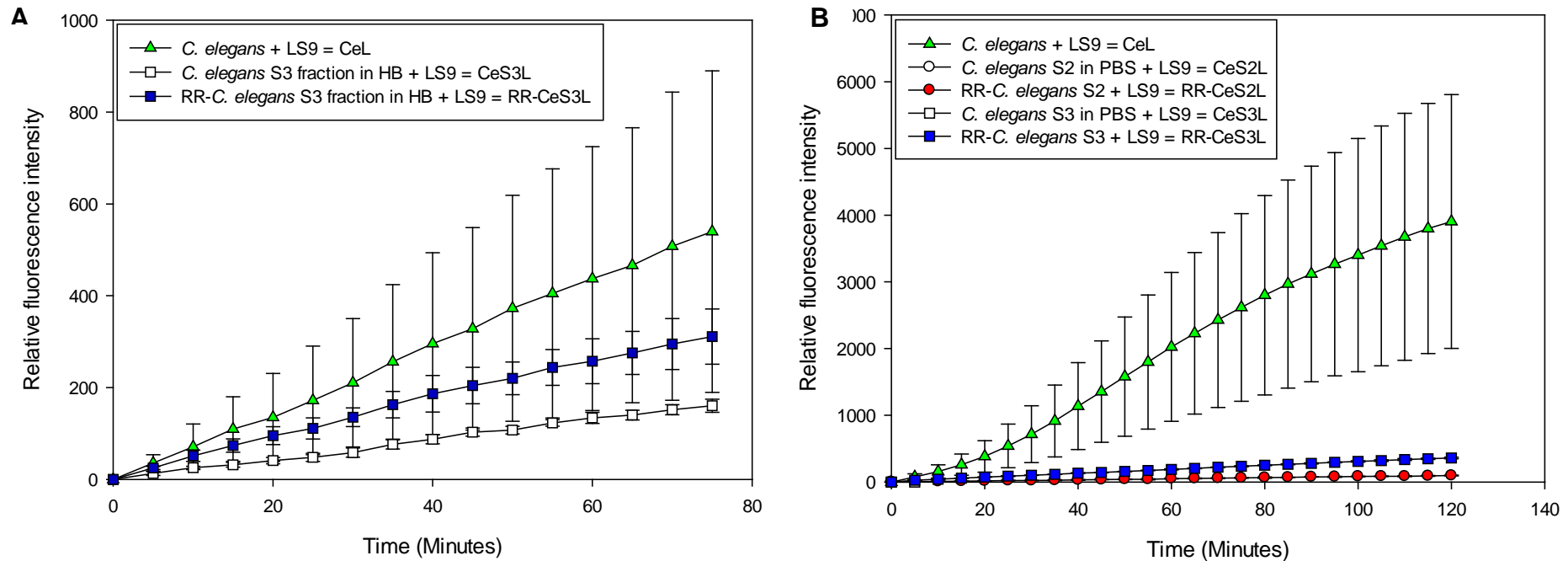


Figure 5.17: LS9 activation by somatic fractions of *C. elegans*.

(A) LS9 activation in membrane-bound fraction (S3) of *C. elegans* extracted with 2% Triton X-100 prepared in homogenizing buffer (HB) at pH7.4. **(B)** LS9 activation in membrane-associated fraction (S2) and membrane-bound fraction (S3) of *C. elegans* extracted with 0.1% Tween 20 and 2% Triton X-100 respectively prepared in Phosphate-Buffered Saline (PBS) solution at pH5. For graph A, *C. elegans* homogenized in HB, S3 fraction of *C. elegans* homogenized in HB or resin-recovered (RR) S3 fraction of *C. elegans* homogenized in HB was treated with LS9 probe (10 μ M) using PCB buffer (pH5) to make up a final volume of 100 μ l per well in a 96 well plate. For graph B, *C. elegans* homogenized in PBS solution, S2 fraction of *C. elegans* homogenized in PBS solution, S3 fraction of *C. elegans* homogenized in PBS solution, RR S2 fraction of *C. elegans* homogenized in PBS solution or RR S3 fraction of *C. elegans* homogenized in PBS solution was treated with LS9 probe (10 μ M) using PCB buffer (pH5) to make up a final volume of 100 μ l per well in a 96 well plate. Treatments were incubated (22 $^{\circ}$ C) in triplicates and fluorescence intensity with excitation and emission wavelength of 544nm and 590nm respectively, was monitored over a 120 minutes' period. Each treatment data recorded by the Omega fluorimetric software (Biostar) was normalized to a starting relative intensity unit of zero. Statistical analysis was performed using two-way ANOVA with error bars representing \pm SD.

5.2.3 Discussion

5.2.3.1 Legumain activity in *C. elegans*

In Figure 5.6, high fluorescence intensity was observed in *C. elegans* homogenate suggesting the presence of legumain in *C. elegans*. Iodoacetamide and N-phenylmaleimide; two known legumain inhibitors lowered the release of fluorescence from the probe (TL11) presumably by reducing legumain activity. While there was no total inhibition of fluorescence, the results showed that N-phenylmaleimide exhibited a stronger inhibitory property. Also, E-64 which inhibits all other protease enzymes but not legumain had some inhibitory effect on probe activation though, this effect was significantly lower than Iodoacetamide and N-phenylmaleimide effect. Since legumain was not isolated or characterized from the *C. elegans* homogenates as with other analysed samples in the study, the term 'legumain-like' activation is preferred to 'legumain' activation. Although the legumain-specific inhibitors did not result in total inhibition of probe activation and E-64 seemed to have reduced probe activation as should not be the case, the trend in Figure 5.6 suggests that a legumain-like type of reaction occurred in *C. elegans*. Whilst it could be argued that the relative fluorescence intensity in Figure 5.6 did not attain the optimal value; that is, the cleavage of the entire probe molecule thus, end of the reaction, it should be noted that the experiment was stopped after a defined time (120 minutes). This was due to two reasons; the first was to enable the velocity of the reaction to be calculated. It is this velocity that helps compare the reactions within sample groups in an experiment; however, velocity is only extrapolated from a linear curve which is characteristic in Figure 5.6 and the steepness of the slope on the progress graph quantitatively defines the activity of legumain in the experiment (Bisswanger, 2014). The second reason for the stopped assay is that, if the assay is allowed to continue after 120 minutes of reaction, the fluorophore might begin to lose its integrity due to photobleaching (Zondervan *et al.*, 2003); leading to errors in the experiment. The results in figure 5.6 demonstrate that a legumain-like enzyme in *C. elegans* was responsible for the cleavage of TL11 resulting in the emission of fluorescence. This also implies that the TL11 probe and subsequently a prodrug could successfully be delivered to target legumain in *C. elegans*.

5.2.3.2 Legumain activity in parasitic helminths

The progress of the experiments utilizing *C. elegans* further encouraged attempts on the parasitic nematodes *T. circumcincta* and *H. contortus*. In Figure 5.7, there was a similar trend of fluorescence reaction between *T. circumcincta* sample with and without E-64 as was observed with *C. elegans* in Figure 5.6 and their progress curves were also linear at the end of the timed reaction. It is not known why E-64 inhibition occurred since it does not inhibit legumain and serine proteases apart from the clan PA serine proteases (Barrett *et al.*, 1982; Chen *et al.*, 1997). On the other hand, the progress curve of the Iodoacetamide-treated *T. circumcincta* homogenate had begun to deviate outside the linear range and into optimal fluorescence production at about 60 minutes of probe-homogenate interaction suggesting inhibition of legumain. Contrastingly in Figure 5.8, the progress curve of *H. contortus* effect on the TL11 cleavage was close to optimal level suggesting the activation of most of the probe molecules by *H. contortus* homogenate hence, a likely presence and activity of legumain (Oliver *et al.*, 2006). Interestingly, the *H. contortus* homogenate treated with Iodoacetamide appeared to have exhibited a competitive inhibition suggesting that the legumain concentration in the *H. contortus* homogenate was not sufficient to convert the whole probe into active product (measured by fluorescence in this case) and allowing Iodoacetamide which should naturally inhibit legumain from the probe probably through alkylation of the probe. E-64 seemingly inhibited the activity of legumain as the rate of reaction and fluorescence were significantly low. A possible explanation of this unexpected observation with E-64 is likely that there may be serine proteases present in *H. contortus* that allowed E-64 to react with the functional thiol group in the enzymes thus modifying the enzymes to cleave the probe. Another plausible explanation is that substrates are commonly assumed to be specific for an enzyme. For example, Z-ala-ala-asn-MCA is commonly assumed to be a legumain-specific substrate (Teng *et al.*, 2010), but this is likely to be relatively rather than absolutely so. This assumption is mostly on the basis of being the available substrate and the lack of studies screening the enzyme substrate against other proteases. Nevertheless, some other endoproteases, for instance, one with cathepsin-like abilities cannot be excluded because they may cleave peptides as small as a dipeptide (Almeida *et al.*, 2001). Thus, if some non-legumain cleavage is seen, it does not mean it occurs at the C-terminus of asparagine. However, aminopeptidases, carboxypeptidases and

several endopeptidases including those with matrix metalloproteinase-like activity can be excluded because they would require a larger peptide sequence in the substrate. It should be noted that these submissions are from a human enzyme perspective and it is probable that nematodes like *C. elegans*, *H. contortus* or *T. circumcincta* have different enzyme substrate specificities. As reassuring as that may be, a comparison between *H. contortus* and *T. circumcincta* activity show a substantial difference in the parasite legumain activities and this suggests again, the possibility of various types of enzyme substrate specificity. Notwithstanding, legumain activity seems relatively conserved across species (Alvarez-Fernandez *et al.*, 1999).

It is necessary to state with caution that while the composition of the homogenates is not known, it is not likely to influence the pattern for the selective protease inhibitor E-64 between *T. circumcincta* and *H. contortus*. A comparative measure that we had for the *T. circumcincta* and *H. contortus* homogenates was the total protein which was 2.27mgml⁻¹ and 2.91mgml⁻¹, respectively though individual protein concentrations are not necessarily dependent on total protein concentration. Since the investigations at this stage is only to show legumain activity, there is no intention to purify legumain in the parasites.

5.2.3.3 pH effect on parasitic helminth activation

Parasitic helminths depend on the chemical environment of the infected site of their host for survival. Also, legumain responds to environmental factors like pH (Dall and Brandstetter, 2016). The arguments put forward so far were based on nematodes in an acidic environment (pH5.0). A comparison to investigate the stability of legumain over a broad range of pH (4-7) was performed. The interaction of *T. circumcincta* and *H. contortus* homogenates with a rhodamine-based probe; LS9, was investigated at pH4, 5, 6 and 7 over a similar time period (120 minutes) using the fluorimetric assay as mentioned earlier. LS9 was chosen over the previous TL11 probe because of its sensitivity to emission; covering a wider fluorescence emission spectrum. In a consistent manner, as was observed in Figure 5.7, *T. circumcincta* maintained a linear curve over 120 minutes at pH5 while the rate of reaction at pH4, 6 and 7 was slow and deviating from a linear curve towards a non-linear. This was observed as early as 20 minutes into the experiment (Figure 5.9). This suggests that pH5 is the optimal for legumain

activation of LS9 in *T. circumcincta*. Also, the *H. contortus* interaction with LS9 was optimal at pH5 (Figure 5.10) and the progress curve was consistent with the one described in Figure 5.8 for TL11 at pH5. While the rate of reaction was initially faster at pH6 the reaction was optimal at a significantly lower RFU than at pH5. A challenge in the experimentation for pH evaluation was that the incubation time should have been increased at least to the point where all reactions would reach optimal peak, however, the photobleaching of the probe's fluorophore could be problematic in the experimental design. Agreed that recombinant mammalian legumain works best at pH5 (Chen *et al.*, 1997) and does not show significant activity at pH7 as observed in one of our experiments (not shown), the same conclusion cannot be reached for helminths. More so, if the incubation time in the Figure 5.10 graph was extended for *H. contortus* homogenate treatment at pH4, there is the likelihood that the optimal relative fluorescence intensity would exceed pH5. Nonetheless, one could infer that helminth parasites can survive at different sites of the host under different chemical situations. For instance, the localisation, growth and multiplication of microbes in the rumen are pH-dependent. In the reticulum of ruminants, pH is between 6 and 7 and may be lower depending on the type of feed given to the animal. Also, the pH of the abomasum, which is the infective site of L3 *H. contortus* and *T. circumcincta* can be as low as 2 (Moran, 2005) depending on the degree of infection. So, the activity of legumain on the probes in these environmental scenarios may be stable.

Cysteine proteases in parasites function in a broader chemical atmosphere than their mammalian host equivalent. The pH of cysteine proteases is rather unstable in mammals apart from cathepsin S which may be using a regulation mechanism to reduce or prevent undesirable proteolysis in cellular units (Turk *et al.*, 1995). On the other hand, parasite cysteine proteases are more active and maintain their pH stability; a characteristic that is in line with their extralysosomal functions (Sajid and McKerrow, 2002), such as the digestion of blood meal.

5.2.3.4 Legumain activity in Sheep plasma

Having considered the pH range of parasitic helminth legumain, experiments were performed to determine the presence of legumain in the plasma of the healthy mammalian host. Healthy sheep plasma was analysed for legumain on

four pH ranges (4-7) using the rhodamine-based prodrug LS9 (Figure 5.11). The legumain activation of LS9 was insignificant over the two-hour incubation period with some negative relative fluorescence intensities observed in the graph. Of course, there is nothing like negative fluorescence but one can assume that the data generated from the fluorimeter is no longer fluorescence but a corrected measurement of fluorescence, which is why it is appropriate to use relativity in context. The fluorimeter (fluorostar Omega, UK) is partly responsible for this negativity as the MARS data analysis software in the fluorostar machine performs an automatic background/baseline correction. Again, normality could be a consequence of this negativity since the direct plotting of data does not give a definitive interpretation on graphs. Generated data is normalized because the fluorimeter, in an attempt to perform baseline correction, does not differentiate the buffers and control samples from other samples; it performs the correction on the entire 96 well plate; so, we still need to normalize to compensate for these errors. Whether or not the sample data is normalized, the standard deviation only changes in decimal fractions. From here on, all observation on so called “negative fluorescence” should be addressed based on the factors above. More so, the anomaly of negative fluorescence in the result could most likely be an issue of the plasma composition rather due to experimental process. A comparison with *H. contortus* extract in Figure 5.12 showed a definite distinction that legumain is probably absent or in its inactive proenzyme form (Dall and Brandstetter, 2016) if present in sheep plasma. This suggests that legumain could easily be targeted in parasites infecting sheep especially in blood.

5.2.3.5 Legumain activity in Sheep liver tissue

The activity of legumain in sheep liver tissue following the interaction with the LS9 probe suggests that legumain is present in sheep liver tissue. N-phenylmaleamide seems to be more efficient in inhibiting legumain activity than Iodoacetamide. The trend was consistent for *C. elegans* and *T. circumcincta* legumain inhibition. The implication of the presence of legumain or any other LS9 probe substrate-cleaving enzyme in the liver is that it might result in release of active anthelmintic in the liver via cleavage of proposed prodrug. This, however, can be prevented by the route of administration of the prodrug. In essence, the

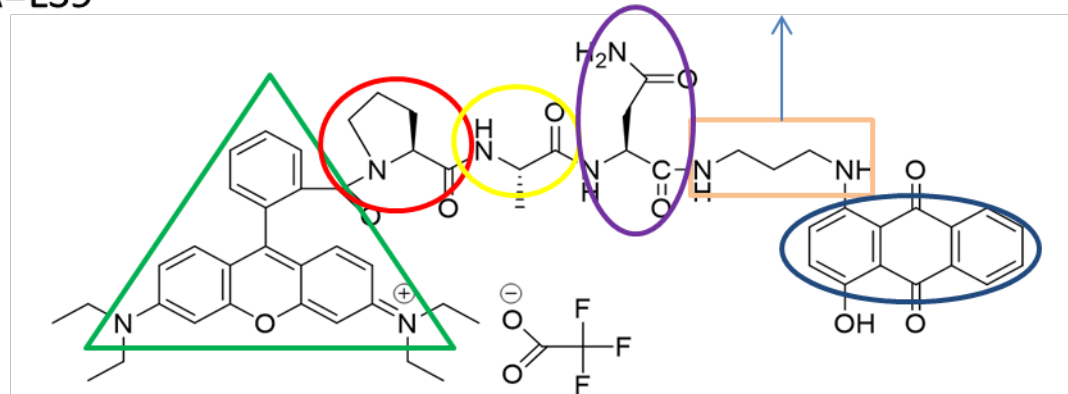
design of the actual prodrug must accommodate consideration for the route of delivery.

5.2.3.6 *In vivo* localization of legumain in *C. elegans*

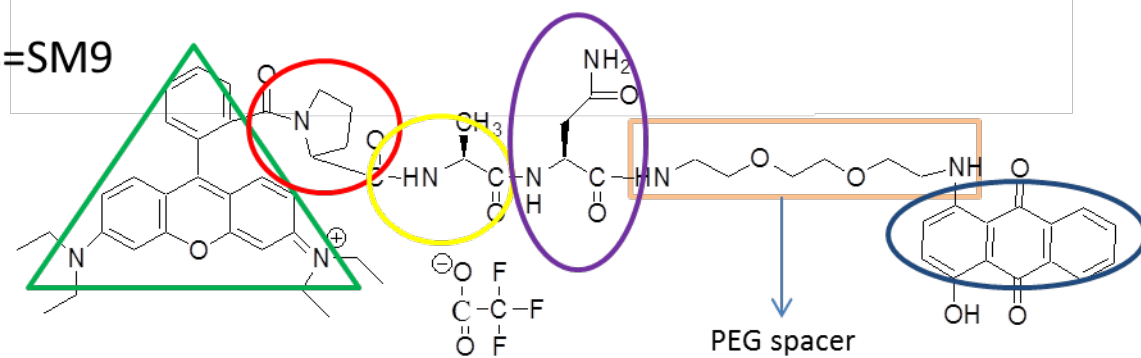
Exposure of worms to TL11 and LS9 probe *in vivo* did not reveal any accumulation and lethal toxicity of the probes in live worms. On the other hand, SM9 which is a slight modification of LS9 at the spacer linking the tripeptide to the quencher was retained in the worms following 24 hour exposure to 1 μ M concentration of the probe as high fluorescence intensity was localized in specific regions of the worm (Figure 5.14). This finding suggests that legumain is likely localized in these regions as fluorescence would only occur following the cleavage of the probe to release the rhodamine fluorophore. Initially, it was assumed that the negative charge on the peptide group might have prevented permeability of LS9 into the worm. One assumption is that the chain could be modified such that the tertiary amide group (amino group on proline in the red circle (see Figure 5.18 below-should be in introduction) is modified to one which would cyclise to form a cyclic compound; leading to the impermeability observed in the rhodamine tripeptide chain. On the contrary, this was not the case as SM9 absorption into the worm suggest two plausible explanations; either that the spacers (orange rectangles in Figure 5.18) could be responsible for the difference in interaction or as a result of errors in the experiments.

The localization of the SM9 is suggested to be around the retrovesicular ganglion (RVG), the haemaphrodite specific neuron (HSN) and the preanal ganglion region, however; a discussion personal discussion with Dr. Emmanuel Busch of the University of Edinburgh suggests that the probe could have affected the structural integrity of the worm as the grinder and pharynx seemed to have shifted towards the posterior of the worm. If this is the case, the morphological change could be a resulting sublethal effect of toxicity. Nevertheless, these localized

A=LS9



B=SM9



LEGEND

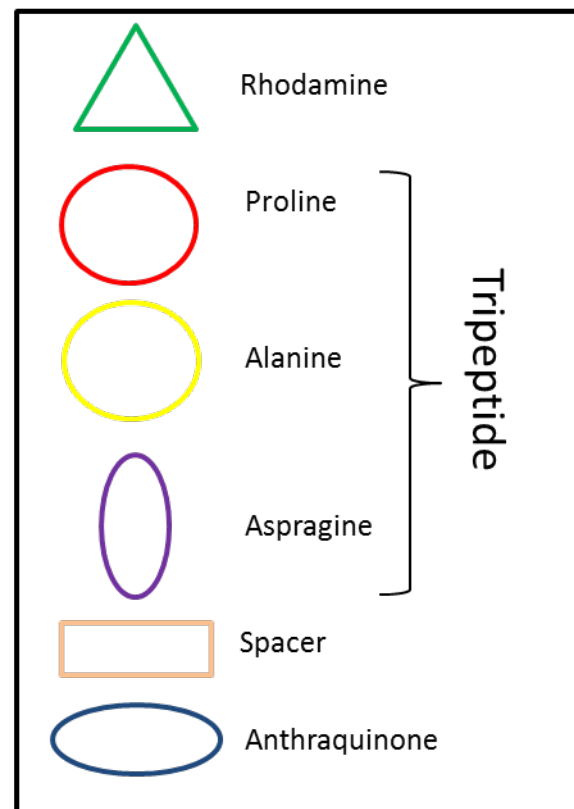


Figure 5.18: Structural representation of probes used for legumain localization.

(A) LS9 containing rhodamine tripeptide linked to the anthraquinone (quencher) with a propyl spacer (1, 3-Diaminopropane) and (B) SM9 containing rhodamine tripeptide linked to the anthraquinone (quencher) with a (polyethylene glycol (PEG) spacer (1, 8-Diamino-3,6-dioxaoctane).

regions are very pivotal in improving the specificity of drugs. For example, neuromuscular collapse in the pharynx would result in prevention of feeding and eventual starvation of worms. Also, a compromise in HSN would affect reproduction. The localization above demonstrates the prospect for the development of better targeted anthelmintics but this would depend on the amenability of the tripeptide with the active anthelmintic compound.

5.2.3.7 Legumain in somatic fractions of *C. elegans*

In vitro analysis of the localization of legumain in *C. elegans* was performed to determine if it is membrane-soluble, -associated or membrane-bound. Using the fluorimetric assay described previously, a designed control experiment to recover legumain from detergents was performed due to the inhibition of legumain activity resulting from the presence of detergent (Figure 5.15). In the control experiment, the recovery of legumain using a resin detergent remover (Thermo Scientific) successfully recovered over 95% of legumain as observed on the fluorescence intensity progress curve where 0.1% Tween 20 was extracted from recombinant mammalian legumain. The result suggests that detergent inhibition of legumain activity was reversible. The implication of this is that the detergents act probably by competitively inhibiting or temporarily preventing active binding of the enzyme to the substrate (LS9 probe) pending extraction. In the actual experiment of extracting somatic fractions of *C. elegans* (Figure 5.17), whilst the linearity of the progress curve indicated activity, the fluorescence intensity was significantly low in somatic fractions compared to pure homogenate of *C. elegans*. In Figure 5.17A, the homogenizing buffer (HB) developed in-house for somatic extraction did not encourage legumain activity probably due to the high pH of the HB (7.4) which exceeded the optimal activation pH for legumain. Conversely, the phosphate buffered salt (PBS) solution (pH5) seemed to reveal an increased yield, however, the differences between HB in Figure 5.17A and PBS in figure 5.17B should be carefully interpreted because of the relative difference between the non-detergent homogenates (CeL) and their resin-recovered S3 fractions. It is most likely that future experiments with preparation of HB at pH5 would yield a similar relationship to that observed in the resin-recovered legumain control test (Figure 5.16). In addressing whether legumain is membrane-bound or – associated, S3 fraction had a higher reaction rate and activity than the resin-

recovered S2 fraction (Figure 5.17B). This suggests that the presence of legumain is higher in membrane-bound fractions of *C. elegans* than in its membrane-associated fraction. Hence, organelles like the mitochondrion and lysosome in *C. elegans* might have more legumain concentration than in the non-membrane bound structures like the cytoskeleton, microfilaments and microtubules external membrane structure. Oliver *et al.* (2006) made mention of a 6-fold increase in legumain activity in membrane-bound fraction (S3) as compared to the water-soluble fraction (S1) in *Haemonchus contortus* although no mention was made of membrane-associated fraction (S2). There is the possibility that *C. elegans* shares similar legumain localization with *H. contortus* in terms of somatic association. *Fasciola hepatica*, legumain does not seem to be membrane-bound nevertheless, a PhD thesis from the University of Glasgow archive (McDougall, 2012) showed that it does, although the author believes his finding was inconclusive.

In summary, the results above support the use of *C. elegans* as a representative model in the application of anthelmintic treatment for parasitic helminth infections as we have shown that legumain cysteine protease can be exploited as a potential for enhanced anthelmintic targeting in parasitic helminths.

Chapter Six

6 General discussion

The suitability of *C. elegans*, and the type of analysis, for toxicity assessment is dependent on the type of chemical to be investigated. For example, in the current research, the consideration for lethality as an endpoint is essentially the first point in assessing the effect of the chemicals. This is most important for the derivatized anthelmintics to ensure that they kill the worm as a representative of helminth parasites. While an endocrine disruptor like diethylstilbestrol (DES) is not lethal to *C. elegans*, it would be acceptable that endpoints such as reproduction and morphology should be given priority when investigating the toxic effect of such chemicals. Notwithstanding, chemicals such as derivatized anthelmintics or DES can still find their way into the environment probably as unused waste from biological systems. For this reason, other endpoints for toxicity can be utilized to investigate the exposure scenarios.

While *C. elegans* shares a high conservation of signalling pathways and genes with the mammalian system (Leung *et al.*, 2008), its success as a toxicity model is highly dependent on good *C. elegans* culture practice (GCeCP) (Hunt, 2016). Consistency with the factors that support a good *C. elegans* culture such as sufficient food source, temperature and salt concentration are critical for reliability and reproducibility of toxicity assessment. Changes to any of these factors might alter toxic effects of tested chemicals. For instance, an increase in temperature may result in the induction of male phenotypes (Corsi *et al.*, 2015) and males produce three times as many eggs than hermaphrodite worms following mating. The offspring would contain 50% male and 50% hermaphrodite that could skew data recorded from reproductive or morphological assays. Worm density is another factor influencing GCeCP and the reliability of toxicological assessment. Dense population of worms in media would result in lack of nutrients and could lead to epigenetic adaptation rather than death (Hall *et al.*, 2010); thus altered toxicity results would be derived from such worm culture. pH can also affect the validity of *C. elegans* for toxicity assessment. While inconsistent pH in culture may not reflect in lethal endpoints, this may not be the case with sublethal endpoints. Culture pH should be checked for separate experiments and same batch samples should always be used for each experiment with different

treatment groups. Again, poor worm synchronization process may result in increased stress resistance of hatched L1 larvae from hypochlorite treatment if not fed after 18 hours in non-nutrient M9 buffer (Jobson *et al.*, 2015).

Apart from GCeCP, the appropriate representation of *C. elegans* and / or its mutants in toxicity experimental design is important. For example, some scientists suggest that the use of transgenic *C. elegans* with a compromised cuticle would encourage easy permeability of chemicals (Dengg and Van Meel, 2004). This might defeat the purpose of toxicological analysis as chemicals like derivatized anthelmintics would most likely produce an expected effect since the natural state of the worm would be compromised. It is often forgotten that predictive assessment using such suitability further deviates from the actual prediction expected. It is implied that in real life scenarios, parasitic worms such as *H. contortus* or *T. circumcincta* would not require an anthelmintic to be displaced from their host if their cuticle is compromised. An argument for the use of transgenics would be better suited for development of biomarkers such as GFP strains which would give insight into mechanisms affected by chemicals in *C. elegans*.

In the current research, not all chemicals considered were evaluated with the same endpoints (Table 6.1) and results varied depending on the chemicals. One major reason for not investigating all endpoints for the three chemicals examined was the available time for the current research. For example, the development of the techniques for accelerated embryonic development (AED) and bag of worms (BOW) phenotype tests, and automated behavioural assessment required several months to establish due to the use of stage-specific worms that required unlimited time and access to the laboratory. Although 24-hour access could have been granted, experiments were designed to accommodate working hour access.

Table 6.1: Toxicological assessment of chemicals performed in the current research

Type of toxicological assessment	Endpoint category	Endpoint sub-category	Endpoint	Chemicals analyzed			
				ZnONP	DES	DAH	
	Lethal	Lethality	Survival	√	√	√	
			Length	√			
			Width	√			
			Body bend frequency		√	√	
			Average speed		√	√	
			Fecundity		√		
			BOW phenotype	√			
			AED phenotype*	√			
	Descriptive and Mechanistic		Transgenic GFP expression	sod-3 GFP expression	√		
			Gene expression	sod-3 gene expression	√		
		Protein expression	SOD-3 protein expression	√			
		MicroRNA expression	MicroRNA array analysis	√			

*AED phenotype endpoint was developed in current research. ZnONP = Zinc oxide nanoparticle, DES = Diethylstilbestrol, DAH = Derivatized anthelmintics

6.1 Lethality as a toxicological endpoint in *C. elegans*

Lethality assessment in *C. elegans* varies from manual prodding of worms for movement to automated movement tracking. For whichever method, high concentrations of chemicals are required to induce a lethal effect on the worms. In the current research, a high concentration of ZnONP was required to induce a lethal effect on *C. elegans*. ZnONP concentrations of 12.5mM (approximately 1g/L) and above were lethal to the worms. These concentrations seemed unrealistic in real life exposure scenarios; however, the dispersion of the ZnONP rather than the dissolution of its Zn²⁺ ions are a likely contributing factor to the high concentration needed to induce lethality. While Williams & Dusenbery (1988) already showed that the LC50 of *C. elegans* correlated with the relative order of some metal toxicity, these metals were in water-soluble forms; thus, this could have contributed to their observations.

The dose of DES, which is a drug, administered to patients during the time of its use was based on the quantitative determination of hormonal levels throughout pregnancy (Smith 1948). Nair & Jacob (2016) explained that allometric scaling which is based on normalizing dose to body surface area can be used to calculate the relative amount of a drug required in a species other than humans but this has only been used for mammalian model systems. Again, conversion of dose based on body weight (mg/kg) may not be the appropriate approach due to the variation in biochemical functions among species as these may alter the pharmacokinetics of the drugs (Nair and Jacob, 2016). DES doses were not based on body weight of patients during its period of use (Reilly *et al.*, 2010) but on how patients' symptoms responded to its use (Karnaky, 1949). The amount of DES given to patients could be between 25 and 1000mg daily (Karnaky, 1949). In the current research, the highest concentration of DES used in the treatment of *C. elegans* was 100µM (26.8mg/L) and this seemed to improve the viability of the worms. One of the challenges with DES, as with some other chemicals, was the extrapolation of concentrations in *C. elegans* to dose administered to patients in real life treatment scenarios.

In addition, variability was observed when analyzing lethality in response to tubulin-targeting derivatized anthelmintics and repeated analyses were not consistent for concentrations that induced lethal effect (200µM to 800µM) on the

worms. While there is no specific explanation for this, an observation of the effect of clorsulon ; a benzenesulphonamide, on *C. elegans* in a separate experiment within our laboratory revealed that worms exposed to concentrations from 150µM (57mg/L) and above experienced total immobility for three minutes immediately after treatment; however, at seven minutes, the worms regained mobility. Since total immobility is usually scored as dead (Burke *et al.*, 2015; Graves *et al.*, 2005; Rogers *et al.*, 2015; Qiuli Wu *et al.*, 2013), the results suggested that there was probably a 'Lazarus effect', a condition in which *C. elegans*, can be described as in temporal paralysis.

Due to the requirement of high concentrations of chemicals used in the current study for the induction of lethal effect, it is suggested that for toxicological studies, sublethal effect of chemicals could yield more sensitive results from lower concentrations that are relevant to real life exposure scenarios. On the other hand, from a pharmaceutical perspective, the requirement of lethality endpoint could be critical in determining the effectiveness of the drugs. Therefore, lethality as is currently measured in *C. elegans* may be an unreliable endpoint; thus, caution may be needed when interpreting data.

6.2 Morphology as a toxicological endpoint in *C. elegans*

Dhawan *et al.* (1999) concluded in their work, which compared sublethal endpoints to lethal endpoint, that chemicals can induce effects on *C. elegans* morphology and unlike lethality, morphological endpoints are easily reproducible, and more sensitive indicators of toxicity. In our study, the assessment of morphology in terms of body length and width of the worms revealed that nanoparticles such as ZnONP can affect the size of the worms. Although the measurement of size was relatively easy to accomplish manually using the worm image captured with a camera on a compound microscope prior to analyzing with imaging software, complete automation could have been used as it can measure more worms over a shorter period of time. However, one concern with automation is that errors from measurements could be underestimated. For example, a lower magnification is required for an image that can capture at least 50 worms in a

single shot while a higher magnification would accommodate fewer worms (typically one to two worms) with larger views. Automated measurement of multiple images with higher magnification would yield lower measurement errors than an image with lower magnification would yield higher measurement errors. Although controls could allay these concerns, the significant differences among treatment groups might still be misrepresented.

One challenge of the assessment of ZnONP effect on *C. elegans* was that the dispersion of nanoparticles rather than their dissolution may have resulted in the worms consuming the nanoparticles which may block the gut; thus, their inability to feed properly with a consequence of becoming lean. This concern could be addressed in future experiments by tagging or coating the particles with probes and monitoring the uptake within the worm but this would require subtlety as the physicochemical properties of the nanoparticles can change; an observation reminiscent with the effect of different dispersant on ZnONP toxicity (see chapter three). Also, for a chemical like DES which was completely dissolved, *E. coli* OP50; the standard laboratory diet of *C. elegans* can be GFP-tagged to monitor its accumulation profile in the intestinal lumen of the worm after feeding in order to understand how this could affect the worm morphology. However, in the current research, worms exposed to DES appeared to be larger in length and width in comparison to the untreated control (data not shown).

6.3 Behavioural endpoints for toxicological assessment

The development of behavioural assessment in the *C. elegans* model was facilitated by the effect of drugs on the nervous system of the worms (Avery and Horvitz, 1990). One characteristic of *C. elegans* is its ability to change its behaviour in response to changes in its external environment and also changes in its internal physiological state. These behavioural alterations are achieved through the activities of the nervous system. *C. elegans* displays a robust behavioural response to changes in its environment. Such changes alter the worm's movement in terms of the effect on locomotion velocity (speed) and turning frequency (body bends per time). The movement of *C. elegans* is affected

by the presence of xenobiotics in its local environment and the worm's neurosensory awareness about these environmental changes is driven by behavioural shifts that are central to survival. In order to understand the *C. elegans* behaviour, the knowledge of how the activity of its muscles translates into movement within the mechanical framework and physical environment is important. The forward movement of the worm is achieved by undulatory waves in a dorsal-ventral plane from head to tail and are affected by responses to conditions in the worm environment that determine the motion behaviour of the worm (Pierce-Shimomura *et al.*, 2008). The alternate contraction and relaxation of two dorsal and two ventral muscle groups running along the length of the body of the worm creates its bending characteristic (Von Stetina *et al.*, 2005).

In *C. elegans*, the connection between the activities of the body wall muscle and the posture of the worm is subject to the environment of the worm. While worms that crawl on solid media display distinct sinusoidal movement patterns that have a wavelength which is shorter than the worm body length, worms that swim in liquid media exhibit bending postures and have longer wavelengths than the worm length (Fang-Yen *et al.*, 2010; Karbowski *et al.*, 2006). Due to the higher frequency of movement in liquid media (Pierce-Shimomura *et al.*, 2008), there is sufficient information gathered on behavioural data over a short period of time (in this research; 15 or 20 seconds). This is one reason for the preference of behavioural tracking in liquid medium over solid medium in the current research.

Previous experiments on motion tracking by other researchers demonstrated dose-dependent decrease in motion to some chemicals (Anderson *et al.*, 2004) while some others observed increase in locomotion (Williams and Dusenbery 1988). In the current research, the speed of worms in liquid media failed to produce consistent phenotypes following exposure to the derivatized anthelmintic drugs. This was consistent with the findings of Beron *et al.* (2015) who showed that a parameter like burrowing is a preferred behavioural assessment tool than speed which failed to produce conspicuous behavioural phenotypes. The results of the body bend frequency revealed a more consistent response. The results suggest that an increase in body bend frequency due to the derivatized anthelmintic drugs is generally concentration-dependent and the TPP-conjugated drugs seem to increase this frequency. The situation where the trend of bend frequency is not progressive is likely as a result of active swimming followed by

an episode of inactivity. Ghosh & Emmons (2008) showed that this dormancy appeared to be caused by high production of acetylcholine (ACh) and is believed to be partly controlled by command interneurons responsible for decision-making. Perhaps, the increased production of ACh which initially increases locomotion may stimulate a secondary process required to halt muscle contraction due to the activation of remote receptors that stop muscle contraction by excess ACh (Ghosh and Emmons, 2008). Another possibility is that the colchicine molecules in the colchicine-based anthelmintics which disrupt the activity of tubulin (Takao & Kaziro, 1977 and Lin & Hamel, 1981) inhibited ACh receptor stimulation of G protein GTPase activity (Ravindra and Aronstam, 1991). Ravindra & Aronstam (1991) further observed that colchicine only inhibited ACh-stimulated GTPase at concentrations below 100 μ M. Since tubulin influences cellular signalling and by virtue of its activity in the cytoskeleton network, the successful binding of colchicine to tubulin may alter the activity of ACh receptor thus resulting in the inhibition of ACh receptor-G protein coupling. This would evidently affect neurotransmission and locomotion behaviour.

With these possibilities in mind, it is likely that while the worms respond to the drug exposure by increasing their body bend frequency; they have the ability to accommodate lower concentrations and attempt to evade the drugs but as the concentration increases more ACh is produced and a reduction in body bend frequency ensues. The body bend frequency of the worm seems to increase with increasing drug concentration.

The variances in the literature of behavioural tracking data is a reflection of some challenges with the techniques and practices involved in performing the test. These include the type of media in which worms are assessed, either solid versus liquid medium; the technique of assessment either manual (Wu *et al.*, 2013) or automated (Truong *et al.*, 2015); the number of worms analysed either random sampling of equal number of worms per treatment (Swierczek *et al.*, 2011) or unequal sample size (Yemini *et al.*, 2013); depending on technique used, single worm assessment (Gomez-Marin *et al.*, 2016; (Contreras *et al.*, 2014); whether or not the worm populations are synchronized (Dhawan *et al.*, 2000), and the time period for monitoring behavioural analysis (Swierczek *et al.*, 2011; (Jiang *et al.*, 2016). Whilst the current research reveals a common trend with two different approaches (see chapter four section 4.2.4). The results are better analyzed

qualitatively rather than quantitatively as change in behavioural endpoints such as speed and body bend frequency can lay on either side of the control group. In addition, it is likely that the combination of neuronal assessments such as calcium imaging with other behavioural endpoints would provide an ideal assessment tool for the effect of chemicals on *C. elegans* behaviour.

6.4 Reproductive and developmental toxicity endpoints should be classified in terms of embryogenesis and egg-laying

Most reproductive toxicity assays in *C. elegans* lay emphasis on the activities of the gravid adult worm (McVey *et al.*, 2016; Walker & Tsui 1968) from the fertilization of its eggs through the process of egg-laying. On the other hand, developmental assessment of the embryo would provide further evidence of the effect of chemicals on reproduction. Reproductive endpoints in the current research included fecundity, bag of worms (BOW) phenotype and in-utero embryogenesis. While these endpoints are considered generally as reproductive toxicity endpoints (Seidel and Kimble, 2011), the current research showed that the bag of worms phenotype; which is an egg-laying defective phenotype that involves in utero hatching, can be induced by the exposure of the adult worms to ZnONP. The finding suggests that the BOW phenotype can be developed to understand the impact of nanoparticles as well as other chemicals on the reproductive process. The BOW phenotype endpoint was more sensitive in identifying toxicity of ZnONP with easy reproducibility and lower variation among repeated experiments in comparison to lethality.

For the first time, a state which was initially thought to be a process leading to the BOW phenotype was identified. While adult worms treated with ZnONP prepared in cationic or anionic dispersants (CZNP or AZNP respectively) revealed BOW phenotypes, adult worms treated with ZnONP prepared in molecular grade water, *E. coli* OP50 supernatant or 0.1% FBS (WZNP, SZNP or FZNP respectively) retained embryos that had developed to the ex utero egg development stage. These embryos had the three-fold elongation which usually develops approximately between 7 and 9 hours after egg-laying. This implied an

accelerated development of the embryo in the gravid adult which was eventually released; preventing the occurrence of BOW. We have termed the phenotype; accelerated embryonic development (AED) phenotype. Although it is not yet known how the AED phenotype occurs, the results revealed that is likely the most sensitive of all the toxicity endpoints used in the current research because it was detected in ZnONP treatments that otherwise did not reveal BOW phenotypes or morphological defect; for example, ZnONP prepared in *E. coli* OP50 supernatant (SZNP)-treated worms had similar morphology to the untreated control groups.

For fecundity assessment, the DES treatment results revealed that despite the increase in brood size of the worms with increasing concentrations of DES, the variances in repeated experiments were wide. It is likely that the BOW and AED phenotype assays would serve as more accurate endpoints because it would take into account the BOW or AED adult instead of the surviving progeny which could either be from a BOW or AED adult. Another advantage of the BOW and AED endpoints as toxicological assessment tools in *C. elegans* is that their combination is representative of reproductive and developmental toxicity assessment of both the adult worm and its offspring. Furthermore, the variance in progeny number in repeated fecundity experiments is avoided in BOW and AED phenotype assessment because the results in the latter are qualitative assessments; hence reproducibility would be more efficient.

As suggested by Harlow *et al.* (2016), since chemical exposure is experienced by the hermaphrodite adult, the combination of egg-laying and embryonic toxicity assessment such as the ones used in the current research is in a way representative of embryonic exposure through maternal contact with the chemical as observed in mammalian tests. Although it is expected that there will be limitations based on differences between *C. elegans* and mammals, the worm still shares a number of developmental processes with mammals. While the BOW and AED phenotypes endpoints mentioned above may be classified as reproductive endpoints, they should in fact be referred to as reproductive and developmental endpoints. This classification is encouraged because the BOW phenotype relates to the viability of the adult hermaphrodite while AED focuses on the viability of the embryo.

Following exposure to ZnONP, while the offspring survives in BOW phenotype probably due to the altruistic action of the hermaphrodite adult worm (Chen & Caswell-Chen, 2004) and in AED phenotype, there is an indication of unfavourable condition resulting from exposure to ZnONP. Although the BOW and AED phenotypes can be measured quantitatively, we propose that qualitative BOW and AED phenotype endpoints can be valuable elements of predictive tools not only for environmental toxicity but also mammalian developmental toxicity.

6.5 Transgenic GFP-reporter expression analysis

Generally, the use of GFP stress reporter strains of *C. elegans* can offer an outline of the patterns of gene response to toxic chemicals and the results are easily amenable to more direct interpretation, due to the existing characterization of some of these genes and their functions. The relevance of GFP-reporter responses is that they can be used as initial screening tools in the identification of patterns of responses which could subsequently be extensively examined using miRNA microarray analysis as applied in the current research. Although more extensive details on mechanisms of action would be available using miRNA microarray analysis as described in section 3.3.7 of chapter three, this would be expensive for testing multiple chemicals; for instance, in this study, the ZnONP in four different dispersants.

The current research presents the response patterns of transgenic *sod-3::GFP* *C. elegans* strain. ZnONP induced the oxidative stress enzyme superoxide dismutase reflecting the increased levels of reactive oxygen species but only CZNP-treated L1 larva revealed reporter responses among the group of treated L1 larva. This suggests that transgenic reporter L1 larva of *C. elegans* could be used in the investigation of the subtler toxic effect of chemicals. There was increased fluorescence in L3 larva treated with AZNP and CZNP but not BZ which seem to imply that the dispersants in which the ZnONP were prepared influenced the responses observed at a specific worm larval stage of development. The reason for this is likely to be the dissolution of Zn²⁺ ions in the dispersant and also the level of expression at different developmental stages of the worm. Using the

gene expression atlas (Kapushesky *et al.*, 2009, Petryszak *et al.*, 2014), microarray and RNA-sequencing data of the *sod-3* expression profile suggest that of the four developmental stages (L1, L3, L4 and gravid adult) considered, L1 larva has the highest baseline level of *sod-3* expression with 4 fragments per kilobase of exon model per million reads mapped (FPKM) while L3 and L4 larva have a baseline expression of 3 and 2 FPKM respectively. The baseline expression for *sod-3* in gravid adult is below the cut off.

Some drawbacks to the *sod-3::GFP* reporter technique described here include the challenge of developing most GFP-reporter strains. For example, because transgenics like *sod-3::GFP* are developed using transcriptional fusions and stable GFP variants (Libina *et al.*, 2003), the induction of stress-response gene expression is reliable but responses that involve the stability of messenger RNA or protein might be missed. The possible explanation for this is that transcriptional responses only become recognized as increased fluorescence after a time lag between the translation of GFP and its autoxidation in the process of becoming fluorescent (David *et al.*, 2003). This might explain the requirement for high concentrations (millimolar) of ZnONP to induce a reporter response in the current research and may be a reflection of a requirement for *C. elegans* gut ZnONP uptake.

Another challenge is the limitation of covering all gene families that are implicated in oxidative stress induction. While transgenics, like *sod-3::GFP* strains, can elucidate the indication of toxic exposure, its predictive power is limited due to the number of possible mechanisms that are implicated. For example, in the current study, a MnSOD (*sod-3*) GFP expression was investigated in transgenic *C. elegans* exposed to ZnONP. While *sod-3* seemed appropriate considering Cu/ZnSOD GFP-marked worm (*sod-1*) could yield false positive results because of its natural affinity for Zn²⁺ ions (Valentine *et al.*, 2005), *sod-3* could be redundant in function as it can be substituted by *sod-2* which is more abundant in the whole organism (Doonan *et al.*, 2008). Furthermore, because *sod-3* is regulated by *daf-16* (Oh *et al.*, 2006) and *elt-3* (Zhou *et al.*, 2011) which both play important roles in ageing, mechanistic toxicity analysis cannot be complete without investigating transgenic worms designed for these regulator genes.

One way of overcoming this challenge is to investigate chemical or toxicant-specific responses. An example of this is the *ajp-1* gene which is induced by arsenite (Sok *et al.*, 2001). Another approach is the utility arrays of biomarkers and knock out strains are likely to offer improved predictability and would facilitate high-throughput screening of chemical effects across multiple stress pathways. GFP reporter strain endpoint assessment such as the use of *sod-3::GFP* *C. elegans* in this case, may result in the misinterpretation of oxidative stress assessment based on the array of genes implicated in controlling oxygen balance in the worm. Following a personal correspondence with Prof. David Gems of the University College London (UCL), an array of GFP reporters and other mutants that can elucidate the descriptive toxicity assessment of chemicals and inform our understanding of possible biochemical pathways implicated in the process of toxic induction was designed; thus, addressing partial mechanistic toxicity assessment. Table 6.2 below describes a rationale for this approach with regards to understanding the effect of induction of oxidative stress by chemicals. *Daf-2* and *daf-16* both act as positive regulators for SOD genes among other genes such as metal binding metallothionein and heat shock protein-regulating genes (Murphy *et al.*, 2003). Consequently, there is cross-regulation of different stress-response pathways by these master regulator genes in *C. elegans*. The amenability of *C. elegans*, makes it possible to investigate the whole stress-response network provided the transgenics can be constructed. For example, the extracellular *sod-4::GFP* has not been constructed because GFP could not be detected in the *sod-4::GFP* lines, probably as a result of the extracellular localization of SOD-4 which leads to the diffusion of GFP; however, its *sod-4* knockout could give information on its importance in free oxygen radical detoxification (Doonan *et al.*, 2008).

Table 6.2: Rationale for the use of transgenic strains for toxicity assessment of chemicals

<i>C. elegans</i> Strain	Mutant description	Availability (e.g. CGC)	Relevance of use in toxicity assessment (oxidative stress assay)
	Null (KO), Hypomorphic (H) or GFP		
GA504	<i>sod-1::GFP</i>	UCL	GFP expression suggests cytosolic superoxide dismutase (SOD) is produced to detoxify drugs/ ZnONP
GA187	<i>sod-1</i> KO	CGC	Survival of strain following treatment suggests possibility that <i>sod-1</i> is not fundamental in drugs/ ZnONP detoxification or <i>sod-5</i> complements its activity.
GA509	<i>daf-2</i> H with <i>sod-1::GFP</i>	UCL	GFP expression in live strain serves as control for <i>sod-1</i> expression in <i>daf-2</i> compromised GA504 strain (treatment could have an effect on <i>daf-2</i>).
GA510	<i>daf-16</i> KO and <i>daf-2</i> H with <i>sod-1::GFP</i>	UCL	GFP expression in live strain serves as control for <i>sod-1</i> expression in <i>daf-2</i> and <i>daf-16</i> compromised GA504 strain (treatment could have an effect on <i>daf-2</i> and <i>daf-16</i>).
GA429	<i>sod-2::GFP</i>	UCL	GFP expression suggests mitochondrial SOD is produced to detoxify drugs/ ZnONP
VC498	<i>sod-2</i> H	CGC	Survival of strain following treatment suggests possibility that <i>sod-2</i> is not fundamental in drugs/ ZnONP detoxification or <i>sod-3</i> complements its activity.
GA459	<i>daf-2</i> H with <i>sod-2::GFP</i>	UCL	GFP expression in live strain serves as control for <i>sod-2</i> expression in <i>daf-2</i> compromised GA5429 strain (treatments could have an effect on <i>daf-2</i>).
GA460	<i>daf-16</i> KO and <i>daf-2</i> H with <i>sod-2::GFP</i>	UCL	GFP expression in live strain serves as control for <i>sod-2</i> expression in <i>daf-2</i> and <i>daf-16</i> compromised GA429 strain (treatments could have an effect on <i>daf-2</i> and <i>daf-16</i>).

CF1553	<i>sod-3::GFP</i>	CGC	GFP expression suggests mitochondrial SOD is produced to detoxify drugs/ ZnONP
GA186	<i>sod-3</i> KO	CGC	Survival of strain following treatment suggests possibility that <i>sod-3</i> is not fundamental in drugs/ ZnONP detoxification or <i>sod-2</i> complements its activity.
CF1580	<i>daf-2</i> H with <i>sod-3::GFP</i>	CGC	GFP expression in live strain serves as control for <i>sod-3</i> expression in <i>daf-2</i> compromised CF1553 strain (treatments could have an effect on <i>daf-2</i>).
CF1588	<i>daf-16</i> KO and <i>daf-2</i> H with <i>sod-3::GFP</i>	CGC	GFP expression in live strain serves as control for <i>sod-3</i> expression in <i>daf-2</i> and <i>daf-16</i> compromised CF1553 strain (treatments could have an effect on <i>daf-2</i> and <i>daf-16</i>).
GA416	<i>sod-4</i> KO	CGC	Survival of strain following treatment suggests possibility that extracellular SOD is not fundamental for drug/ ZnONP detoxification
GA411	<i>sod5::GFP</i>	UCL	GFP expression suggests cytosolic SOD is produced to detoxify drugs/ ZnONP
GA503	<i>sod-5</i> KO	CGC	Survival of strain following treatment suggests possibility that <i>sod-5</i> is not important in drugs/ ZnONP detoxification or <i>sod-1</i> complements its activity.
GA412	<i>daf-2</i> H with <i>sod-5::GFP</i>	UCL	GFP expression in live strain serves as control for <i>sod-5</i> expression in <i>daf-2</i> compromised GA411 strain (treatments could have an effect on <i>daf-2</i>).
GA414	<i>daf-16</i> KO and <i>daf-2</i> H with <i>sod-5::GFP</i>	UCL	GFP expression in live strain serves as control for <i>sod-3</i> expression in +++ <i>daf-2</i> and <i>daf-16</i> compromised GA411 strain. Treatments could have an effect on <i>daf-2</i> and <i>daf-16</i> .
GA480	<i>sod-2</i> KO and <i>sod-3</i> KO	CGC	Death of strain following treatment suggests that mitochondrial SOD is important in drugs/ ZnONP detoxification.

The colour-coded rows represent the smallest array of SOD transgenic *C. elegans* strains suggested for the investigation of toxicity. Strains were supplied by (Doonan *et al.*, 2008) from the University College, London (UCL) and the Caenorhabditis Genetics Centre (CGC).

Previous research has focused on multiple toxicity assessments classified as either descriptive or mechanistic assessment assays, the use of transgenic *C. elegans* strains combines both (Table 6.2) and would improve initial insight to chemical toxicity in comparison to humans and their environment as well as the quality and time spent on performing the assessments. Whilst the current research with transgenic strains focused on ZnONP toxicity, the same technique can be used for exploring complex patterns of stress responses (Anbalagan *et al.*, 2012) in other nanoparticles (Ma *et al.*, 2009; Blinova *et al.*, 2010) and even drugs like DES and anthelmintic derivatives to give insight into the mechanisms by which they work.

In terms of reproducibility of transgenic GFP reporter assays, seemingly inconsequential environmental changes can be misrepresented as toxic, while toxic conditions may go undetected or there might be a wide variability among repeated experiments. For example, in the work of Power *et al.* (1998) control values in expression responses may differ by as much as 4-fold between repeat experiments. This could be as a result of subtle changes in environmental conditions such as temperature or oxygen content. Whilst all experiments are performed under the same conditions, these subtle changes cannot be completely eliminated and although data can be normalized to controls for standardization, it is better to run experiments concurrently as with qPCR analysis to avoid wide variations in data.

Conclusively, the GFP-reporter expression assay offers an extensive prospect for stress-gene expression patterns in the assessment of chemical toxicity which would otherwise require expensive gene arrays. The data generated can be used to determine the process by which chemicals cause adverse effect to biological systems. Future work will extend this approach as a predictive tool via reference of already investigated or tested chemicals and, where information is not sufficient, the parameters investigated could be increased accordingly to cover a desired theme. The continuous update of the library of assessed chemicals would become progressively more accurate over time thus leading the reduction in the used of animal models for toxicity assessment.

6.6 MiRNA expression as a biomarker for toxicity

Some studies have utilized miRNA expression as a tool for toxicological assessment in the *C. elegans* model system (Wu *et al.*, 2015, Yang *et al.*, 2016, Zhao *et al.*, 2016) but there is not enough information on how microarray analysis of miRNA expression can be maximized as a biomarker for chemical toxicity. The current research was conducted to investigate the use of miRNA expression as a marker of toxicity. Previous studies have shown that chemicals can induce genotoxic effects on biological systems (Eom *et al.*, 2013, Kim *et al.*, 2016, Park and Choi 2017). In most of these studies, the quantification of RNA transcripts using real-time PCR (qPCR) in combination with protein assays like western blot are considered as the definitive endpoints for genes implicated in toxicological pathways. In the current research, there was no change in superoxide dismutase III (SOD-3) protein and gene expression, where SOD-3 was used as a marker of oxidative stress resulting from exposure to ZnONP. On the other hand, the confidence of the microarray analysis of miRNA expression as a useful biomarker was strengthened by its consistency with the results obtained from sub-lethal endpoint assessments in the evaluation of ZnONP. Many genes and biochemical pathways are implicated in chemical toxicity and this places miRNA microarray analysis at an advantage over gene or protein analysis because the number of miRNAs describing a marker of toxicity is less than the number of genes implicated in that production of the marker. For example, miRNAs implicated in the regulation of *sod-3* are less than the number of genes associated with *sod-3*. Although a lot is yet to be understood about miRNAs, it could be adopted for predictive assessment of chemical toxicity. Furthermore, target mRNAs of miRNAs implicated in toxicity can be investigated to understand the pathways involved for specific chemicals.

6.7 Designing realistic exposure scenarios

The present study suggests that the dispersants used in the preparation of ZnONP may influence the adverse effect of ZnONP on *C. elegans*. The low effect of ZnONP prepared in *E. coli* OP50 supernatant or 0.1% FBS on *C. elegans* morphology in comparison to the adverse effect of ZnONP prepared in proprietary ionic dispersants suggests that a likely protein-coating of ZnONP by the dispersants alleviated the toxicological effect of the ZnONP in comparison to the proprietary ionic dispersants. This was previously demonstrated by Tiedemann *et al.* (2014) who showed that serum-coated gold and silver nanoparticles reduced the toxic effect of the nanoparticles. While *E. coli* OP50 supernatant and 0.1% FBS may likely mimic a protein corona that coats nanoparticles; their availability in the environment could be contrary to the controlled exposure scenarios simulated in the laboratory. Of course, a controlled environment allows for reproducibility and standardization of methods, however, there would be unavoidable differences compared to real environmental situations. Also, synthetic dispersants such as the proprietary ionic dispersants used for ZnONP preparation (CZNP and AZNP) are not likely present in actual environmental scenarios. From a domestic point of view, cosmetic products such as sunscreens contain about 155mg/g ZnONP and the major emission routes for such products are air, surface water, waste water and soil waste (Boxall *et al.*, 2007). These routes accommodate different concentrations of ZnONP; for example, a simulation predicted that if 10% of sunscreen products in the United Kingdom market are used, the ZnONP content that would be released into water would be less than 80µg/L and more than 3.1 mg/kg in the soil (Boxall *et al.*, 2007). While the current research on ZnONP may not be appropriate for environmental water exposure scenarios; unless in accidental or disaster situations like spillage, it could be better suited for soil exposure scenarios.

6.8 The *C. elegans* model in the application of anthelmintic drug delivery

C. elegans appears to be an acceptable model for the development of a novel drug delivery system against helminth parasites. Assessment of legumain activity in *C. elegans* as well as nematode parasites, using fluorophore-labelled prodrugs, suggests that legumain is present in *C. elegans* as well as in parasitic nematodes. The experiments carried out so far point to legumain being the effector or activator of the prototype fluorogenic probes. Moreover, legumain activity seems to be conserved across species due to the similarities in the inhibitor profiles of *C. elegans*, *H. contortus* and *T. circumcincta*. Also, legumain is not present in the water-soluble fraction of *C. elegans* but in *H. contortus* and *T. circumcincta* is active at acidic to neutral pH. Again, there are suggestions that sheep plasma does not contain legumain. Under such circumstances, legumain would be a possible target for drugs and its delivery.

6.9 Conclusion

The current research revealed that *C. elegans* is a suitable model system for the evaluation of chemical toxicity but different toxicity endpoints would be required depending on the type of chemicals evaluated. Toxicological sub-lethal endpoints are likely to be more sensitive than lethal endpoint by order of the requirement for lower concentration of chemicals. The accelerated embryonic development (AED) phenotype is classified for the first time and is exclusive of the bag of worm (BOW) phenotype. The AED phenotype can be utilized with the BOW phenotype as reproductive and developmental toxicity endpoints. Furthermore, microarray analysis of miRNA expression is a suitable biomarker of chemical toxicity. We therefore propose that an AED phenotype test and microarray analysis of miRNA expression be developed and incorporated into toxicological evaluation techniques.

Also, we have shown that the *C. elegans* model system can be developed to show proof of concept for anthelmintic drug delivery against helminth parasites.

The findings in the current research point to legumain being the effector or activator of the prototype fluorogenic probes that are representative of anthelmintic prodrugs; therefore, more research will continue to refine and define structure-activity relationships and to determine the effect of the novel agents on worm viability.

References

- Adelsberger H., Lepier A. and Dudel J. (2000). Activation of rat recombinant alpha 1 beta 2 gamma 3 GABA_A receptor by the insecticide ivermectin. *European Journal of Pharmacology*, 394: 163–170.
- Adisakwattana P., Viyanant V., Chaicumpa W., Vichasri-Grams. S, Hofmann A, Korge G., Sobhon. P and Grams R (2007). Comparative molecular analysis of two asparaginyl endopeptidases and encoding genes from *Fasciola gigantica*. *Molecular and Biochemical Parasitology*, **156**(2): 102–116.
- Ahn J.M., Eom H.J., Yang X., Meyer J.N. and Choi J. (2014). Comparative toxicity of silver nanoparticles on oxidative stress and DNA damage in the nematode, *Caenorhabditis elegans*. *Chemosphere*, Elsevier Ltd. 108: 343–352.
- Aleyasin H., Karuppagounder S.S., Kumar A., Sleiman S., Basso M., Ma T., Siddiq A., Chinta S.J., Brochier C., Langley B., Haskew-Layton R., Bane S.L., Riggins G.J., Gazaryan I., Starkov A., Andersen J.K. and Ratan R.R. (2014). Antihelminthic benzimidazoles are novel HIF activators that prevent oxidative neuronal death via binding to tubulin. *Antioxidants & redox signaling*. **0**(0): 121–134.
- Almeida P.C., Nantes I.L., Chagas J.R., Rizzi C.C.A., Faljoni-Alario A., Carmona E., Julianoi L., Nader H.B. and Tersariol I.L.S. (2001). Cathepsin B activity regulation. Heparin-like glycosaminoglycans protect human cathepsin B from alkaline pH-induced inactivation. *Journal of Biological Chemistry*. **276**(2): 944–951.
- Alvarez-Fernandez M., Barrett A.J., Gerhartz B., Dando P.M., Ni J. and Abrahamson M. (1999). Inhibition of mammalian legumain by some cystatins is due to a novel second reactive site. *Journal of Biological Chemistry*, 274(27): 19195–19203.
- Anand K and Varghese S (2015) Role of surfactants on the stability of nano-zinc oxide dispersions. *Particulate Science and Technology*, Taylor & Francis **0**(0): 1–4. .
- Anbalagan C., Lafayette I., Antoniou-Kourouniotti M., Haque M., King J., Johnsen B., Baillie D., Gutierrez C., Martin J.A.R. and Pomerai D. (2012). Transgenic nematodes as biosensors for metal stress in soil pore water samples. *Ecotoxicology*, **21**(2): 439–455.
- Anderson G.L., Cole R.D. and Williams P.L. (2004). Assessing behavioral toxicity with *Caenorhabditis elegans*. *Environmental Toxicology and Chemistry*. **23**(5): 1235–1240.
- Andrade V., Guerra M., Jardim C., Melo F., Silva W., Ortega J.M., Robert M., Nathanson M.H. and Leite F. (2011). Nucleoplasmic calcium regulates cell proliferation through legumain. *Journal of Hepatology*. European Association for the Study of the Liver, **55**(3): 626–635.
- De Angelis I., Barone F., Zijno A., Bizzarri L., Russo M.T., Pozzi R., Franchini F., Giudetti G., Uboldi C., Ponti J., Rossi F. and De Berardis B. (2012). Comparative

study of ZnO and TiO₂ nanoparticles: physicochemical characterisation and toxicological effects on human colon carcinoma cells. *Nanotoxicology*, **7**(8): 1361–1372.

Angelo G. and Gilst M.R. Van (2009). Starvation Protects Germline Stem Cells and Extends Reproductive Longevity in *C. elegans*. *Science*, **326**(5955): 954–958.

Antebi A., Norris C.R., Hedgecock E.M., Garriga G. Cell and Growth Cone Migrations. (1997). In: Riddle DL, Blumenthal T, Meyer B.J., Priess J.R., editors. *C. elegans* II. 2nd edition. Cold Spring Harbor (NY): Cold Spring Harbor Laboratory Press. Chapter 21

Armstrong, J. S. (2007). Mitochondrial Medicine: Pharmacological targeting of mitochondria in disease. *British Journal of Pharmacology*. **151**(8): 1154–1165.

Arzate-Mejía R.G., Valle-García D. and Recillas-Targa F. (2011). Signaling epigenetics: Novel insights on cell signaling and epigenetic regulation. *IUBMB Life*, **63**(10): 907–921.

Avery L. and Horvitz H.R. (1990). Effects of starvation and neuroactive drugs on feeding in *Caenorhabditis elegans*. *Journal of Experimental Zoology*, **253**(3): 263–270.

Balaban R.S., Nemoto S., Finkel T. (2005). Mitochondria, oxidants, and aging. *Cell*. **120**(4):483-95.

Barrett A. J., Kembhavi A. A., Brown M. A., Kirschke H., Knight C.G., Tamai M. and Hanada K. (1982). L-trans-Epoxy succinyl-leucylamido(4-guanidino)butane (E-64) and its analogues as inhibitors of cysteine proteinases including cathepsins B, H and L. *The Biochemical journal*, **201**(1): 189–198.

Bartel D.P. (2009). MicroRNAs: Target Recognition and Regulatory Functions. *Cell*, **136**(2): 215–233.

Beron C., Vidal-Gadea A.G., Cohn J., Parikh A., Hwang G. and Pierce-Shimomura J.T. (2015). The burrowing behavior of the nematode *Caenorhabditis elegans*: A new assay for the study of neuromuscular disorders. *Genes, Brain and Behavior*, **14**(4): 357–368.

Berven L., Johansen H.T., Solberg R., Kolset S.O. and Samuelsen A.B.C. (2013). Autoactivation of prolegumain is accelerated by glycosaminoglycans. *Biochimie Elsevier Masson SAS*, **95**(4): 772–781.

Bhuvaneshwari M., Iswarya V., Archana S., Madhu G.M., Kumar G.K.S., Nagarajan R., Chandrasekaran N. and Mukherjee A. (2015). Cytotoxicity of ZnO NPs towards fresh water algae *Scenedesmus obliquus* at low exposure concentrations in UV-C, visible and dark conditions. *Aquatic Toxicology*. Elsevier B.V, **162**: 29–38.

Bisswanger H. (2014). Enzyme assays. *Perspectives in Science*. Elsevier, **1**(1–6): 41–55.

Blaxter M., Aslett M., Guiliano D. and Daub J. (1999). Parasitic helminth

genomics. *Parasitology*, 118: S39–S51.

Blaxter M., Daub J., Guiliano D., Parkinson J. and Whitton C. (2002). The *Brugia malayi* genome project: expressed sequence tags and gene discovery. *Transactions of the Royal Society of Tropical Medicine and Hygiene*, **96**(1): 7–17.

Blinova I., Ivask A., Heinlaan M., Mortimer M. and Kahru A. (2010). Ecotoxicity of nanoparticles of CuO and ZnO in natural water. *Environmental Pollution*. Elsevier Ltd, **158**(1): 41–47.

Blouin M.S., Yowell C.A., Courtney C.H. and Dame J.B. (1995). Host movement and the genetic structure of populations of parasitic nematodes. *Genetics*, **141**(3): 1007–1014.

Boholm M. and Arvidsson R. (2016). A Definition Framework for the Terms Nanomaterial and Nanoparticle. *NanoEthics*, **10**(1): 25–40.

de Bono M. and Maricq A.V. (2005). Neuronal substrates of complex behaviors in *C. elegans*. *Annual Review of Neuroscience* **28**(1): 451–501.

Braendle C. (2012). Pheromones: Evolving language of chemical communication in nematodes. *Current Biology*. Elsevier Ltd, **22**(9): R294–R296.

Brenner S. (2009). In the beginning was the worm. *Genetics*, **182**(2): 413–415.

Brun N.R., Lenz M., Wehrli B. and Fent K. (2014). Comparative effects of zinc oxide nanoparticles and dissolved zinc on zebrafish embryos and eleuthero-embryos: Importance of zinc ions. *Science of the Total Environment*, 476–477: 657–666.

Bucher E. A. and Seydoux G. (1994). Gastrulation in the nematode *Caenorhabditis elegans*. *Developmental Biology* 5: 121–130.

Burke S.L., Hammell M. and Ambros V. (2015). Robust distal tip cell pathfinding in the face of temperature stress is ensured by two conserved microRNAs in *Caenorhabditis elegans*. *Genetics*, **200**(4): 1201–1218.

C. elegans Consortium (1998). Genome Sequence of the Nematode *C. elegans*: A Platform for Investigating Biology. *Science (New York, N.Y.)*, **282**(5396): 2012–2018.

Caffrey, C. R. (2012). Parasitic Helminth: Targets, Screens, Drugs and Vaccines. Drug Discovery in Infectious Diseases. (Vol 3) Ed. Selzer, P. M. pp. v. ISBN 978-3-527-33059-1 -Wiley-VCH, Weinheim

Chalfie M. and Sulston J. (1981). Developmental genetics of the mechanosensory neurons of *Caenorhabditis elegans*. *Developmental Biology*, **82**(2): 358–370.

Chatterjee S., Fasler M., Büssing I. and Großhans H. (2011). Target-Mediated Protection of Endogenous MicroRNAs in *C. elegans*. *Developmental Cell*, **20**(3): 388–396.

- Chatterjee S. and Grosshans H. (2009). Active turnover modulates mature microRNA activity in *Caenorhabditis elegans*. *Nature*. **461**(7263): 546–549.
- Chen J. and Caswell-Chen E.P. (2003). Why *Caenorhabditis elegans* adults sacrifice their bodies to progeny. *Nematology*, **5**(4): 641–645.
- Chen J. and Caswell-Chen E.P. (2004). Facultative Vivipary is a Life-History Trait in *Caenorhabditis elegans*. *Journal of nematology*, **36**(2): 107–113.
- Chen J., Dando P.M., Neil D., Brown M.A., Young N.E., Stevens R.A., Hewitt E., Watts C., Barrett A.J. and Rawlings N.D. (1997). Cloning, isolation, and characterization of mammalian legumain, an asparaginyl endopeptidase. *J Biol Chem*, **272**(12):8090-8098.
- Chen P.S., Su J.L., Cha S.T., Tarn W.Y., Wang M.Y., Hsu H.C., Lin M.T., Chu C.Y., Hua K.T., Chen C.N., Kuo T.C., Chang K.J., Hsiao M., Chang Y.W., Chen J.S., Yang P.C. and Kuo M.L. (2011). miR-107 promotes tumor progression by targeting the let-7 microRNA in mice and humans. *Journal of Clinical Investigation*, **121**(9): 3442–3455.
- Chitwood D.J., Lusby W.R., Lozano R., Thompson M.J. and Svoboda J.A. (1983). Novel nuclear methylation of steckols by the nematode *Caenorhabditis elegans*. *Steroids*, **42**(3): 311–319.
- Chun L., Gong J., Yuan F., Zhang B., Liu H., Zheng T., Yu T., Xu X.Z.S. and Liu J. (2015). Metabotropic GABA signalling modulates longevity in *C. elegans*. *Nature Communications*, **6**: 8828.
- Contreras E.Q., Puppala H.L., Escalera G., Zhong W. and Colvin V.L. (2014). Size-dependent impacts of silver nanoparticles on the lifespan, fertility, growth, and locomotion of *Caenorhabditis elegans*. *Environmental Toxicology and Chemistry*, **33**(12): 2716–2723.
- Contreras L., Drago I., Zampese E., Pozzan T. (2010). Mitochondria: the calcium connection. *Biochim Biophys Acta*. **1797**(6-7):607-18.
- Corsi A.K., Wightman B. and Chalfie M. (2015). A Transparent window into biology : A primer on *Caenorhabditis elegans*. 1–31.
- Dalbeth N., Lauterio T.J. and Wolfe H.R. (2014). Mechanism of action of colchicine in the treatment of gout. *Clinical Therapeutics*. **36**(10): 1465–1479.
- Dall E. and Brandstetter H. (2016). Structure and function of legumain in health and disease. *Biochimie*. **122**: 126–150.
- Dallaire A., Garand C., Paquet E.R., Mitchell S.J., de Cabo R.D., Simard M.J. and Lebel M. (2012). Down regulation of miR-124 in both Werner syndrome DNA helicase mutant mice and mutant *Caenorhabditis elegans wrn-1* reveals the importance of this microRNA in accelerated aging. *Aging*, **4**(9): 636–647.
- Danza A., Conte A., Mastromatteo M. and Matteo Alessandro Del Nobile (2015). A New Example of Nanotechnology Applied to Minimally Processed Fruit: The Case of Fresh-Cut Melon. *Journal of Food Processing & Technology*, **6**(4): 4–7.

David H.E., Dawe A.S., de Pomerai D.I., Jones D., Candido E.P.M. and Daniells C. (2003). Construction and evaluation of a transgenic hsp16-GFP-lacZ *Caenorhabditis elegans* strain for environmental monitoring. *Environmental toxicology and chemistry; SETAC* **22**(1): 111–118.

Dengg M. and Van Meel J.C.A. (2004). *Caenorhabditis elegans* as model system for rapid toxicity assessment of pharmaceutical compounds. *Journal of Pharmacological and Toxicological Methods*, **50**(3): 209–214.

Dennis J.L., Mutwakil M.H.A.Z., Lowe K.C. and De Pomerai D.I. (1997). Effects of metal ions in combination with a non-ionic surfactant on stress responses in a transgenic nematode. *Aquatic Toxicology*, **40**(1): 37–50.

Dhawan R., Dusenbery D.B. and Williams P.L (2000). A comparison of metal-induced lethality and behavioral response in the nematode *Caenorhabditis elegans*. *Environmental Toxicology and Chemistry* **19**(12): 3061–3067.

Dhawan R., Dusenbury D. and Williams P. (1999). Comparison of Lethality, Reproduction, and Behavior As Toxicological Endpoints in the Nematode *Caenorhabditis elegans*. *Journal of Toxicology and Environmental Health, Part A* **58**(7): 451–462.

Dickinson B.C. and Chang C.J. (2012). Chemistry and biology of reactive oxygen species in signaling or stress responses. *Nat Chem Biol.* **7**(8): 504–11.

Diers A.R., Higdon A.N., Ricart K.C., Johnson M.S., Agarwal A., Kalyanaraman B., Landar A., Darley-Usmar V.M. (2010). Mitochondrial targeting of the electrophilic lipid 15-deoxy-Delta12,14-prostaglandin J2 increases apoptotic efficacy via redox cell signalling mechanisms. *Biochem J.* **426**(1):31-41

Ding Y. (2014). Design, synthesis and evaluation of novel endoprotease-activated prodrugs and fluorogenic probes with theranostic applications in chemotherapy. Doctor of Philosophy, Edinburgh Napier University, United Kingdom.

Dinusson W.E., Andrews F.N. and Beeson W.M. (1950). The effect of stilbestrol, testosterone, thyroid alteration and spaying on the growth and fattening of beef heifers. *J. Anim. Sci.* **9**: 321–330.

Doonan R., McElwee J., Matthijssens F., Walker G., Houthoofd K., Back P., Matscheski A., Vanfleteren and Gems D. (2008). Against the oxidative damage theory of aging: Superoxide dismutases protect against oxidative stress but have little or no effect on lifespan in *C. elegans*. *Genes & Development* **22**: 3236–3241.

Driscoll M. (1995) Methods for the Study of Cell Death in the Nematode *Caenorhabditis elegans*. *Methods Cell Biol.* **46**: 323–353.

Edgington L.E., Verdoes M., Ortega A., Withana N.P., Lee J., Syed S., Bachmann M.H., Blum G. and Bogyo M. (2013). Functional imaging of legumain in cancer using a new quenched activity-based probe. *Journal of the American Chemical Society*, **135**(1): 174–182.

Eom H.J., Ahn J.M., Kim Y. and Choi J. (2013). Hypoxia inducible factor-1 (HIF-

1)-flavin containing monooxygenase-2 (FMO-2) signaling acts in silver nanoparticles and silver ion toxicity in the nematode, *Caenorhabditis elegans*. *Toxicology and Applied Pharmacology*. **270**(2): 106–113.

Erden A., Karagoz H., Gümüscü H.H., Karahan S., Basak M., Aykas F., Bulut K., Cetinkaya A., Avcı D. and Poyrazoglu O.K. (2013). Colchicine intoxication: A report of two suicide cases. *Therapeutics and Clinical Risk Management* **9**(1): 505–509.

Fakhravar Z., Ebrahimnejad P., Daraee H. and Akbarzadeh A. (2015). *Nanoliposomes: Synthesis Methods and Applications in Cosmetics*. *Journal of Cosmetic and Laser Therapy*.

Falzon L.C., Menzies P.I., Shakya K.P., Jones-Bitton A., Vanleeuwen J., Avula J., Jansen J.T. and Peregrine A.S. (2013). A longitudinal study on the effect of lambing season on the periparturient egg rise in Ontario sheep flocks. *Preventive Veterinary Medicine*. **110**(3–4): 467–480.

Fan Q., Cheng K., Yang Z., Zhang R., Yang M., Hu X., Ma X., Bu L., Lu X., Xiong X., Huang W., Zhao H. and Cheng Z. (2015). Perylene-diimide-based nanoparticles as highly efficient photoacoustic agents for deep brain tumor imaging in living mice. *Advanced Materials*, **27**(5): 843–847.

Fang-Yen C., Wyart M., Xie J., Kawai R., Kodger T., Chen S., Wen Q. and Samuel A.D. (2010). Biomechanical analysis of gait adaptation in the nematode *Caenorhabditis elegans*. *Proc Natl Acad Sci*, **107**(47): 20323–20328.

Fasseas M.K., Fasseas C., Mountzouris K.C. and Syntichaki P. (2013). Effects of *Lactobacillus salivarius*, *Lactobacillus reuteri*, and *Pediococcus acidilactici* on the nematode *Caenorhabditis elegans* include possible antitumor activity. *Applied Microbiology and Biotechnology* **97**(5): 2109–2118.

Fielenbach N. and Antebi A. (2008). *C. elegans* dauer formation and the molecular basis of plasticity. *Genes and Development*, **22**(16): 2149–2165.

Fitch D.H.A. and Kelley-Thomas W. (1997). Evolution. *In*: Riddle D.L., Blumenthal T., Meyer B.J., Priess J.R., *C. elegans* II. 2nd edition. Cold Spring Harbor (NY): Cold Spring Harbor Laboratory Press. Chapter 29

Finichiu P.G., James A.M., Larsen L., Smith R.A.J. and Murphy M.P. (2013). Mitochondrial accumulation of a lipophilic cation conjugated to an ionisable group depends on membrane potential, pH gradient and pK_a: Implications for the design of mitochondrial probes and therapies. *Journal of Bioenergetics and Biomembranes*, **45**(1–2): 165–173.

George S., Pokhrel S., Xia T., Gilbert B., Ji Z., Schowalter M., Rosenauer A., Damoiseaux R., Bradley K.A., Mädler L. and Nel AE (2010). Use of a rapid cytotoxicity screening approach to engineer a safer zinc oxide nanoparticle through iron doping. *ACS Nano*, **4**(1): 15–29.

Geurden T., Hoste H., Jacquiet P., Traversa D., Sotiraki S., Frangipane di Regalbono A., Tzanidakis N., Kostopoulou D., Gaillac C., Privat S., Giangaspero A., Zanardello C., Noé L., Vanimisetti B. and Bartram D. (2014). Anthelmintic

resistance and multidrug resistance in sheep gastro-intestinal nematodes in France, Greece and Italy. *Veterinary Parasitology*. **201**(1–2): 59–66.

Ghosh R. and Emmons S.W. (2008). Episodic swimming behavior in the nematode *C. elegans*. *The Journal of experimental biology*, **211**(Pt 23): 3703–3711.

Giglio A.M., Hunter T., Bannister J.V., Bannister W.H., Hunter GJ (1994) The copper/zinc superoxide dismutase gene of *Caenorhabditis elegans*. *Biochem Mol Biol Int* 33:41–44.

Giovanni M., Yue J., Zhang L., Xie J., Ong C.N. and Leong D.T. (2015). Pro-inflammatory responses of RAW264.7 macrophages when treated with ultralow concentrations of silver, titanium dioxide, and zinc oxide nanoparticles. *Journal of Hazardous Materials*. . 297: 146–152.

Global Nanotechnology Market Analysis & Trends - Industry Forecast to 2025 (2016). <http://www.businesswire.com/news/home/20160928005566/en/Global-Nanotechnology-Market-Worth-USD-173.95-Billion>. [Accessed 10th March, 2017]

Golden J.W. and Riddle D.L. (1984). The *Caenorhabditis elegans* dauer larva: Developmental effects of pheromone, food, and temperature. *Developmental Biology*, **102**(2): 368–378.

Gomez-Marin A., Stephens G.J. and Brown A.E.X. (2016). Hierarchical compression of *Caenorhabditis elegans* locomotion reveals phenotypic differences in the organization of behaviour. *Journal of The Royal Society Interface* **13**(121): 20160466.

Gonzalez-Moragas L., Roig A. and Laromaine A. (2015). *C. elegans* as a tool for in vivo nanoparticle assessment. *Advances in Colloid and Interface Science*. 219: 10–26.

Gonzalez-Moragas L., Yu S.M., Carenza E., Laromaine A. and Roig A. (2015). Protective Effects of Bovine Serum Albumin on Superparamagnetic Iron Oxide Nanoparticles Evaluated in the Nematode *Caenorhabditis elegans*. *ACS Biomaterials Science & Engineering* acsbiomaterials.5b00253. Available at: <http://pubs.acs.org/doi/10.1021/acsbiomaterials.5b00253>.

Gore M. and Desai N.S. (2014). Computer-aided drug designing. *Methods Mol Biol*. 1168: 313–321.

Gosens I., Kermanizadeh A., Jacobsen N.R., Lenz A.G., Bokkers B., De Jong W.H., Krystek P., Tran L., Stone V., Wallin H., Stoeger T. and Cassee F.R. (2015) Comparative hazard identification by a single dose lung exposure of zinc oxide and silver nanomaterials in mice. *PLoS ONE* **10**(5): 1–17.

Graves A.L., Boyd W.A. and Williams P.L. (2005). Using transgenic *Caenorhabditis elegans* in soil toxicity testing. *Archives of Environmental Contamination and Toxicology*, **48**(4): 490–494.

Greenwald, I. (1997). Development of the Vulva. In *C. elegans* II. (ed. D. Riddle,

T Blumenthal, B. Meyer and J. Priess), 33: 519-541. Cold Spring Harbor, New York: Cold Spring Harbor Laboratory Press.

Guggisberg A.M., Amthor R.E. and Odom A.R. (2014). Isoprenoid biosynthesis in *Plasmodium falciparum*. *Eukaryotic Cell*. **13**(11): 1348–1359.

Guo P., Zhu Z., Sun Z., Wang Z., Zheng X. and Xu H. (2013). Expression of legumain correlates with prognosis and metastasis in gastric carcinoma. *PLoS one* **8**(9): e73090.

Hägerbäumer A., Höss S., Heininger P. and Traunspurger W. (2015). Experimental Studies with Nematodes in Ecotoxicology: An Overview. *Journal of Nematology*. **47**(1): 11–27.

Hall S.E., Beverly M., Russ C., Nusbaum C. and Sengupta P. (2010). A Cellular Memory of Developmental History Generates Phenotypic Diversity in *C. elegans*. *Current Biology*. Elsevier Ltd **20**(2): 149–155. Available at: <http://dx.doi.org/10.1016/j.cub.2009.11.035>.

Hancock J.T., Desikan R. and Neill S.J. (2001). Role of reactive oxygen species in cell signalling pathways. *Biochemical Society transactions*. **29**(2): 345–50.

Harris R.M. and Waring R.H. (2012). Diethylstilboestrol - A long-term legacy. *Maturitas*. **72**(2): 108–112.

Hartung T. and Rovida C. (2009). Chemical regulators have overreached. *Nature* **460**(7259): 1080–1081.

Haugen M.H., Johansen H.T., Pettersen S.J., Solberg R., Brix K., Flatmark K. and Maelandsmo G.M. (2013). Nuclear Legumain Activity in Colorectal Cancer. *PLoS ONE*. **8**(1).

Heggeness M.H., Simon M. and Singer S.J. (1978). Association of mitochondria with microtubules in cultured cells. *Proceedings Of The National Academy Of Sciences Of The United States Of America* **75**(8): 3863–3866.

Herbst A.L., Ulfelder H. and Poskanzer D.C. (1971). Adenocarcinoma of the Vagina: Association of Maternal Stilbestrol Therapy with Tumor Appearance in Young Women. *New England Journal of Medicine*. **284**(16): 878–881.

Hirokawa N. and Takemura R. (2005). Molecular motors and mechanisms of directional transport in neurons. *Nature reviews. Neuroscience*. **6**(3): 201–214.

Hoberg E.R., Lichtenfels J.R. and Gibbons L. (2004). Phylogeny for species of *Haemonchus* (Nematoda: Trichostrongyloidea): considerations of their evolutionary history and global biogeography among Camelidae and Pecora (Artiodactyla). *The Journal of parasitology*. **90**(5): 1085–102.

Hodgkin J. (1988). In "The nematode *C. elegans*" (W. B. Wood ed.) pp243-280. Cold Spring Harbor Laboratory Press. New York.

Honda Y. and Honda S. (1999). The *daf-2* gene network for longevity regulates oxidative stress resistance and Mn-superoxide dismutase gene expression in *Caenorhabditis elegans*. *The FASEB journal: official publication of the*

Federation of American Societies for Experimental Biology. **13**(11): 1385–1393.

Honda Y., Tanaka M. and Honda S. (2008). Modulation of longevity and diapause by redox regulation mechanisms under the insulin-like signaling control in *Caenorhabditis elegans*. *Experimental Gerontology*. **43**(6): 520–529.

Hoogewijs D., Houthoofd K., Matthijssens F., Vandesompele J. and Vanfleteren J.R. (2008). Selection and validation of a set of reliable reference genes for quantitative sod gene expression analysis in *C. elegans*. *BMC molecular biology* **9**(1): 9.

Hoover R.H., Hyer M., Pfeiffer R.M., Adam E., Bond B., Cheville A.L., Colton T., Hartge P., Hatch E.E., Herbst A.L., Karlan B.Y., Kaufman R., Noller K.L., Palmer J.R., Robboy S.J., Saal R.C., Strohsnitter W., Titus-Ernstoff L. and Troisi R. (2011). Adverse Health Outcomes in Women Exposed In Utero to Diethylstilbestrol. *New England Journal of Medicine*. **365**(14): 1304–1314.

Horiguchi H., Oguma E., Sakamoto T., Murata K. and Kayama F. (2014). Suppression of erythropoietin induction by diethylstilbestrol in rats. *Archives of Toxicology*. **88**(1): 137–144.

Höss S., Jänsch S., Moser T., Junker T. and Römbke J. (2009). Assessing the toxicity of contaminated soils using the nematode *Caenorhabditis elegans* as test organism. *Ecotoxicology and Environmental Safety*. **72**(7): 1811–1818.

Hradil J., Pisarev A., Babič M. and Horák D. (2007). Dextran-modified iron oxide nanoparticles. *China Particuology*. **5**(1–2): 162–168.

Huang C.C., Aronstam R.S., Chen D.R. and Huang Y.W. (2010). Oxidative stress, calcium homeostasis, and altered gene expression in human lung epithelial cells exposed to ZnO nanoparticles. *Toxicology in vitro : an international journal published in association with BIBRA*. **24**(1): 45–55.

Hughes S.E., Evason K., Xiong C. and Kornfeld K. (2007). Genetic and pharmacological factors that influence reproductive aging in nematodes. *PLoS Genetics*. **3**(2): 0254–0265.

Hunt P.R. (2016). The *C. elegans* model in toxicity testing. *Journal of Applied Toxicology*. **37**(1):50-59.

Hunter T., Bannister W.H. and Hunter G.J. (1997). Cloning, expression, and characterization of two manganese superoxide dismutases from *Caenorhabditis elegans*. *The Journal of biological chemistry*. **272**(45): 28652–9.

Hurd D.D., Miller R.M., Núñez L. and Portman D.S. (2010). Specific alpha- and beta-tubulin isotypes optimize the functions of sensory Cilia in *Caenorhabditis elegans*. *Genetics*. **185**(3): 883–896.

Ilanchezhiyan P., Zakirov A.S., Kumar G.M., Yuldashev S.U., Cho H.D., Kang T.W. and Mamadalimov A. T. (2015). Highly efficient CNT functionalized cotton fabrics for flexible/wearable heating applications. *RSC Adv*. **5**(14): 10697–10702.

Iorio M.V. and Croce C.M. (2012). Causes and Consequences of microRNA Dysregulation. *Cancer journal*. **18**(3): 215–222.

- Jasmer D.P., Roth J. and Myler P.J. (2001). Cathepsin B-like cysteine proteases and *Caenorhabditis elegans* homologues dominate gene products expressed in adult *Haemonchus contortus* intestine. *Molecular and Biochemical Parasitology* **116**(2): 159–169.
- Jensen L.T. and Culotta V.C. (2005). Activation of CuZn superoxide dismutases from *Caenorhabditis elegans* does not require the copper chaperone CCS. *Journal of Biological Chemistry*. **280**(50): 41373–41379.
- Jiang Y., Chen J., Wu Y., Wang Q. and Li H. (2016). Sublethal toxicity endpoints of heavy metals to the nematode *Caenorhabditis elegans*. *PLoS ONE*. **11**(1): 1–12.
- Jobson M.A., Jordan J.M., Sandrof M.A., Hibshman J.D., Ashley L. and Baugh L.R. (2015). Transgenerational effects of early life starvation on growth, reproduction and stress resistance in *C. elegans*. 1–37.
- Johnson, T. E. (1984). Analysis of the biological basis of aging in the nematode, with special emphasis on *Caenorhabditis elegans*. In: *Invertebrate Models in Aging Research*. Johnson, T.E. and Mitchell, D.H. (Eds.), CRC, Boca Raton, FL, pp. 59-93
- Jones N., Ray B., Ranjit K.T. and Manna A.C. (2008). Antibacterial activity of ZnO nanoparticle suspensions on a broad spectrum of microorganisms. *FEMS Microbiology. Letters*. **279**(1): 71–76.
- Ju J.W., Joo H.N., Lee M.R., Cho S.H., Cheun H.I.I., Kim J.Y., Lee Y.H., Lee K.J., Sohn W.M., Kim D.M., Kim I.C., Byoung C.P. and Kim T.S. (2009). Identification of a serodiagnostic antigen, legumain, by immunoproteomic analysis of excretory-secretory products of *Clonorchis sinensis* adult worms. *Proteomics* **9**(11): 3066–3078.
- Kaletta T. and Hengartner M.O. (2006). Finding function in novel targets: *C. elegans* as a model organism. *Nature Reviews*. **5**(5): 387–398.
- Kaminsky R., Gauvry N., Schorderet Weber S., Skripsky T., Bouvier J., Wenger A., Schroeder F., Desaulles Y., Hotz R., Goebel T., Hosking B.C., Pautrat F., Wieland-Berghausen S. and Ducray P. (2008). Identification of the amino-acetonitrile derivative monepantel (AAD 1566) as a new anthelmintic drug development candidate. *Parasitology Research*. **103**(4): 931–939.
- Kaplan R.M. and Vidyashankar A.N. (2012). An inconvenient truth: Global worming and anthelmintic resistance. *Veterinary Parasitology*. **186**(1–2): 70–78.
- Kapushesky M., Emam I., Holloway E., Kurnosov P., Zorin A., Malone J., Rustici G., Williams E., Parkinson H. and Brazma A. (2009). Gene expression Atlas at the European Bioinformatics Institute. *Nucleic Acids Research*. **38**(SUPPL.1): 690–698.
- Karbowski J., Cronin C.J., Seah A., Mendel J.E., Cleary D. and Sternberg P.W. (2006). Conservation rules, their breakdown, and optimality in *Caenorhabditis* sinusoidal locomotion. *Journal of Theoretical Biology*. **242**(3): 652–669.

Karbowski M., Spodnik J.H., Teranishi M., Wozniak M., Nishizawa Y., Usukura J. and Wakabayashi T. (2001). Opposite effects of microtubule-stabilizing and microtubule-destabilizing drugs on biogenesis of mitochondria in mammalian cells. *Journal of Cell Science*. **114**(2): 281–291.

Karnaky K.J. (1949). Diethylstilbestrol dosage in threatened and habitual abortion and premature labor. *American Journal of Obstetrics and Gynecology* **58**(3): 622–623.

Kaszuba M. (2015). Dynamic Light Scattering. *Malvern Guides*. 1–26.

Khare P., Sonane M., Nagar Y., Moin N., Ali S., Gupta K.C. and Satish A. (2014). Size dependent toxicity of zinc oxide nano-particles in soil nematode *Caenorhabditis elegans*. *Nanotoxicology*. 5390: 1–10.

Kim D.H., Puthumana J., Kang H.M., Lee M.C., Jeong C.B., Han J., Hwang D.S., Kim I.C., Lee J.W. and Lee J.S. (2016). Adverse effects of MWCNTs on life parameters, antioxidant systems, and activation of MAPK signaling pathways in the copepod *Paracyclops nana*. *Aquatic Toxicology*. 179: 115–124.

Kimble J. and Hirsh D. (1979). The postembryonic cell lineages of the hermaphrodite and male gonads in *Caenorhabditis elegans*. *Developmental Biology*. **70**(2): 396–417.

Kimble J.E. and White J.G. (1981). On the control of germ cell development in *Caenorhabditis elegans*. *Developmental Biology*. **81**(2): 208–219.

Kimura K.D., Tissenbaum H.A., Liu Y. and Ruvkun G. (1997). *daf-2*, an insulin receptor-like gene that regulates longevity and diapause in *Caenorhabditis elegans*. *Science*. **277**(5328): 942–946.

Kingston I.B. (1991). Collagen genes in *Ascaris*. M Kennedy (Ed.), Parasitic nematodes-antigens, membranes and genes. Taylor & Francis. London. pp. 66–83

Kitchen D., Decornez H., Furr J. and Bajorath J. (2004). Docking and scoring in virtual screening for drug discovery: methods and applications. *Nat Rev Drug Discov*. **3**(11): 935–949.

Kurzchalia T. and Ward S. (2003). Why do worms need cholesterol? *Nature cell biology*. **5**(8): 684–688.

Kuzbari O., Peterson C.M., Franklin M.R., Hathaway L.B., Johnstone E.B., Hammoud A.O. and Lamb J.G. (2013). Comparative analysis of human CYP3A4 and rat CYP3A1 induction and relevant gene expression by bisphenol A and diethylstilbestrol: Implications for toxicity testing paradigms. *Reproductive Toxicology*. 37: 24–30.

Lacey E. (1988) The role of the cytoskeletal protein, tubulin, in the mode of action and mechanism of drug resistance to benzimidazoles. *International Journal for Parasitology*. **18**(7): 885–936.

Lagos-quintana M., Rauhut R., Lendeckel W. and Tuschl T. (2001). Identification of novel genes Coding for RNAs of Small expressed RNAs. *Science*. **294**(5543):

853–858.

Laronda M.M., Unno K., Butler L.M. and Kurita T. (2012). The development of cervical and vaginal adenosis as a result of diethylstilbestrol exposure in utero. *Differentiation*. **84**(3): 252–260.

Lau N.C. and Lim L.P., Weinstein E.G., Bartel D.P. (2001). An abundant class of tiny RNAs with probable regulatory roles in *Caenorhabditis elegans*. *Science*. 294: 858–862.

Lee R.C. and Ambros V. (2001). An extensive class of small RNAs in *Caenorhabditis elegans*. *Science*. **294**(5543): 862–4.

Lee R.C., Feinbaum R.L. and Ambros V. (1993). The *C. elegans* heterochronic gene *lin-4* encodes small RNAs with antisense complementarity to *lin-14*. *Cell*. **75**(5): 843–854.

Leung M.C.K., Williams P.L., Benedetto A., Au C., Helmcke K.J., Aschner M. and Meyer J.N. (2008). *Caenorhabditis elegans*: An emerging model in biomedical and environmental toxicology. *Toxicological Sciences*. **106**(1): 5–28.

Levitan D. and Greenwald I. (1995). Facilitation of *lin-12*-mediated signalling by *sel-12*, a *Caenorhabditis elegans* S182 Alzheimer's disease gene. *Nature*. **377**(6547):351-4.

Li W.H., Ju Y.R., Liao C.M. and Liao V.H.C. (2014). Assessment of selenium toxicity on the life cycle of *Caenorhabditis elegans*. *Ecotoxicology*. **23**(7): 1245–1253.

Libina N., Berman J.R. and Kenyon C. (2003). Tissue-Specific Activities of *C. elegans* DAF-16 in the Regulation of Lifespan. *Cell*. **115**(4): 489–502.

Lin C.M. and Hamel E. (1981). Effects of Inhibitors of Tubulin Polymerization on GTP Hydrolysis. **256**(17): 9242–9245.

Lindblom T.H., Pierce G.J. and Sluder A.E. (2001). A *C. elegans* orphan nuclear receptor contributes to xenobiotic resistance. *Current Biology*. **11**(11): 864–868.

Little P.R., Hodge A., Maeder S.J., Wirtherle N.C., Nicholas D.R., Cox G.G. and Conder G.A. (2011). Efficacy of a combined oral formulation of derquantel-abamectin against the adult and larval stages of nematodes in sheep, including anthelmintic-resistant strains. *Veterinary Parasitology*. **181**(2–4): 180–193.

Liu C., Sun C., Huang H., Janda K. and Edgington T. (2003). Overexpression of legumain in tumors is significant for invasion/metastasis and a candidate enzymatic target for prodrug therapy. *Cancer Research*. **63**(11): 2957–2964.

Lu Y., Chen J., Xiao M., Li W. and Miller D.D. (2012). An overview of tubulin inhibitors that interact with the colchicine binding site. *Pharmaceutical Research*. **29**(11): 2943–2971.

Luc M., Taylor D.P. and Netscher C. (1979). On *endotokia matricida* and intra-uterine development and hatching of nematodes. *Nematologica*. 25: 268–274.

- Luque-Ortega R.J., Reuther P., Rivas L. and Dardonville C. (2010). New Benzophenone-derived bisphosphonium salts as leishmanicidal leads targeting mitochondria through inhibition of respiratory complex II. *Journal of Medicinal Chemistry*. **53**(4): 1788–1798.
- Lynagh T., Webb T.I., Dixon C.L., Cromers B.A. and Lynch J.W. (2011). Molecular determinants of ivermectin sensitivity at the glycine receptor chloride channel. *Journal of Biological Chemistry*. **286**(51): 43913–43924.
- Ma H., Bertsch P.M., Glenn T.C., Kabengi N.J. and Williams P.L. (2009). Toxicity of manufactured zinc oxide nanoparticles in the nematode *Caenorhabditis elegans*. *Environmental toxicology and chemistry / SETAC*. **28**(6): 1324–1330.
- Ma H., Williams P.L. and Diamond S.A. (2013). Ecotoxicity of manufactured ZnO nanoparticles - A review. *Environmental Pollution*. **172**: 76–85.
- Maeda N., Okumura K., Tanaka E., Suzuki T., Miyasho T., Haeno S., Ueda H., Hoshi N., Yokota H. (2014). Downregulation of cytochrome P450_{scc} as an initial adverse effect of adult exposure to diethylstilbestrol on testicular steroidogenesis. *Environ Toxicol*. **29**(12):1452-9.
- Maehr R., Hang H.C., Mintern J.D., Kim Y., Cuvillier A., Nishimura M., Yamada K., Shirahama-noda K., Hara-nishimura I and Ploegh HL. (2005). Asparagine endopeptidase is not essential for class II MHC antigen presentation but is required for processing of cathepsin L in mice. *Journal of Immunology* **174**(11): 7066–7074.
- Magner D.B., Wollam J., Shen Y., Hoppe C., Li D., Latza C., Rottiers V., Hutter H. and Antebi A. (2013). The NHR-8 nuclear receptor regulates cholesterol and bile acid homeostasis in *C. elegans*. *Cell Metabolism*. **18**(2): 212–224.
- Mahalingaiah S., Hart J.E., Wise L.A., Terry K.L., Boynton-Jarrett R. and Missmer S.A. (2014). Prenatal diethylstilbestrol exposure and risk of uterine leiomyomata in the nurses' health study II. *American Journal of Epidemiology*. **179**(2): 186–191.
- Manoury B., Mazzeo D., Li D.N., Billson J., Loak K., Benaroch P. and Watts C. (2003). Asparagine endopeptidase can initiate the removal of the MHC class II invariant chain chaperone. *Immunity*. **18**(4): 489–498.
- Maranghi F., Tassinari R., Moracci G., Macrì C. and Mantovani A. (2008). Effects of a low oral dose of diethylstilbestrol (DES) on reproductive tract development in F1 female CD-1 mice. *Reproductive Toxicology*. **26**(2): 146–150.
- Martin R.J. and Robertson A.P. (2010). Control of nematode parasites with agents acting on neuro-musculature systems: lessons for neuropeptide ligand discovery. *Advances in experimental medicine and biology* **692**: 138–54.
- Martínez-Valladares M., Martínez-Pérez J.M., Robles-Pérez D., Cordero-Pérez C., Famularo M.R., Fernández-Pato N., Castañón-Ordóñez L. and Rojo-Vázquez F.A. (2013). The present status of anthelmintic resistance in gastrointestinal nematode infections of sheep in the northwest of Spain by in vivo and in vitro techniques. *Veterinary Parasitology*. **191**(1–2): 177–181.

McAllister H.C., Nisbet A.J., Skuce P.J. and Knox D.P. (2011). Using lectins to identify hidden antigens in *Fasciola hepatica*. *Journal of Helminthology*. **85**(2): 121–127.

McClements J. and McClements D.J. (2015). Standardization of nanoparticle characterization: Methods for testing properties, stability and functionality of edible nanoparticles. *Critical Reviews in Food Science and Nutrition* 56:1334–1362.

McDougall H.C. (2012). Identifying 'hidden' antigens in the liver fluke, *Fasciola hepatica*. PhD. United Kingdom: University of Glasgow. Available at: <http://theses.gla.ac.uk/3661/1/2012mcdougallphd.pdf>. [Accessed 10th May, 2017]

McVey K.A., Snapp I.B., Johnson M.B., Negga R., Pressley A.S. and Fitsanakis V.A. (2016). Exposure of *C. elegans* eggs to a glyphosate-containing herbicide leads to abnormal neuronal morphology. *Neurotoxicology and Teratology*. 55: 23–31.

Mendenhall A.R., Wu D., Park S.K., Cypser J.R., Tedesco P.M., Link C.D., Phillips P.C. and Johnson T.E. (2011). Genetic dissection of late-life fertility in *Caenorhabditis elegans*. *Journals of Gerontology - Series A Biological Sciences and Medical Sciences*. **66A**(8): 842–854.

Meng X.Y., Zhang H.X., Mezei M. and Cui M. (2011). Molecular Docking: A powerful approach for structure-based drug discovery. *Current Computational Aided Drug Design* **7**(2): 146–157.

Meyer J.N., Lord C.A., Yang X.Y., Turner E.A., Badireddy A.R., Marinakos S.M., Chilkoti A., Wiesner M.R. and Auffan M. (2010). Intracellular uptake and associated toxicity of silver nanoparticles in *Caenorhabditis elegans*. *Aquatic Toxicology*. **100**(2): 140–150.

Mihaylova V.T., Borland C.Z., Manjarrez L., Stern M.J. and Sun H. (1999). The PTEN tumor suppressor homolog in *Caenorhabditis elegans* regulates longevity and dauer formation in an insulin receptor-like signaling pathway. *Proceedings of the National Academy of Sciences of the United States of America*. **96**(13): 7427–7432.

Miranda K.C., Huynh T., Tay Y., Ang Y.S., Tam W.L., Thomson A.M., Lim B. and Rigoutsos I. (2006). A Pattern-Based Method for the Identification of MicroRNA Binding Sites and Their Corresponding Heteroduplexes. *Cell*. **126**(6): 1203–1217.

Mitchell P.S., Parkin R.K., Kroh E.M., Fritz B.R., Wyman S.K., Pogosova-Agadjanyan E.L., Peterson A., Noteboom J., O'Briant K.C., Allen A., Lin D.W., Urban N., Drescher C.W., Knudsen B.S., Stirewalt D.L., Gentleman R., Vessella R.L., Nelson P.S., Martin D.B. and Tewari M. (2008). Circulating microRNAs as stable blood-based markers for cancer detection. *Proc. Natl. Acad. Sci. U.S.A.* **105**(30): 10513–10518.

Mitreva M., Blaxter M.L., Bird D.M. and McCarter J.P. (2005). Comparative genomics of nematodes. *Trends in Genetics*. **21**(10): 573–581.

Modica-Napolitano J.S., Aprille J.R. (2001). Delocalized lipophilic cations selectively target the mitochondria of carcinoma cells. *Adv Drug Deliv Rev.* **49**(1-2):63-70.

Modica-Napolitano J.S., Weiss M.J., Chen L.B., Aprille J.R. (1984). Rhodamine 123 inhibits bioenergetic function in isolated rat liver mitochondria. *Biochem Biophys Res Commun.* **118**(3):717-23.

Moran B.J. and Press L. (2005). How the rumen works. *Tropical Dairy Farming: Feeding Management for Small Holder Dairy Farmers in the Humid Tropics.* 41–49.

Murphy C.T., McCarroll S.A., Bargmann C.I., Fraser A., Kamath R.S., Ahringer J., Li H. and Kenyon C. (2003). Genes that act downstream of DAF-16 to influence the lifespan of *Caenorhabditis elegans*. *Nature.* **424**(6946): 277–283.

Nair A.B. and Jacob S. (2016). A simple practice guide for dose conversion between animals and human. *Journal of basic and clinical pharmacy.* **7**(2): 27–31.

Nakae J., Biggs W.H., Kitamura T., Cavenee W.K., Wright C.V.E., Arden K.C. and Accili D. (2002). Regulation of insulin action and pancreatic beta-cell function by mutated alleles of the gene encoding forkhead transcription factor Foxo1. *Nature genetics.* **32**(2): 245–53.

Newbold R.R., Padilla-Banks E. and Jefferson W.N. (2009). Environmental estrogens and obesity. *Molecular and Cellular Endocrinology.* **304**(1–2): 84–89.

Nieuwhof G.J. and Bishop S.C. (2005). Costs of the major endemic diseases of sheep in Great Britain and the potential benefits of reduction in disease impact. *Animal Science.* **81**(1): 23–29.

Nikolaou S. and Gasser R.B. (2006). Prospects for exploring molecular developmental processes in *Haemonchus contortus*. *International Journal for Parasitology.* **36**(8): 859–868.

Nohynek G.J., Lademann J., Ribaud C. and Roberts M.S. (2007). Grey goo on the skin? Nanotechnology, cosmetic and sunscreen safety. *Critical Reviews in Toxicology.* **37**(3): 251–277.

Noller K.L., Blair P.B., O'Brien P.C., Melton L.J., Offord J.R., Kaufman R.H. and Colton T. (1988). Increased occurrence of autoimmune disease among women exposed in utero to diethylstilbestrol. *Fertility and sterility.* **49**(6): 1080–2.

Noller K.L. and Fish C.R. (1974). Diethylstilbestrol Usage: Its Interesting Past, Important Present, and Questionable Future. *Medical Clinics of North America.* **58**(4): 793–810.

Nowack B. and Bucheli T.D. (2007). Occurrence, behavior and effects of nanoparticles in the environment. *Environmental Pollution.* **150**(1): 5–22.

Nussbaum-Krammer C.I., Neto M.F., Brielmann R.M., Pedersen J.S. and Morimoto R.I. (2015). Investigating the spreading and toxicity of prion-like proteins using the metazoan model organism *C. elegans*. *Journal of visualized*

experiments : JoVE (95): 52321.

O'Connor L.J., Walkden-Brown S.W. and Kahn L.P. (2006). Ecology of the free-living stages of major trichostrongylid parasites of sheep. *Veterinary Parasitology*. **142**(1–2): 1–15.

Oberdörster G. (2010). Safety assessment for nanotechnology and nanomedicine: Concepts of nanotoxicology. *Journal of Internal Medicine*. **267**(1): 89–105.

Obiol-Pardo C., Rubio-Martinez J. and Imperial S. (2011). The methylerythritol phosphate (MEP) pathway for isoprenoid biosynthesis as a target for the development of new drugs against tuberculosis. *Current medicinal chemistry*. **18**(9): 1325–38.

Ogg S., Paradis S., Gottlieb S., Patterson G.I., Lee L., Tissenbaum H. A. and Ruvkun G. (1997). The Fork head transcription factor DAF-16 transduces insulin-like metabolic and longevity signals in *C. elegans*. *Nature*. **389**(6654): 994–999.

Oh S.W., Mukhopadhyay A., Dixit B.L., Raha T., Green M.R. and Tissenbaum H.A. (2006). Identification of direct DAF-16 targets controlling longevity, metabolism and diapause by chromatin immunoprecipitation. *Nat.Genet.* **38**(2): 251–257.

Ohno Y., Nakashima J., Ohori M., Hashimoto T., Hatano T. and Tachibana M. (2010). Association of the Legumain Expression Pattern With Prostate Cancer Invasiveness and Aggressiveness. *The Journal of Urology*. **183**(4): e266.

Oliver E.M., Skuce P.J., McNair C.M. and Knox D.P. (2006). Identification and characterization of an asparaginyl proteinase (legumain) from the parasitic nematode, *Haemonchus contortus*. *Parasitology*. **133**(2): 237–44.

Pandurangan M., Veerappan M. and Kim D.H. (2014). Cytotoxicity of zinc oxide nanoparticles on antioxidant enzyme activities and mRNA expression in the cocultured C2C12 and 3T3-L1 Cells. *Applied Biochemistry and Biotechnology*. **175**(3): 1270–1280.

Park S.Y. and Choi J. (2017). Molecular Characterization and Expression Analysis of P38 MAPK Gene and Protein in Aquatic Midge, *Chironomus riparius* (Diptera: Chironomidae), Exposed to Environmental Contaminants. *Archives of environmental contamination and toxicology*. **72**(3): 428–438.

Pasquinelli A.E., Reinhart B.J., Slack F., Martindale M.Q., Kurodak M.I., Maller B, Hayward D.C., Ball E.E., Degnan B., Ller P.M., Spring J., Srinivasan A., Fishman M., Finnerty J., Joseph E.D. and Ruvkun G. (2000). Conservation of the sequence and temporal expression of let-7 heterochronic regulatory RNA. *Nature*. **408**(6808): 86–89.

Patel N.R., Hatziantoniou S., Georgopoulos A., Demetzos C., Torchilin V.P., Weissig V., D'Souza G.G. (2010). Mitochondria-targeted liposomes improve the apoptotic and cytotoxic action of sclareol. *J Liposome Res*. **20**(3):244-9.

Payne, B. A. I., & Chinnery, P. F. (2015). Mitochondrial dysfunction in aging:

Much progress but many unresolved questions. *Biochimica et Biophysica Acta*. **1847**(11): 1347–1353.

Pederson J.S. (n.d.). *C. elegans* motility analysis in ImageJ - A practical approach. 1–15. <http://phage.dk/plugins/download/wrMTrck.pdf>. [Accessed 19th August, 2016].

Petryszak R., Burdett T., Fiorelli B., Fonseca N.A., Gonzalez-Porta M., Hastings E., Huber W., Jupp S., Keays M., Kryvych N., McMurry J., Marioni J.C., Malone J., Megy K., Rustici G., Tang A.Y., Taubert J., Williams E., Mannion O., Parkinson H.E. and Brazma A. (2014). Expression Atlas update - A database of gene and transcript expression from microarray- and sequencing-based functional genomics experiments. *Nucleic Acids Research*. **42**(D1): 926–932.

Pettersson S. (2004). Biochemistry of topoisomerase inhibition and cellular mechanisms of anthraquinone-amino acid conjugates in vitro. Edinburgh Napier University.

Pickett C.L. and Kornfeld K. (2013). Age-related degeneration of the egg-laying system promotes matricidal hatching in *Caenorhabditis elegans*. *Aging Cell* **12**(4): 544–553.

Piekny A.J., Johnson J.L.F., Cham G.D. and Mains P.E. (2003). The *Caenorhabditis elegans* nonmuscle myosin genes *nmy-1* and *nmy-2* function as redundant components of the *let-502*/Rho-binding kinase and *mel-11*/myosin phosphatase pathway during embryonic morphogenesis. *Development*. **130**(23): 5695–5704.

Pierce-Shimomura J.T., Chen B.L., Mun J.J., Ho R., Sarkis R. and McIntire S.L. (2008). Genetic analysis of crawling and swimming locomotory patterns in *C. elegans*. *Proceedings of the National Academy of Sciences*. **105**(52): 20982–20987.

Polak N., Read D.S., Jurkschat K., Matzke M., Kelly F.J., Spurgeon D.J. and Stürzenbaum S.R. (2014). Metalloproteins and phytochelatin synthase may confer protection against zinc oxide nanoparticle induced toxicity in *Caenorhabditis elegans*. *Comparative Biochemistry and Physiology - C Toxicology and Pharmacology*. **160**(1): 75–85.

Power R.S., David H.E., Mutwakil M.H. A.Z., Fletcher K., Daniells C., Nowell M. A., Dennis J.L., Martinelli A., Wiseman R., Wharf E. and Pomerai D.I. (1998). Stress-inducible transgenic nematodes as biomonitors of soil and water pollution. *Journal of Biosciences*. **23**(4): 513–526.

Prach M., Stone V. and Proudfoot L. (2013). Zinc oxide nanoparticles and monocytes: Impact of size, charge and solubility on activation status. *Toxicology and Applied Pharmacology*. **266**(1): 19–26.

Prichard R.K. (2001). Genetic variability following selection of *Haemonchus contortus* with anthelmintics. *Trends in Parasitology*. **17**(9): 445–453.

Prichard R.K., Basáñez M.G., Boatman B.A., McCarthy J.S., García H.H., Yang G.J., Sripa B. and Lustigman S. (2012). A research agenda for helminth diseases

of humans: Intervention for control and elimination. *PLoS Neglected Tropical Diseases*. **6**(4).

Pritchard C.C., Cheng H.H. and Tewari M. (2012). MicroRNA profiling: approaches and considerations. *Nature Reviews Genetics*. Nature Publishing Group. **13**(5): 358–369.

Raizen D., Song B., Trojanowski N. and Young-Jai Y. (2012). Methods for measuring pharyngeal behaviors. *WormBook: The Online Review of C. elegans Biology*. **7**(6): 533–544.

Ranganathan R., Sawin E.R., Trent C. and Horvitz H.R. (2001). Mutations in the *Caenorhabditis elegans* serotonin reuptake transporter MOD-5 reveal serotonin-independent and -independent activities of fluoxetine. *The Journal of neuroscience : the official journal of the Society for Neuroscience*. **21**(16): 5871–84.

Ravelli R.B.G., Gigant B., Curmi P.A., Jourdain I., Lachkar S., Sobel A. and Knossow M. (2004). Insight into tubulin regulation from a complex with colchicine and a stathmin-like domain. *Letters To Nature*. 428: 198–202.

Ravindra R. and Aronstam R.S. (1991). Colchicine Inhibits Acetylcholine Receptor Stimulation of G Protein GTPase Activity in Rat Striatum : s. 259–262.

Read D.S., Matzke M., Gweon H.S., Newbold L.K., Heggelund L., Ortiz M.D., Lahive E., Spurgeon D. and Svendsen C. (2016). Soil pH effects on the interactions between dissolved zinc, non-nano- and nano-ZnO with soil bacterial communities. *Environmental Science and Pollution Research*. **23**(5): 4120–4128.

Reilly J.O., Mirzaei F., Forman M.R. and Ascherio A. (2010). Original Contribution Diethylstilbestrol Exposure in Utero and Depression in Women. **171**(8): 876–882.

Reinhart B.J., Slack F.J., Basson M., Pasquinelli A.E., Bettinger J.C., Rougvie A.E., Horvitz H.R. and Ruvkun G. (2000). The 21-nucleotide let-7 RNA regulates developmental timing in *Caenorhabditis elegans*. *Nature*. **403**(6772): 901–906.

Riddle D.L. and Albert P.S. (1997). Genetic and environmental regulation of dauer larva development. *In: D Riddle, T Blumenthal, B Meyer, J Priess (Eds.), C. elegans II*, Cold Spring Harbor Laboratory Press. Cold Spring Harbor. New York pp. 739–768

Rogers S., Rice K.M., Manne N.D., Shokuhfar T., He K., Selvaraj V. and Blough E.R. (2015). Cerium oxide nanoparticle aggregates affect stress response and function in *Caenorhabditis elegans*. *SAGE open medicine* 3: 2050312115575387. doi: 10.1177/2050312115575387. [Accessed 4th August, 2016]

Roh J.Y., Lee J. and Choi J. (2006). Assessment of stress-related gene expression in the heavy metal-exposed nematode *Caenorhabditis elegans*: a potential biomarker for metal-induced toxicity monitoring and environmental risk assessment. *Environmental toxicology and chemistry / SETAC*. **25**(11): 2946–56.

Roh J.Y., Sim S.J., Yi J., Park K., Chung K.H., Ryu D.Y., Choi J. (2009).

Ecotoxicity of silver nanoparticles on the soil nematode *Caenorhabditis elegans* using functional ecotoxicogenomics. *Environ Sci Technol.* **43**(10):3933-40

Roskov Y., Kunze T., Orrell T., Abucay L., Culham A., Bailly N., Kirk P., Bourgoin T., Decock W., De Wever A., eds. (2014). Species 2000 & ITIS Catalogue of Life,. Digital resource at www.catalogueoflife.org/col. Species 2000: Naturalis, Leiden, the Netherlands. [Accessed 19th August, 2014]

Rothstein N., Stoller T. and Rajan T. (1988). DNA base composition of filarial nematodes. *Parasitology.* **97**(1): 75–79.

Rüegger S. and Großhans H. (2012). MicroRNA turnover: When, how, and why. *Trends in Biochemical Sciences.* **37**(10): 436–446.

Sager H., Hosking B., Bapst B., Stein P., Vanhoff K. and Kaminsky. R (2009). Efficacy of the amino-acetonitrile derivative, monepantel, against experimental and natural adult stage gastro-intestinal nematode infections in sheep. *Veterinary Parasitology.* **159**(1): 49–54.

Sajid M. and McKerrow J.H. (2002). Cysteine proteases of parasitic organisms. *Molecular and Biochemical Parasitology.* **120**(1): 1–21.

Saptarshi S.R., Feltis B.N., Wright P.F. and Lopata A.L. (2015). Investigating the immunomodulatory nature of zinc oxide nanoparticles at sub-cytotoxic levels in vitro and after intranasal instillation in vivo. *Journal of nanobiotechnology.* 13: 6. doi: 10.1186/s12951-015-0067-7. [Accessed 17th June 2016]

Sargison N.D., Jackson F., Bartley D.J., Wilson D.J., Stenhouse L.J. and Penny C.D. (2007). Observations on the emergence of multiple anthelmintic resistance in sheep flocks in the south-east of Scotland. *Veterinary Parasitology.* **145**(1–2): 65–76.

Schindelin J., Arganda-Carreras I., Frise E., Kaynig V., Longair M., Pietzsch T., Preibisch S., Rueden C., Saalfeld S., Schmid B., Tinevez J.Y, White D.J., Hartenstein V., Eliceiri K., Tomancak P., Cardona A., Liceiri K., Tomancak P. and A.C. (2012). Fiji: an open source platform for biological image analysis. *Nature Methods.* **9**(7): 676–682.

Scott I. and Sutherland I. (2010). Gastrointestinal Nematodes of Sheep and Cattle: Biology and Control. *Oxford.* Wiley-Blackwell.

Scott I., Pomroy W.E., Kenyon P.R., Smith G., Adlington B. and Moss A. (2013). Lack of efficacy of monepantel against *Teladorsagia circumcincta* and *Trichostrongylus colubriformis*. *Veterinary Parasitology.* **198**(1–2): 166–171.

Seidel H.S. and Kimble J. (2011). The oogenic germline starvation response in *C. elegans*. *PLoS ONE* 6(12):e28074. doi: 10.1371/journal.pone.0028074. [Accessed 7th January, 2017]

Shaye D.D. and Greenwald I. (2011). Ortholist: A compendium of *C. elegans* genes with human orthologs. *PLoS ONE* 6(5):e20085. doi: 10.1371/journal.pone.0020085. [Accessed 7th January, 2017]

Sherrington R., Rogaev E.I., Liang Y., Rogaeva E.A., Levesque G., Ikeda M., Chi

H., Lin C., Li G., Holman K., Tsuda T., Mar L., Foncin J.F., Bruni A.C., Montesi M.P., Sorbi S., Rainero I., Pinessi L., Nee L., Chumakov I., Pollen D., Brookes A., Sanseau P., Polinsky R.J., Wasco W., Da Silva H.A., Haines J.L., Perkick-Vance M.A., Tanzi R.E., Roses A.D., Fraser P.E., Rommens J.M. and St George-Hyslop P.H. (1995). Cloning of a gene bearing missense mutations in early-onset familial Alzheimer's disease. *Nature*, 754–60.

Shibata Y., Branicky R., Landaverde I.O. and Hekimit S. (2003). Redox regulation of germline and vulval development in *Caenorhabditis elegans*. *Science*. **302**(5651): 1779–1782.

Shimkin M.B. and Grady H.G. (1941). Toxic and carcinogenic effects of stilbestrol in strain c3h male mice. *Journal of the National Cancer Institute*. **2**(1): 55–60.

Shirahama-Noda K., Yamamoto A., Sugihara K., Hashimoto N., Asano M., Nishimura M. and Hara-Nishimura I. (2003). Biosynthetic processing of cathepsins and lysosomal degradation are abolished in asparaginyl endopeptidase-deficient mice. *Journal of Biological Chemistry*. **278**(35): 33194–33199.

Shook D.R. and Johnson T.E. (1999). Quantitative trait loci affecting survival and fertility-related traits in *Caenorhabditis elegans* show genotype-environment interactions, pleiotropy and epistasis. *Genetics*. **153**(3): 1233–1243.

Silvestre F., Dierick J.F., Dumont V., Dieu M., Raes M. and Devos P. (2006). Differential protein expression profiles in anterior gills of *Eriocheir sinensis* during acclimation to cadmium. *Aquatic Toxicology*. **76**(1): 46–58.

Skelly P.J. and Shoemaker C.B. (2001). *Schistosoma mansoni* proteases Sm31 (cathepsin B) and Sm32 (legumain) are expressed in the cecum and protonephridia of cercariae. *The Journal of parasitology*. **87**(5): 1218–1221.

Slatko B. E., Taylor M. J., and Foster J. M. (2010). The *Wolbachia* endosymbiont as an anti-filarial nematode target. *Symbiosis*. **51**(1), 55–65.

Sliwoski G., Kothiwale S., Meiler J. and Lowe E.W. (2013). Computational Methods in Drug Discovery. *Pharmacological Reviews*. **66**(1): 334–395.

Smith O.W. (1948). Diethylstilbestrol in the prevention and treatment of complications of pregnancy. *American Journal of Obstetrics and Gynecology*. **56**(5): 821–834.

Sok J., Calfon M., Lu J., Lichtlen P., Clark S.G. and Ron D. (2001). Arsenite-inducible RNA-associated protein (AIRAP) protects cells from arsenite toxicity. *Cell stress & chaperones*. **6**(1): 6–15.

Sokolov S. V., Tschulik K., Batchelor-McAuley C., Jurkschat K. and Compton R.G. (2015). Reversible or not? Distinguishing agglomeration and aggregation at the nanoscale. *Analytical Chemistry*. **87**(19): 10033–10039.

Steele A., Bayer I. and Loth E. (2009). Inherently superoleophobic nanocomposite coatings by Spray Atomization. *Nano Letters*. **9**(1): 501–505.

Steinmetz R., Brown N.G., Allen D.L., Bigsby R.M. and Ben-Jonathan N. (1997).

- The environmental estrogen bisphenol A stimulated prolactin release in vitro and in vivo. *Endocrinology*. **138**(5): 1780–1786.
- Von Stetina S.E., Treinin M. and Miller D.M. (2005). The Motor Circuit. *International Review of Neurobiology*. **69**(5): 125–167.
- Stiernagle T. (2006) Maintenance of *C. elegans*. *WormBook* (1999): 1–11. Review. PubMed PMID: 18050451. [Accessed 18th April, 2014].
- De Strooper B., Annaert W., Cupers P., Saftig P., Craessaerts K., Mumm J.S., Schroeter E.H., Schrijvers V., Wolfe M.S., Ray W.J., Goate A. and Kopan R. (1999). A presenilin-1-dependent gamma-secretase-like protease mediates release of Notch intracellular domain. *Nature*. **398**: 518–522.
- Sulston J. (1988). *Cell lineage*. In: *The Nematode Caenorhabditis elegans*. Cold Spring Harbour. United Kingdom. pp123-155.
- Sulston J., Dew M. and Brenner S. (1975) Dopaminergic neurons in the nematode *Caenorhabditis elegans*. *The Journal of comparative neurology*. **163**(2): 215–226.
- Sulston J. and Hodgkin J. (1988) Methods. *The Nematode Caenorhabditis elegans*. 587–606.
- Sulston J.E. and Horvitz H.R. (1977). Post-embryonic cell lineages of the nematode, *Caenorhabditis elegans*. *Developmental Biology*. **56**(1): 110–156. Available
- Sulston J.E., Schierenberg E., White J.G. and Thomson J.N. (1983) The embryonic cell lineage of the nematode *Caenorhabditis elegans*. *Developmental Biology*. **100**(1): 64–119.
- Sun X., Wong J.R., Song K., Hu J., Garlid K.D., Chen L.B. (1994). AA1, a newly synthesized monovalent lipophilic cation, expresses potent in vivo antitumor activity. *Cancer Res*. **54**(6):1465-71.
- Sundaram M. and Greenwald I. (1993). Suppressors of a *lin-12* hypomorph define genes that interact with both *lin-12* and *glp-1* in *Caenorhabditis elegans*. *Genetics*. **135**(3): 765–783.
- Sustainable Control of Parasites in Sheep (SCOPS). (2012). Faecal Egg Count (FEC) monitoring. Available at:<http://www.scops.org.uk/endoparasites-using-fecs.html>. [Accessed 8th June, 2014]
- Sutherland I.A. and Leathwick D.M. (2011). Anthelmintic resistance in nematode parasites of cattle: A global issue? *Trends in Parasitology*. **27**(4): 176–181.
- Swierczek N.A., Giles A.C., Rankin C.H. and Kerr R.A. (2011). High-throughput behavioral analysis in *C. elegans*. *Nature Methods*. **8**(7): 592–598.
- Syama S., Reshma S.C., Sreekanth P.J., Varma H.K. and Mohanan P.V. (2013). Effect of Zinc oxide nanoparticles on cellular oxidative stress and antioxidant defense mechanisms in mouse liver. *Toxicological & Environmental Chemistry*. **95**(3): 495–503.

- Takao A. and Kaziro Y. (1977). Role of GTP in the assembly of microtubules. *Journal of biochemistry*. **82**(4): 1063–1071.
- Taylor C.M., Fischer K., Abubucker S., Wang Z., Martin J., Jiang D., Magliano M., Rosso M.N., Li B.W., Fischer P.U., Mitreva M. (2011). Targeting protein-protein interactions for parasite control. *PLoS One*. **6**(4):e18381. doi: 10.1371/journal.pone.0018381. [Accessed on 17th August, 2017]
- Teng L., Wada H. and Zhang S. (2010). Identification and functional characterization of legumain in amphioxus *Branchiostoma belcheri*. *Bioscience reports*. **30**(3): 177–186.
- Trajkovski M., Hausser J., Soutschek J., Bhat B., Akin A., Zavolan M., Heim M.H. and Stoffel M. (2011). MicroRNAs 103 and 107 regulate insulin sensitivity. *Nature*. **474**(7353): 649–53.
- Tran D.Q., Jin L., Chen J., McLachlan J.A. and Arnold S.F. (1997). Evaluation of clinical and environmental anti-estrogens with human estrogen receptor expressed in *Saccharomyces cerevisiae*: a novel role for ABC-cassette transporters in mediating anti-estrogenic activity. *Biochem Biophys Res Commun* **235**(3): 669–674.
- Truong-Tran Q., Carter J., Ruffin R. and Zalewski P.D. (2001). New insights into the role of zinc in the respiratory epithelium. *Immunology and cell biology*. **79**(2): 170–177.
- Truong T., Karlinski Z.A., O'Hara C., Cabe M., Kim H. and Bakowska J.C. (2015). Oxidative stress in *Caenorhabditis elegans*: Protective effects of spartin. *PLoS ONE*. **10**(6): 1–14.
- Turk B., Bieth J.G., Björk I., Dolenc I., Cimerman N., Kos J., Öolic A., Stoka V. and Turk V. (1995). Regulation of the activity of lysosomal cysteine proteinases by pH-Induced inactivation and/or endogenous protein inhibitors, cystatins. *Biol Chem Hoppe Seyler*. **376**(4):225-30.
- Valentine J.S., Doucette P.A. and Potter S.Z. (2005). Copper-zinc superoxide dismutase and amyotrophic lateral sclerosis. *Annu. Rev. Biochem.* **74**: 563–593.
- Vinaud M.C., Ferreira C.S., Lino Junior Rde S., Bezerra J.C. (2008). *Taenia crassiceps*: energetic and respiratory metabolism from cysticerci exposed to praziquantel and albendazole in vitro. *Exp Parasitol*. **120**(3):221-6.
- Walker J.T. and Tsui R.K. (1968). Induction of ovoviviparity in Rhabditis by S02. *Nematologica*. **14**: 148–149.
- Waller P.J., Rudby-Martin L., Ljungström B.L. and Rydzik A. (2004). The epidemiology of abomasal nematodes of sheep in Sweden, with particular reference to over-winter survival strategies. *Veterinary Parasitology*. **122**(3): 207–220.
- Walter D. (2013). Primary particles - agglomerates - aggregates. *Nanomaterials* **9**–24.
- Wang K., Zhang S., Marzolf B., Troisch P., Brightman A., Hu Z., Hood L.E. and

- Galas D.J. (2009). Circulating microRNAs, potential biomarkers for drug-induced liver injury. *Proceedings of the National Academy of Sciences of the United States of America*. **106**(11): 4402–7.
- Wang L., Chen S., Zhang M., Li N., Chen Y., Su W., Liu Y., Lu D., Li S., Yang Y., Li Z., Stupack D., Qu P., Hu A. and Xiang R. (2012). Legumain: A biomarker for diagnosis and prognosis of human ovarian cancer. *Journal of Cellular Biochemistry*. **113**(8): 2679–2686.
- Wawrzyniak I., Texier C., Poirier P., Viscogliosi E., Tan K.S.W., Delbac F. and E.I. Alaoui H. (2012). Characterization of two cysteine proteases secreted by Blastocystis ST7, a human intestinal parasite. *Parasitology International*. **61**(3): 437–442.
- Wehmas L.C., Anders C., Chess J., Punnoose A., Pereira C.B., Greenwood J.A. and Tanguay R.L. (2015). Comparative metal oxide nanoparticle toxicity using embryonic zebrafish. *Toxicology reports*. **2**: 702–715.
- White J.G., Southgate J.N. and Thomson J.N. (1986). The structure of the nervous system of the nematode *Caenorhabditis elegans*. *Phil. Trans. R. Soc.* **314**: 1–340.
- White R., Jobling S., Hoare S.A., Sumpter J.P., Parker M.G. (1994). Environmentally persistent alkylphenolic compounds are estrogenic. *Endocrinology*. **135**(1):175-82
- Williams P.L. and Dusenbery D.B. (1988). Using the nematode *Caenorhabditis elegans* to predict mammalian acute lethality to metallic salts. *Toxicology and Industrial Health*. **4**: 469–478.
- Wu H., Huang C., Taki F.A., Zhang Y., Dobbins D.L., Li L., Yan H. and Pan X. (2015). Benzo- α -pyrene induced oxidative stress in *Caenorhabditis elegans* and the potential involvements of microRNA. *Chemosphere*. **139**: 496–503.
- Wu Q., Nouara A., Li Y., Zhang M., Wang W., Tang M., Ye B., Ding J. and Wang D. (2013). Comparison of toxicities from three metal oxide nanoparticles at environmental relevant concentrations in nematode *Caenorhabditis elegans*. *Chemosphere*. **90**(3): 1123–1131.
- Xiao Y., Vijver M.G., Chen G. and Peijnenburg W.J.G.M. (2015). Toxicity and accumulation of Cu and ZnO nanoparticles in *Daphnia magna*. *Environmental Science and Technology*. **49**(7): 4657–4664.
- Yanase S., Onodera A., Tedesco P., Johnson T.E. and Ishii N. (2009). SOD-1 deletions in *Caenorhabditis elegans* alter the localization of intracellular reactive oxygen species and show molecular compensation. *Journals of Gerontology - Series A Biological Sciences and Medical Sciences*. **64**(5): 530–539.
- Yang R., Ren M., Rui Q. and Wang D. (2016). A *mir-231*-regulated protection mechanism against the toxicity of graphene oxide in nematode *Caenorhabditis elegans*. *Scientific reports*. **6**: 1–12.
- Yemini E., Jucikas T., Grundy L.J., Brown A.E., Schafer W.R, Brown E.X. and

- Schafer W.R. (2013). A database of *Caenorhabditis elegans* behavioral phenotypes. *Nat Methods* **10**(9): 877–879.
- Yen K., Narasimhan S.D. and Tissenbaum H.A. (2011). DAF-16 = Forkhead Box O Transcription Factor : Many Paths to a Single Fork (head) in the Road. **14**(4).
- Zielonka J., Joseph J., Sikora A., Hardy M., Ouari O., Vasquez-Vivar J., Cheng G., Lopez M., Kalyanaraman B. (2017). Mitochondria-targeted triphenylphosphonium-based compounds: syntheses, mechanisms of action, and therapeutic and diagnostic applications. *Chem Rev.* **117**(15):10043-10120.
- Zhang X., Li J.H., Duan S.X., Lin Q.J., Ke S., Ma L., Huang T.H. and Jiang X.W. (2014). G protein-coupled estrogen receptor-protein kinase A-ERK-CREB signaling pathway is involved in the regulation of mouse gubernaculum testis cells by diethylstilbestrol. *Archives of Environmental Contamination and Toxicology.* **67**(1): 97–103.
- Zhang Y., Chen D., Smith M.A., Zhang B. and Pan X. (2012). Selection of reliable reference genes in *Caenorhabditis elegans* for analysis of nanotoxicity. *PLoS ONE* **7**(3).
- Zhao Y., Yang J. and Wang D. (2016). A MicroRNA-mediated insulin signaling pathway regulates the toxicity of multi-walled carbon nanotubes in nematode *Caenorhabditis elegans*. *Scientific reports.* **6**: 23234. doi: 10.1038/srep23234. [Accessed 10th December, 2016].
- Zhou K.I., Pincus Z. and Slack F.J. (2011). Longevity and stress in *Caenorhabditis elegans*. *Aging.* **3**(8): 733–753.
- Zijno A., De Angelis I., De Berardis B., Andreoli C., Russo M.T., Pietraforte D., Scorza G., Degan P., Ponti J., Rossi F. and Barone F. (2015). Different mechanisms are involved in oxidative DNA damage and genotoxicity induction by ZnO and TiO₂ nanoparticles in human colon carcinoma cells. *Toxicology in Vitro.* **29**(7): 1503–1512.
- Zondervan R., Kulzer F., Kol M.A. and Orrit M. (2003). Photobleaching of Rhodamine 6G in poly (vinyl alcohol) at the ensemble and single-molecule level. *J. Phys. Chem.* **108** (10):1657–1665.

Appendices

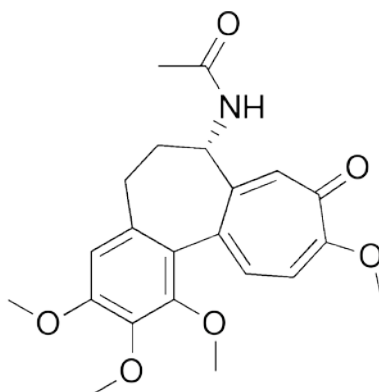
Appendix A: Synchronization

C. elegans synchronization is important in the current research because it could help monitor if the stage-specific effects resulting from exposure to toxicants. Also, as a helminth parasite model, the worm can easily be used to mimic the target parasite's infective stage since this is usually difficult to isolate and maintain successfully outside the host. This is a significant attribute of *C. elegans* over using helminth parasite directly in experiments. A description of the procedure for synchronization is seen below.

1. Worms were chunked onto 3 *E. coli* OP50-seeded 60mm NGM plates. The worms were allowed to grow for 3 days
2. On the third day, with the number of eggs/adults on the plates increased, 5ml of M9 was poured into each of the plates and gently swirled to dislodge the worms.
3. Using a 5ml pipette, the worms were transferred to a 15ml conical tube and centrifuged for 2 minutes at 5000rpm to pellet the worms.
4. This was followed by aspiration of 14.5ml of the M9 without disturbing the worm pellet.
5. A 14.5ml volume of 20% NaOCl solution was added to the tube.
6. The tube was mixed by inverting gently for approximately 5 minutes or until a decrease in the number of intact adult worms was seen. The bleaching should not exceed 5 minutes or the eggs would be killed.
7. Once most of the bodies had dissolved, the tube was centrifuged at maximum speed for 1 minute.
8. A 14.5ml volume of the 20% NaOCl solution (see section D of the appendix) was aspirated without disturbing the worm pellet.
9. 14.5ml of M9 was added to the tube and mixed well.
10. The tube was centrifuged again at 5000rpm for 2 minutes.
11. Most of the M9 was aspirated without disturbing the worm pellet.
12. Steps 9 -11 were repeated twice to take off the hypochlorite.
13. 10ml of M9 was added and agitated to resuspend the pellet and this was transferred into a 250ml flask containing 40ml M9.

14. The eggs were allowed to hatch with gentle rocking at 160rpm and 20°C.
15. After 8 hours of incubation, mid L1 larvae were observed to confirm hatching and worms were centrifuged and the pellets were collected.
16. 7ml of S medium was added and agitated to resuspend the pellet, this was transferred into a 500ml flask containing 100ml S. medium inoculated with *E. coli* OP50 and incubated for 29 hours to allow the larvae develop into mid L4 stage.
17. Dead worms, debris and waste were removed from the synchronized population by centrifuging at 5000rpm for 1minute and aspirating the supernatant containing living worms into a fresh tube.
18. The tube containing living synchronized worms was place on ice for 10 minutes to allow the worms settle.
19. The supernatant is aspirated and the worms are collected at the bottom of the tube.

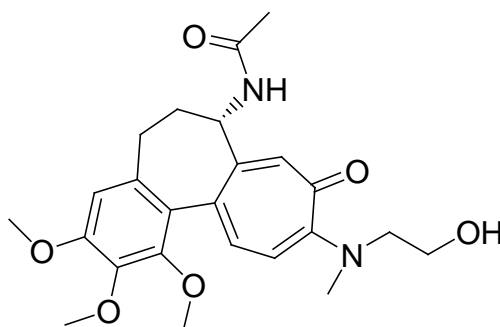
Appendix B: Anthelmintic derivatives



$C_{22}H_{25}NO_6$

Mol. Wt.: 399.437

Figure 1: Colchicine



GEO 1

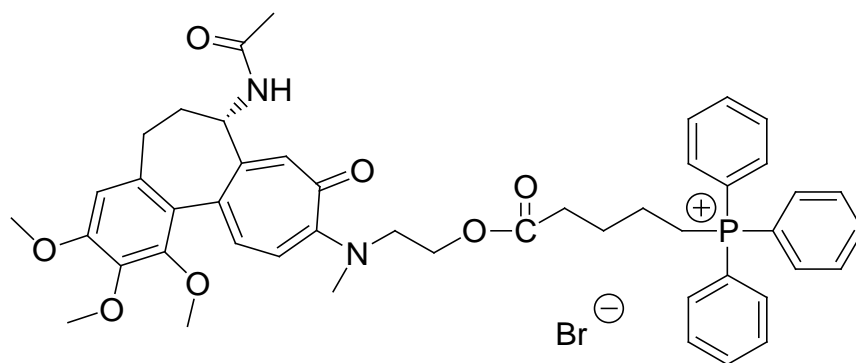
$C_{24}H_{30}N_2O_6$

Exact Mass: 442.21

Mol. Wt.: 442.50

C, 65.14; H, 6.83; N, 6.33; O, 21.69

Figure 2: Colchicine derivative

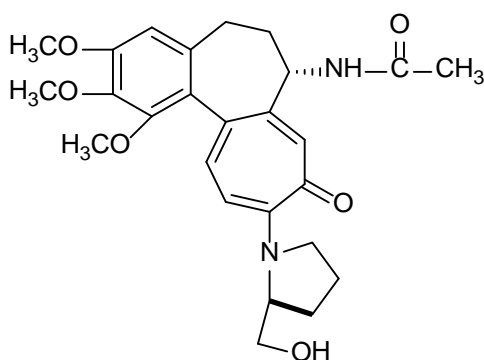


GEO 2

$C_{47}H_{52}BrN_2O_7P$
 Exact Mass: 866.27
 Mol. Wt.: 867.80

C, 65.05; H, 6.04; Br, 9.21; N, 3.23; O, 12.91; P, 3.57

Figure 3: Colchicine derivative + Triphenylphosphonium

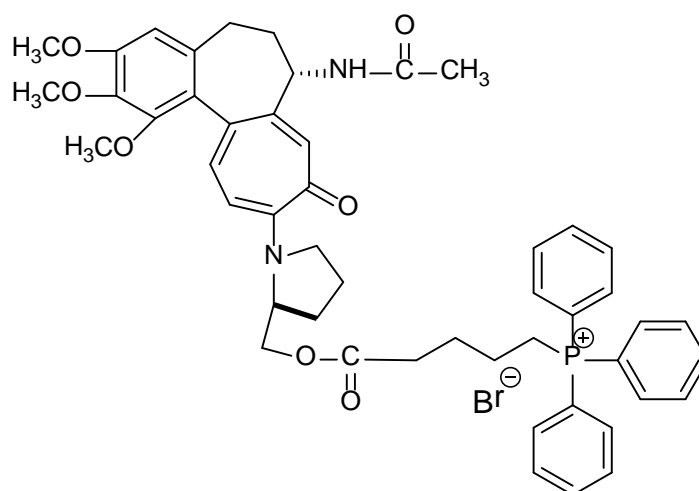


AM1

$C_{26}H_{32}N_2O_6$
 Exact Mass: 468.23
 Mol. Wt.: 468.54

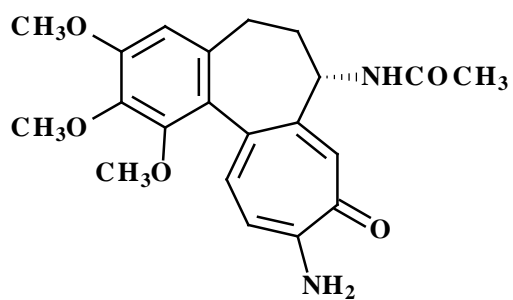
C, 66.65; H, 6.88; N, 5.98; O, 20.49

Figure 4: Colchicine-prolinol



AM2

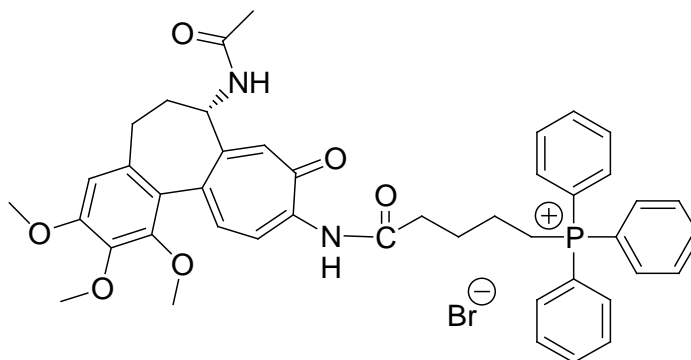
Figure 5: Colchicine-prolinol + Triphenylphosphonium



MB2

Mol. Wt.: 384

Figure 6: Colchicineamide



MB2-TPP

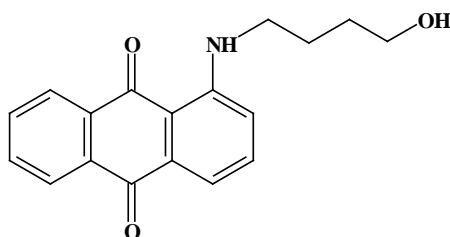
$C_{44}H_{46}BrN_2O_6P$

Exact Mass: 808.23

Mol. Wt.: 809.72

C, 65.27; H, 5.73; Br, 9.87; N, 3.46; O, 11.86; P, 3.83

Figure 7: Colchicineamide + Triphenylphosphonium

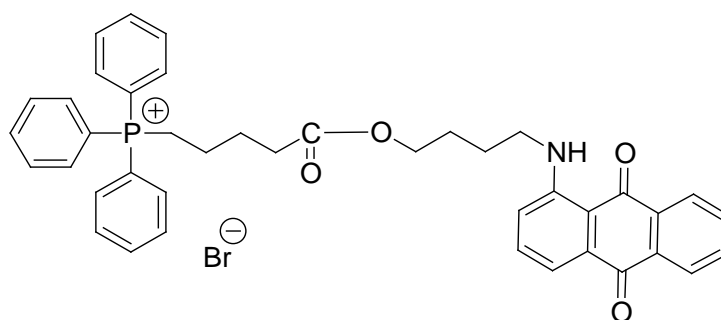


NU:UB 238

$C_{18}H_{17}NO_3$

Mol. Wt.: 295

Figure 8: 1-[(4-Hydroxybutyl) amino]-9,10-anthraquinone



SH1

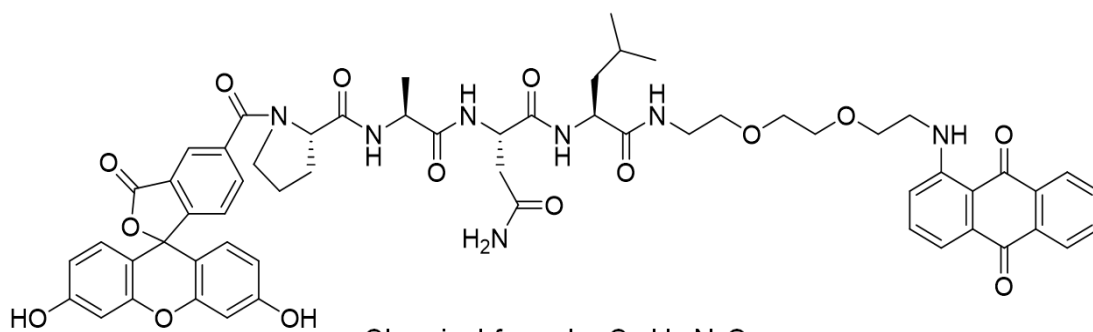
$C_{41}H_{39}BrNO_4P$

Exact Mass: 719.18

Mol. Wt.: 720.63

C, 68.33; H, 5.45; Br, 11.09; N, 1.94; O, 8.88; P, 4.30

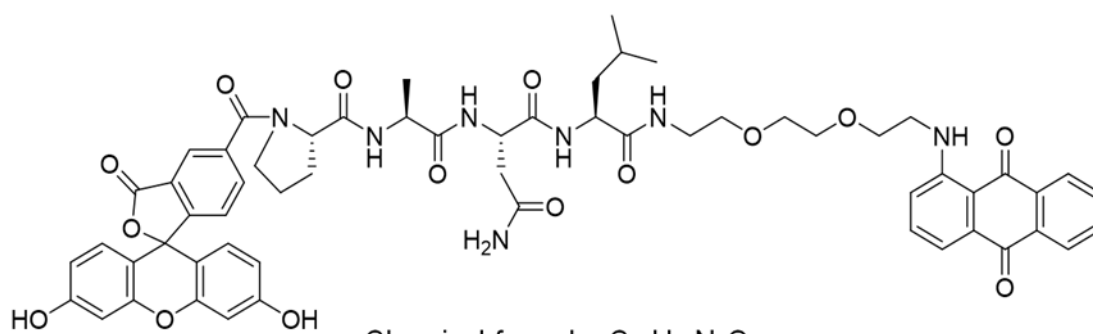
Figure 9: 1-[(4-Hydroxybutyl) amino]-9,10-anthraquinone +
Triphenylphosphonium



Chemical formula: $C_{59}H_{61}N_7O_{15}$

Exact formula weight: 1107.42

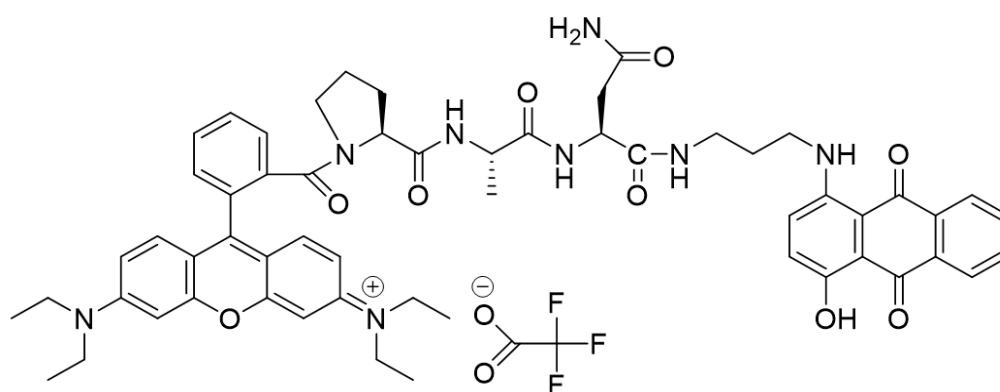
Appendix C: Fluorophore-based probes



Chemical formula: $C_{59}H_{61}N_7O_{15}$

Exact formula weight: 1107.42

Figure 1: Chemical structure of TL11. Fluorescein-labelled probe.



Chemical formula: $C_{59}H_{63}F_3N_8O_{11}$

Exact formula weight: 1116.46

Figure 2: Chemical structure of LS9. Rhodamine-labelled probe.

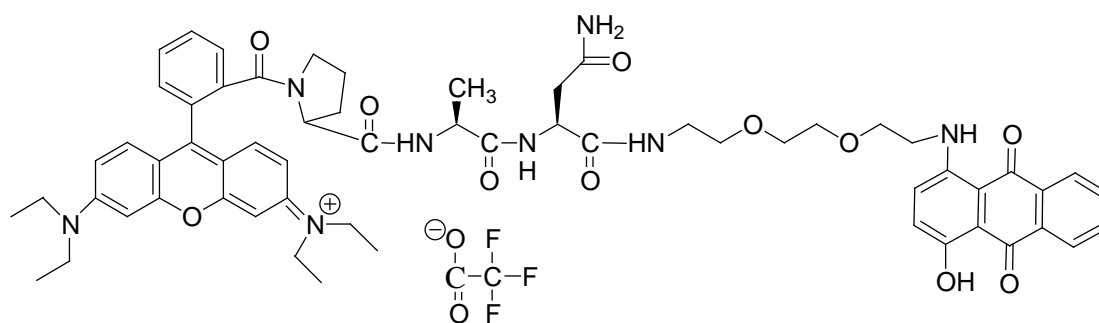


Figure 3: Chemical structure of SM9. Rhodamine-labelled probe.

Appendix D: Reagents and treatment preparation

I. LB agar preparation

Four grams of LB (Oxoid; Basingstoke Hampshire, UK) was weighed into a 1 litre flask. A 200ml volume of deionised water was added into the 1 litre flask and a magnetic stirrer was used to dissolve the LB solute in the solution. The weighing balance was used to measure 2.4g agar (Agar technical number 3 from Oxoid; Basingstoke Hampshire, UK) into the flask and the solution was mixed using the magnetic stirrer and heating on the hot plate avoiding boiling while ensuring total dissolution of the agar. Aliquots of 20ml were transferred into 10 universal glass bottles and screwed loosely with their lid to avoid breakage during sterilization before placing the bottles in the autoclave and sterilizing at a holding temperature of 121°C for 15 minutes. After cooling in a water bath (50°C), each universal bottle carefully poured aseptically into Petri dishes. Once the agar was set after cooling, the plates were stacked appropriately and kept in the 4°C fridge for storage.

II. NGM preparation

Using a calibrated balance, 17g of agar was weighed into a 2-litre flask. The weighing balance was used to measure 2.5g bacterial peptone and 3g of NaCl into the 2-litre flask. The flask was filled with 975ml deionized water and aliquots of 200ml were transferred into 300ml Wheaton bottles with their lids loosely screwed to avoid breakage during sterilization. The bottles were autoclaved at 121°C for a holding time of 15 minutes and allowed to cool in a water bath to 50°C. Using sterile pipettes, 200µl each of sterilized 1M MgSO₄, 1M CaCl and 5mgml⁻¹ cholesterol were added aseptically to each 200ml Wheaton bottle. Also, 5ml of 1M KPO₄ was added to each bottle aseptically and gently mixed avoiding bubbles. Aliquots of 15ml were aseptically poured into either 60mm or 100mm Petri dishes. The plates were allowed to set and carefully placed in an inverted position, stacked and stored in a 4°C fridge until needed for usage.

III. Concentrated *E. coli* OP50 (Pellets)

Twenty grams of LB Broth powder (Fischer New Jersey, USA) was weighed into a 2-litre flask. Deionized water was added into the 2-litre flask to a volume of 1 litre to dissolve the powder. The flask was then placed on a hotplate and mixed using a magnetic stirrer to allow the powder to dissolve completely. Aliquots of 100ml were transferred from the 2-litre flask into ten 500ml flasks.

The 500ml flasks were covered with a stopper and placed in the autoclave and sterilized at 121°C holding temperature for 15 minutes.

After cooling in a water bath (50°C), colonies of *E. coli* OP50 were aseptically taken from a starter culture plate into the 500ml flask containing 100ml LB broth. The flask was incubated overnight in a shaker incubator at 37°C and 180rpm. After incubation, the broth culture was transferred into 50ml centrifuge tubes and centrifuge at 4000rpm for 15 minutes. The supernatant was aspirated, leaving about 1ml containing bacterial pellet. The 1ml culture from the 50ml tubes were transferred into 1.5ml Eppendorf tubes and centrifuged for 2 minutes at 12,000rpm. The supernatant was aspirated and the pellets were kept in a -80°C freezer until needed.

IV. M9 Buffer

To make up 1L M9; 3g KH_2PO_4 , 7.52g $\text{Na}_2\text{HPO}_4 \cdot 2\text{H}_2\text{O}$ and 5g of NaCl were added into a 2L flask.

The mixture was dissolved in 500ml deionized water and 1ml of 1M MgSO_4 (24.65g $\text{MgSO}_4 \cdot 7\text{H}_2\text{O}$ in 100ml deionized water) was added.

Deionized water was added to make up a total volume of 1L in the flask and the preparation was sterilized by autoclaving at 121°C for a holding time of 15 minutes.

V. S Basal solution

In order to make up 1L of S Basal; 5.85g NaCl, 1g K_2HPO_4 and 6g KH_2PO_4 were added into a 2L flask.

The mixture was dissolved in 500ml deionized water.

Having prepared 5mgml^{-1} cholesterol by adding 50mg cholesterol to 10ml of 99% ethanol, 1ml of the resulting cholesterol was added to the 2L flask and mixed with a magnetic stirrer.

Deionized water was added to make up a total volume of 1L in the flask and the preparation was sterilized by autoclaving at 121°C for a holding time of 15 minutes.

VI. Potassium Citrate (pH6)

1M Potassium Citrate (200ml) was prepared by adding 4g citric acid monohydrate and 58.7g tri-potassium citrate monohydrate into a 500ml flask and adding deionized water to make a total volume of 200ml. The preparation was sterilized by autoclaving.

VII. Trace metal solution

Disodium EDTA (1.86g), FeSO₄·7H₂O (0.69g), MnCl₂·4H₂O (0.2g), ZnSO₄·7H₂O (0.29g) and CuSO₄·5H₂O (0.025g) were measured into a 2L flask and filled with deionized water to a total volume of 1L. The preparation was transferred into a dark bottle and sterilized by autoclaving.

VIII. S medium

To make up 1.026 litres S. medium, 1L S basal solution was aseptically added into an already sterilized 2L flask by flaming the tip of the flask containing the S basal solution before transferring into the 2L flask. Trace metal solution (10ml), 1M Potassium Citrate (10ml), 1M MgSO₄ (3ml) and 3ml of sterilized CaCl₂ (11.1g CaCl₂ in 200ml deionized water) were aseptically added to the 1L S basal solution. The preparation is mixed carefully and not autoclaved.

IX. 20% Sodium hypochlorite (NaOCl)

To make up 150ml 20% NaOCl, 100ml of 1M NaOH was prepared by adding 4g NaOH to 100ml of deionized water. A 37.5ml volume of the 1M NaOH was added to a 250ml flask and 30ml of hypochlorite (Sigma Aldrich) was added. The flask was filled with deionized water (82.5ml) to make a total of 150ml of the preparation.

X. Zinc Oxide nanoparticle treatment preparation

Zinc Oxide nanoparticles (ZnO NPs) dispersed in either cationic, ionic and non-ionic dispersants produced by Alfa Aesar were used. The manufacturer's preparation contained 50% ZnO NP in water. In order to prepare stock for treatments, the molarity of the ZnO NPs in water was calculated thus:

Since 50% ZnO is contained in water, this means 50g of ZnO NP in 100ml of water or 500g in 1L of water which is the mass concentration of the stock. Now

$$Molarity = \frac{Mass\ concentration}{Relative\ molecular\ mass\ (RMM)}$$

Where Mass concentration of the ZnO NPs = 500g/L and RMM of ZnO = 81.41g/mol.

$$\text{So Molarity} = \frac{500\text{g/L}}{81.41\text{g/mol}} = 6.14175\text{M} \left(\frac{\text{mol}}{\text{L}}\right).$$

In order to prepare 5ml of 1M solution for each ZnO NP type, 815 μ l of 6.14175M stock was diluted in 4.185ml filtered (0.2 μ m) deionised water. The calculation is as described below.

Using $C_aV_a = C_bV_b$ where $C_a = 1\text{M}$

$C_b = 6.14175\text{M}$ and $V_a = 5\text{ml}$, the volume of 1mM per treatment can be calculated.

$$V_b = \frac{C_aV_a}{C_b}$$

$$V_b = \frac{1\text{M} * 5\text{ml}}{6.14175\text{M}} = 0.815\text{ml} = 815\text{ul}$$

1 part of 1M of each ZnONP (CZNP or AZNP) suspension was added to nine part molecular grade water to get 100mM working stock. A 5ml stock of 100mM solution for each ZnONP type was probe-sonicated for 30 minutes with a 15 second pulse every 10 minutes.

The ZnO NP concentrations investigated were 3.125mM, 6.25mM, 12.5mM and 25mM in 1ml total volume of treatment and these were prepared as described below.

Where $V_a = 1\text{ml}$, $C_a = 3.125\text{mM}$, 6.25mM, 12.5mM or 25mM, and $C_b = 100\text{mM}$ ZnO NP

For 3.125mM concentration:

$$V_b = \frac{3.125\text{mM} * 1\text{ml}}{100\text{mM}} = 0.03125\text{ml} = 31.25\text{ul}$$

So 31.25 μ l of 1M ZnO NP is needed in 1ml *C. elegans* culture to get a total concentration of 3.125mM.

For 6.25mM concentration:

$$Vb = \frac{6.25mM * 1ml}{100mM} = 0.00625ml = 62.5ul$$

So 62.5µl of 1M ZnO NP is needed in 1ml *C. elegans* culture to get a total concentration of 6.25mM.

For 12.5mM concentration:

$$Vb = \frac{12.5mM * 1ml}{100mM} = 0.0125ml = 125ul$$

So 125µl of 1M ZnO NP is needed in 1ml *C. elegans* culture to get a total concentration of 12.5mM.

For 25mM concentration:

$$Vb = \frac{25mM * 1ml}{100mM} = 0.025ml = 250ul$$

So 250µl of 1M ZnO NP is needed in 1ml *C. elegans* culture to get a total concentration of 25mM.

Table A1: Organisation of samples for qPCR for reference gene selection

		RG 1 Actin				RG 2 EIF3C				RG 3 MDH1			
		1	2	3	4	5	6	7	8	9	10	11	12
	A	Control 1		Heat Shock 1		Control 1		Heat Shock 1		Control 1		Heat Shock 1	
	B	Control 2		Heat Shock 2		Control 2		Heat Shock 2		Control 2		Heat Shock 2	
	C	Control 3		Heat Shock 3		Control 3		Heat Shock 3		Control 3		Heat Shock 3	
	D	Control 4		Heat Shock 4		Control 4		Heat Shock 4		Control 4		Heat Shock 4	
	E	CZNP-treated 1		Water		CZNP-treated 1		Water		CZNP-treated 1		Water	
	F	CZNP-treated 2				CZNP-treated 2				CZNP-treated 2			
	G	CZNP-treated 3				CZNP-treated 3				CZNP-treated 3			
	H	CZNP-treated 4				CZNP-treated 4				CZNP-treated 4			

		RG 4 CANX				RG 5 TUBULIN				RG 6 UBC3			
		1	2	3	4	5	6	7	8	9	10	11	12
	A	Control 1		Heat Shock 1		Control 1		Heat Shock 1		Control 1		Heat Shock 1	
	B	Control 2		Heat Shock 2		Control 2		Heat Shock 2		Control 2		Heat Shock 2	
	C	Control 3		Heat Shock 3		Control 3		Heat Shock 3		Control 3		Heat Shock 3	
	D	Control 4		Heat Shock 4		Control 4		Heat Shock 4		Control 4		Heat Shock 4	
	E	CZNP-treated 1		Water		CZNP-treated 1		Water		CZNP-treated 1		Water	
	F	CZNP-treated 2				CZNP-treated 2				CZNP-treated 2			
	G	CZNP-treated 3				CZNP-treated 3				CZNP-treated 3			
	H	CZNP-treated 4				CZNP-treated 4				CZNP-treated 4			

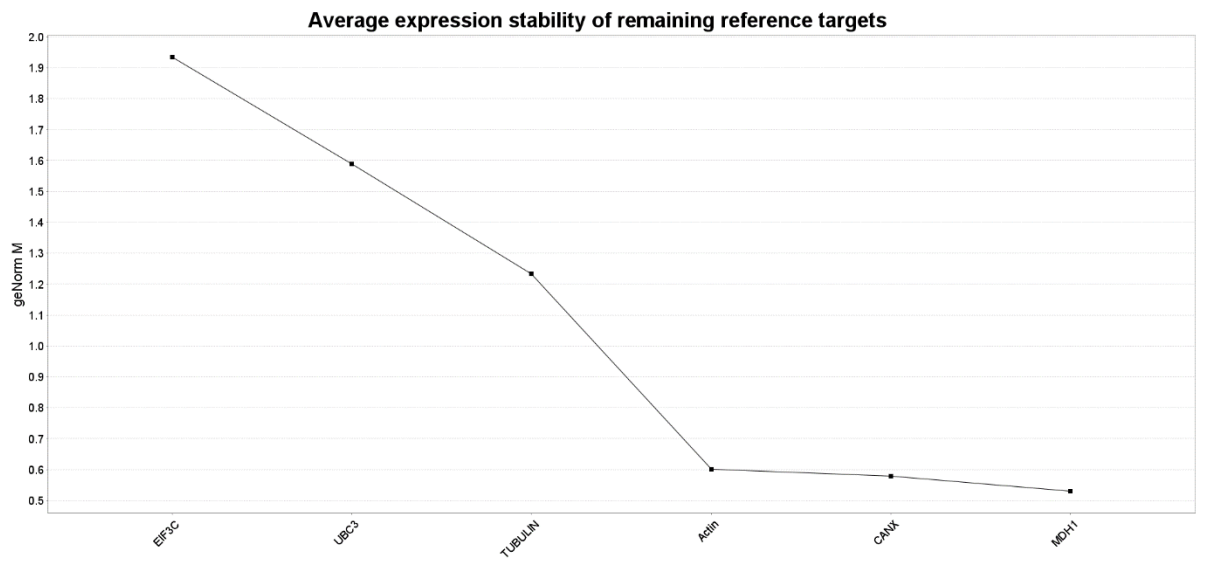


Figure 1: Stability of *C. elegans* reference genes

Table A2: Organisation of 96 well plate for *sod-3* qPCR

		SOD 3			Actin			Canx			MDH1		
		1	2	3	4	5	6	7	8	9	10	11	12
+RT	A												
+RT	B												
+RT	C												
-RT	D												
+RT	E												
+RT	F												
+RT	G												
-RT	H												

		SOD 3			Actin			Canx			MDH1		
		1	2	3	4	5	6	7	8	9	10	11	12
+RT	A												
+RT	B												
+RT	C												
-RT	D												
+RT	E												
+RT	F												
+RT	G												
-RT	H												

XI. Preparation of Phosphate-Citrate Buffer

Phosphate citrate buffer was required for legumain-prodrug treatment and was prepared by mixing varying volumes of 0.2M Na₂HPO₄ and 0.1M citrate with deionized water. Below is a description of the preparation of the acid and base as well as the final buffer.

0.2M Na₂HPO₄: The preparation of 0.2M Na₂HPO₄ (500ml) was carried out by dissolving 14.2g Na₂HPO₄ in 500ml of deionized water in a 1 litre flask. The solution was filter sterilized into a 500ml hybex media bottle and stored at 4°C.

0.1M citrate: This was prepared by dissolving 10.505g of citric acid in 500ml of deionized water in a 1 litre flask. The solution (500ml) was filtered into a 500ml hybex media bottle and stored at 4°C.

Phosphate-citrate buffer: The table below illustrates the preparation of the Phosphate citrate buffer at pH of 4, 5, 6 and 7.

pH	0.2M Na ₂ HPO ₄ (ml)	0.1M Citrate (ml)	Deionized water (ml)	Total volume (ml)
4	19.3	30.7	50.0	100
5	25.7	24.3	50.0	100
6	32.1	17.9	50.0	100
7	43.6	6.5	49.9	100

The pH values may vary slightly, so either the acid or base is added in drops to achieve the exact pH required by measuring with a pH electrode. The buffers were stored in the 4°C fridge.

XII. Preparation of MES buffer

MES buffer at pH of 5 was also used for legumain-prodrug treatment. In order to make 100ml of 100mM MES at pH 5, 1.95g of MES was added to a 250ml beaker with 70ml deionized water. A pH electrode was used to measure the pH and 1M NaOH was titrated into the beaker until the pH was adjusted to 5. Once pH of 5 was achieved, the solution was transferred into a graduated cylinder and diluted to a final volume of 100ml. The final solution was filtered into a 100ml hybex media bottle and stored at 4°C.

XIII. Preparation of Cysteine Protease Inhibitors

Three protease inhibitors; E-64, N-phenylmaleimide or iodoacetamide were used for legumain expression experiments. The inhibitors were provided by Dr. David Mincher's laboratory at Edinburgh Napier University. Iodoacetamide and N-phenylmaleimide are known to inhibit mammalian legumain while E-64 has no effect on legumain (Chen *et al.*, 1997). The concentration of E-64 used in treatment was 100 μ M while N-phenylmaleimide and Iodoacetamide required in treatments had a concentration of 1mM.

N-phenylmaleimide: In a total volume of 100 μ l per well, 1mM N-phenylmaleimide was required from a 5mgml⁻¹ (Relative molecular mass = 173.17gmol⁻¹) stock solution provided. The total volume of 5mgml⁻¹ (28.87mM) stock solution of N-Phenylmaleimide needed in a total of 100 μ l treatment per well to give 1mM N-Phenylmaleimide is 3.5 μ l.

E-64: 100 μ M E-64 (Relative molecular mass = 357.41gmol⁻¹) was prepared from 1mgml⁻¹ (2.79mM) stock solution provided and the required volume of E-64 needed to make up 100 μ l total volume of treatment was 3.6 μ l.

Iodoacetamide: 1mM Iodoacetamide was prepared from a 27mM stock solution provided and the required volume in a total of 100 μ l to give a final concentration of 1mM concentration was 3.7 μ l.

XIV. Preparation of LS9 and TL11 probes

LS9: Given an 895.7 μ M stock solution, and a required 10 μ M concentration in the treatment, the volume of LS9 needed in a 100 μ l volume treatment was 1.1 μ l.

TL11: Like LS9, 10 μ M TL11 was similarly prepared from a 902.5 μ M stock solution

So the total volume of stock solution of TL11 required in a 100 μ l treatment is 1.1 μ l.

XV. Preparation of *C. elegans* treatments with different pH

Homogenate or somatic fraction (40 μ l) from mixed population of worms was diluted in 58.9 μ l buffer (buffer with pH4, 5, 6 or 7) with 1.1 μ l TL11 or LS9 to make up a total of 100 μ l per micro well. Also, 40 μ l homogenates or ES from either L1

or L4 larvae was diluted in 60µl buffer (buffer with pH4, 5, 6 or 7) without TL11 or LS9 to make up 100µl per micro well.

XVI. Preparation of nematode parasite treatments at different pH

H. contortus or *T. circumcincta* lysate (40µl) was diluted in 58.9µl buffer (buffer with pH4, 5, 6 or 7) with 1.1µl TL11 or LS9 to make up a total of 100µl per micro well. Similarly, 40µl *H. contortus* or *T. circumcincta* lysate was diluted in 60µl buffer (buffer with pH4, 5, 6 or 7) without TL11 or LS9 to make up 100µl per micro well.

XVII. Legumain assay plate plan

<p>CONTROL WELL</p> <p>Buffer----- 98.9µl Probe----- 1.1µl <u>100µl</u></p> <p>Final volume in well contains 10µM probe</p>	<p>CONTROL WELL</p> <p>Buffer----- 98.9µl Rhodamine----- 1.1µl <u>100µl</u></p> <p>Final volume in well contains 10µM rhodamine</p>
<p>CONTROL WELL</p> <p>Buffer----- 60.0µl Sample----- 40.0µl <u>100µl</u></p>	<p>CONTROL WELL</p> <p>R. Legumain----- 98.9µl Probe----- 1.1µl <u>100µl</u></p> <p>Final volume in well contains 10µM probe</p>
<p>TREATMENT WELL</p> <p>Buffer----- 58.9µl Sample----- 40.0µl Probe----- 1.1µl <u>100µl</u></p> <p>Final volume in well contains 10µM probe</p>	<p>TREATMENT WELL</p> <p>Buffer----- 55.4µl Sample----- 40.0µl N-Phenylmaleamide-- 3.5µl Probe----- 1.1µl <u>100µl</u></p> <p>Final volume in well contains 10µM probe and 1mM N-Phenylmaleamide</p>
<p>TREATMENT WELL</p> <p>Buffer----- 55.3µl Sample----- 40.0µl E-64----- 3.6µl Probe----- 1.1µl <u>100µl</u></p> <p>Final volume in well contains 10µM probe and 100µM E-64</p>	<p>TREATMENT WELL</p> <p>Buffer----- 55.2µl Sample----- 40.0µl Iodoacetamide----- 3.7µl Probe----- 1.1µl <u>100µl</u></p> <p>Final volume in well contains 10µM probe and 1mM Iodoacetamide</p>

LEGEND

Sample

- Sheep plasma or
- Sheep liver tissue homogenate or
- *C. elegans* homogenate or
- *H. contortus* homogenate or
- *T. circumcincta* homogenate or
- Water soluble fraction of *C. elegans* (S1) or
- Membrane-associated fraction of *C. elegans* (S2)
or
- Membrane-bound fraction of *C. elegans* (S3)

Buffer

- MES (pH5) or
- Phosphate citrate (pH4, 5, 6 or 7)

Probe

- LS9 or TL11

Inhibitor

- N-Phenylmaleamide (28.87mM stock) or
- E-64 (2.79mM stock) or
- Iodoacetamide (27mM stock)

Legumain

- R. Legumain (2.5ng/1µl or 1.67/1µl buffer)

Rhodamine

- Rhodamine B (897.6µM stock)

Figure 2: Schematic representation of treatment plan for legumain assay